

January 2020

Synthesis Of Bradyrhizose And The Equatorial Glycosides Of 3-Deoxygenation-D-Mango-Oct-2-Ulosonic Acid

Philemon O. Ngoje
Wayne State University

Follow this and additional works at: https://digitalcommons.wayne.edu/oa_dissertations

 Part of the [Organic Chemistry Commons](#)

Recommended Citation

Ngoje, Philemon O., "Synthesis Of Bradyrhizose And The Equatorial Glycosides Of 3-Deoxygenation-D-Mango-Oct-2-Ulosonic Acid" (2020). *Wayne State University Dissertations*. 2498.
https://digitalcommons.wayne.edu/oa_dissertations/2498

This Open Access Dissertation is brought to you for free and open access by DigitalCommons@WayneState. It has been accepted for inclusion in Wayne State University Dissertations by an authorized administrator of DigitalCommons@WayneState.

**SYNTHESIS OF BRADYRHIZOSE AND THE EQUATORIAL GLYCOSIDES OF 3-
DEOXY-D-MANNO-OCT-2-ULOSONIC ACID**

by

PHILEMON NGOJE

DISSERTATION

Submitted to the Graduate School

of Wayne State University,

Detroit, Michigan

in partial fulfillment of the requirements

for the degree of

DOCTOR OF PHILOSOPHY

2020

MAJOR: CHEMISTRY (Organic)

Approved By:

Advisor

Date

DEDICATION

I dedicate this dissertation to my dear parents Wilson and Pamela Ngoje, my wife Jovia Akinyi, my brothers and sisters and to my relatives and friends for their candid and unwavering support and guidance they gave me in my PhD journey.

ACKNOWLEDGEMENTS

I'm honored and greatly thankful to my supervisor and mentor, Prof. David Crich for the rare opportunity he gave me to conduct research in his lab. Indeed, the completion of my thesis as well as the success of my graduate studies journey were as a result of his dedication, solid support, guidance and his patience towards my short comings. His in-depth knowledge of chemistry in general was worth emulating. I extend my gratitude to all my dissertation committee members, Prof. Jennifer L. Stockdill, Prof. Steven Sucheck, and Prof. Bernhard Schlegel for being part of my Phd journey. Their time and dedication, as well as advice made it possible for the completion of this thesis.

Many thanks to past and present members of the Crich laboratory for their insightful ideas which were readily availed to me at the time when I needed them most. Their genuine friendship created a peaceful work environment that I will forever be thankful for. My sincere thanks to my wife Jovia for her patience, love and encouragement she showed me both during the bad and good days. I will forever be thankful for my mum and dad for their solid support which they have continually shown me through their love, encouragement and prayers.

TABLE OF CONTENTS

Dedication.....	ii
Acknowledgements.....	iii
List of Tables.....	viii
List of Figures.....	x
List of Schemes.....	xii
List of Abbreviations.....	xvi
CHAPTER 1. INTRODUCTION.....	1
1.1 Carbohydrates as essential chemical messengers in intercellular communication.....	1
1.1.1 Significance of the lectin-carbohydrate interactions in leguminous plants.....	4
1.1.2 The symbiotic nitrogen cycle, its mechanism and significance in leguminous plants growth.....	5
1.1.3 The role and structure of Nod-factors	6
1.1.4 Structure and role of <i>O</i> -antigen lipopolysaccharides.....	7
1.2 Photosynthetic <i>Bradyrhizobia</i>	9
1.2.1 Isolation and structure elucidation of bradyrhizose.....	11
1.3 Literature total syntheses of bradyrhizose.....	14
1.3.1 Bradyrhizose synthesis by Yu group.....	14
1.3.2 Synthesis of bradyrhizose oligosaccharides with α -(1 \rightarrow 7) glycosidic linkages that are relevant to the bradyrhizobium <i>O</i> -antigen.....	16
1.3.3 Bradyrhizose synthesis by Lowary group.....	18
1.3.4 Comparison of ^1H and ^{13}C spectral data of bradyrhizose syntheses by the Yu ⁴⁷ and the Lowary ⁵⁰ laboratories and the Molinaro ⁴⁷ material from degradation of a polymer	21
1.4 Synthesis of structurally related bradyrhizose motifs.....	23

1.5 Occurance and role of ulosonic acids in Gram-negative bacteria.....	26
1.5.1 Biosynthesis of KDO in Gram-negative bacteria.....	27
1.5.2 Occurance of KDO in bacterial lipopolysaccharides	28
1.5.3 Occurance of KDO in bacterial capsular polysaccharides	31
1.5.4 Development of KDO containing glycoconjugate vaccines as potential therapeutics for treatment of pathogenic infections	33
1.6 Challenges and opportunities in KDO glycoside chemistry.....	34
1.6.1 Stereoselective synthesis of axial and equatorial KDO glycosides.....	34
1.7 Role of side chain conformation in stereo-controlled glycosylation reactions	41
1.7.1 Influence of side chain conformation in stereoselective synthesis of sialosides.....	46
1.8 Literature studies on the existence of a <i>tg</i> side chain conformation in KDO residues...	53
1.9 Goals.....	54
CHAPTER 2. INTRODUCTION.....	55
2.1 Results and discussion.....	55
2.1.1 Retrosynthetic analysis of bradyrhizose.....	55
2.1.2 Synthesis of bradyrhizose from methyl α -D-glucopyranoside.....	56
2.1.2.1 Derivatization of compound 247.....	56
2.1.2.2 Exploration of various C-C bond formation reactions for side chain elongation at the glucopyranoside 6-position of compound 247.....	57
2.1.2.2.1 Methallylation via the cross-coupling reaction of methallylmagesium chloride with the iodo sugar derivative.....	57
2.1.2.2.2 C-C bond formation via radical methallylation using methallylsulfones.....	58

2.1.2.3 Synthesis of the key bicyclic intermediate 278.....	61
2.1.2.4 Stereoselective synthesis of the epoxide 279.....	64
2.1.2.5 Regio- and stereoselective ring opening of the epoxide 288.....	66
2.1.3.1 Preparation of benzyl 2,3-di- <i>O</i> -benzyl-6-deoxy-6-iodo- α -D-glucopyranoside from D-glucose.....	69
2.1.3.2 Exploration of various C-C bond formation reactions for side chain elongation at the glucopyranoside 6-position of benzyl 2,3-di- <i>O</i> -benzyl-6-deoxy-6-iodo- α -D-glucopyranoside.....	70
2.1.3.2.1 C-C bond formation via radical methallylations using methallylsulfones or methallyltri- <i>n</i> -butylstannane.....	70
2.1.3.2.2 Visible-light mediated C-C bond formation using (<i>fac</i> -Ir(ppy) ₃) and methallylsulfone.....	73
2.1.3.3 Construction of the bicyclic scaffold.....	75
2.1.3.4 Stereoselective synthesis of oxiranes 241 and 317.....	76
2.1.3.5 Deprotection of 242 to give 20.....	82
2.1.4 Comparison of ¹ H and ¹³ C spectral data of bradyrhizose	82
2.2 Conclusions.....	84
CHAPTER 3. STEREOSELECTIVE SYNTHESIS OF THE EQUATORIAL GLYCOSIDES OF 3-DEOXY-D-MANNO-OCT-2-ULOSONIC ACID.....	86
3.1 Background.....	86
3.2 Results and discussion.....	87
3.2.1 Synthesis of KDO key acetonide intermediate.....	87
3.2.2 Synthesis of KDO thioglycosyl donors.....	88
3.2.3 Preparation of acceptors.....	91
3.3 Glycosylation reactions of KDO thioglycosyl donors.....	94
3.3.1 Assignment of configuration for coupled KDO glycosides.....	95

3.4 Conclusions.....	103
CHAPTER 4. PROGRESS TOWARDS A STEREOCONTROLLED CONVERGENT SYNTHESIS OF A PENTASACCHARIDE CONTAINING A TETRASACCHARIDE REPEATING UNIT OF <i>K. KINGAE</i> TYPE C CAPSULAR POLYSACCHARIDE.....	104
4.1 Background.....	104
4.2 Results and discussion.....	106
4.2.1 Retrosynthesis of compound 404.....	106
4.2.2 Preparation of KDO donor 330 and acceptor 398.....	108
4.2.3 Preparation of the ribofuranosyl imidate donor 393 and the ribose acceptor 389.....	109
4.3 Intended completion of synthesis.....	111
4.3.1 Preparation of key trisaccharide acceptor 398.....	111
4.3.2 Preparation of key imidate donor 392.....	112
4.3.3 Stereocontrolled construction of β -(1 \rightarrow 2)-linkage via a convergent 3+2 glycosylation approach	113
4.5 Conclusions.....	114
CHAPTER 5. CONCLUSIONS.....	116
CHAPTER 6. EXPERIMENTAL SECTION.....	117
References.....	162
Abstract.....	174
Autobiographical Statement.....	177

LIST OF TABLES

Table 1	Spectral analysis of bradyrhizose 12 by Molinaro and co-workers.....	12
Table 2	Comparison of ^1H and ^{13}C spectral data of bradyrhizose syntheses by the Yu ⁴⁷ and the Lowary ⁵⁰ laboratories and the Molinaro ⁴⁷ material from degradation of a polymer.....	22
Table 3	Synthesis of β -KDO glycosides using peracetylated KDO-1- <i>C</i> -arylglcyl donor.....	35
Table 4	Synthesis of β -KDO glycosides using peracetylated KDO-glycyl donor.....	36
Table 5	Synthesis of β -KDO glycosides using peracetylated and perbenzoylated KDO-thioglycoside donors.....	37
Table 6	Synthesis of β -KDO glycosides using peracetylated KDO-thioglycoside donor appended with 4'-methoxyphenacyl ester.....	38
Table 7	Synthesis of β -KDO glycosides using KDO-thioglycoside donor appended with 2-quinolinecarboxyl group.....	40
Table 8	Synthesis of β -KDO glycosides using ortho-hexynylbenzoate KDO donors.....	41
Table 9	Synthesis of β -mannosyl glycosides using mannosyl sulfoxide donors.....	43
Table 10	Relative hydrolysis rates of glucopyranosides as examined by Bols and co-workers.....	44
Table 11	Relative hydrolysis rates of galactopyranosides as examined by Crich and co-workers.....	45
Table 12	The selectivity trends of bicyclic thiomannoside donors as reported by Crich and co-workers.....	46
Table 13	The coupling reactions of compound 201 and 202 with selected acceptors.....	48
Table 14	The ESI mass spectrometry fragmentation experiments of compounds 209 and 210.....	49
Table 15	The coupling reactions of compound 214 with selected acceptors.....	51
Table 16	The coupling reactions of compound 219 with selected acceptors.....	52
Table 17	Attempted methallylation by use of a Grignard reagent in the presence of a catalyst.....	58

Table 18	Methallylation under various radical initiated conditions using methallylsulfones or methallyltri- <i>n</i> -butylstannane.....	71
Table 19	Attempted regioselective epoxide ring opening under various conditions	79
Table 20	Regioselective epoxide ring opening under various acidic conditions	81
Table 21	Comparison of ^1H and ^{13}C spectral data of bradyrhizose synthesis with literature syntheses.....	83
Table 22	Chemical shift and the multiplicity of the synthesized KDO thioglycosyl donors.....	99
Table 23	$^2J_{\text{H,H}}$ and $^3J_{\text{H,H}}$ coupling constants around the pyranoside ring of the synthesized KDO thioglycosyl donors.....	100
Table 24	Comparison of ^1H and ^{13}C chemical shifts of a mixture of compounds 420 and 421 in relation to compound 417.....	111

LIST OF FIGURES

Figure 1	General structure of nodulation factors with ‘n’ indicating variation in oligosaccharide chain length.....	7
Figure 2	Rhizobial LPS structure.....	8
Figure 3	Structures of the repeating units of <i>O</i> -antigen side chain of rhizobial strains.....	9
Figure 4	General structure of rhizobial nodulating factors 4 and the structure of the repeating units of <i>O</i> -antigen side chain of bradyrhizobial (ORS278, BTail) strains 9.....	10
Figure 5	The polysaccharide unit of bradyrhizose with an α -(1→7) glycosidic linkage 9, the monomeric unit of bradyrhizose 10 and its Fischer projection 11.....	11
Figure 6a	The ^1H NMR spectrum of the isolated bradyrhizose <i>O</i> -antigen from <i>Bradyrhizobium sp.</i> BTail.....	13
Figure 6b	The ^{13}C NMR and DEPT spectra of the isolated bradyrhizose <i>O</i> -antigen from <i>Bradyrhizobium sp.</i> BTail reproduced with permission from reference 47.....	13
Figure 7	Different forms of bradyrhizose 12 in solution.....	22
Figure 8	Examples of 2-ulosonic acids commonly found as constituents of glycoconjugates	26
Figure 9	The Structure of KDO and its Fischer configuration.....	27
Figure 10	Structures of KO and KDO8N.....	27
Figure 11	Structures of KDO containing oligosaccharides present in the LPS of various Gram-negative bacteria	30
Figure 12	Structures of KDO containing oligosaccharides present in the CPS of various Gram-negative bacteria.....	32
Figure 13	Carbohydrate-based glycoconjugate vaccine bearing diphtheria toxin mutant or BSA.....	33
Figure 14	The three staggered conformations of hexopyranoses 172 and 173 in solution.....	42
Figure 15	Inversion of the configuration at C7 of compound 201.....	47
Figure 16	Inversion of the configuration at C5 of compound 208.....	50

Figure 17	Inversion of the configuration at C5, C7 and C8 of compound 213.....	52
Figure 18	The Investigation of the $^3J_{H6, H7}$ coupling constants of KDO anomers	53
Figure 19	Pseudo-enantiomeric relationship of pseudaminic acid 228 and KDO 102.....	58
Figure 20	NOE correlations between H4' and H3 and H5 in compound 274.....	62
Figure 21	NOE correlations of H9, C8-methyl group, H3, H5 and H7 in compound 271.....	63
Figure 22	NOE correlations between H9, H3, H5 and H7 in compound 288.....	66
Figure 23	Hypothesized role of Cram chelation in the stereo-controlled addition of vinyl Grignard reagent to compound 291.....	68
Figure 24	NOE correlations between H4' and H3 and H5 in compound 237.....	76
Figure 25	NOE correlations between H9, C8-methyl group and the benzylic methylene hydrogens in compound 317.....	78
Figure 26	NOE correlations of H9, C8-methyl group, H3, H5 and H7 in compound 241.....	80
Figure 27	NOE correlations between H9, H3, H5 and H7 in compound 242.....	82
Figure 28	Pseudaminic donor with a predominant <i>tg</i> conformation about its exocyclic C6-C7 bond.....	86
Figure 29	Synthesis of equatorially linked KDO glycosides.....	95
Figure 30	Karplus relationship showing the dihedral angle of equatorial and axial KDO glycoside and the corresponding coupling constants.....	96
Figure 31	Determination of the configuration of KDO glycosides using IPAP-HSQMBC experiment	97
Figure 32	<i>K. kingae</i> capsule c repeating unit 119 and its derivative 403 containing a linker	105
Figure 33	Equatorially selective peracetylated donor 330.....	105

LIST OF SCHEMES

Scheme 1	Enzymatic catalyzed assembly of a complex carbohydrate.....	1
Scheme 2	A one-pot automated assembly of Globo H analogue 7.....	2
Scheme 3	The automated solid phase assembly of a Le ^y -Le ^x antigen 14.....	3
Scheme 4	The Yu synthesis of bradyrhizose from D-glucal.....	15
Scheme 5	Synthesis of bradyrhizose oligosaccharides with α -(1→7) glycosidic linkages.....	17
Scheme 6	The Lowary synthesis of bradyrhizose from <i>myo</i> -inositol.....	20
Scheme 7	Synthesis of deca-5,6-diulose by Ziegler and co-workers.....	23
Scheme 8	Synthesis of 2,10-dioxadecalins by Ziegler and co-workers.....	24
Scheme 9	Synthesis of structurally related bradyrhizose compounds by Crich and co-workers.....	25
Scheme 10	Synthesis of of enantiomeric diplopyrone analogue by Giuliano and co-workers.....	26
Scheme 11	The biosynthesis of KDO.....	28
Scheme 12	Synthesis of β -KDO glycosides using peracetylated KDO-thioglycoside donor.....	34
Scheme 13	Oxidation of 132 to the corresponding KDO derivative 135.....	36
Scheme 14	Deiodination of 139 to the corresponding KDO derivative 142.....	37
Scheme 15	Mechanistic hypothesized role of 4'-methoxyphenacyl ester in favoring formation of β -KDO glycosides.....	39
Scheme 16	Competition glycosylation experiment involving donors 201, 202 and acceptor 211.....	49
Scheme 17	Mechanistic explanation of the role of <i>tg</i> conformation in formation of β -sialosides.....	53
Scheme 18	Retrosynthesis of a planned bradyrhizose 20.....	56
Scheme 19	Synthesis of the iodo compound from methyl α -D-glucopyranoside.....	57

Scheme 20	Example of a metal catalyzed C-C bond construction using Grignard reagent.....	58
Scheme 21	Synthesis of methallylsulfones 257 and 259.....	59
Scheme 22	Lauroyl peroxide radical initiated reaction using 2-pyridyl methallylsulfone.....	59
Scheme 23	Lauroyl peroxide radical initiated reaction using 4-toluyll methallylsulfone.....	59
Scheme 24	Proposed mechanism for the formation of product 253 and byproducts 260 and 261.....	61
Scheme 25	Oxidation under Parikh-Doering conditions.....	61
Scheme 26	Stereo-controlled Grignard addition reactions in related glucopyranoside systems.....	62
Scheme 27	Stereo-controlled formation of compound 274.....	62
Scheme 28	Synthesis of trisubstituted cyclohexene as reported by Plenio and co-workers.....	63
Scheme 29	Construction of the bicyclic scaffold.....	64
Scheme 30	Regioselective allylic oxidation on compound 279.....	64
Scheme 31	Proposed mechanism leading to enone 279.....	65
Scheme 32	Stereoselective synthesis of epoxide 288.....	65
Scheme 33	Proposed mechanism for epoxidation leading to compound 288.....	66
Scheme 34	Acid catalyzed regio- and stereoselective opening of epoxide 288.....	67
Scheme 35	Proposed mechanism leading to tetraol 291.....	67
Scheme 36	Proposed mechanism for the regeneration of enone 279.....	68
Scheme 37	Attempted hydrolysis of the glycosidic bond.....	69
Scheme 38	A five-step synthesis of compound 234 from D-glucose.....	70
Scheme 39	Synthesis of methallylsulfones 301 and 304.....	70
Scheme 40	Et ₃ B-induced radical reaction by Brown and co-workers.....	72
Scheme 41	Et ₃ B-induced radical transformation by Crich and co-workers.....	73

Scheme 42	Visible-light mediated reductive dehalogenation of unactivated alkyl, alkenyl or aryl iodides.....	74
Scheme 43	Proposed mechanism for the visible-light mediated formation of compound 235 using <i>fac</i> -Ir(ppy) ₃ as a catalyst.....	75
Scheme 44	Synthesis of the bicyclic intermediate 238.....	75
Scheme 45	Derivatization of 241 and 317 from intermediate 240.....	76
Scheme 46	Proposed mechanism for epoxidation leading to compound 317.....	77
Scheme 47	Completion of synthesis.....	82
Scheme 48	Synthesis of bradyrhizose 20 from D-glucose 229.....	85
Scheme 49	Preparation of phosphonate ester 322.....	88
Scheme 50	Preparation of KDO key intermediate 327 from D-mannose	88
Scheme 51	Preparation of thioglycoside 328 from compound 327.....	89
Scheme 52	Preparation of KDO thioglycosyl donor 330 from the acetonide derivative 328...89	
Scheme 53	Synthesis of benzylated thioglycoside 331 from tetraol 329.....	90
Scheme 54	Synthesis of a silyl protected KDO donor 334.....	90
Scheme 55	Preparation of methyl glucosyl acceptor 338.....	91
Scheme 56	Synthesis of mannosyl acceptor 341 from D-mannose.....	91
Scheme 57	Synthesis of methyl ribofuranosyl acceptor 346.....	92
Scheme 58	Preparation of acceptor 351.....	92
Scheme 59	Synthesis of acceptor 360.....	93
Scheme 60	Preparation of methyl galactosyl acceptor 368.....	94
Scheme 61	Enhancement of α -selectivity by distortion of the ⁵ C ₂ chair conformation of donor 380.....	101
Scheme 62	Synthesis of axial KDO glycosides using 5,7-di- <i>O</i> - <i>tert</i> -butylsilyl donor 383.....	102

Scheme 63	Mechanistic hypothesis outlining the importance of side chain conformation on reactivity and selectivity of KDO glycosyl donors.....	103
Scheme 64	Synthesis of a β -ribofuranoside via the neighboring participation of <i>p</i> -nitrobenzoyl group.....	106
Scheme 65	Retrosynthetic analysis of the synthesis of pentasaccharide 404.....	107
Scheme 66	Retrosynthetic analysis of the synthesis of trisaccharide acceptor 398 and ribofuranosyl donor 392.....	108
Scheme 67	Preparation of KDO acceptor 398 from donor 330.....	109
Scheme 68	Synthesis of acceptor 389 from diol 417 and the proposed preparation of imidate donor 393 from 420.....	110
Scheme 69	Proposed preparation of disaccharide acceptor 398.....	112
Scheme 70	Proposed stereoselective synthesis of 390 and preparation of imidate donor 392.....	113
Scheme 71	Proposed preparation of the pentasaccharide via a stereocontrolled convergent 3+2 glycosylation approach.....	114

LIST OF ABBREVIATIONS

α	Alpha anomeric configuration
NeuAc	<i>N</i> -acetyl neuraminic acid
Ara4N	4-amino-4-deoxy- β -L-arabinose
KDO8N	8-amino-3,8-dideoxy-D-manno-oct-2-ulosonic acid
GAlNAc	2-acetamido-2-deoxygalactose
GlcNAc	2-acetamido-2-deoxyglucose
AIBN	Azobisisobutyronitrile
β	Beta anomeric configuration
BSA	Bovine serum albumin
BnOH	Benzyl alcohol
BnBr	Benzyl bromide
CPS	Capsular polysaccharides
CIP	Contact ion pair
CSA	10-Camphorsulfonic acid
CMP	Cytidine-5'-monophosphonate
CPS	Capsular polysaccharides
^{13}C NMR	Carbon nuclear magnetic resonance
CMP	Cytidine-5'-monophosphonate
<i>m</i> -CPBA	<i>meta</i> -Chloroperoxybenzoic acid
KDO	3-Deoxy-D-manno-oct-2-ulosonic acid
KDN	3-Deoxy-D- <i>glycero</i> -D-galacto-2-nonulosonic acid
KO	D- <i>glycero</i> -D-talo-oct-2-ulosonic acid

Glc	D-glucose
Hep	D-heptose
DNA	Deoxyribonucleic acid
DMF	Dimethyl formamide
EPS	Exopolysaccharides
Fe-Mo-co	Ferrous-molybdenum cofactor
HSQMBC	Heteronuclear single quantum and multiple bond Coherence
HWE	Horner–Wadsworth–Emmons
Pi	Inorganic phosphate
LPS	Lipopolysaccharides
Mo-Fe	Molybdenum-ferrous complex
Mg-ATP	Magnesium-adenosine triphosphate
Mann	D-mannose
(<i>S</i>)MTPA	(<i>S</i>)- α -methoxy- α - (trifluoromethyl) phenylacetyl chloride
NIS	<i>N</i> -iodosuccinimide
Nod	Nodulating gene
IBr	Iodine monobromide
LPS	Lipopolysaccharides
LA	Lipid layer
^1H NMR	Proton nuclear magnetic resonance
P-cluster	Phosphorous forms
<i>fac</i> -Ir(ppy) ₃	<i>fac</i> -tris[2-phenylpyridinato-C2,N]iridium(III)

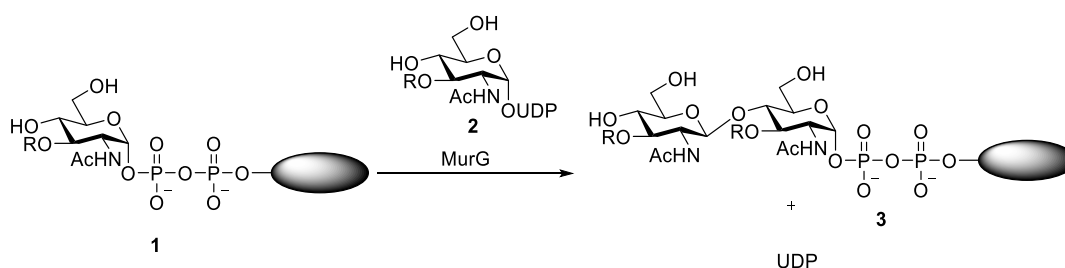
Rib	D-ribose
Rha	L-rhamnose
ROS	Reactive oxygen species
RNA	Ribonucleic acid
RRV	Relative reactivity value
UDP	Uridine diphosphate
TEMPO	(2,2,6,6-tetramethylpiperidin-1-yl)oxidanyl
SSIP	Solvent separated ion pair
TBSCl	<i>tert</i> -butyldimethylsilyl chloride
TIPDSC	1,3-dichloro-1,1,3,3-tetra-isopropyldisiloxane
Tal	L-talose
KpsS &KpsC	Transferase enzyme

CHAPTER 1. INTRODOCTION

1.1 Carbohydrates as essential chemical messengers in intercellular communication

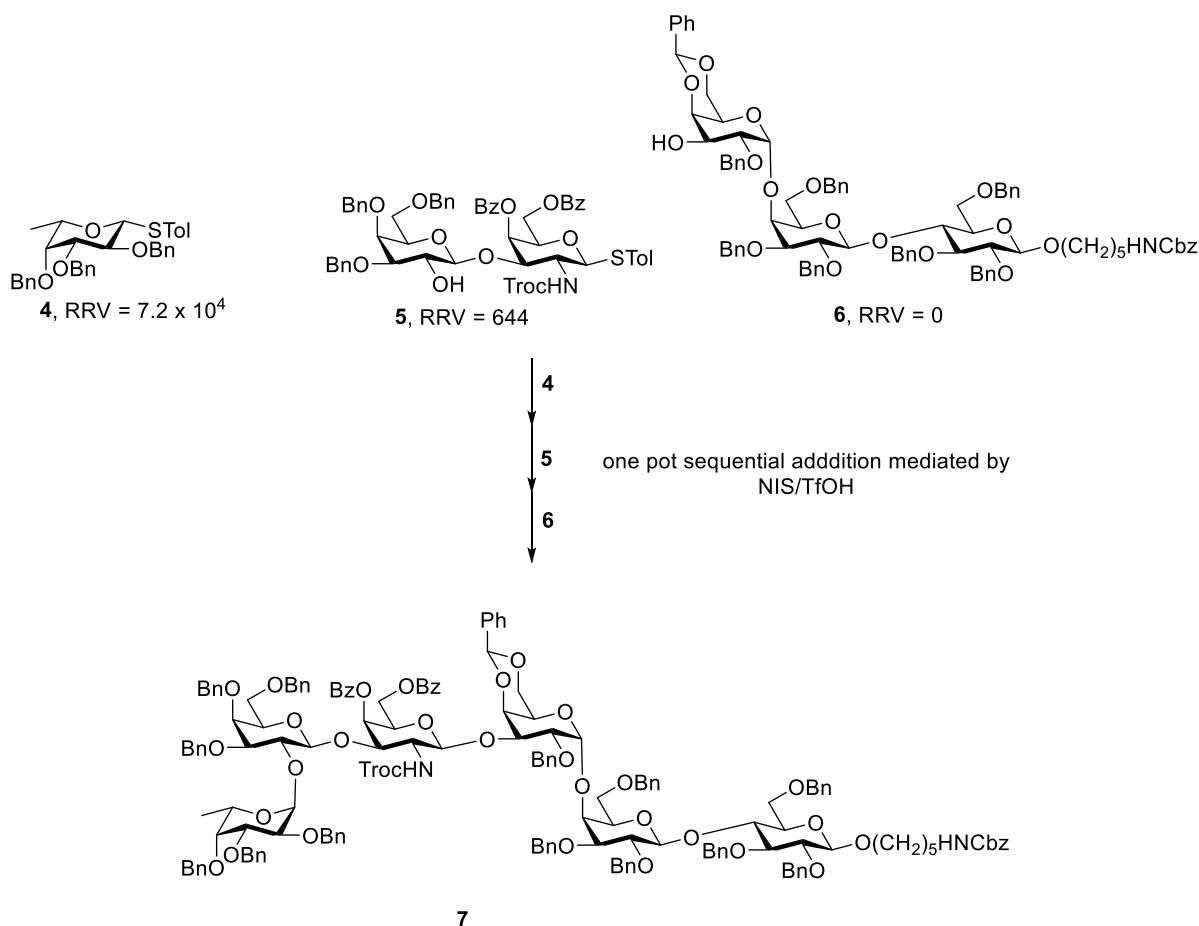
Carbohydrates are polyhydroxylated aldehydes or ketones with the empirical formula $(\text{CH}_2\text{O})_n$ and are by far the most abundant organic molecules found in nature. Nearly all organisms synthesize and metabolize carbohydrates. Most carbohydrates found in nature exist as polysaccharides, glycoconjugates, or glycosides, in which simple sugar units such as the hexoses (glucose, galactose, mannose, and fucose), or the *N*-acetyl aminosugars (*N*-acetylglucosamine and *N*-acetylgalactosamine) are attached to one another or to aglycones through *O*-glycosidic bonds.¹ The structural variability and complexity of carbohydrates allows them to function as energy source molecules, signaling molecules, recognition molecules and adhesion molecules.²

Biologically, the biosynthesis of such *O*-glycosidic linkages is engineered by the glycosyltransferases that assemble monosaccharide units into linear and branched glycan chains with excellent regio- and stereospecificity. These enzymes generally utilize nucleotide phosphate sugar donors such as UDP-*N*-acetylglucosamine, UDP-galactose, GDP-fucose, or CMP-sialic acid that are transferred onto the acceptors such as monosaccharides, oligosaccharides, lipids and proteins (**Scheme 1**).²



Scheme 1. Enzyme catalyzed assembly of a complex carbohydrate

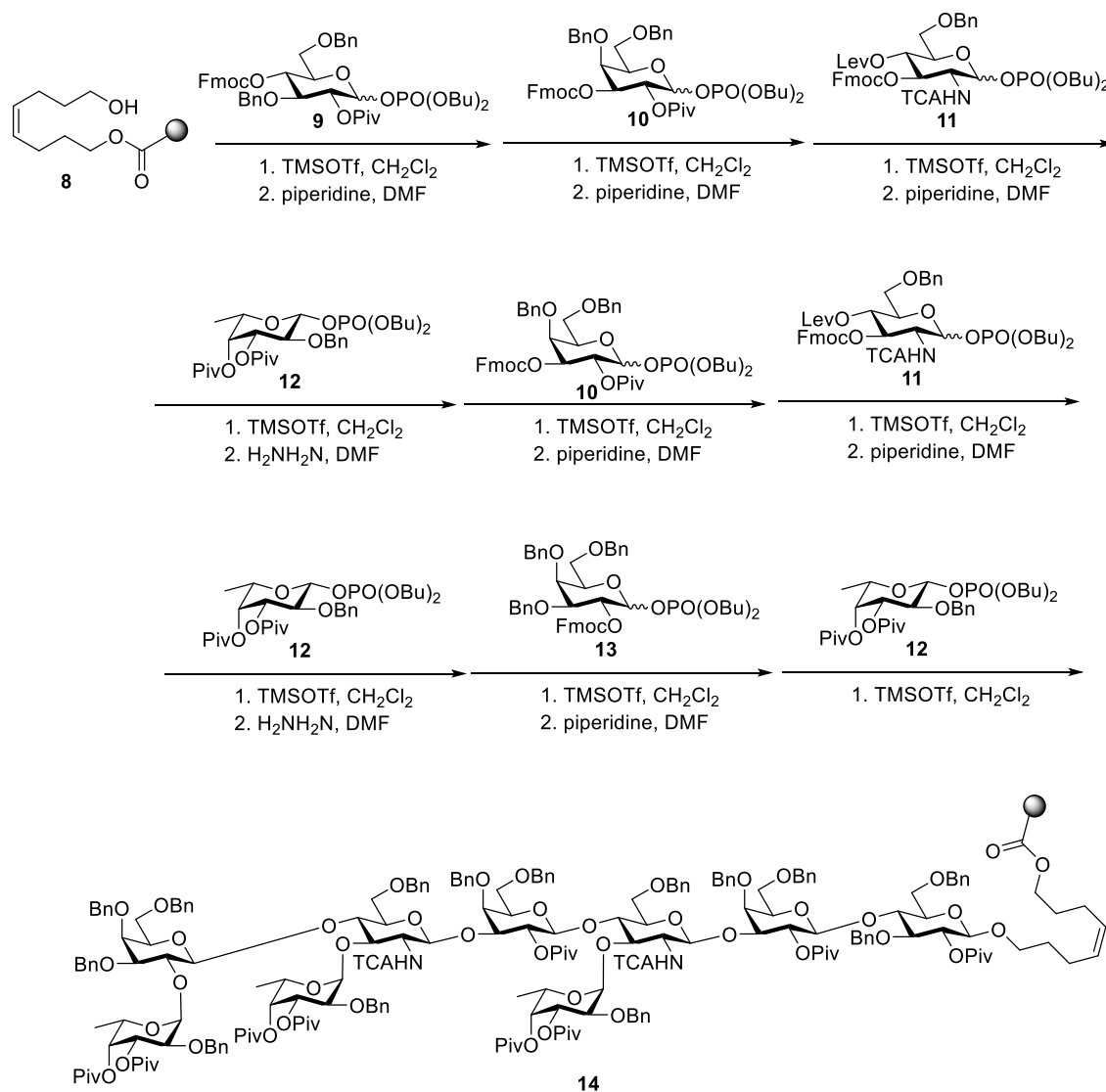
Other chemical methods that have evolved for the assembly of such complex structures include the automated one pot solution phase and solid phase glycan assembly.³ The automated solution phase method involves synthesis of glycans by exploiting the differences in the anomeric reactivity of a large set of diverse thioglycoside building blocks. Wong and co-workers described the automated synthesis of the Globo H analogue **7** by employing the reactivity difference between the thioglycosides **4** and **5** (**Scheme 2**).⁴



Scheme 2. A one-pot automated assembly of Globo H analogue **7**

The automated solid phase glycan assembly method uses a sugar acceptor often attached to the solid polymer surface via a cleavable linker. An example in this case was the synthesis of Le^y-Le^x antigen analogue **14** by Seeberger and co-workers (**Scheme 3**).⁵ Since its inception,⁶ the

automated approach has received wide application in synthesis of bacterial and plant oligosaccharides,⁷⁻⁸ *cis*- and *trans*-glycosidic linkages,⁹⁻¹⁰ assembly of glycosamino sugars¹¹ as well as the sialylated glycans.¹²



Scheme 3. Automated solid phase assembly of the Le^y - Le^x antigen **14**

Complex carbohydrates coat the surfaces of cells and have the potential to carry the information necessary for cell-cell recognition. Most cells are completely covered with a glycan layer, which consists of glycoproteins and glycolipids inserted in the cell membrane, and

proteoglycans, which may be more loosely associated with the cell surface.¹³⁻¹⁴ Many investigators have demonstrated that cell-surface carbohydrates and sugar-specific receptors (lectins) mediate cell-cell communication.¹² Such carbohydrate-directed cell communication appears to be important in many intercellular activities where glycans function as receptors for phages and bacteriocins; specific surface antigens that can determine the pathogenicity of microbes as well as functioning as highly specific receptors in eukaryotes for viruses, bacteria, hormones, and toxins.¹⁵⁻¹⁶

1.1.1 Significance of lectin-carbohydrate interactions in leguminous plants

Carbohydrates on the cell surface of bacteria can function in the intercellular recognition process as in the case between rhizobia and the plant root hair cells. Furthermore, studies have shown that the bacterial recognition of its host (leguminous plant) is related to the carbohydrates on its cell surface and the rhizobial species with different host specificity have different cell surface carbohydrates, respectively.¹⁷

Lectins comprise a structurally very diverse class of proteins characterized by their ability to covalently bind carbohydrates with high specificity and in a reversible manner. They are found in organisms ranging from viruses and plants to humans and serve to mediate biological recognition events occurring in the terminal or intermediate positions of the glycan structure. Legume lectins represent the largest family of carbohydrate binding proteins, and their biological properties have been broadly studied.¹⁸⁻²⁵ For example, studies by Bohlool and co-workers on the specificity of the interaction of the rhizobia with legumes provide an example of an interaction between specific carbohydrates on a cell surface and a lectin protein from the legume plant cell.

That is, Bohlool's group attempted to correlate the binding of lectins to the surface of rhizobium cells with the ability of the rhizobium to establish a symbiotic relationship with the

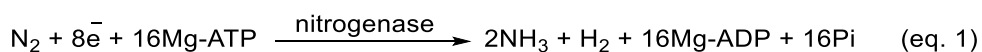
legume from which the lectin was isolated. They found that soybean lectin binds specifically to *R. japonicum*, but not to other *rhizobia* species. Thus, these results indicated that the rhizobium which nodulated soybeans had a surface distinct from the rhizobium which did not nodulate soybeans. This suggested that binding between the plant's lectin proteins, and carbohydrates on the surface of rhizobium cells determined which legumes the rhizobium could nodulate.²⁶

1.1.2 The symbiotic nitrogen cycle, its mechanism and significance in leguminous plants growth

Nitrogen as an element plays a vital role in the formation of DNA or RNA nucleotides, amino acids, proteins and in the growth of tissues of all animals, plants, and other living organisms. Nitrogen in its inert form (N_2) accounts for approximately 78% of the atmosphere's volume; yet because of its features such as a strong covalent $N \equiv N$ triple bond ($226 \text{ kcal mol}^{-1}$), high ionization potential, and negative electron affinity, most organisms, including plants, are unable to metabolize nitrogen. The process of converting nitrogen gas into ammonia is referred to as nitrogen fixation and can be accomplished via any of the following processes: (i) through geochemical processes such as lightning, (ii) industrially through the Haber–Bosch process, and (iii) biologically through the action of specific microorganisms such as endophytic diazotrophic bacteria through a nitrogenase that is rich in Fe and Mo.²⁷

Rhizobium is a symbiotic soil bacteria that induces root nodule formation on leguminous plants, in which they are able to fix atmospheric nitrogen gas to a form utilizable ammonia, thus providing the host plant with all of its essential nitrogen requirement. In return the plant provides the bacterium with carbohydrates. The infectious process often occurs via the deformation or curling of the developing root hairs by the plant host. Within infected cells, molecular nitrogen is reduced to ammonia by the bacteroids, which synthesize nitrogenase

enzymes that catalyze the reduction of atmospheric nitrogen gas to ammonia. The nitrogenase enzyme is a two-component system composed of the Mo-Fe protein dinitrogenase, the electron-transfer Fe protein dinitrogenase reductase, and Mg-ATP required for the catalysis cycle. The Fe protein and Mo-Fe protein associate and dissociate in a catalytic cycle involving single electron transfer and Mg-ATP hydrolysis. Additionally, the Mo-Fe protein contains two metal clusters: the iron–molybdenum cofactor, which provides the active site for substrate binding and reduction, and the P-cluster, that is involved in electron transfer from the Fe protein to iron–molybdenum cofactor. The reduction catalytic cycle is summarized in **Equation 1**.²⁸⁻³¹



This process, and the ensuing nodule development, are host specific, in that a particular rhizobium species will only nodulate a small, defined range of plants. Conversely, bacterial mutation analysis has shown that nodule development is controlled by the rhizobial nodulating genes, that are involved in the production of secreted rhizobial signals called Nod factors. The Nod factors are sufficient to initiate root-hair deformations and to trigger nodule development, albeit only on specific host legumes.³²

1.1.3 The structure and role of Nod-factors

Nod factors are a group of biologically active oligosaccharide signals that are secreted by symbiotic bacteria of the family rhizobiaceae. Their biosynthesis and secretion are determined by rhizobial nodulation (*nod*) genes and are specifically induced in response to flavonoids secreted from the roots of host leguminous plants. The nodulation genes are often categorized as regulatory (*nodD*), or (*nodABC*). The presence of *nodABC* genes in all symbiotically rhizobial species suggests that they are involved in the biosynthesis of a common structural feature present in all

Nod factors.³³⁻³⁵ The *NodC* protein has been shown to have *N*-acetylglucosamine β -(1,4)-transferase activity,³⁶ while *NodB* has chitin oligosaccharide terminal *N*-deacetylase activity,³⁷ and *NodA* is an *N*-acyltransferase.³⁸ Structurally, all Nod factors are short oligomers of β -1,4-linked *N*-acetylglucosamine (**Figure 1**). This core structure may be modified by a number of specific substituents and the modifications are often governed by rhizobial host specificity nod genes. The biological activity of purified Nod factors mirrors the host specificity, indicating that the symbiotic host range of individual rhizobium species is, at least partially, determined by the variety of Nod factors they are able to produce.³⁵

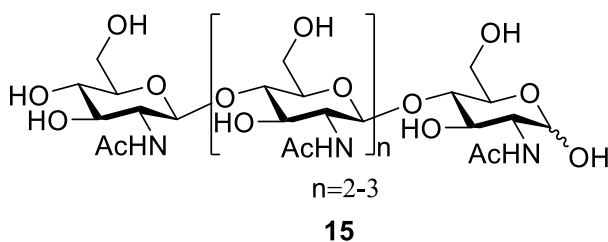


Figure 1. General structure of nodulation factors with ‘n’ indicating variation in oligosaccharide chain length

1.1.4 Structure and role of *O*-antigen lipopolysaccharides

Lipopolysaccharides are glycoconjugates that form part of the outer membrane surface of Gram-negative bacteria. Previous studies have identified these conjugates as undergoing structural modifications during symbiotic processes to allow them to perform functions such as root hair infection and suppression or triggering of host defense responses.³⁹⁻⁴⁰ In general, the structure of many of these polysaccharides are still not fully elucidated, however, well-known components include the KDO, which interconnects the lipid A with the outer core glycans and the *O*-antigenic polysaccharide (**Figure 2**).

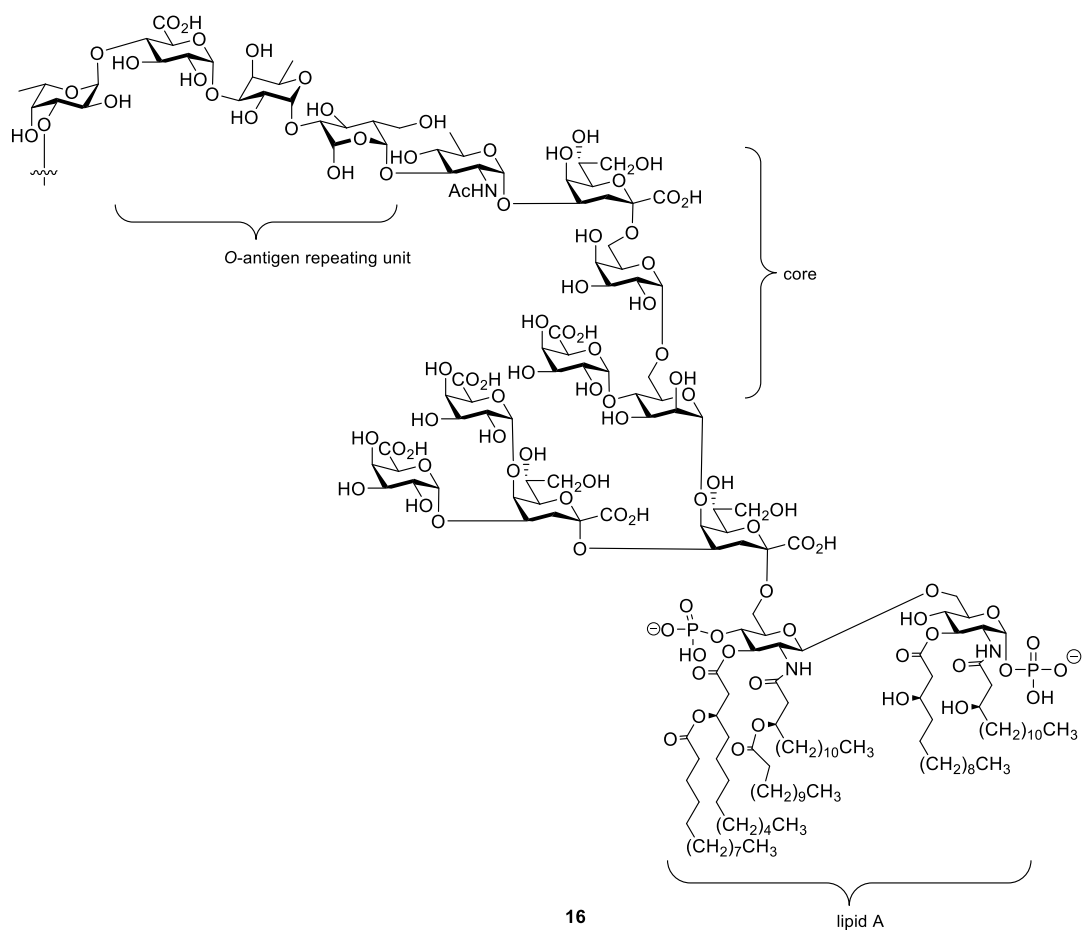


Figure 2. Rhizobial LPS structure

The *O*-antigen side chain is the most significant component and varies from one strain of bacteria to another. For example, studies indicate that different strains of rhizobia possess variations in their *O*-antigen side chain (**Figure 3**). The putative role of the *O*-antigen side chain could be facilitation of establishment of symbiosis through provision of a direct contact channel between the plant and the rhizobia for molecular signal exchange.^{35, 39}

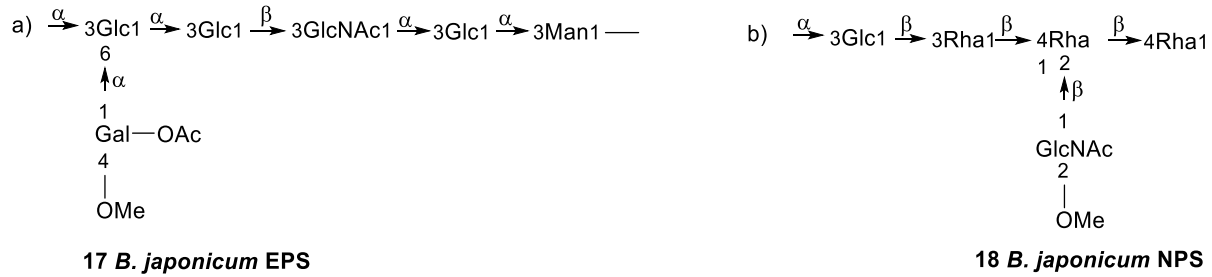


Figure 3. Structures of the repeating units of *O*-antigen side chain of rhizobial strains

1.2 Photosynthetic *Bradyrhizobia*

As a subclass of proteobacteria, *Bradyrhizobia* are symbiotic nitrogen fixers generally found in specific leguminous plant roots. As is evident from the literature, almost all leguminous plants forming a symbiotic relationship with rhizobia have a universal signal transduction mechanism.⁴¹ As such, studies by the Giraud and Chaintreuil groups have demonstrated that *Bradyrhizobia* species strains (ORS285) contain the known nodulation genes *nodABC* that induces nodulation in most *Aeschynomene* plant species via the classical known molecular transduction mechanism.⁴² However, recent studies have revealed that *Aeschynomene indica* and *sensitiva* plant species are able to have a mutual relationship with specific *bradyrhizobia* strains in the absence of nod factors. For example, Giraud and co-workers in their preceding works discovered that the *Aeschynomene indica* and *sensitiva* plant species could still be nodulated by the *Bradyrhizobia* strains (ORS285 and BTail) even after mutation of the *nodABC* genes present in ORS285. This Nod-independent symbiotic process indicates a new alternative molecular signaling pathway for the nitrogen fixation. However, a great challenge in identifying the factors that entirely control the whole process still exists.⁴³

Many hypotheses have been used to explain the occurrence of this new phenomena, based on a closer look at the outer membrane structure of the *Bradyrhizobia* strains of interest. First, *Bradyrhizobia* is thought to be coated by non-immunogenic surface polysaccharides such as

exopolysaccharides (EPS), and capsular polysaccharides (CPS) that have previously been shown to be involved in symbiosis by suppressing plant innate immunity, masking surface antigens or directly functioning as molecular signals.^{44,45} Secondly, it has also been suggested that *Bradyrhizobia* release yet to be determined non-nod signals that initiate the symbiotic process as well as suppressing the plant innate immunity.⁴⁶

Through their recent study on the structure of lipopolysaccharide *O*-antigen side chain of *Bradyrhizobium* species (BTail) strains, Molinaro and co-workers proposed a new hypothesis that could further explain the unknown mechanism involved in the symbiotic process between the *Bradyrhizobia* (ORS278, BTail) strains and the *A. indica* and *sensitiva* plant species. Unlike the presence of lipochitooligosaccharides in LPS of *rhizobia*³² **15** (**Figure 4**), they discovered that the LPS *O*-antigen of photosynthetic *Bradyrhizobia* consisted of monomeric repeating units **19** with a unique bicyclic chemical structure called bradyrhizose, whose presence is thought to result in suppression of the plant innate immune system as well as triggering of the release of transduction signals.⁴⁷

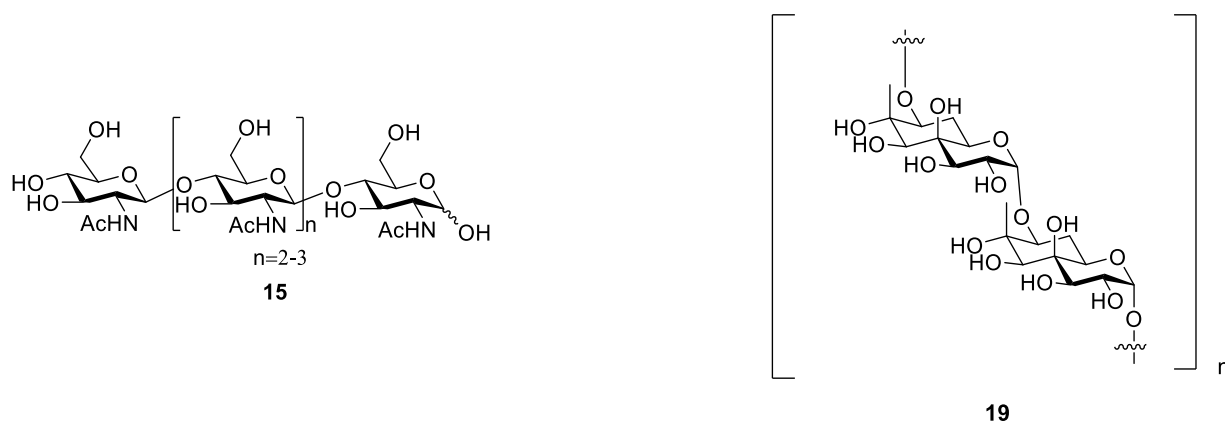


Figure 4. General structure of rhizobial nodulating factors **15** and the structure of the repeating units of *O*-antigen side chain of bradyrhizobial (ORS278, BTail) strains **19**.

1.2.1 Isolation and structure elucidation of bradyrhizose

Bradyrhizose is an inositol-fused monosaccharide that forms a polymeric unit via an α -(1 \rightarrow 7) glycosidic linkage (**Figure 5**). The findings of Molinaro and co-workers revealed that the monomeric unit **20** is made up of an inositol ring which is *trans*-fused onto another six-membered ring resulting into a ten-carbon bicyclic compound. Interestingly, further conformational analysis revealed that the polymer adopts a compact two-fold right-handed helicoidal structure with all methylene groups pointing inwards while the hydroxy and methyl groups are exposed outwards.⁴⁷

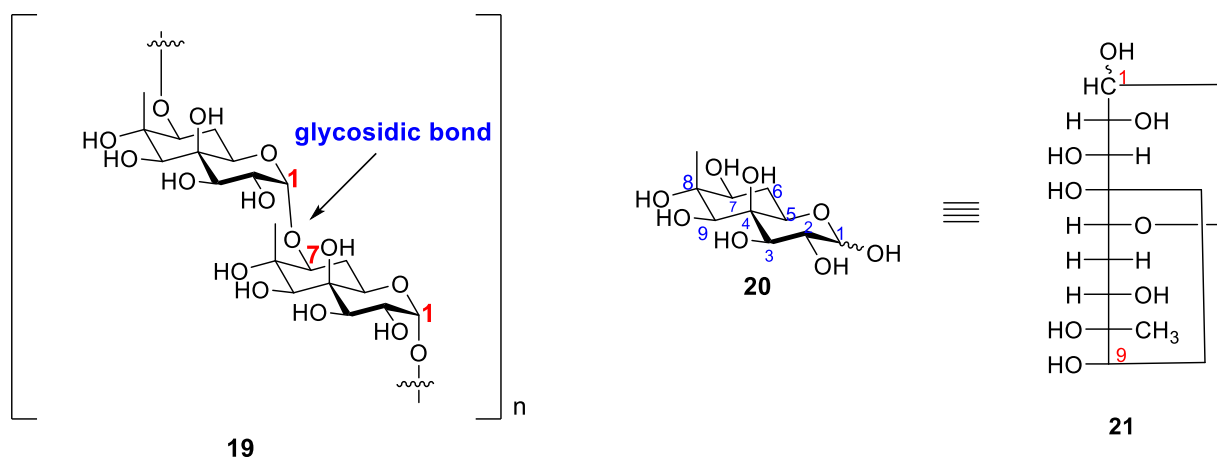
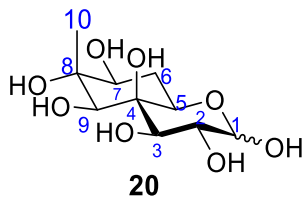


Figure 5. The polysaccharide unit of bradyrhizose with an α -(1 \rightarrow 7) glycosidic linkage **19**, the monomeric unit of bradyrhizose **20** and its Fischer projection **21**.

Indeed, ^1H NMR spectral analysis revealed nine signals that confirmed the monomeric structure of bradyrhizose **20** and its α -configuration (**Figure 6a**). Thus, the characteristic single peak observed in the anomeric region at 4.97 ppm corresponded to an α -anomeric configuration as was supported by the $^3J_{\text{H-1,H-2}}$ coupling constant of 3.9 Hz (**Table 1**). Additionally, the 2D experimental analysis done by Molinaro and co-workers confirmed the correlation of the anomeric proton at δ_{H} 4.97 with H-2 at 3.77 ppm and H-3 at 4.06 ppm, with the $^3J_{\text{H-2,H-3}}$ coupling constant of 10 Hz confirming the axial orientation of H-2 and H-3. Similarly, further 2D analysis showed a

correlation between the diastereotopic methylene protons (H6_{ax} and H-6_{eq}) at 1.73-1.97 ppm and both the H-5 proton at 4.26 ppm and the H-7 proton at 3.72 ppm. Molinaro and co-workers also showed by NMR data analysis that the singlet observed at 1.34 ppm corresponded to a methyl group located on a tetra-substituted carbon. The isolation of **20** as a single anomer with the α -configuration was further confirmed by both ^{13}C and DEPT NMR analysis. Such analysis by Molinaro and group showed the presence of ten carbon signals, two of which were quaternary carbons at δ_{C} 75.0, corresponding to C-4, and at δ_{C} 74.5, which corresponded to C-8. The methylene carbon at δ_{C} 27.5 was associated with the H-6_{ax} and H-6_{eq}, while the anomeric carbon at δ_{C} 96.6 (**Figure 6b**) confirmed the α -configuration of the monomer. (**Table 1**). Subsequently, they demonstrated that carbon peaks observed at δ_{C} 69.2, 75.0, 65.8, and 75.0 corresponded to C-2, C-3, C-5 and C-9, respectively, with the C-methyl peak being observed at δ_{C} 19.9.

Table 1. ^1H and ^{13}C spectral analysis of bradyrhizose **20** by Molinaro and co-workers



¹ H and ¹³ C of 20	Signal assignment										
	1	2	3	4	5	6 _{ax}	6 _{eq}	7	8	9	10
δ _H	4.97	3.77	4.06	-	4.26	1.73	1.97	3.72	-	3.65	1.34
multiplicity	d	dd	d		dd	m	q	dd		s	s
³ J _{H, H}	(3.9 Hz)	(3.9, 10.0 Hz)	(10.0 Hz)		(3.5, 11.6 Hz)		(11.6 Hz)	(4.5, 11.6 Hz)			
δ _C	96.6	69.2	75.0	75.0	65.8	27.5	27.5	77.2	74.5	75.0	19.9

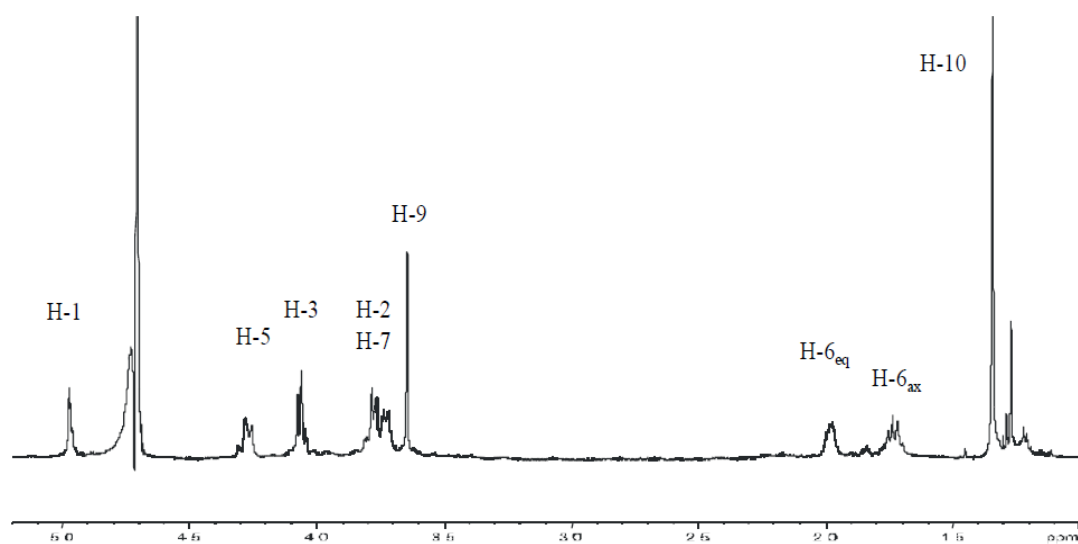


Figure 6a. The ^1H NMR spectrum of the isolated bradyrhizose *O*-antigen from *Bradyrhizobium* *sp.* BTAil reproduced with permission from reference 47

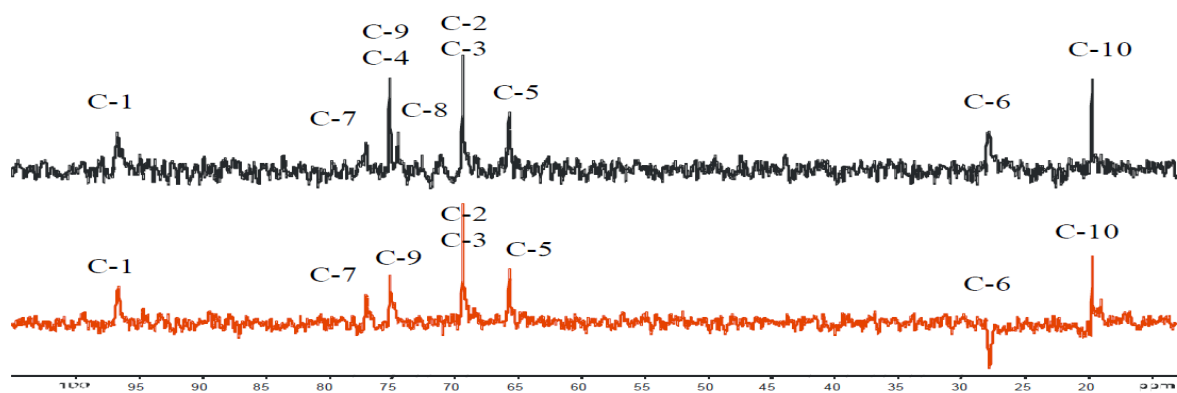
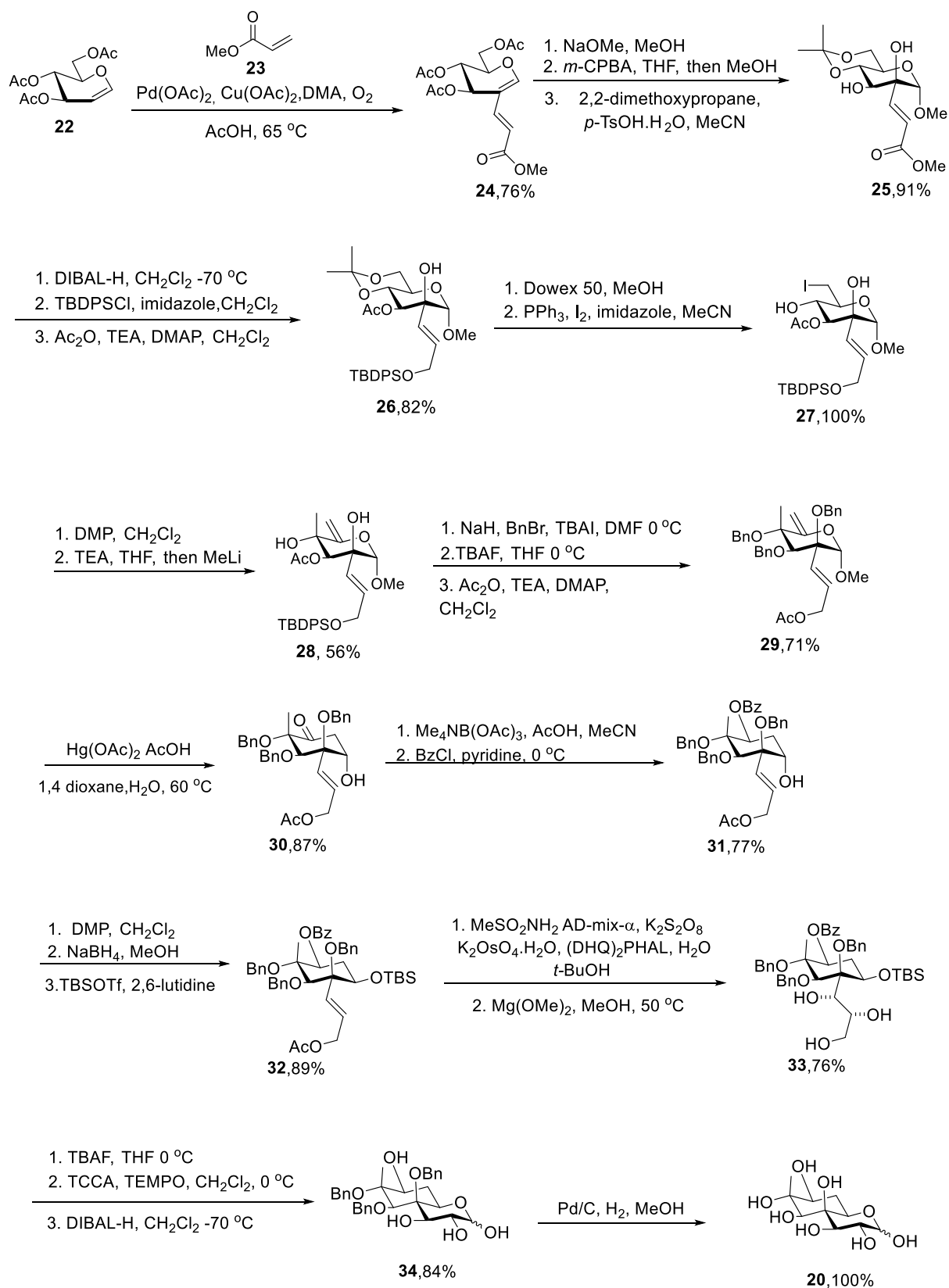


Figure 6b. The ^{13}C NMR and DEPT spectra of the isolated bradyrhizose *O*-antigen from *Bradyrhizobium* *sp.* BTAil reproduced with permission from reference 47

1.3 Literature total syntheses of bradyrhizose

1.3.1 Bradyrhizose synthesis by Yu group

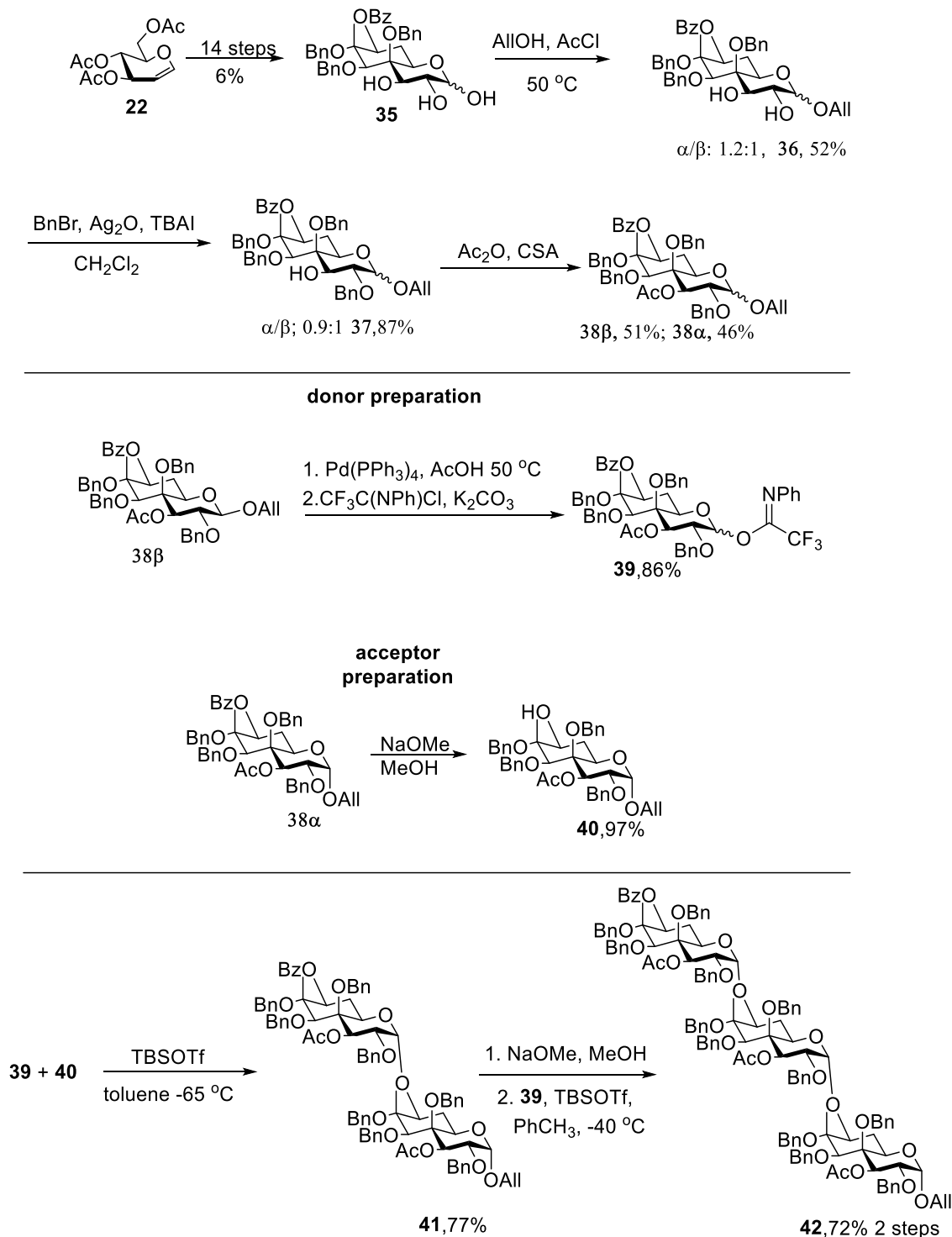
Yu and co-workers reported a total synthesis of bradyrhizose **20** (**Scheme 4**) from D-glucal **22** which involved 26 steps with an overall yield of 9%. Their strategy involved key steps such as the preparation of the conjugated glycal **24** via the Pd(OAc)₂-catalyzed C(2)-functionalization of the activated glycal, the regio- and stereoselective introduction of the *trans* 1,2-diol via epoxidation-hydrolysis on the conjugated glycal **24**, and the Ferrier type II rearrangement of a glucopyranoside derivative **29** mediated by the mercuric acetate system. The rearrangement on the pyranoside derivative **29** proved to be an effective method for accessing the polyhydroxy inositol scaffold. Further functional group adjustment gave **32** in good yield. The Yu group also demonstrated that the construction of the galactose scaffold was of equal importance and they achieved this by further elaboration on the *trans*-ene scaffold **32** via the Sharpless asymmetric dihydroxylation conditions. This transformation led to installation of the galactose 2,3-diol. Subsequently, a selective elaboration on the anomeric aldehyde mediated by the TEMPO/trichloroisocyanuric acid system followed by simultaneous formation of the hemiacetal from a polyol resulted in **34**, which upon subjection to hydrogenolysis conditions gave **20** as a mixture.⁴⁸ With an overall yield of 6%, Yu and co-workers synthesis was characterized by use of multiple protecting groups and of numerous synthetic steps.



Scheme 4. The Yu synthesis of bradyrhizose from D-glucal

1.3.2 Synthesis of bradyrhizose oligosaccharides with α -(1 \rightarrow 7) glycosidic linkages that are relevant to the bradyrhizobium *O*-antigen

In a subsequent communication, Yu and co-workers demonstrated that the bradyrhizose dimer, tetramer, and pentamer having an α -(1 \rightarrow 7) glycosidic linkages could be achieved in good yields in a TBSOTf-mediated glycosylation reaction using 3-*O*-acetyl-2-*O*-benzyl protected imidate donors and bradyrhizopyranoside acceptors in toluene at temperatures between -40 to -65 °C (**Scheme 5**).⁴⁹ The benzyl ethers were used as protecting groups to enhance the reactivity of the donors given that the rigid structure of bradyrhizose renders it less reactive. Such protecting groups were also strategically installed to minimize the laborious work of the selective installation and removal of protecting groups.



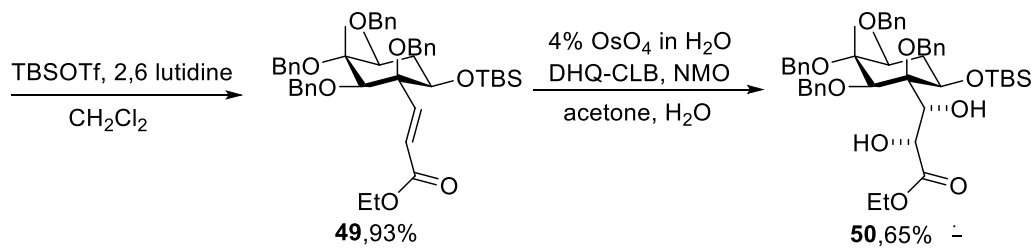
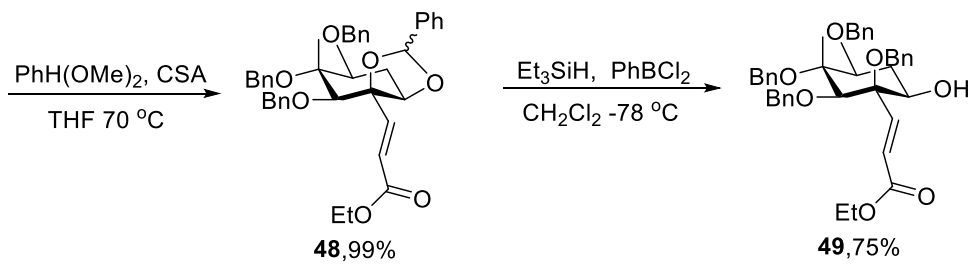
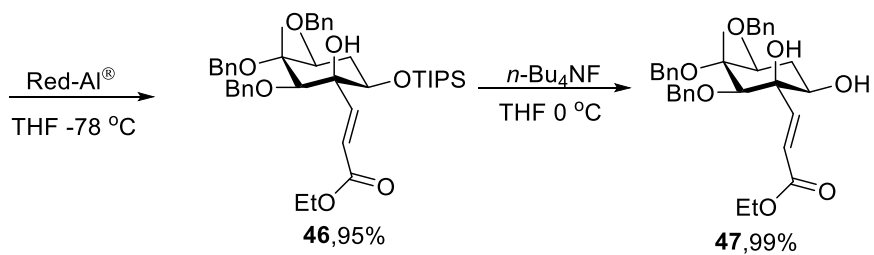
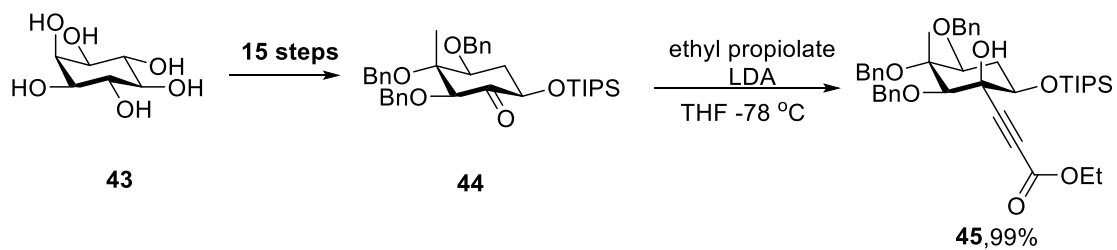
Scheme 5. Synthesis of bradyrhizose oligosaccharides with α -(1 \rightarrow 7) glycosidic linkages

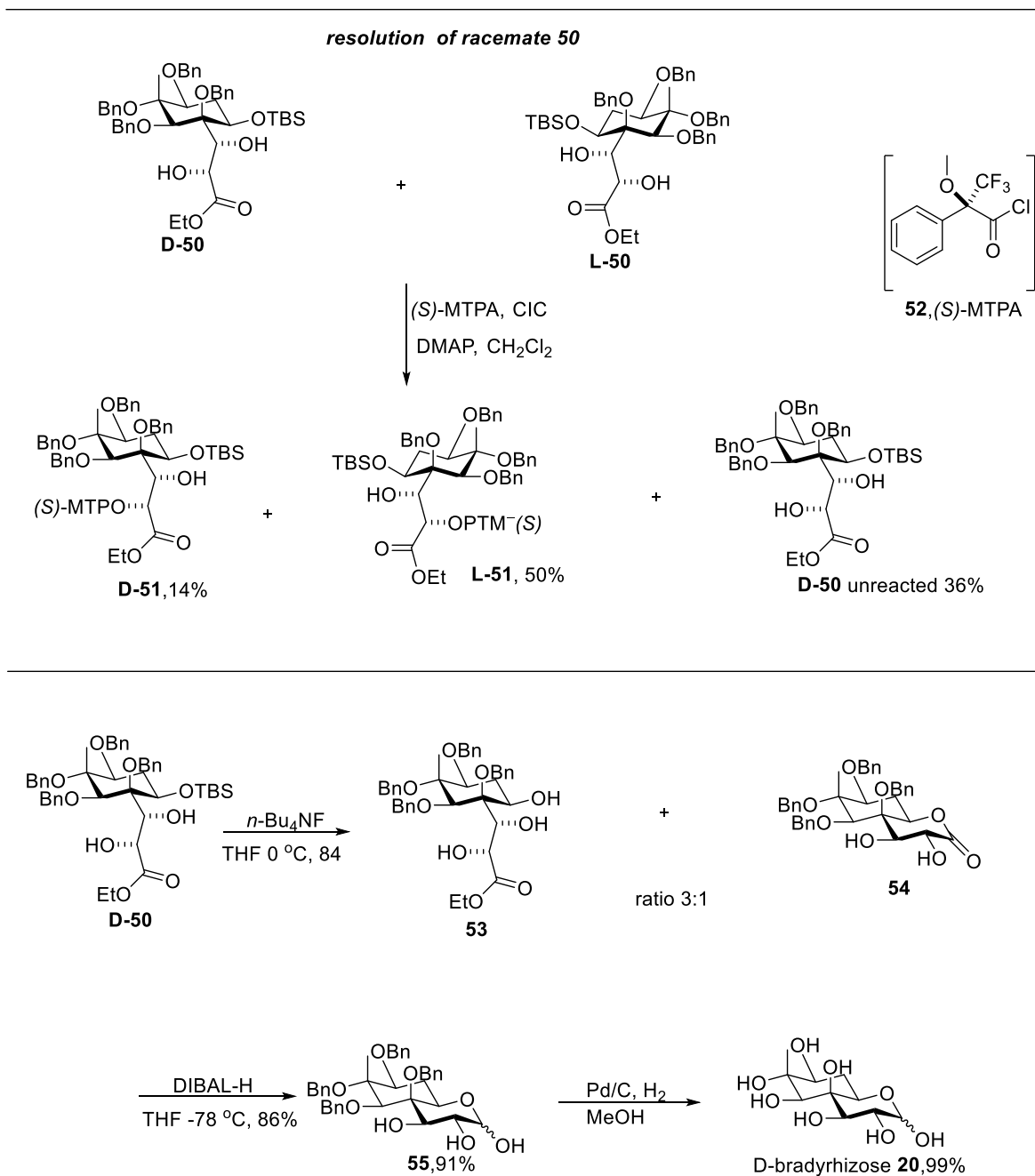
Additionally, the immunogenicity studies conducted on the deprotected oligo-bradyrhizopyranosides revealed that they did not induce ROS in *Xanthomonas campestris* pv.

campestris LPS. This observation was consistent with previous studies that had shown that the whole LPS of bradyrhizobium did not induce any immune responses in its host plant or in other plant families.⁴⁷

1.3.3 The Lowary synthesis of bradyrhizose

Lowary and co-workers have recently demonstrated that they could synthesize bradyrhizose **20** from *myo*-inositol **43** in 25 steps with an overall yield of 6% (**Scheme 6**).⁵⁰ The key transformations in their synthesis involved the derivatization of the ketone intermediate **44** from inositol **43** in 15 steps as well as the stereoselective introduction of the propargylic alcohol **45** onto the ketone **44** using LDA and a propargyl ester. Subsequent functional group adjustments followed by the asymmetric dihydroxylation on *trans*-ene intermediate **49** yielded the desired *trans*-1,2-diol **50** as a racemic mixture. Studies on the resolution of the racemate revealed that upon treatment of **50** with (*S*)-(-)- α -methoxy- α -(trifluoromethyl)phenylacetic acid **52**, enantiomer **D-50** reacted preferentially to give **L-51** in 50% yield, while the other reacted with (*S*)-MTPA to give **D-51** in 14% yield. The unreacted **D-50** was recovered and its purity determined by chiral HPLC. Construction of the galactose framework then began by treatment of the enantiopure **D-50** with tetra-*n*-butylammonium fluoride giving **53** and **54** as inseparable mixture. Subsequent reduction of the mixture using DIBAL-H followed by global deprotection on **55** led to **20** that was obtained as a mixture. Similar to the observations previously made in the Yu synthesis of bradyrhizose, the synthesis of **20** by the Lowary group was also characterized by the use of multiple steps, as well as the intermediacy of racemate **50** that had to be resolved. Additionally, the generation of intermediates **53** and **54** as inseparable mixtures also was a major challenge in this synthesis.





Scheme 6. Key steps in the Lowary synthesis of bradyrhizose from *myo*-inositol

1.3.4 Comparison of ^1H and ^{13}C spectral data from the bradyrhizose syntheses by the Yu⁴⁸ and the Lowary⁵⁰ laboratories and the Molinaro⁴⁷ material from degradation of the polymer

An inspection of the ^1H NMR spectra of **20** in D_2O with acetone as an internal standard by the Yu group revealed that this bicyclic structure gave rise in solution to an equilibrium mixture consisting of two different pyranose forms **a** and **b**, the regioisomer **c**, and the furanose forms **d** and **e** (**Figure 7**). Similar observations were made by Lowary group using acetone as an external standard. These observations contradicted the report by Molinaro group who observed a single anomer of **20**.

Based on the Yu data, the ^1H NMR spectrum of **20** in D_2O shows anomeric signals of H-1 at δ_{H} 4.50 and 5.10 ppm corresponding to the β - and α -anomers of pyranose forms **a** and **b** with $^3J_{\text{H1,H2}}$ coupling constants of 8.07 and 3.90 Hz, respectively (**Table 2**). In the same manner the Lowary group report shows the anomeric signals at δ_{H} 4.62 and 5.23 ppm corresponding to the H-1 β - and α -anomers of pyranose forms **a** and **b** with $^3J_{\text{H1,H2}}$ coupling constants of 8.1 and 4.0 Hz, respectively. In contrast, Molinaro and co-workers reported the existence of only the α -anomer at 4.97 ppm with $^3J_{\text{H1,H2}}$ coupling constant value of 3.9 Hz. Subsequently, the Yu group indicated that the further H-1 anomeric signals observed at δ_{H} 4.93 and 5.14 ppm corresponded to the α - and β -anomers of furanose forms **d** and **e**, respectively, while the anomeric signal observed at 4.93 ppm was attributed to the regioisomeric form **c** with a $^3J_{\text{H1,H2}}$ coupling constant of 5.0 Hz (**Table 2**). On the other hand, the Lowary data revealed that the H-1 anomeric signals they observed between 5.07-5.05 ppm corresponded to the α - and β -anomers of furanose forms **d** and **e** respectively, while the anomeric signal observed at 5.27 ppm was attributed to the regioisomeric form **c** with a $^3J_{\text{H1,H2}}$ coupling constant of 5.3 Hz. The deviations in both the ^1H and ^{13}C NMR spectra chemical shifts observed in (**Table 2**) possibly resulted from the use of acetone as either

an internal standard as in the case of Yu and Molinaro, or as an external standard as in the case of the Lowary group.

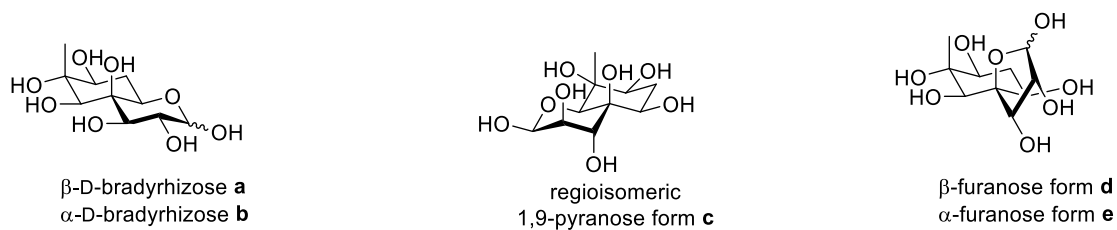


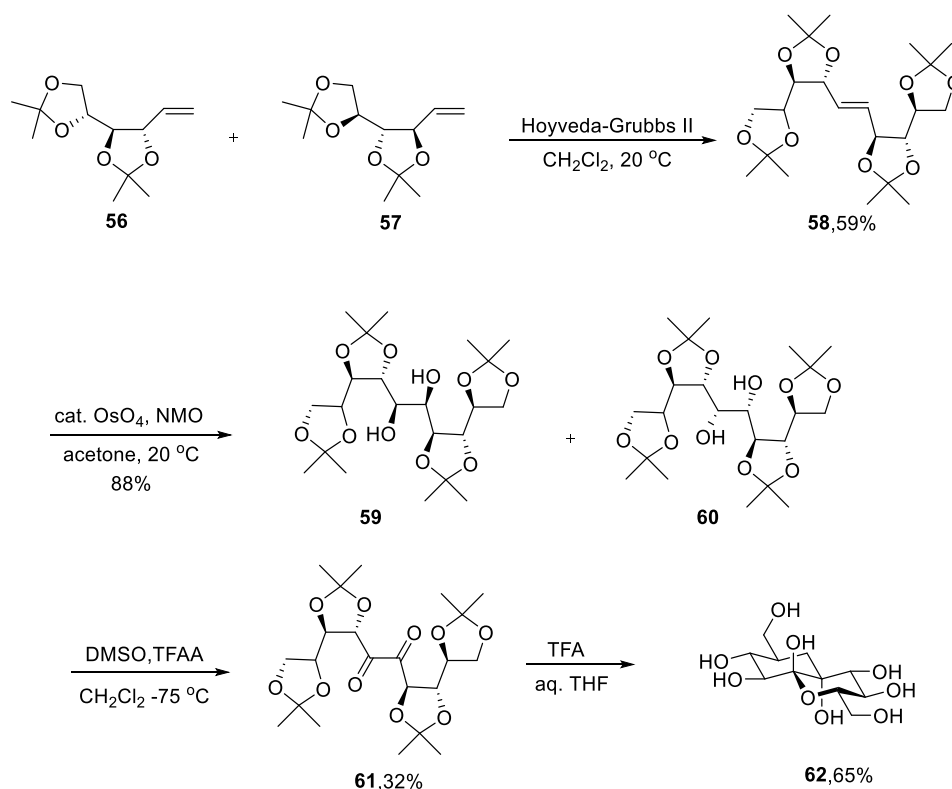
Figure 7. Different forms of bradyrhizose **20** in solution

Table 2. Comparison of ^1H and ^{13}C spectral data of bradyrhizose syntheses by the Yu⁴⁷ and the Lowary⁵⁰ laboratories and the Molinaro⁴⁷ material from degradation of a polymer

Data source	20a	20b	20c	20d	20e	Solvent	Chemical shift reference
Yu data ⁴⁸							
δ_{H}	4.50	5.10	4.93	4.93	5.14		internal acetone at δ_{H} 2.225, δ_{C} 31.45
multiplicity	d	d	d	d		D ₂ O	
$^3J_{\text{H1,H2}}$	(8.07 Hz)	(3.9 Hz)	(5.0 Hz)	(1.9 Hz)			
δ_{C}	96.5	92.2	100.0	93.2	93.6		
Lowary data ⁵⁰							
δ_{H}	4.62	5.23	5.07-5.05	5.07-5.05	5.27		external acetone at δ_{H} 2.225, δ_{C} 31.07
multiplicity	d	d	m	m	d	D ₂ O	
$^3J_{\text{H1,H2}}$	(8.1 Hz)	(4.0 Hz)			(5.3 Hz)		
δ_{C}	97.6	93.3					
Molinaro data ⁴⁷							
δ_{H}		4.97					internal acetone at δ_{H} 2.225, δ_{C} 31.45
multiplicity		d				D ₂ O	
$^3J_{\text{H1,H2}}$		(3.9 Hz)					
δ_{C}		96.6					

1.4 Synthesis of structurally related bradyrhizose motifs

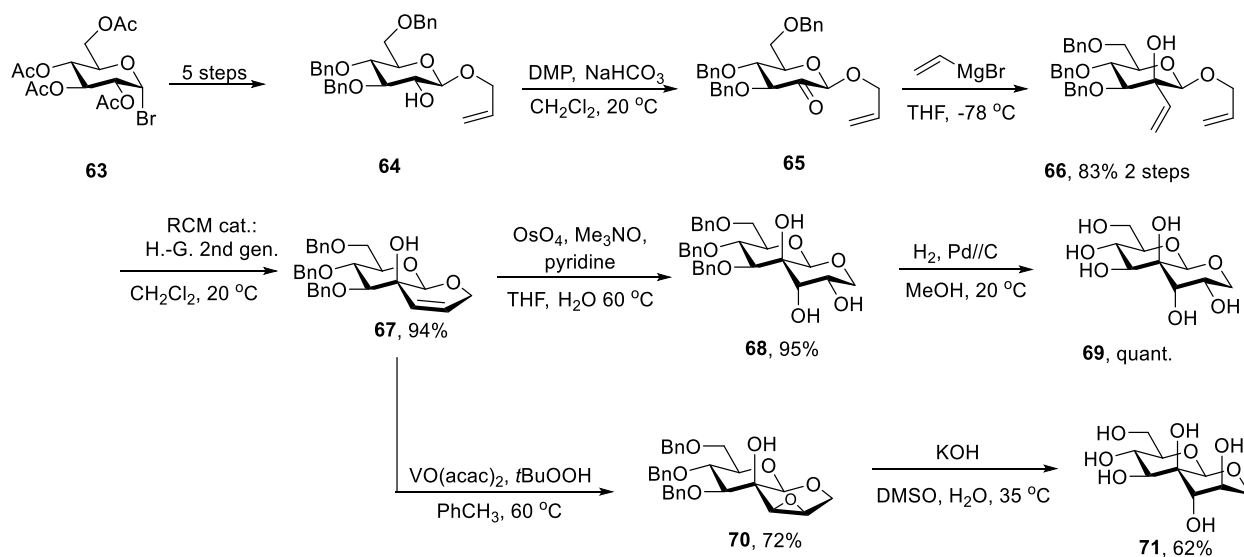
In addition to the total syntheses of bradyrhizose reported by the Yu and Lowary labs, the construction of bicyclic mimetics of bradyrhizose and of related compounds has also been reported. Thus, in 2014, Ziegler and co-workers described the synthesis of deca-5,6-diulose **62** from the hex-1-enitols **56** and **57**. Key steps in this synthesis involved the generation of the *trans*-dec-5-enitol **58** through a cross-coupling reaction of **56** with **57** in the presence of Hoyveda-Grubbs catalyst, dihydroxylation of dec-5-enitol **58** by treatment with osmium tetroxide and *N*-methylmorpholine *N*-oxide, oxidation and subsequent formation of the bicyclic framework via cyclization.⁵¹



Scheme 7. Synthesis of deca-5,6-diulose **62** by Ziegler and co-workers

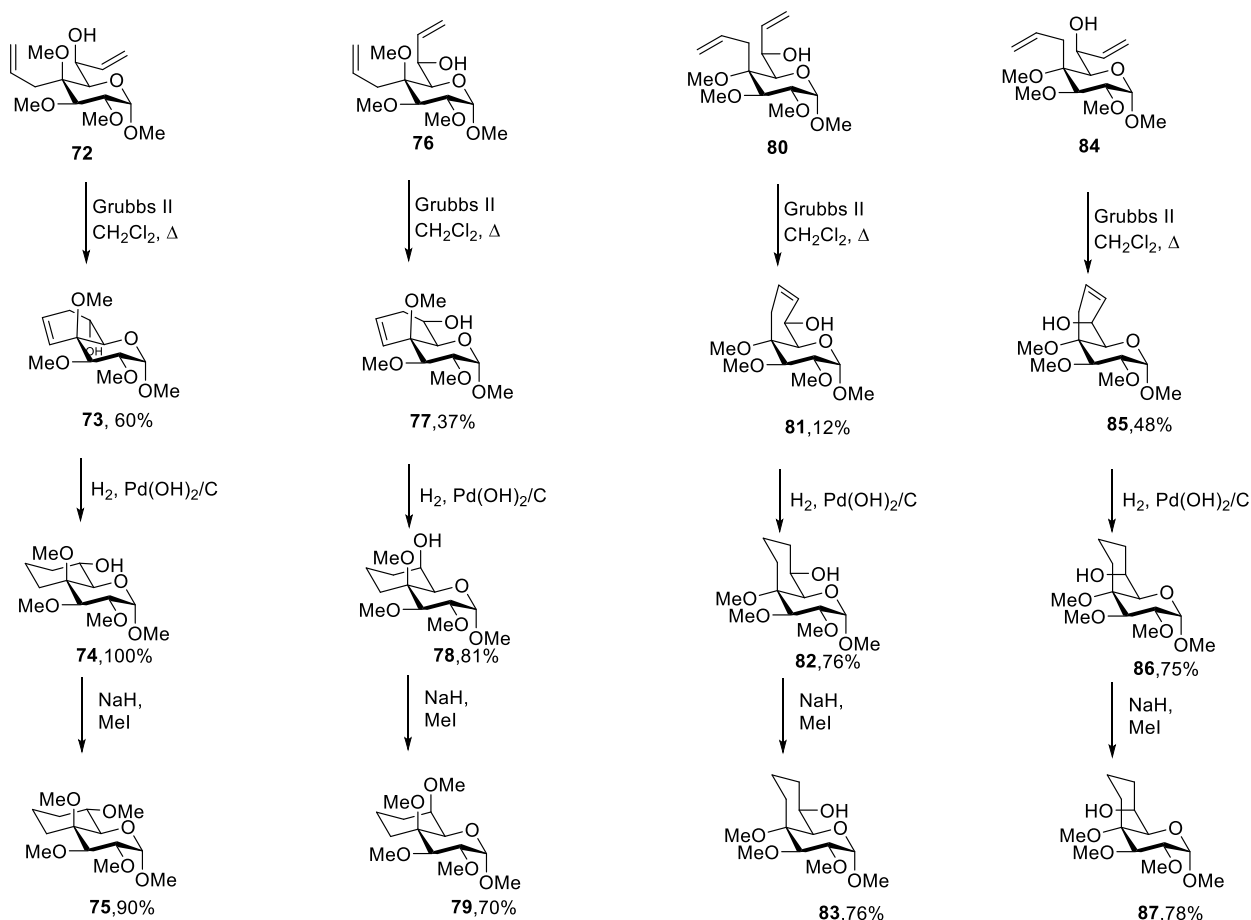
Subsequently, Ziegler and co-workers described the synthesis of 2,10-dioxadecalins **69** and **71** (**Scheme 8**) featuring a mannose ring *trans*-fused onto a pyranose moiety. In this work, the

synthesis of the bicyclic compound **69** bearing *syn*-configuration at the vicinal stereogenic centers was achieved via a reaction sequence that consisted of a manno-selective vinylation on the ketone **65**, construction of the 1,2-annulated alkene **67** through a ring-closing metathesis, and the diastereoselective dihydroxylation on alkene **67**, followed by hydrogenation that afforded the polyhydroxylated bicyclic compound **69**. Compound **71** bearing the *anti*-configuration at the vicinal stereogenic centers was achieved via a reaction sequence that consisted of the epoxidation on the 1,2-annulated alkene **67** followed by subsequent nucleophilic epoxide opening on **70**.⁵²



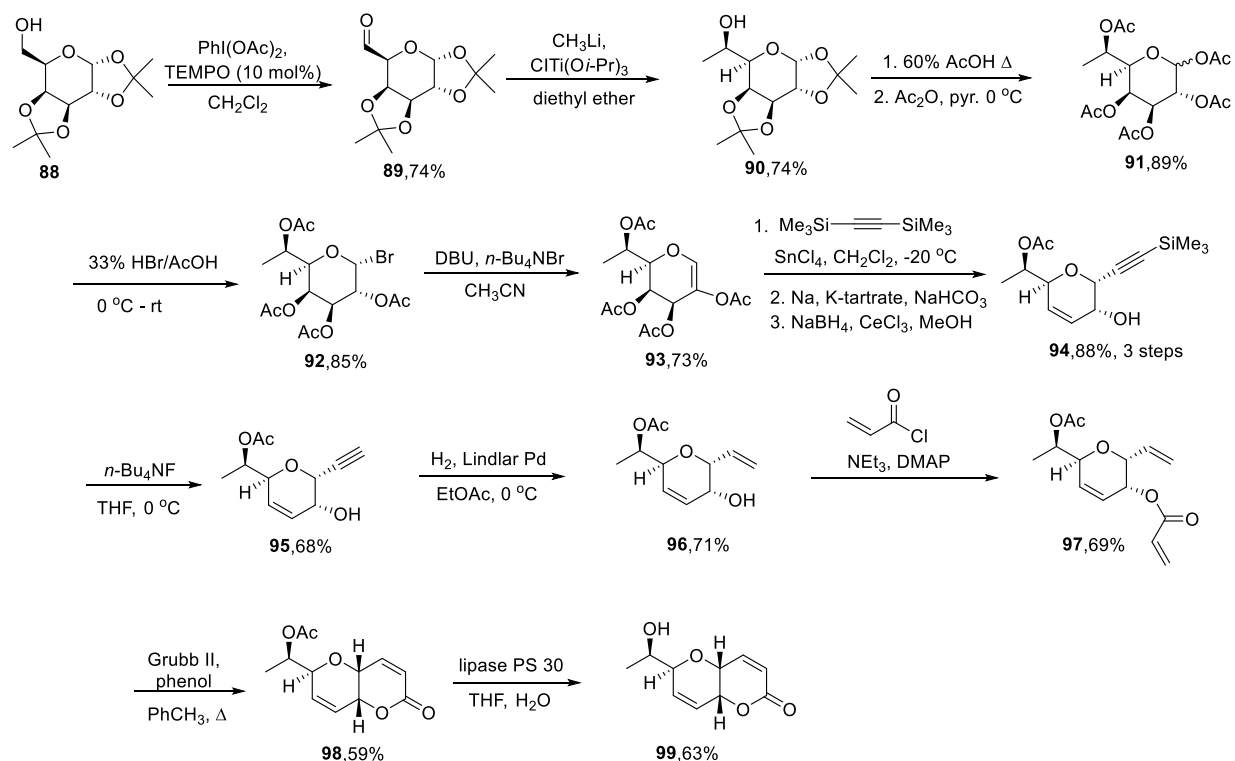
Scheme 8. Synthesis of 2,10-dioxadecalins **69** and **71** by Ziegler and co-workers

Crich and co-workers reported the synthesis of similar bicyclic scaffolds and demonstrated their application as models in an in-depth study of the $^3J_{H5,H6}$ coupling constants for the prediction of the side chain conformation of hexopyranoses. Their work relied on the synthesis and use of the diastereomeric mixtures of **72**, **76**, **80** and **84**, by a series of Grignard reactions. The bicyclic derivatives **75**, **79**, **83** and **87** were obtained in good yields through a general reaction sequence of ring closing metathesis, hydrogenation, and finally methylation (**Scheme 9**).⁵³



Scheme 9. Synthesis of structurally related compounds by Crich and co-workers

Similarly, the importance of these complex bicyclic motifs is evident from the recent work by Giuliano and co-workers resulting in an asymmetric carbohydrate-based synthesis of diplopyrone analogue **99**. This molecule displayed good antibacterial activity against common bacterial pathogens such as *Edwardsiella ictaluri* and *Flavobacterium columnare* that cause enteric septicemia and columnaris disease, respectively. Key steps in this work involved the pyranose side chain elongation via a *C*-alkynylation-rearrangement of the glycal **93** with bis(trimethylsilyl)-acetylene, the Lindlar reduction on **95**, and the construction of the pyranopyran **98** via ring closing metathesis (Scheme 10).⁵⁴



1.5 Occurrence and role of ulosonic acids in Gram-negative bacteria

2-ulosonic acids are a diverse family of monosaccharides that play important roles as components of natural glycoconjugates. Neuraminic acid **100** is found in bacterial glycoconjugates where it occupies the non-reducing end of oligosaccharide chains. Other 2-ulosonic acids structurally related to NeuAc include 3-deoxy-D-*glycero*-D-galacto-2-nonulosonic acid (KDN) **101**, commonly identified as a constituent of polysialoglycoproteins in mammalian tissues, and 3-deoxy-D-manno-oct-2-ulosonic acid **102** (Figure 8).⁵⁵

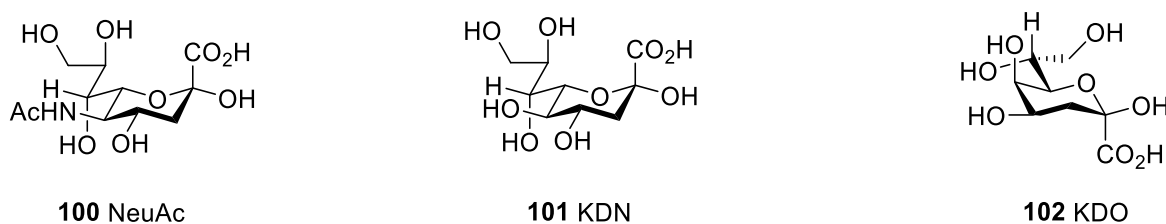


Figure 8. Examples of 2-ulosonic acids commonly found as constituents of glycoconjugates

3-Deoxy-D-manno-oct-2-ulosonic acid **102** is an 8-carbon sugar consisting of an α -keto carboxylic acid and four consecutive hydroxylated carbon atoms of D-manno configuration linked together through one methylene unit (**Figure 9**).⁵⁶ This sugar is found in the lipopolysaccharides of a wide variety of Gram-negative bacteria and is a component of bacterial capsular polysaccharides as well.⁵⁷

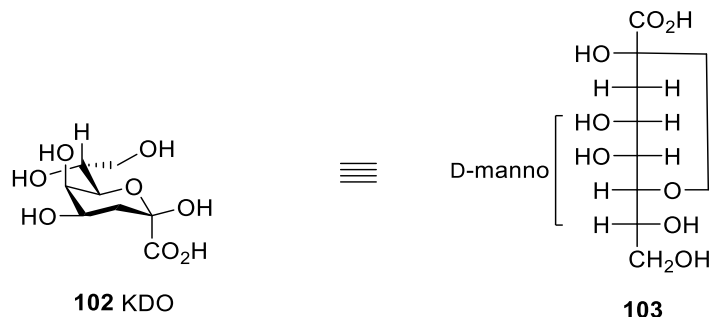


Figure 9. The Structure of KDO and its Fischer configuration

Other oct-2-ulosonic acids structurally related to KDO that are found in Gram-negative bacteria are shown in (**Figure 10**).⁵⁸

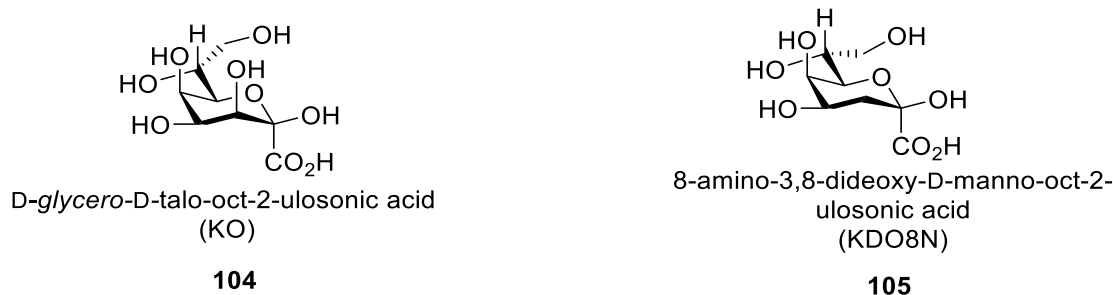
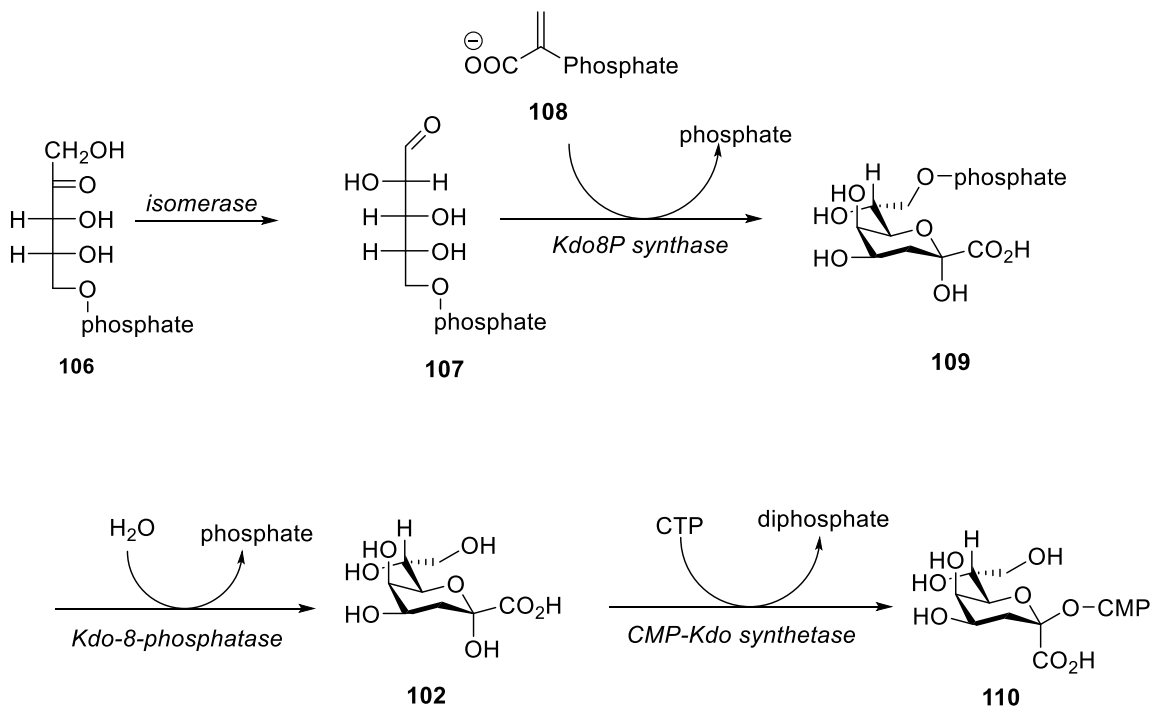


Figure 10. Structures of KO and KDO8N

1.5.1 Biosynthesis of KDO in Gram-negative bacteria

Biosynthesis of KDO begins from D-ribulose 5-phosphate **106**, which is converted into D-arabinose 5-phosphate **107** with the aid of D-arabinose-5-phosphate isomerase. Condensation of D-arabinose 5-phosphate with phosphoenol-pyruvate **108** is catalyzed by KDO 8-phosphate synthase and affords KDO 8-phosphate **109**. Then, KDO 8-phosphate phosphatase hydrolyzes

KDO 8-phosphate to KDO **102** and releases an inorganic phosphate. Finally, the formation of the activated sugar nucleotide derivative KDO cytidine monophosphate (CMP) **110** from KDO and cytidine triphosphate is catalyzed by CMP-KDO synthetase. CMP-KDO is the substrate of monofunctional or bifunctional glycosyltransferases, which sequentially add one or two KDO residues to lipid A to initiate the core biosynthesis.^{59,60}



Scheme 11. The biosynthesis of KDO

1.5.2 Occurrence of KDO in bacterial lipopolysaccharides

Lipopolysaccharides are major surface components of Gram-negative bacteria and in the LPS that have been studied, α -linked KDO residues located at the reducing ends of the polysaccharide domain, provide a bridge between lipid A and the core oligosaccharide.⁶⁰ Most Gram-negative bacterial lipopolysaccharides share an α -(2 \rightarrow 4) linked KDO-KDO disaccharide unit as a common inner core structure (**Figure 11**). This core disaccharide can be further linked to KDO or other pyranose moieties mostly with α -glycosidic linkages. For example, the investigation

of the *E. coli* K12 W3100 LPS **111** by Raina and co-workers revealed that a substitution of the C5 of the KDO-KDO disaccharide with an α -D-heptose or α -L-rhamnose residue forms the inner core tetrasaccharide of Rha- α -L-(1 \rightarrow 5)-KDO- α -D-(2 \rightarrow 4)-KDO- α -D-(2 \rightarrow 4)-KDO- α -D-(1 \rightarrow 5)-Hep.⁶¹ The structural elucidation of the lipopolysaccharides from *Legionella pneumophila* **112** by Helbig and co-workers revealed that the oligosaccharide is constituted of GalNAc- α -D-(1 \rightarrow 4)-Man- α -D-(1 \rightarrow 5)-KDO- α -D-(2 \rightarrow 4)-KDO glycosidic linkages.⁶² Additionally, 4-amino-4-deoxy- β -L-arabinose (Ara4N) residues have been detected glycosidically-linked to the LPS core sugar 3-deoxy-D-manno-oct-2-ulonic acid. In particular, Ara4N has been found in a α -(1 \rightarrow 8) linkage to KDO in the LPS of *Burkholderia pyrrocinia* BTS7 **113**.⁶³

As facultative pathogens, *Providencia alcalifaciens* are considered to cause infections such as urinary tract infections and wound infections. Structural studies of the *Providencia alcalifaciens* O36 lipopolysaccharide **114** by Rozalski and co-workers⁶⁴ showed that the O-polysaccharide unit consists of a linear tetrasaccharide repeating unit containing 2-acetamido-2-deoxygalactose, 6-deoxy-L-talose, and 3-deoxy-D-manno-oct-2-ulonic acid with a Tal- α -L-(1 \rightarrow 4)-GalNAc- β -D-(1 \rightarrow 7)-KDO- α -D-(2 \rightarrow 3)-Tal glycosidic linkage pattern. Additionally, *Neisseria meningitidis* serotype B, that is perceived to cause life-threatening illness in individuals who lack the necessary protective antibodies, has been shown to contain a repeating pentasaccharide unit composed of D-heptose, 2-acetamido-2-deoxy-D-galactose and 3-deoxy-manno-oct-2-ulonic acid residues with GalNAc- α -D-(1 \rightarrow 2)-Hep- α -D-(1 \rightarrow 3)-Hep- α -D-(1 \rightarrow 5)-KDO- α -D-(2 \rightarrow 4)-KDO glycosidic linkages **115**.⁶⁵ A bacterial lipopolysaccharide of *Acinetobacter baumannii* NCTC 10303 has also been shown to be composed mainly of tetrasaccharide repeating oligosaccharide units of KDO- α -D-(2 \rightarrow 5)-KDO- α -D-(2 \rightarrow 5)-KDO- α -D-(2 \rightarrow 4) **116** with substitution at the C8 and C4 positions with L-rhamnose and D-glucose respectively.⁶⁶

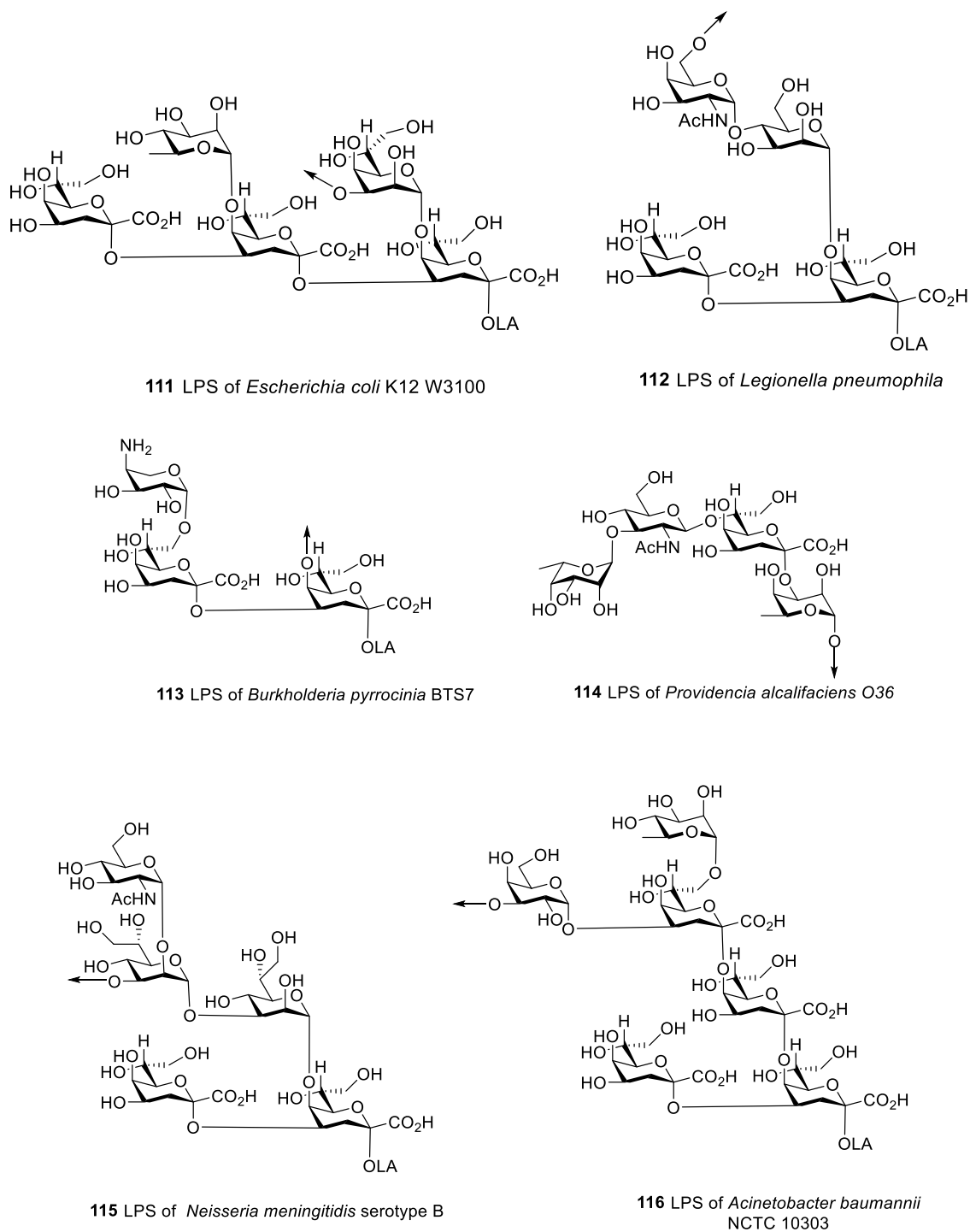


Figure 11. Structures of KDO containing oligosaccharides present in the LPS of various Gram-negative bacteria

1.5.3 Occurrence of KDO in bacterial capsular polysaccharides

Polysaccharide capsules are often involved in virulence and possess functions that range from masking of bacterial surface antigens and protection against serum killing, to prevention of phagocytosis. A bacterial capsular polysaccharide is composed mainly of repeating oligosaccharide units that frequently contain the KDO residue that is equatorially linked to another pyranose moiety at the KDO C2 position (**Figure 12**).⁶⁷

The structural elucidation of the capsule of *Cronobacter dublinensis* HPB 3169⁶⁸ by Perry group indicated that the the repeating unit of the capsule is made up of 2-acetamido-2-deoxyglucose, L-rhamnose, and 3-deoxy-D-manno-oct-2-ulosonic acid that forms a polymer of Rha- α -L-(1 \rightarrow 5)-KDO- β -D-(2 \rightarrow 3)-Rha- β -D-(1 \rightarrow 4)-GlcNAc **117**. Similarly, a Rha- α -L-(1 \rightarrow 5)-KDO- β -D-(2 \rightarrow 3)-Rha- α -L-(1 \rightarrow 2)-Rha polymeric unit has been isolated from *E. coli* K12 antigen capsule by Jann and co-workers.⁶⁹ Such findings have been supported by the recent work by Whitfield and co-workers who demonstrated that KpsS and KpsC in *E. coli* and *N. meningitidis* are β -KDO transferases that insert poly- β -KDO linkers onto a phosphatidyl-glycerol lipid moiety in such bacteria.⁷⁰

The structural analysis of *K. kingae* type b, *K. kingae* strain **269-492** and type c capsules by St. Geme and co-workers⁷¹ revealed that type b and the *K. kingae* strain 269-492 capsules are a polymer of GalNAc- α -D-(1 \rightarrow 5)-KDO- β -D-(2 \rightarrow 3)-GalNAc **120** while the type c capsule is a polymer of Rib- β -D-(1 \rightarrow 2)-Rib- β -D-(1 \rightarrow 2)-Rib- β -D-(1 \rightarrow 4)-KDO- β -D-(2 \rightarrow 3)-Rib **119**, respectively. Heulin and co-workers have described the structure of the capsule expressed by *Burkholderia caribensis* strain MWAP7172 as a polymer composed of D-glucose, 6-deoxy-L-talose and 3-deoxy-D-manno-oct-2-ulosonic acid with a structure comprised of KDO- β -D-(2 \rightarrow 3)-Tal- β -L-(1 \rightarrow 3)-Glc **122**. Moreover, similar KDO- β -D-(2 \rightarrow 3)-Tal glycosidic connections have

also been observed in *Pseudoalteromonas flavipulchra* NCIMB 2033.⁷³ KDO- β -D-(2 \rightarrow 6)-GalNAc glycosidic linkages **123** have also been identified in the capsular polysaccharide of *K. kingae* strain PYKK181 as well as in the CPS of *Moraxella nonliquefaciens* **123**.⁷⁴

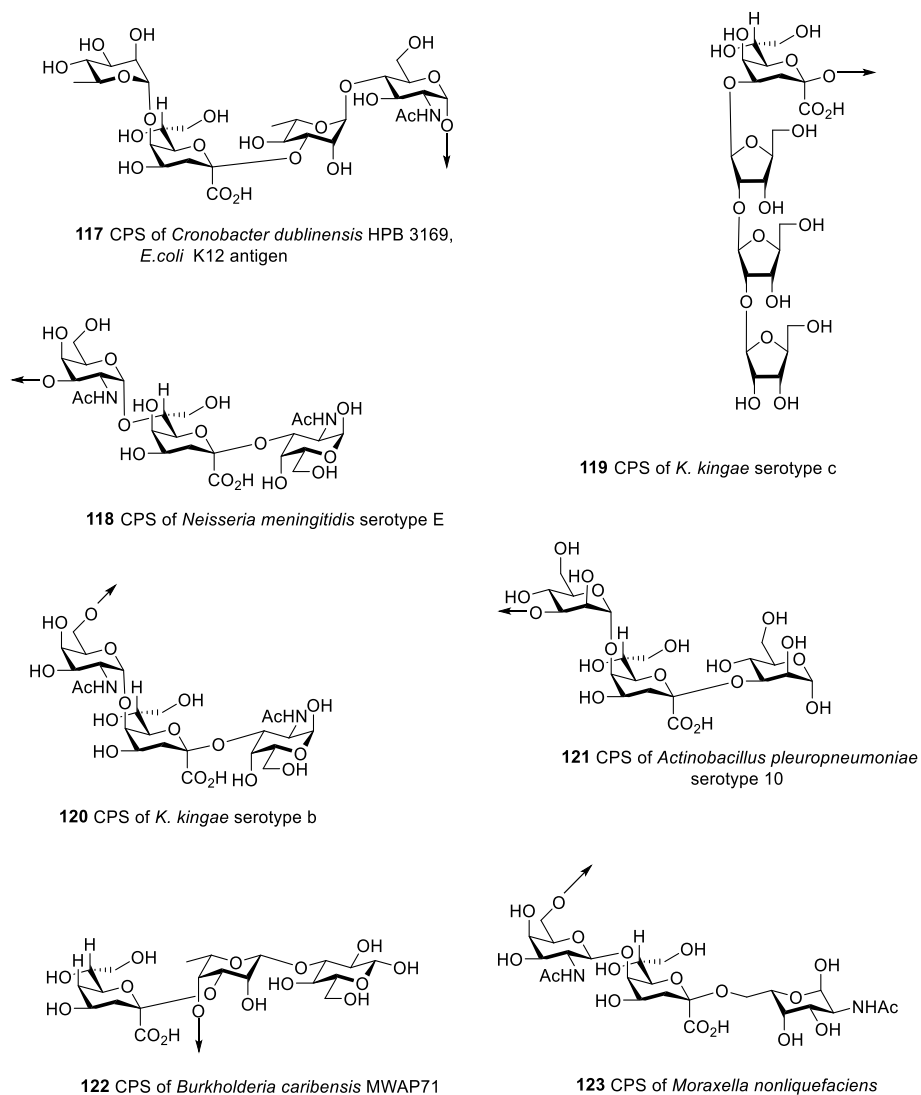


Figure 12. Structures of KDO containing oligosaccharides present in the CPS of various Gram-negative bacteria.

1.5.4 Development of KDO containing glycoconjugate vaccines as potential therapeutics for treatment of pathogenic infections

The incorporation of KDO is a vital step in both the LPS and CPS biosynthesis, and indeed, in growth of the Gram-negative bacteria. Therefore, the immunochemistry, biochemistry, and synthetic carbohydrate chemistry involving KDO has become of increasing interest in scientific research. Noteworthy, the use of defined synthetic and pure oligosaccharides is of necessity in order to provide a rational basis for future vaccine development. As such, several stereo-controlled glycosylation methodologies have been used in the synthesis of larger oligosaccharide containing KDO fragments equipped with reactive spacer group.⁷⁵ For example, Davis and co-workers have described the synthesis of a carbohydrate-based glycoconjugate vaccine bearing diphtheria toxin (DT-Lys51Glu/Glu148Lys) mutant or BSA (Figure 13). Immunochemical studies involving the (Hep₂Kdo₂)₄-DT or (Hep₂Kdo₂)₄-BSA conjugates revealed that they induced specific serum antibodies in rabbit.⁷⁶ Such immunochemical and structural studies on KDO specific antibodies clearly support the immune-relevance of KDO residues in the discovery of carbohydrate-based vaccines.

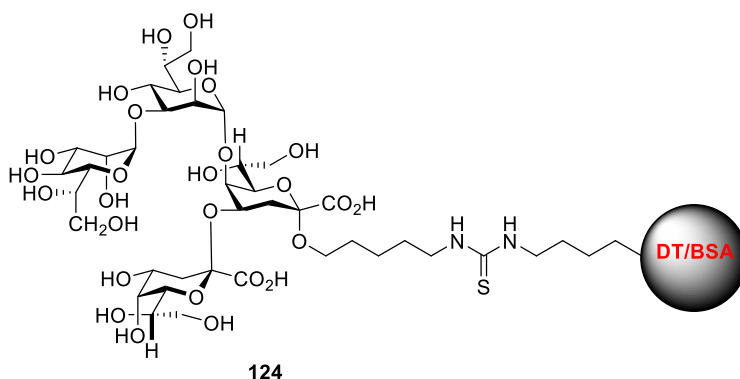


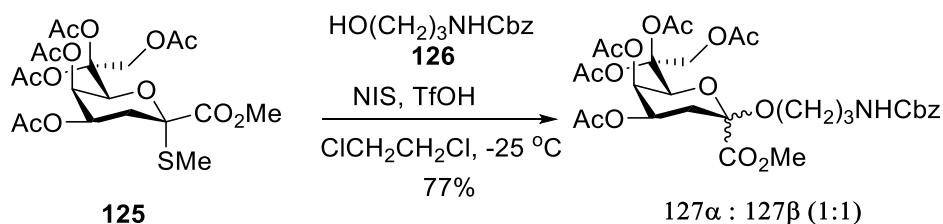
Figure 13. Carbohydrate-based glycoconjugate vaccine bearing diphtheria toxin mutant or BSA

1.6 Challenges and opportunities in KDO glycoside chemistry

The enzymatic or chemical synthesis of KDO-containing portions of capsular polysaccharides has continued to draw much attention amongst scientists due to their relevance in pharmaceutical research. However, the stereoselective synthesis of KDO glycosides has been met with various challenges that stem from the lack of a hydroxyl group at the C-3 position, which excludes the use of the neighboring group participation effect. Secondly, the presence of an electron-withdrawing carboxylic group at C-1 deactivates and hinders the anomeric position and in some cases results in formation of the undesirable glycal esters.⁷⁷

1.6.1 Stereoselective synthesis of axial and equatorial KDO glycosides

Much progress has been made in the development of efficient and stereoselective glycosylation methodologies for synthesizing KDO glycosides with the axial configuration.⁷⁸⁻⁸¹ In contrast, the synthesis of KDO glycosides having the thermodynamically less stable equatorial configuration has been less explored. In this respect, it is worth mentioning the work by Boons and co-workers who described the synthesis of β -KDO glycosides **127** mediated by NIS/TfOH in a 1,2-dichloroethane solvent system using peracetylated KDO thioglycoside donor **125** with spacer **126** (Scheme 12).⁸² However, such conditions are not stereoselective as α -KDO glycosides were obtained in equal quantities.

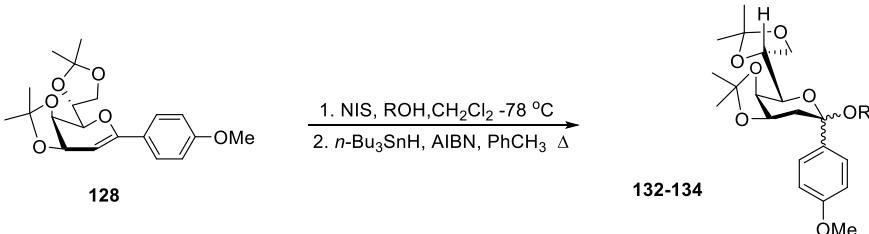
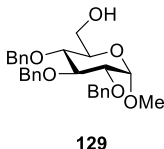
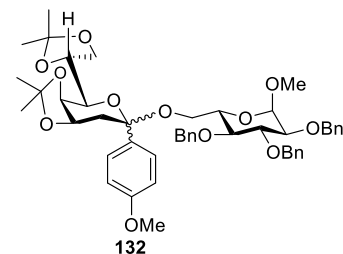
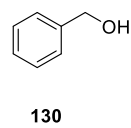
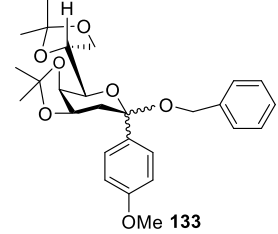
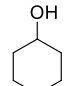
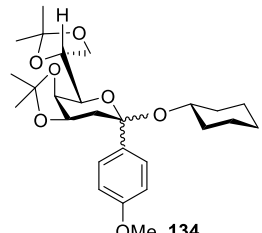


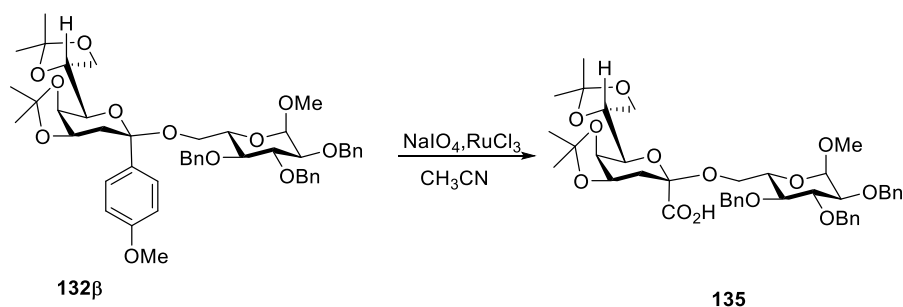
Scheme 12. Synthesis of β -KDO glycosides using peracetylated KDO thioglycoside donor

Ling and co-workers have demonstrated that they could furnish β -glycosides **132-134** in great selectivity and better yields using KDO 1-*C*-aryl glycal donor under NIS-mediated

glycosylations (**Table 3**).⁸³ Isolation of the major β -isomer followed by oxidation in the presence of a $\text{RuCl}_3/\text{NaIO}_4$ reagent, gave the corresponding KDO glycoside **139** (**Scheme 13**). The access of β -KDO glycosides relied on radical deiodination using toxic tin reagents which are often difficult to isolate from products, as well as use of strong oxidizing agents such as RuCl_3 to cleave the arene to the carboxylate functional group.

Table 3. Synthesis of β -KDO glycosides using peracetylated KDO 1-*C*-aryl glycol donor

					
Entry	Donor	Acceptor	Glycoside	Yield (%)	Product (α/β)
1	128	 129	 132	76	1:8
2	128	 130	 133	82	1:15
3	128	 131	 134	78	1:8

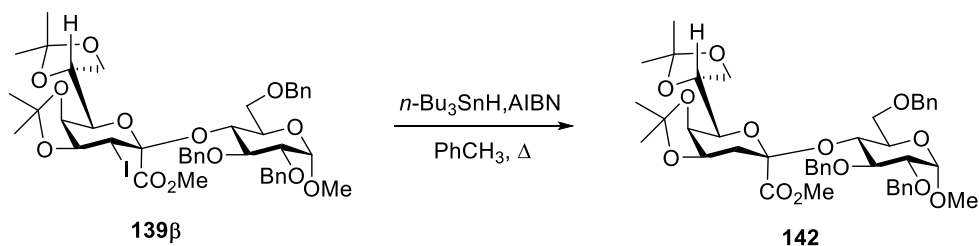


Scheme 13. Oxidation of **132** to the corresponding KDO derivative **135**

Similarly, Mong and co-workers reported a β -selective glycosylation method for the synthesis of β -KDO glycosides using a KDO donor having a pre-installed carboxylate at C1 (**Table 4**). The coupling reactions were mediated by NIS/TMSOTf in a 1:2 $\text{CH}_2\text{Cl}_2/\text{CH}_3\text{CN}$ solvent system and resulted in the formation of α - and β -KDO glycosides with ratios of up to 1:20. Subsequent radical deiodination on the β -anomer in the presence of tributyltin hydride and azo-bis(isobutyro)nitrile furnished the deoxy derivative **142** (**Scheme 14**).⁸⁴

Table 4. Synthesis of β -KDO glycosides using peracetylated KDO glycal donor

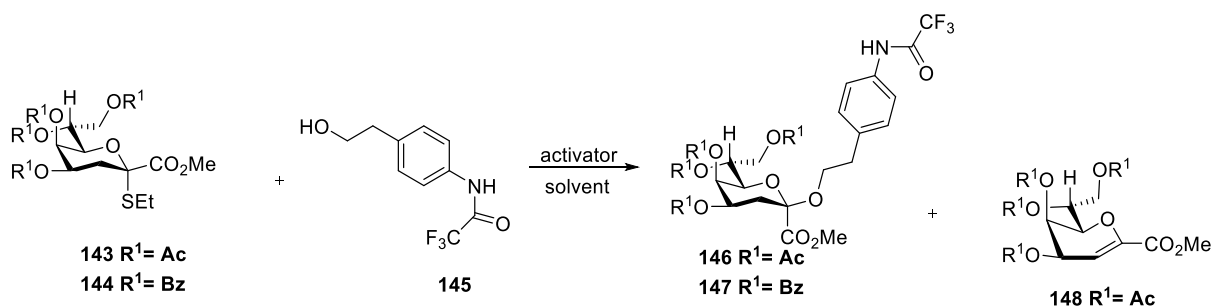
Entry	Donor	Acceptor	Glycoside	Yield (%)	Product (α/β)
1	136	 129	 139	70	1:5
2	136	 137	 140	65	1:20
3	136	 138	 141	72	1:14



Scheme 14. Deiodination of **139** to the corresponding KDO derivative **142**

Synthesis of β -KDO glycosides with nonglycal donors has also been reported by Oscarson and co-workers who described the synthesis of β -KDO glycosides using various KDO thioglycoside donors under different promoter systems (**Table 5**). Their findings revealed that formation of β -KDO glycosides bearing the 2-(4-(trifluoroacetamidophenyl)ethyl) as a spacer were best achieved when peracetylated KDO thioglycosides were activated at low temperatures using IBr/AgOTf as a promoter in a $\text{CH}_2\text{Cl}_2/\text{CH}_3\text{CN}$ solvent system. However, NIS/AgOTf-mediated glycosylations only led to the formation of α -KDO glycosides with the isolation of the glycal ester in large quantities.⁸⁵

Table 5. Synthesis of β -KDO glycosides using peracetylated and perbenzoylated KDO thioglycoside donors

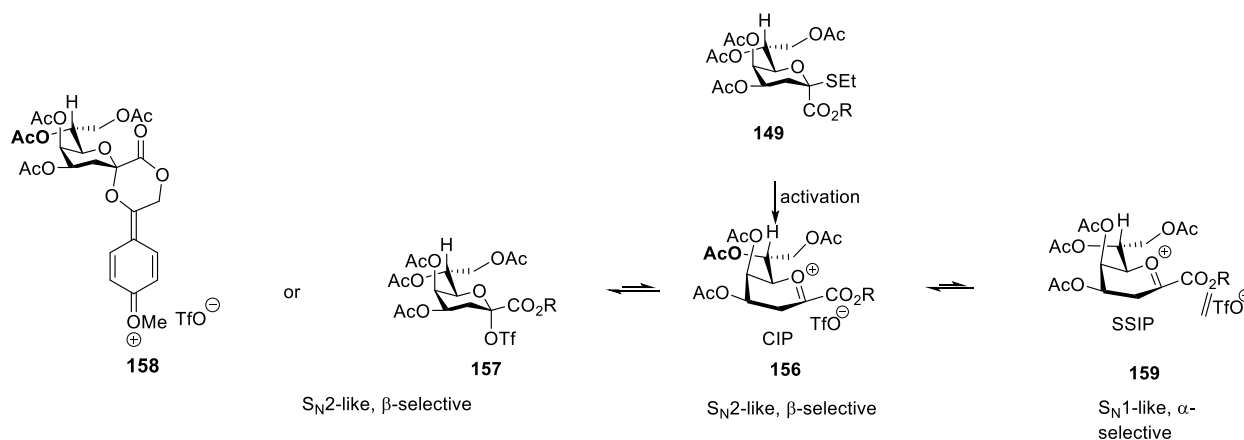


Entry	Donor	Promoter	Temp. (°C)	Solvent	Yield (%)	Product (α/β)	Elimination (%)
1	143	DMTST	-15	CH_2Cl_2	81	146 (1:3)	
2	143	NIS/AgOTf	-30	CH_2Cl_2	54	146 (1:0)	148 (46)
3	144	IBr/AgOTf	-70	3:2 $\text{CH}_3\text{CN}/\text{CH}_2\text{Cl}_2$	81	147 (0:1)	

Recently, Gauthier and co-workers developed a novel class of peracetylated KDO thioglycoside donor bearing the participating 4'-methoxyphenacyl ester at C1, which upon activation with NIS/AgOTf, in CH₃CN at -10 °C led to the stereoselective formation of β -KDO glycosides with ratios of up to 1:11 (**Table 6**).⁸⁶ The observed β -selectivity was rationalized as rising from the long range participating effect of 4'-methoxyphenacyl ester auxiliary group which forms a covalent six-membered α -spiro intermediate **158** that would then be preferentially attacked by the acceptor from the β -face, furnishing the desired glycoside (**Scheme 15**).

Table 6. Synthesis of β -KDO glycosides using peracetylated KDO thioglycoside donor appended with 4'-methoxyphenacyl ester

Entry	Donor	Acceptor	Glycoside	Yield (%)	Product (α/β)
1	149			61	1:5
2	149			58	1:4.3
3	149			80	1:11



Scheme 15. Mechanistic hypothesized role of 4'-methoxyphenacyl ester in favoring formation of β -KDO glycosides

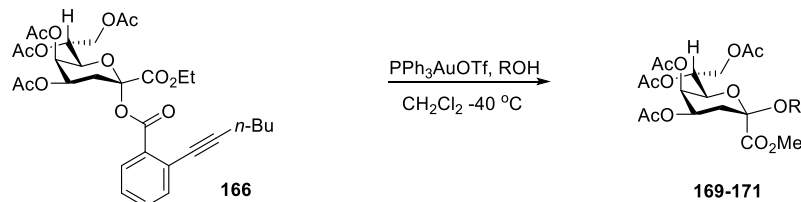
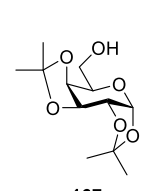
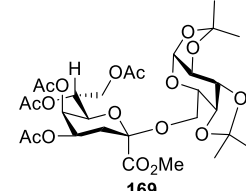
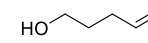
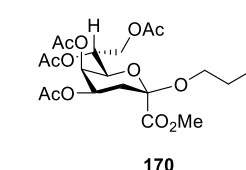
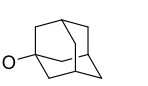
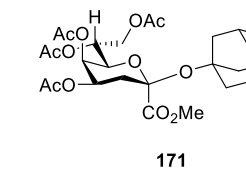
The enhancement of β -selectivity via the hydrogen bond directing effect has also been described by the Yang group. In this work, Yang and co-workers discovered that KDO thioglycosides equipped with a 2-quinolinecarboxyl group at C5-position could undergo β -glycosylation with primary alcohols, mediated by NIS/TfOH (**Table 7**). Despite the fact that β -selectivity was realized in good yields with reactive primary alcohols, a complete reversal in selectivity was observed when secondary and tertiary acceptors were employed under the activation of NIS/TfOH system or IBr/AgOTf system.⁸⁷ Moreover, a considerable amount of eliminated product was isolated in the latter case.

Table 7. Synthesis of β -KDO glycosides using KDO thioglycoside donor appended with 2-quinolinecarboxyl group

Entry	Donor	Acceptor	Conditions	Glycoside	Yield (%)	Product (α/β)
1	160	 161	NIS, TfOH, ROH CH ₂ Cl ₂ -78 °C	 163	82	β -only
2	160	 162	NIS, TfOH, ROH CH ₂ Cl ₂ -78 °C	 164	12	α -only
3	160	 151	IBr/AgOTf CH ₂ Cl ₂ , -78 °C	 165	78	α -only

More recently, Yang and co-workers reported a β -glycosylation of *o*-hexynylbenzoate KDO donor under the activation by gold(I)-catalyst that furnished β -KDO glycosides in good yields (Table 8).⁸⁸ However, this approach employs an expensive catalyst.

Table 8. Synthesis of β -KDO glycosides using *o*-hexynylbenzoate KDO donor

					
Entry	Donor	Acceptor	Glycoside	Yield (%)	Product (α/β)
1	166			64	β -only
2	166			73	β -only
3	166			69	β -only

1.7 Role of side chain conformation in stereo-controlled glycosylation reactions

The stereoselective formation of glycosidic bonds in glycosylation reactions is not straightforward, as such, a considerable effort has been made to better understand factors that play key roles in such reactions. In a recent review, Crich and co-workers discussed in a broader scope the influence factors such as the leaving group and protecting group, solvent, promoter, temperature and additives have on glycosylation reaction outcome.⁸⁹ Similarly, the pyranosyl side chain configuration and conformation have been shown to be important contributing factors in influencing the reactivity and selectivity of glycosyl donors.

The importance of side chain configuration and conformation stems from earlier experimental findings, which have shown that in solution, the side chain of the hexopyranoses **172**

and **173** exist in an equilibrium mixture of three staggered conformations: *gauche,gauche* (*gg*), *gauche,trans* (*tg*), and *trans,gauche* (*gt*) conformers. The description of these is based on the relationship of the C6-O6 bond to the C5-C4 and C5-O5 bonds (**Figure 14**).⁹⁰ Additionally, it has also been revealed that the three staggered conformations for the glucose series **172a-c** are populated in an approximate ratio of 6:4:0, *gg:gt:tg*, while in the galactose series **173a-c** an approximate population ratio of 2:6:2, *gg:gt:tg* has been reported. Of note is that these values vary slightly in different solvent systems.

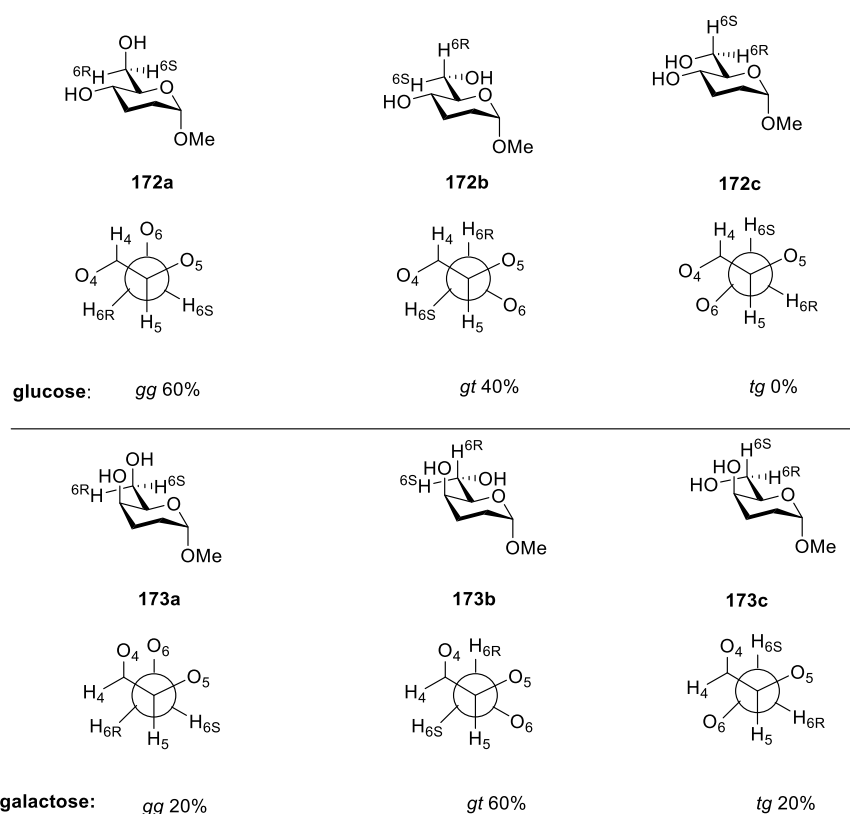


Figure 14. The three staggered conformations of hexopyranoses **172** and **173** in solution

In a study of the coupling reactions of mannosyl sulfoxide donors with primary and secondary alcohols, Crich and co-workers found that working with 4,6-*O*-benzylidene-protected mannosyl sulfoxides in dichloromethane at $-78\text{ }^{\circ}\text{C}$ with pre-activation with triflic anhydride prior to addition of an acceptor gave excellent β -selectivities compared to the 4,6-di-*O*-benzyl mannosyl

sulfoxide donors (**Table 9**).⁹¹ Consistent with the previous observations made by Fraser-Reid on the disarming effect of a 4,6-*O*-benzylidene group,⁹² the Crich group reasoned that the conformational deformation imposed on the pyranose ring by the 4,6-*O*-benzylidene group, favored the formation of the covalently bonded axial triflate intermediate which was displaced by an acceptor from the β -face leading to formation of β -mannosides.

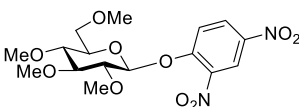
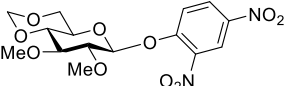
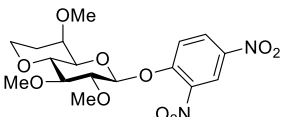
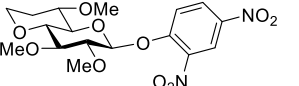
Table 9. Synthesis of β -mannosyl glycosides using mannosyl sulfoxide donors

<div style="text-align: center;"> <p> 174 $R^1, R^1 = \text{PhH}$ 175 $R^1 = R^1 = \text{Bn}$ </p> <p> 180-181 $R^1, R^1 = \text{PhH}$ 182 $R^1 = R^1 = \text{Bn}$ </p> </div>					
Entry	Donor	Acceptor (R^2)	Glycoside	Yield (%)	Product (α/β)
1	174			95	1:25
2	174			96	1:1.5
3	175			-	1:2

Further information on the influence of C–O bonds on the anomeric reactivity of glycosyl donors was highlighted in the work of Bols and co-workers. Thus, it was demonstrated that the acid-catalyzed hydrolysis of methyl or dinitrophenyl glucopyranosides occurred faster with torsionally free monocyclic derivative **184** than with torsionally restricted **186**, **187** and the 4,6-*O*-methylidene derivative **185** (**Table 10**). Noteworthy, the locked *gg* conformer **186** and the *gt* conformer **187** both lacking the O6 were 0.3 and 0.4 times more reactive than the *tg* conformer

185 respectively. Bols group concluded that the less reactivity nature of compound **185** was influenced by torsional disarming effect as well as the imposition of the *tg* conformation on the glucopyranosyl side chain by 4,6-*O*-acetal. Thus, the resulting conformational change maximized the electron-withdrawing effect of the C6–O6 bond thereby destabilizing the formation of the solvent separated ion pair (SSIP) intermediate.⁹³

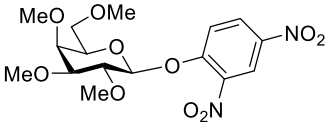
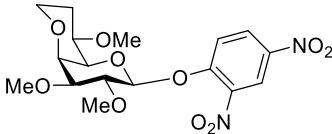
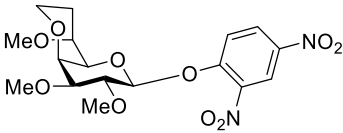
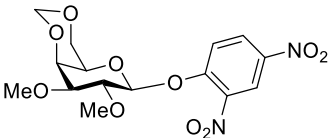
Table 10. Relative hydrolysis rates of glucopyranosides as examined by Bols and co-workers

Compound	Structure	Relative hydrolysis rate	O5-C5-O6-C6
184		1	-
185		0.07	<i>tg</i>
186		0.24	<i>gg</i>
187		0.16	<i>gt</i>

In yet a further study on the influence of C–O bonds on the anomeric reactivity of glycosyl donors, Crich and co-workers conducted experiments to determine the relative rates of hydrolysis of methyl or dinitrophenyl galactopyranosides under acidic conditions (**Table 11**).⁹⁴ These studies revealed that the bicyclic dinitrophenyl galactopyranosides were less reactive in comparison to the monocyclic derivatives and that compound with the 4,6-*O*-alkylidene group **191** was the least reactive. Thus, it was concluded that the imposition of a *tg* conformation on the galactocopyranosyl

side chain by 4,6-*O*-acetal retarded the formation of the solvent separated ion pair (SSIP). These observations were consistent with Bols observations in the glucose series.

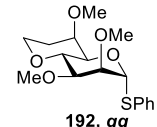
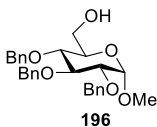
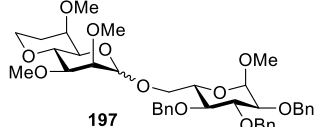
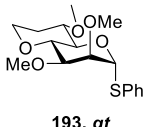
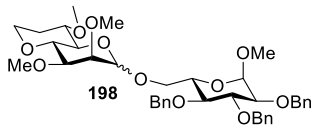
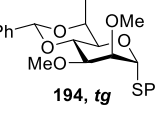
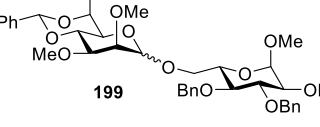
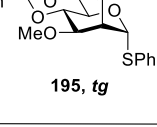
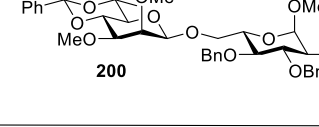
Table 11. Relative hydrolysis rates of galactopyranosides as examined by Crich and co-workers

Compound	Structure	Relative hydrolysis rate	O5-C5-O6-C6
188		1	
190R		0.23	<i>gt</i>
190S		0.17	<i>tg</i>
191		0.43	<i>gg</i>

In 2016, Crich and co-workers prepared a series of bicyclic mannopyranosyl donors **192**, **193**, **194**, **195** with the C6–O6 bond locked in either the *gg*, *gt*, or *tg* conformations respectively, and investigated how the side chain conformation influenced selectivity trend in glycosylation reactions. Such studies revealed that the mannopyranosyl donor **195** with a *tg* conformation was the most β -selective while mannopyranosyl donor **192** with a *gg* conformation was the least β -selective (**Table 12**). It was reasoned that in a *tg* conformation the electron-withdrawing effect of the C6–O6 bond is maximized thereby stabilizing the

covalently bonded axial triflate intermediate. Therefore, the acceptor would preferentially approach from the β -face resulting to the formation of β -glycosides.⁹⁵

Table 12. The selectivity trends of bicyclic thiomannoside donors as reported by Crich and co-workers

Entry	Compound	Acceptor	Conditions	Glycoside	Yield (%)	Product (α/β)
1	 192, <i>gg</i>	 196	TTBP,BSP Tf ₂ O, CH ₂ Cl ₂ -78 °C	 197	84	1:4.4
2	 193, <i>gt</i>	196	TTBP,BSP Tf ₂ O, CH ₂ Cl ₂ -78 °C	 198	85	1:8.4
3	 194, <i>tg</i>	196	TTBP,BSP Tf ₂ O, CH ₂ Cl ₂ -78 °C	 199	83	1:7.2
4	 195, <i>tg</i>	196	TTBP,BSP Tf ₂ O, CH ₂ Cl ₂ -78 °C	 200	79	β -only

1.7.1 Influence of side chain conformation in stereoselective synthesis of sialosides

Crich and co-workers have successfully synthesized and applied various sialic acid thioglycosyl donors as models in glycosylation reactions to gain a further understanding of how changes in the side chain configuration and conformation of a sialic acid pyranosyl ring influences the reactivity and selectivity of such donors. Focusing on the neuraminic acid, specifically the O4,N5-oxazolidinone thioglycoside donors, the Crich group demonstrated that a change in the configuration of a single stereogenic center in the side chain of *N*-acetyl neuraminic acid donor **201** to the 7-*epi*-isomer **202** (Figure 15) resulted to a change in a conformation of the O7-C7 bond from *gg* in **201** to *gt* in **202**.⁹⁶ The change in side chain conformation was supported by the ¹H

NMR studies that revealed a $^3J_{6,7}$ coupling constant of 2.4 Hz for donor **202**, suggesting that a *gt* conformation about the C6–C7 bond predominated while a $^3J_{6,7}$ coupling constant of 1.5 Hz was reported for the donor **201** suggesting that a *gg* conformation about the C6–C7 bond predominated.

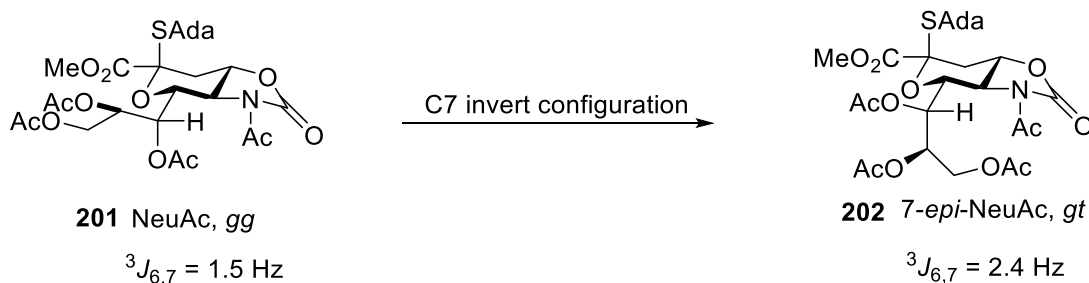
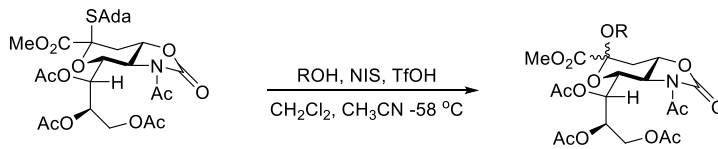
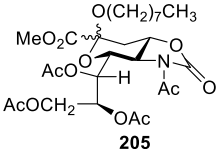
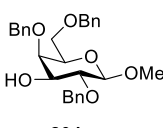
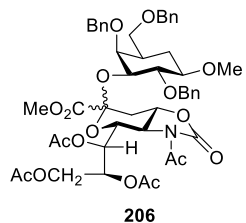
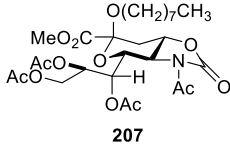
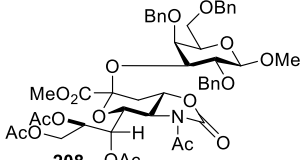


Figure 15. Inversion of the configuration at C7 of compound **201**

Employing 7-*epi*-thioglycoside donor **202**, primary and secondary acceptors in glycosylation reactions under the mediation of NIS/TfOH in CH₂Cl₂/CH₃CN at -78 °C furnished both α,β -neuraminic acid glycosides in modest yields (**Table 13**).⁹⁶ Conversely, excellent α -selectivity was observed under the same glycosylation conditions when the natural thioglycoside donor **201** was used. Crich and co-workers concluded that the less selectivity nature observed in coupling reactions involving donor **202** was as a result of a change in its side conformation to a *gt*, whereby in such a conformation the α -face of the SSIP is shielded thereby preventing approach of the acceptor from α -face while promoting a competing β -selective associative mechanism.

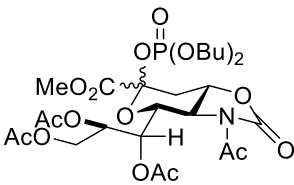
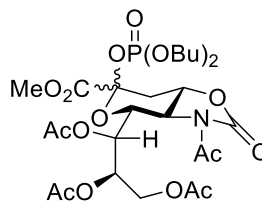
Table 13. The coupling reactions of compound **201** and **202** with selected acceptors

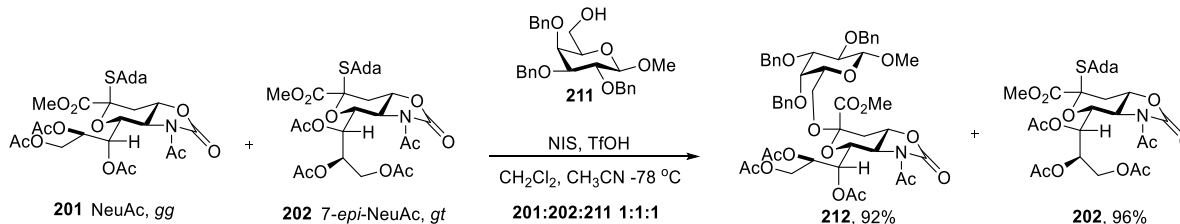
					
		202 7- <i>epi</i> NeuAc donor 201 natural NeuAc donor		205-206 7- <i>epi</i> NeuAc glycosides 207-208 natural NeuAc glycosides	
Entry	Donor	Acceptor	Glycoside	Yield (%)	Product (α/β)
1	202	203 CH ₃ (CH ₂) ₇ OH	 205	76	10:1
2	202	204 	 206	83	1:3
3	201	203	 207	85	α -only
4	201	204	 208	89	α -only

Noteworthy, ESI mass spectrometry fragmentation experiments using a standard cone voltage of 40 V, revealed that the fragmentation for the natural phosphate isomer **209** was detectable at a cone voltage of 85 V, while the 7-*epi*-phosphate isomer **210** required a cone voltage of 98 V in order for the fragmentation to occur (**Table 14**). Such experiments clearly demonstrated that a change in the side chain conformation from a *gg* to *gt* had an effect on the reactivity of the donors as donor **209** with a *gg* conformation proved to be readily fragmented hence more reactive compared to phosphate donor **210** with a *gt* conformation. In fact, competitive glycosylation experiments done by the Crich group (**Scheme 16**) was in support of the latter observation made

in the fragmentation studies as donor **201** with a *gg* conformation was easily activated and consumed in the presence of donor **202** with a *gt* conformation which was recovered in large quantities.

Table 14. The ESI mass spectrometry fragmentation experiments of compounds **209** and **210**

Compound	Structure	Cone voltage (V)	O6-C6-O7-C7
209		85	<i>gg</i>
210		98	<i>gt</i>



Scheme 16. Competition glycosylation experiment involving donors **201**, **202** and acceptor **211**

In their subsequent communication on related works, the Crich group demonstrated that a change in the configuration of a stereogenic center in the side chain of the 5-Azido thioglycosyl donor **213** to the 5-*epi*-isomer **214** (**Figure 16**) resulted to a change in the conformation of the O7-C7 bond from *gauche,gauche* (*gg*) in **213** to *gauche,trans* (*gt*) in **214**.⁹⁷ This notable change in side chain conformation was supported by the ¹H NMR studies that revealed ³J_{6,7} coupling constants of 2.2 Hz and 8.8 Hz that were observed for compounds **213** and **214** respectively.

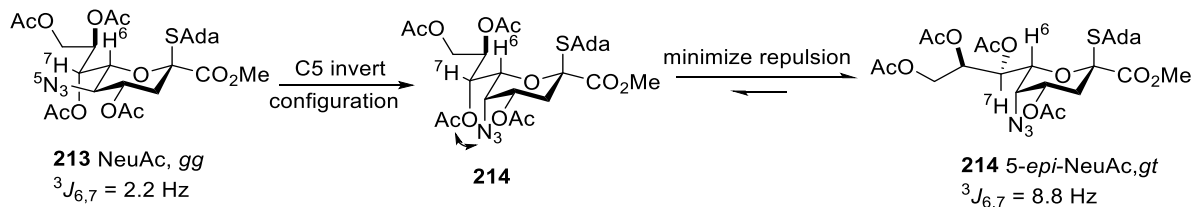


Figure 16. Inversion of the configuration at C5 of compound **213**

Additionally, experimental results revealed that the neuraminic acid thioglycoside donor **214** was β -selective even in cases where less reactive acceptors such as **215** were used (**Table 15**). Considering the fact that 5-azido group in **214** occupies the axial position it would be expected that axial glycosides would be formed in good amounts since the axial C–N bond would be *gauche* to the O6 ring oxygen thereby stabilizing the developing positive charge at the ring oxygen during glycosylation. However, the above observations were not made by the Crich group. Therefore, it was concluded that the β -selectivity observed with donor **214** was as a result of the influence of the predominant *gt* side chain conformation of **214** that did offset the effect of the axial azide group. Conducting such glycosylation experiments at low temperatures was noted to be equally important.⁹⁷

Table 15. The coupling reactions of compound **214** with selected acceptors

Reaction scheme showing the coupling of compound **214** with acceptors to form products **216-218**. Reagents: ROH, NIS, TfOH; Solvents: CH₂Cl₂, CH₃CN; Temperature: -78 °C.

Entry	Donor	Acceptor	Glycoside	Yield (%)	Product (α/β)
1	214			72	β-only
2	214			44	β-only
3	214			79	β-only

Most recently, Crich and co-workers demonstrated that epimerization at each of the C5, C7 and C8 centers of compound **213** followed by functional group adjustment resulted to 5,7,8-tris-*epi*-thioglycoside donor **219** (Figure 17). These configurational changes led to a change in the conformation of the exocyclic bond from *gauche,gauche* (*gg*) in **213** to *trans,gauche* (*tg*) in **219**. Indeed, an inspection of ¹H NMR spectrum revealed a ³*J*_{6,7} coupling constant of 10.5 Hz for the H6, H7 spin system of the pseudaminic acid glycosyl donor **219** that confirmed the existence of a *tg* conformation as the values were consistent with the reported literature values.

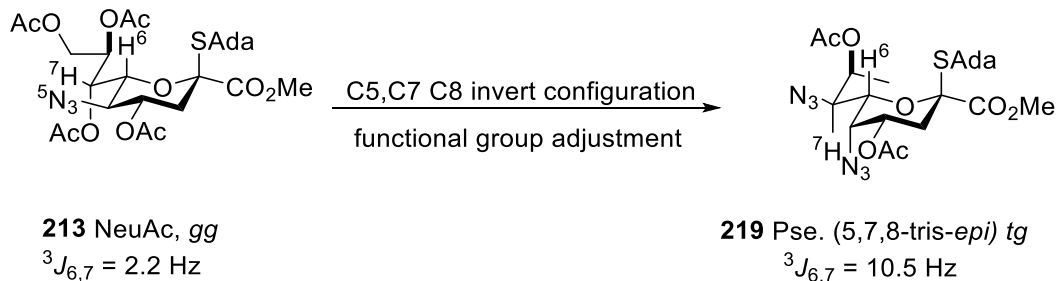


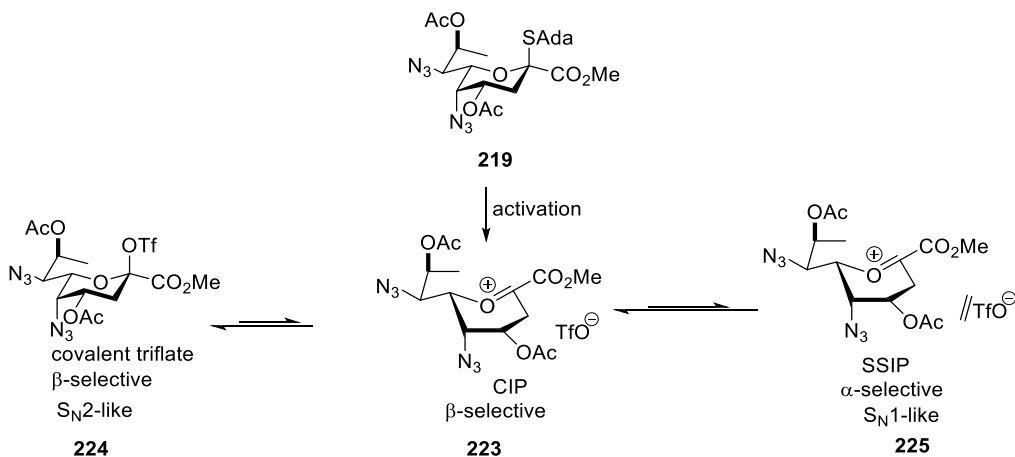
Figure 17. Inversion of the configuration at C5, C7 and C8 of compound **213**

Consistent with their predictions, it was observed that activation of the pseudaminic acid donor **219** by the NIS/TfOH combination led to the stereoselective formation of equatorial-sialosides. (Table 16).⁹⁸

Table 16. The coupling reactions of compound **219** with selected acceptors

Entry	Donor	Acceptor	Glycoside	Yield (%)	Product (α/β)
		<p>219</p>	<p>220-222</p>		
1	219	<p>211</p>	<p>220</p>	74	β -only
2	219	<p>204</p>	<p>221</p>	76	β -only
3	219	<p>130</p>	<p>222</p>	85	β -only

The conclusions arrived at were that in a *tg* conformation, the electron withdrawing effect of the C6–O6 bond is maximized thereby stabilizing the covalently bonded intermediate **224** with an S_N2 -like character, resulting in the formation of the equatorial anomers (Scheme 17).



Scheme 17. Mechanistic explanation of the role of *tg* conformation in the formation of β-sialosides

1.8 Literature evidence on the existence of a *tg* side chain conformation in KDO residues

In 1980, Unger and co-workers synthesized the methyl α- and β-KDO pyranosides **226** and **227** and an inspection of the ^1H NMR spectrum of the compounds revealed a $^3J_{\text{H6}, \text{H7}}$ coupling constant of 9.7 Hz for the H6, H7 spin system, suggesting the predominance of the *tg* conformation (**Figure 18**).⁹⁹ Most recently, computational work by Kiessling and co-workers has also pointed KDO adopting the *tg* side chain conformation.¹⁰⁰

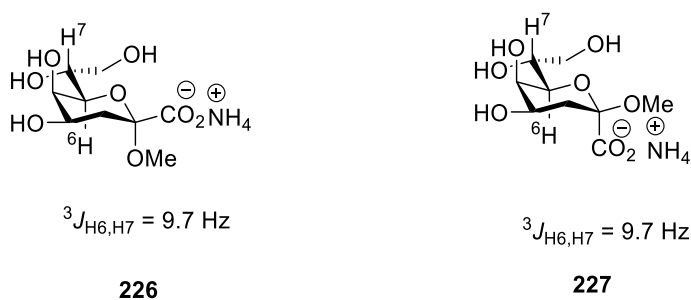


Figure 18. Investigation of the $^3J_{\text{H6}, \text{H7}}$ coupling constants of KDO anomers

1.9 Goals

The unique bicyclic chemical structure of bradyrhizose poses a synthetic challenge and indeed presents an opportunity for the development of efficient methods for its synthesis before its biological application is investigated. Both the Yu and Lowary syntheses above employ several steps with purification challenges encountered along the way. Moreover, the two approaches involved fusion of a pyranose ring onto a preformed inositol skeleton. In view of these problems, the research described in this thesis set out to develop a simple and a shorter method for accessing bradyrhizose from D-glucose. This protocol is based on the fusion of the bicyclic ring onto an existing pyranose framework as opposed to the fusion of a pyranose ring onto a preformed inositol skeleton.

As discussed above, there exists fewer methods for accessing β -KDO glycosides and only a few cases display high level of β -selectivity. Inspired by the pseudo-enantiomeric relationship between pseudaminic acid **228** and 3-deoxy-D-manno-oct-2-ulosonic acid **102** (KDO) (**Figure 19**), and building upon the work by Unger and co-workers as well as the majority of the 3-deoxy-D-manno-oct-2-ulosonic acid thioglycoside donors synthesized and employed in this study as models have a *tg* conformation about their exocyclic bond.

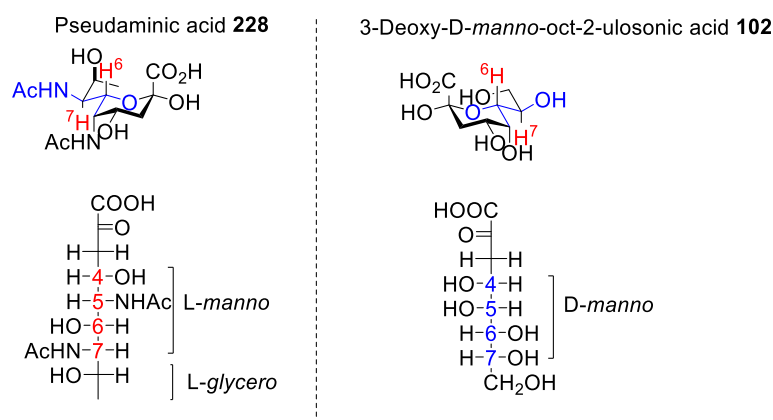


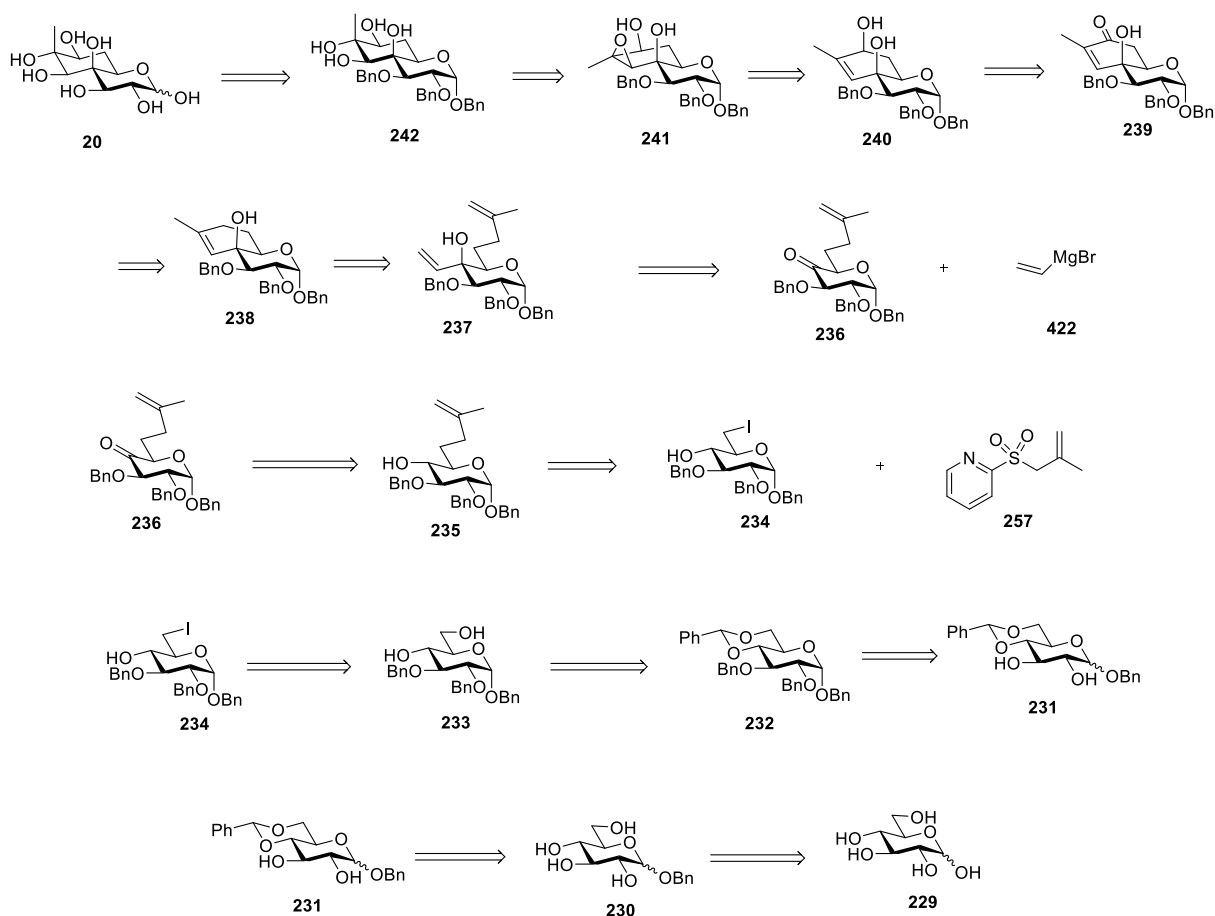
Figure 19. Pseudo-enantiomeric relationship of pseudaminic acid **228** and KDO **102**

CHAPTER 2 SYNTHESIS OF BRADYRHIZOSE FROM D-GLUCOSE

2.1 Results and discussion

2.1.1 Retrosynthetic analysis of bradyrhizose

Bradyrhizose **20** can be obtained from the benzyl protected tetraol **242** through hydrogenolysis. The tetraol **242** can be straightforwardly obtained from methallyl derivative **237** via a sequence of transformations involving ring closing metathesis, regioselective allylic oxidation, regio- and stereoselective reduction on the enone, stereoselective epoxidation and acid-catalyzed regio- and stereoselective epoxide ring opening. As a key intermediate, compound **237** can be synthesized from a reaction involving the ketone compound **236** and the vinyl Grignard **422**. Oxidation of the C4-OH on compound **235** is expected to yield to ketone derivative **236**. As a key intermediate, the methallylated compound **235** can be obtained via a side chain elongation at the glucopyranoside 6-position of compound **234** under radical initiated methallylation conditions using the iodo compound **234** and the sulfone **257** as precursors. Compound **234** can be obtained from compound **232** via a sequence of reactions involving the selective cleavage of the benzylidene group in compound **232** and conversion of the C6 hydroxy group in compound **233** to the iodo group. Finally, the benzyl protected intermediate **232** can be obtained from D-glucose **229** via a sequence of reactions involving the Fischer glycosylation on compound **229** leading to compound **230**, selective benzylidene protection of the O4 and O6 hydroxy groups on compound **230** leading to compound **231** and benzylation on the α -anomer of compound **231**.



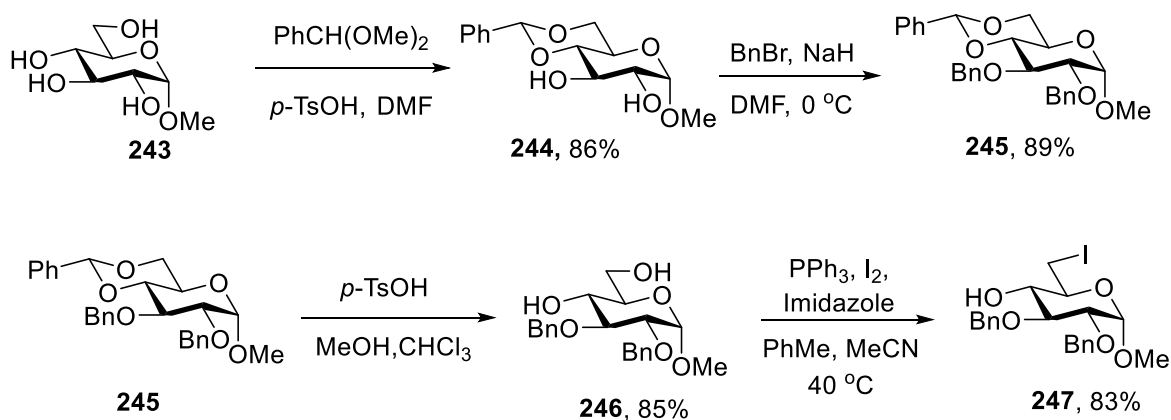
Scheme 18. Retrosynthesis of a planned bradyrhizose **20**

2.1.2 Synthesis of bradyrhizose from methyl α -D-glucopyranoside

2.1.2.1 Derivatization of compound **247**

The initial planned synthesis of bradyrhizose was based on using a single anomer of a glucopyranoside in order to avoid unnecessary complications in the NMR spectra. Following the retrosynthetic analysis, methyl α -D-glucopyranoside **243** was chosen as the starting material (**Scheme 19**): the preliminary steps involved selective installation of a benzylidene acetal¹⁰¹ on the C4 and C6 hydroxyl groups of **243** followed by benzylation¹⁰² of the free C2 and C3 hydroxyl groups, which led to compound **245** in 89% yield. Liberation of the C4 and C6 hydroxyl groups was achieved by cleavage of the benzylidene acetal under acid-catalyzed conditions;¹⁰³ this paved

the way for selective installation of the iodo group on the free primary hydroxyl group under Appel conditions¹⁰⁴ resulting in compound **247**.



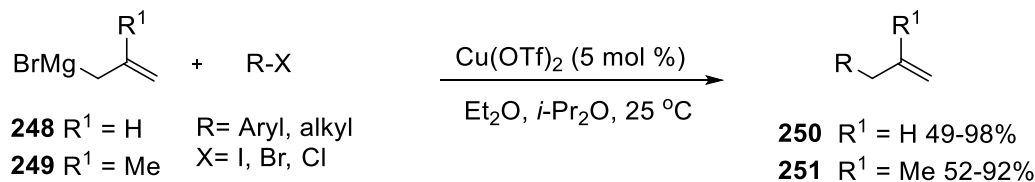
Scheme 19. Synthesis of the iodo compound from methyl α -D-glucopyranoside

2.1.2.2 Exploration of various C-C bond formation reactions for side chain elongation at the glucopyranoside 6-position of compound **247**

Methallylation of **247** under thermal conditions using lauroyl peroxide as the initiator, as well methallylation using methallyl Grignard reagents and metal catalysts were investigated.

2.1.2.2.1 Methallylation via the cross-coupling reaction of methallylmagnesium chloride with the iodo sugar derivative

Metal-catalyzed allylation or methallylation reactions of alkyl halides with allyl or methallyl Grignard reagents have been demonstrated to be an effective way of forming C-C bonds (**Scheme 20**). The most commonly employed transition-metal catalysts in such transformations include copper (I) iodide, $(\text{Pd}(\text{PPh}_3)_4)$,¹⁰⁵ Li_2CuCl_4 ,¹⁰⁶ $[\text{NiCl}_2(\text{dppp})]$,¹⁰⁷ $[\text{CoCl}_2(\text{dppp})]$,¹⁰⁸ $\text{Cu}(\text{OTf})_2$ ¹⁰⁹ and AgNO_3 .¹¹⁰



Scheme 20. Example of metal catalyzed C-C bond construction using Grignard reagent

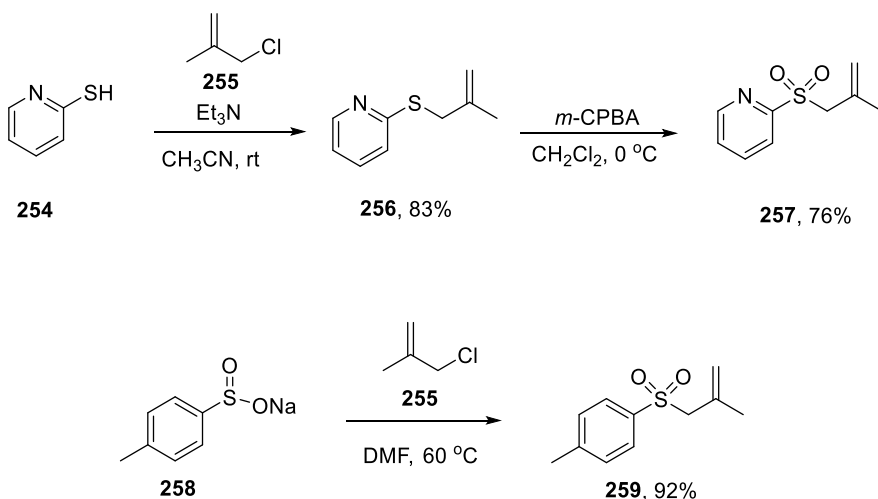
Therefore, methallylation using methallyl Grignard reagent **252** in the presence of $(Pd(PPh_3)_4)$, CuI, or Li_2CuCl_4 were attempted (**Table 17**). However, starting materials were recovered essentially unchanged under such conditions. It was reasoned that these failures in part arose from the protonation of the hydroxy group at the C4 position of the substrate. This problem could potentially have been overcome by the inclusion of an extra protecting group but, as would have added two steps to the planned synthesis, attention was turned instead to C-C bond forming reactions compatible with the presence of a free alcohol.

Table 17. Attempted methallylation by use of a Grignard reagent in the presence of a catalyst

Entry	Catalyst (mol %)	Time (h)	253 Yield (%)
1	CuI (5)	12	NR
2	$Pd(PPh_3)_4$ (5)	8	NR
3	Li_2CuCl_4 (5)	10	NR

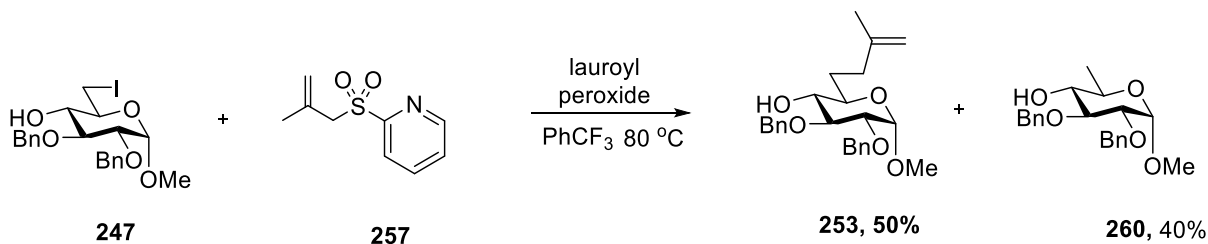
2.1.2.2.2 C-C bond formation via radical methallylation using methallylsulfones

Attention was therefore focused on radical conditions with initiation by the readily available stable peroxide lauroyl peroxide.¹¹¹ Methallylsulfones **257**, and **259** (**Scheme 21**) were synthesized in good yields and employed in the radical coupling reactions.

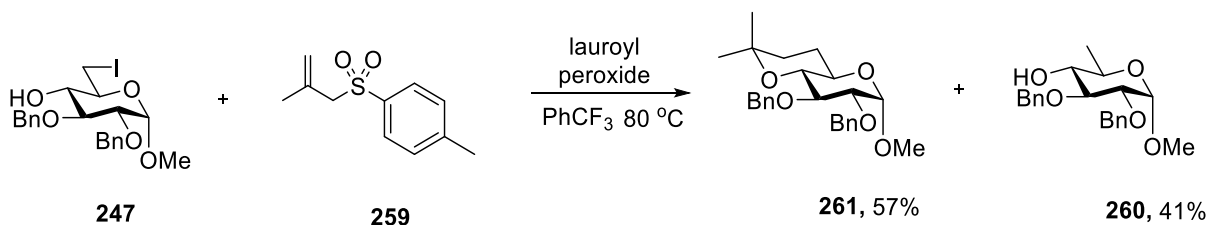


Scheme 21. Synthesis of methallylsulfones **257** and **259**

Subjection of compound **247** to radical methallylation conditions yielded the desired **253** in 50% yield with the formation of the reduced substrate **260** in 40% yield (**Scheme 22**). In the course of yield optimization, it was discovered that replacing 2-pyridyl methallylsulfone **257** by 4-toluylyl methallylsulfone **259** gave a cyclized compound **261** in 57% yield (**Scheme 23**) as was confirmed by ^1H NMR studies.



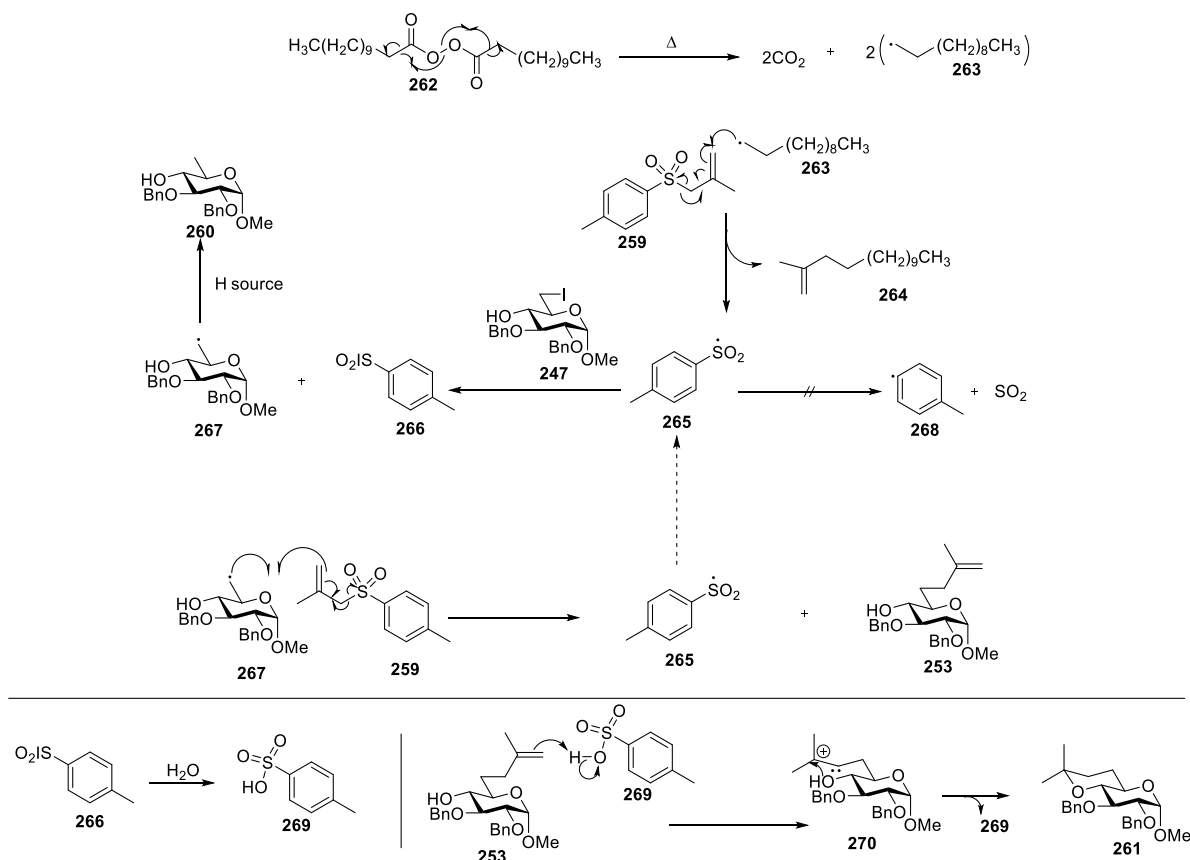
Scheme 22. Lauroyl peroxide radical initiated reaction using 2-pyridyl methallylsulfone



Scheme 23. Lauroyl peroxide radical initiated reaction using 4-toluylyl methallylsulfone

The proposed mechanism for the radical methallylation leading to compound **261** is illustrated in (Scheme 24). In the initiation step radical **263** is generated from the thermal fragmentation/decarboxylation of lauroyl peroxide **262**. This alkyl radical adds onto the 4-toluy methylsulfone **259** to generate the 4-toluy sulfonyl radical **265** with the generation of byproduct **264**. Desulfonylation of **265** is considered unlikely since it would generate a high energy aryl radical **268**. The 4-toluy sulfonyl radical **265** abstracts iodine atom from the iodo glucopyranoside **247** to form the radical **267** with the liberation of the sulfonyl iodide **266**. The reactive radical **267** then couples irreversibly to the 4-toluy methylsulfone **259** to form compound **253** with regeneration of radical **265** that propagates the radical chain reaction.

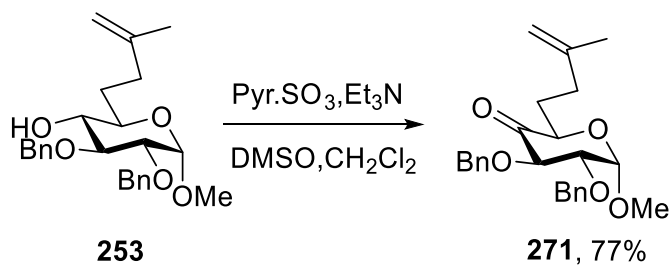
The sulfonyl iodide **266** can be hydrolyzed to 4-toluenesulfonic acid **269** in the presence of moisture thereby generating an acidic medium. Under such acidic conditions, compound **253** is protonated generating the tertiary cation **270**. Finally, the C4 hydroxy group in **270** being in proximity with the carbocation attacks the tertiary center resulting to the formation of the bicyclic compound **261**. When the pyridyl methylsulfone **257** was employed as reagent, the internal base buffers the reaction conditions and suppresses this acid-catalyzed cyclization. Formation of the reduction product **260** is presumably the product of hydrogen atom abstraction from the allylic position of the reagent or from one of the many C-H bonds in the initiator.



Scheme 24. Proposed mechanism for the formation of product **253** and byproducts **260** and **261**

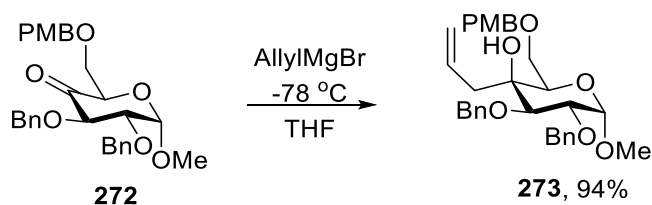
2.1.2.3 Synthesis of the key bicyclic intermediate **278**

Compound **271** was obtained in moderate yields from oxidation of **253** under Parikh-Doering conditions (**Scheme 25**). Parikh-Doering conditions, often known as the industrial Swern conditions, were employed as they are relatively green and do not involve tedious workup procedures.¹¹²



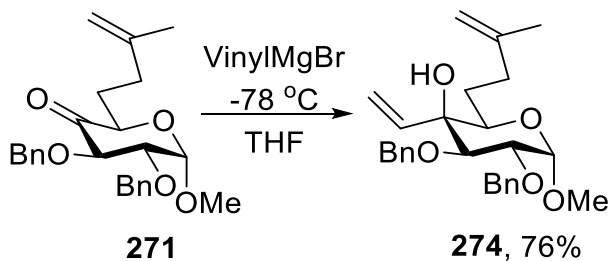
Scheme 25. Oxidation under Parikh-Doering conditions

La Ferla and co-workers reported a stereo-controlled addition of Grignard reagents that led to the isolation of compound **273** in 94% as a single diastereoisomer (**Scheme 26**).¹¹³



Scheme 26. Stereo-controlled Grignard addition reactions in related glucopyranoside systems

Considering La Ferla's work, reaction of compound **271** with vinyl magnesium bromide gave compound **274** as a single diastereoisomer in 76% yield (**Scheme 27**).



Scheme 27. Stereo-controlled formation of compound **274**

The observed desired stereoselectivity was confirmed by NOE studies that revealed the existence of NOE correlations between $\text{H4}'$ and H3 and, $\text{H4}'$ and H5 (**Figure 20**).

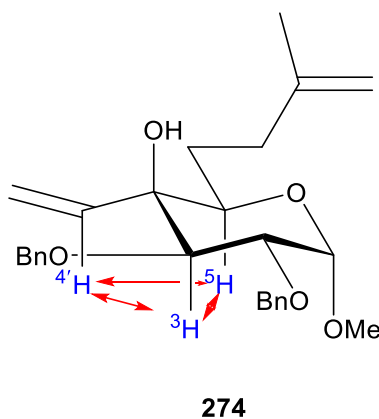


Figure 20. NOE correlations between $\text{H4}'$ and H3 and H5 in compound **274**

The stereo-controlled addition of the vinyl Grignard was proposed to be influenced by formation of a Cram chelated intermediate **271** that allows the nucleophile to approach from the less hindered side thus leading to compound **274** (**Figure 21**).¹¹⁴

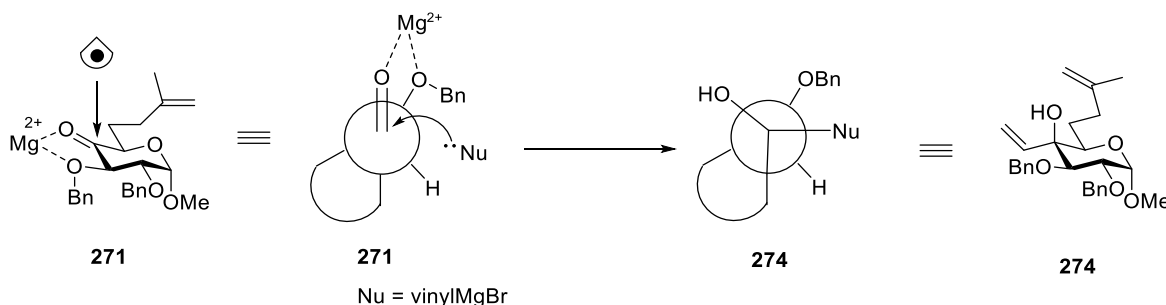
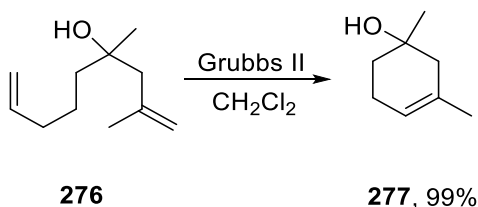


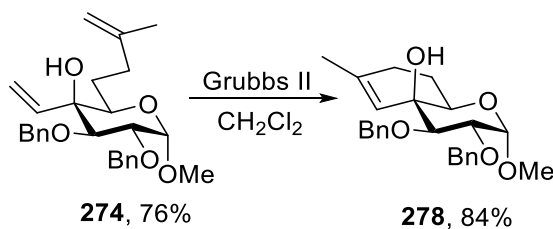
Figure 21. Hypothesized role of Cram chelation in the stereo-controlled addition of vinyl Grignard reagent to compound **271**

Plenio and co-workers demonstrated that trisubstituted cyclohexenes could be effectively formed in excellent yields from methallyl type precursors in the presence of a Grubbs catalyst (**Scheme 28**).^{115e}



Scheme 28. Synthesis of trisubstituted cyclohexene as reported by Plenio and co-workers

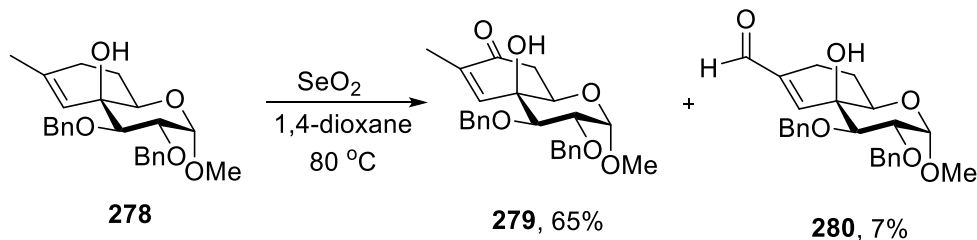
Therefore, the bicyclic scaffold was constructed by the ring closing metathesis on compound **274** using Grubbs cat. 2nd generation thus giving compound **278** in 84% yield (**Scheme 29**).^{115a-d}



Scheme 29. Construction of the bicyclic scaffold

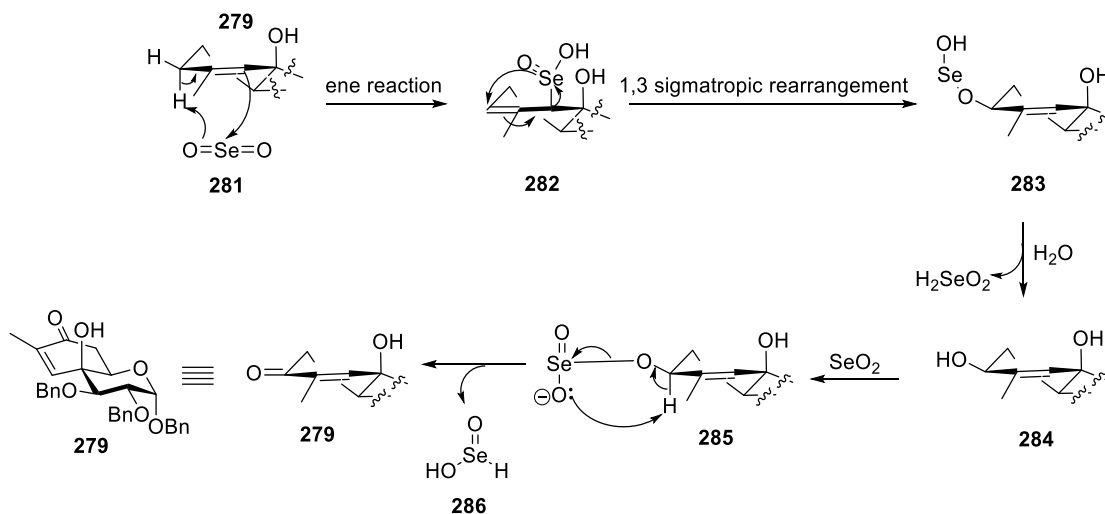
2.1.2.4 Stereoselective synthesis of the epoxide **279**

Subsequently, compound **278** was subjected to allylic oxidation conditions using SeO_2 to regioselectively give enone **279** as the major compound. The regioisomeric aldehyde **280** was also isolated in 7% yield from this reaction (**Scheme 30**).



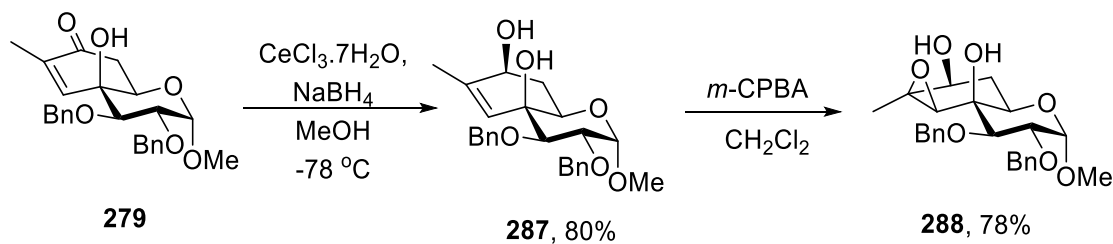
Scheme 30. Regioselective allylic oxidation on compound **279**

The regioselectivity observed is consistent with Guillemonat's rules and subsequent work.¹¹⁶ According to Guillemonat's rule, the selenium dioxide catalyzed allylic oxidation at the endocyclic secondary (CH_2) position is preferred over the exocyclic primary (CH_3) position. This is because the secondary C-H bonds are weaker than the primary ones in the methyl group. The regioselective formation of enone **279** begins with a heteroene reaction, to give the seleninic acid **282**, which undergoes a 1,3 sigmatropic rearrangement that results in **283**. Hydrolysis of **283** gives the alcohol **284** that reacts with another equivalent of selenium dioxide to generate intermediate **285**. Subsequent cleavage of the Se-O bond results to enone **279** (**Scheme 31**).

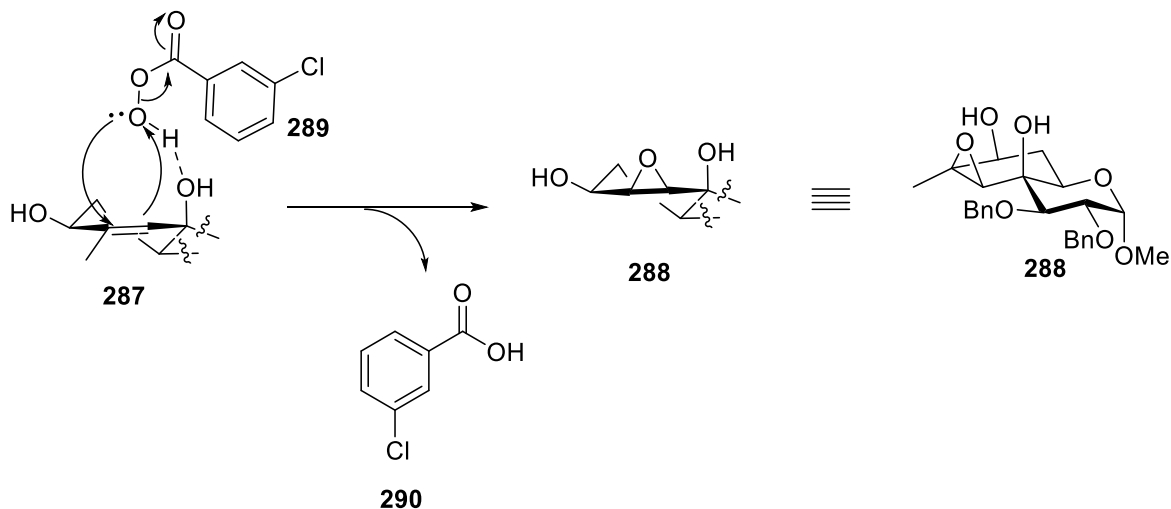


Scheme 31. Proposed mechanism leading to enone **279**

Regio- and stereoselective reduction of the enone **279** was performed under Luche's reduction conditions,¹¹⁷ resulting in compound **287** in 80% yield (**Scheme 32**). The observed stereoselectivity is thought to arise by approach of the hydride to the carbonyl center from the bottom face, which is less hindered in comparison to the top face. A hydrogen bond directed epoxidation¹¹⁸ (**Scheme 33**) on enol **287** then stereoselectively gave the epoxide **288** in 78% yield as a single diastereoisomer.



Scheme 32. Stereoselective synthesis of epoxide **288**



Scheme 33. Proposed mechanism for epoxidation leading to compound **288**

The relative configuration of epoxide **288** was determined by the observation of strong NOE correlations of H9 with the C8-methyl group, H3, H5 and H7 (**Figure 22**).

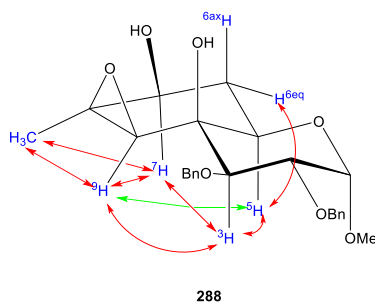
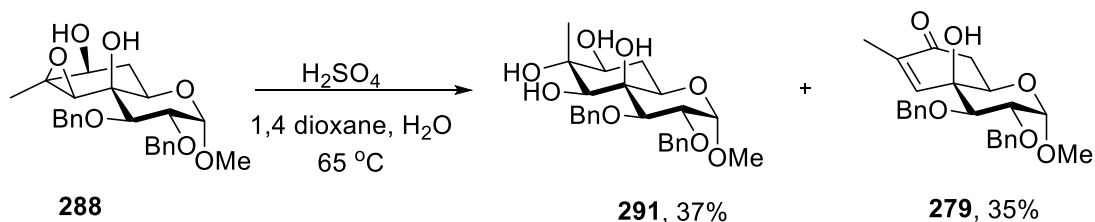


Figure 22. NOE correlations of H9, C8-methyl group, H3, H5 and H7 in compound **288**

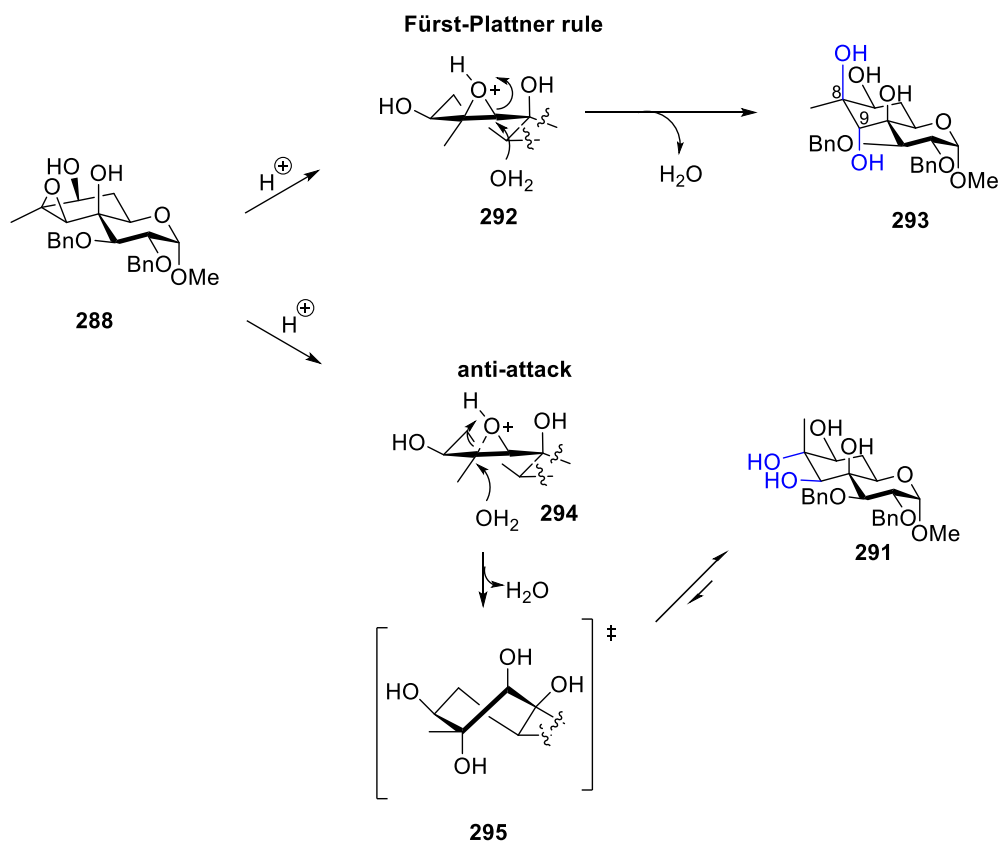
2.1.2.5 Regio- and stereoselective ring opening of the epoxide **288**

The regio- and stereoselective opening of **288** was conducted using sulfuric acid as catalyst in a 1,4-dioxane:water 1:2 mixture and yielded tetraol **291** in 37% yield alongside 35% of the enone **279** that was recycled (**Scheme 34**).



Scheme 34. Acid catalyzed regio- and stereoselective opening of epoxide **288**

The regiochemical and stereochemical outcome of this ring opening observed derives from the well-known anti attack of nucleophiles at the more substituted position of trisubstituted epoxides under acidic conditions (**Scheme 35**).¹¹⁹ This observation deviates from the Fürst-Plattner rule¹²⁰ that involves attack of nucleophiles at the less substituted position of a trisubstituted epoxide thereby directly leading to tetraol **293** with wrong stereochemistry at both C8 and C9 positions.



Scheme 35. Proposed mechanism leading to tetraol **291**

The relative configuration of **291** was established by the NOE studies that revealed the proximity of H9 with H3, H5 and H7. Similarly, a strong NOE correlation of the axial C8 methyl group to H6_{axial} was observed and supported the assigned structure (**Figure 23**).

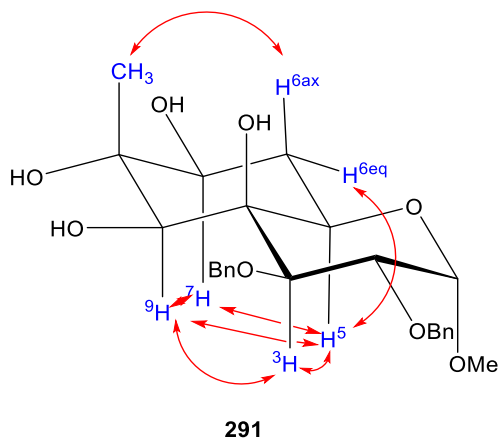
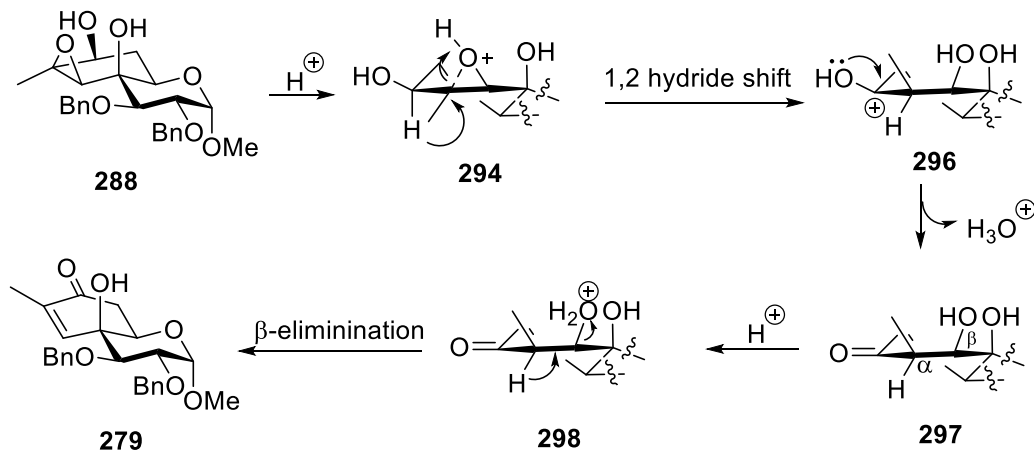


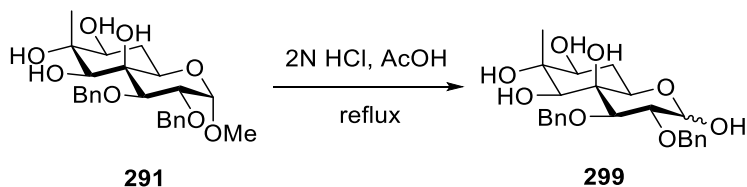
Figure 23. NOE correlations between H9, H3, H5 and H7 in compound **291**

The formation of compound **279** is suggested to have occurred as a result of a 1,2-hydride shift followed by β -elimination (**Scheme 36**).



Scheme 36. Proposed mechanism for the regeneration of enone **279**

An attempt to hydrolyze the glycosidic bond in **291** under acidic conditions were complicated by apparent decomposition of tetraol **291** as was judged by thin layer chromatography and mass spectrometry of the crude reaction mixtures (**Scheme 37**).

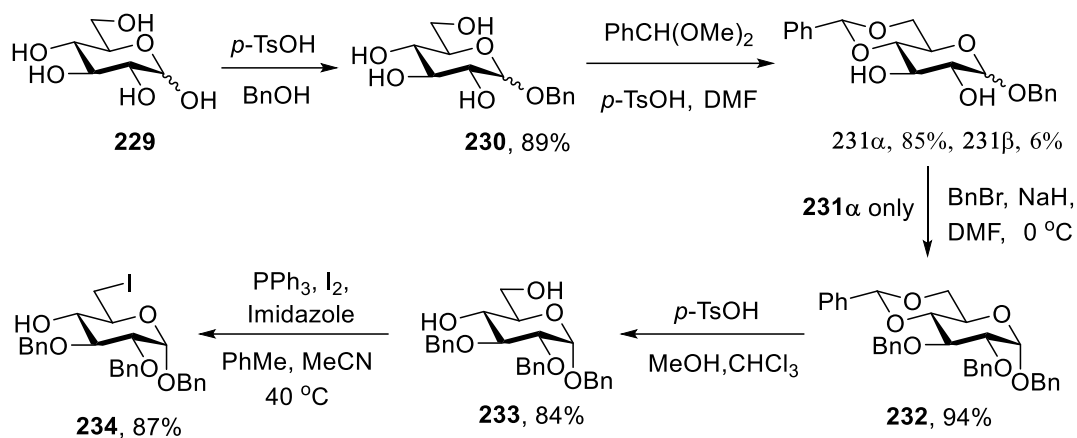


Scheme 37. Attempted hydrolysis of the glycosidic bond

These complications lead to a redesign of the synthesis to incorporate a benzyl glycoside, cleavable by hydrogenolysis, rather than a methyl glycoside.

2.1.3.1 Preparation of benzyl 2,3-di-*O*-benzyl-6-deoxy-6-iodo- α -D-glucopyranoside from D-glucose

As outlined in (**Scheme 38**), the synthesis of **234** from D-glucose **229** was achieved in five steps with the first step involving subjection of **229** to Fischer glycosylation¹²¹ in benzyl alcohol at reflux resulting in **230**. Subsequently, the benzylidene group was selectively installed on O4 and O6 under acidic conditions furnishing **231** in 31g scale, 91% yield as a mixture of two anomers with a ratio of 14:1 α : β .¹⁰¹ In order to minimize complications in purifications of the anomeric mixtures in later stages of synthesis, and simplify NMR spectral analysis, the pure α -anomer of **231** was isolated in 85% yield and subjected to benzylation with benzyl bromide and sodium hydride to afford compound **232**.¹⁰² Acid-catalyzed removal of the benzylidene acetal,¹⁰³ followed by selective Appel¹⁰⁴ iodination of the primary hydroxyl group resulted in compound **234**. All of these steps proceeded with excellent yields

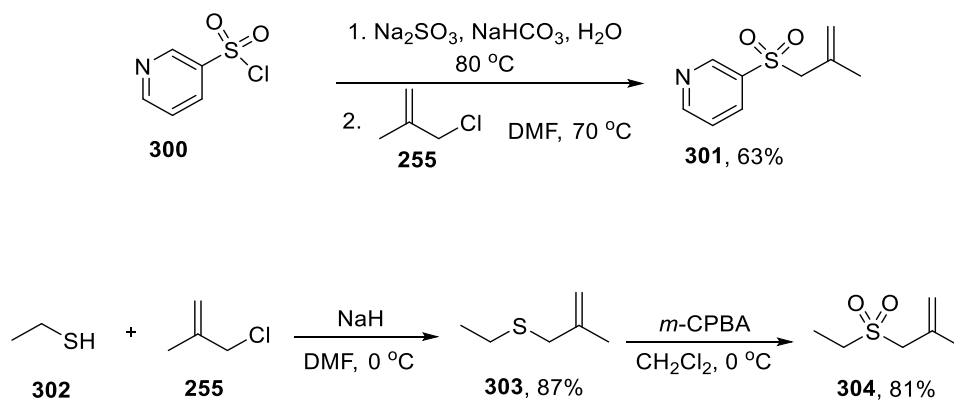


Scheme 38. A five-step synthesis of compound **234** from D-glucose

2.1.3.2 Exploration of various C-C bond formation reactions for side chain elongation at the glucopyranoside 6-position of benzyl 2,3-di-*O*-benzyl-6-deoxy-6-iodo- α -D-glucopyranoside

2.1.3.2.1 C-C bond formation via radical methallylations using methallylsulfones or methallyltri-*n*-butylstannane

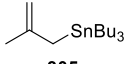
In an attempt to improve the yield of the radical methallylation step, further methallyl sulfones were prepared as outlined in (**Scheme 39**). As previously, the methallylation reactions were conducted under thermal conditions with initiation by lauroyl peroxide or azoisobutyronitrile as summarized in (**Table 18**).



Scheme 39. Synthesis of methallylsulfones **301** and **304**

Table 18. Methallylation under various radical initiated conditions using methallylsulfones or methallyltri-*n*-butylstannane

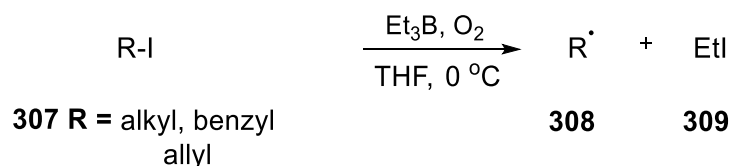
$\text{234} + \text{257, 301, 304, 306} \xrightarrow[\text{solvent}]{\text{initiator}}$
 $\text{235} + \text{306}$

Entry	Iodo	Sulfone (R2)	Initiator	Solvent	Temp.(°C)	Yield (%)	
						235	306
1	234	2-pyridyl 257	lauroyl peroxide	PhCF ₃	80	54	36
2	234	3-pyridyl 301	lauroyl peroxide	PhCF ₃	80	50	38
3	234	2-pyridyl 257	AIBN	PhCF ₃	80	7	16
4	234	2-pyridyl 257	Et ₃ B/O ₂	PhCF ₃	0 - rt	40	51
5	234	 305	AIBN	PhCF ₃	80	58	31
6	234	ethyl 304	AIBN	heptane/PhCl	85	10	6
7	234	2-pyridyl 257	<i>fac</i> -Ir(ppy) ₃ (5 mol%) Bu ₃ N	CH ₃ CN	rt	68	13

The radical methallylation reactions on iodo glucopyranoside **234** with 2-pyridyl methallylsulfone **257** under thermal initiation by lauroyl peroxide gave compound **235** in 54% yield while replacement of the 2-pyridyl methallylsulfone with the regioisomeric 3-pyridyl methallylsulfone¹²² **301** gave the corresponding methallylated product **235** in 50% yield albeit with the formation of the reduced compound **306** (Table 18, entries 1 and 2). Based on these observations, it was concluded that a change of nitrogen position in the pyridine ring did not have a major impact in yield optimization as the yield obtained in methallylation reactions involving 2-pyridyl methallyl sulfone were similar to those of 3-pyridyl methallylsulfone. The construction of

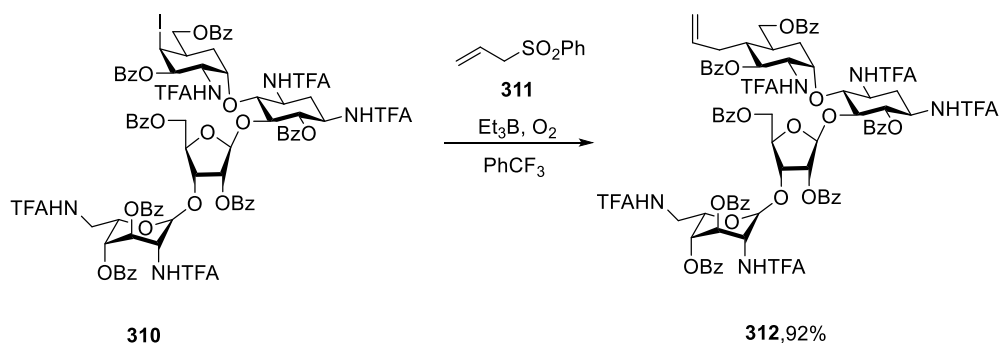
the C-C bond via thermal initiation by AIBN using 2-pyridyl methallylsulfone **257** (Table 1 entry 3) equally resulted in low yields of the desired compound.

Attention was therefore focused on investigating radical methallylation using triethylborane as an initiator. Precedent by Brown and co-workers on reaction of organoboranes with alkyl, benzylic and allylic iodides in the presence of oxygen¹²³ to generate radicals revealed that organoboranes are excellent sources of free radicals for use in chain reactions in the presence of oxygen (**Scheme 40**). Subsequently, these initiation conditions were developed by Oshima and coworkers and have been very widely employed in subsequent years.¹²⁴



Scheme 40. Et₃B-induced radical reaction by Brown and co-workers

Most recently, Crich and co-workers demonstrated in their synthesis of the 4'-C-alkyl paromomycin derivative **312**, that the key C-C bond forming step was possible by employing allyl phenylsulfone **311** and the iodo derivative **310** in α,α,α trifluorotoluene with initiation by triethylborane and air (**Scheme 41**).¹²⁵ α,α,α -Trifluorotoluene was selected as an environmentally friendly radical-compatible solvent for such transformation and the reaction was successfully conducted on scales of up to 100 g.¹²⁶

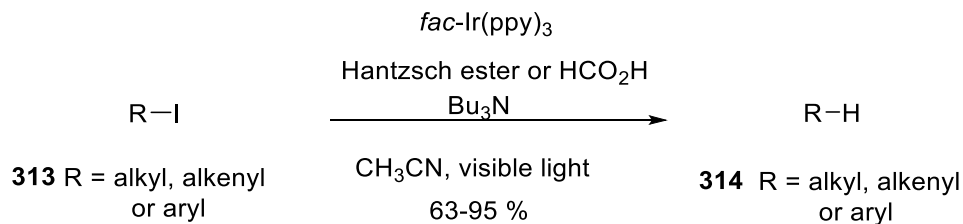


Scheme 41. Et₃B-induced radical transformation by Crich and co-workers

Therefore, methallylation using 2-pyridyl methallylsulfone **257** and triethylborane¹²⁷ as initiator in the presence of oxygen at room temperature was attempted (Table 18, entry 4). However, the construction of the C-C bond under such conditions proved inefficient and resulted in the formation of significant quantities of the simple reduction product **306**. Subsequently, chemical initiation with AIBN was investigated with the methallyltri-*n*-butylstannane derivative **305** (Table 18, entry 5).¹²⁸ However, the methallylated compound **235** proved rather difficult to obtain in pure form.

2.1.3.2.2 Visible-light mediated C-C bond formation using (*fac*-Ir(ppy)₃) and methallylsulfone

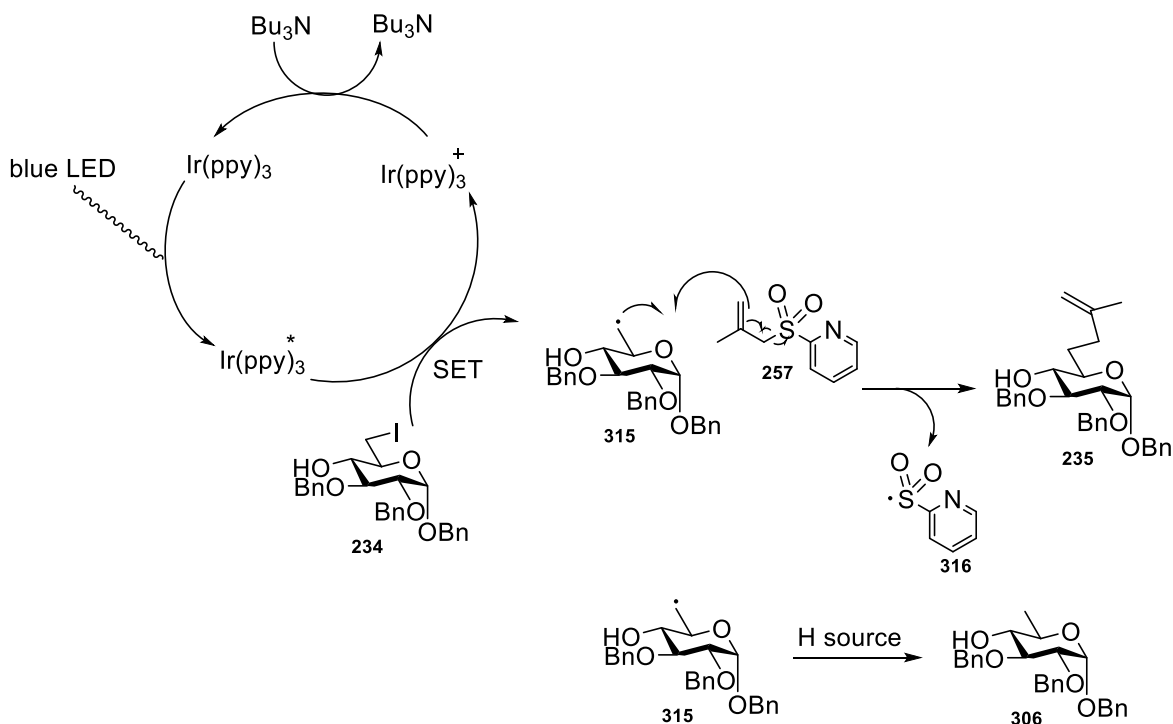
Stephenson and co-workers reported a visible-light mediated reductive dehalogenation of unactivated carbon-iodide bonds using photocatalyst *fac*-Ir(ppy)₃ having a strong reduction potential of -2.19 V (versus SCE) under mild conditions. Such photocatalytic transformations required the use of tributylamine as a sacrificial electron donor and either the Hantzsch ester or formic acid as hydrogen atom donor (**Scheme 42**).¹³⁰



Scheme 42. Visible-light mediated reductive dehalogenation of unactivated alkyl, alkenyl or aryl iodides

In the light of Stephenson's work, visible-light mediated methallylation using (*fac*-Ir(ppy)₃), 2-pyridyl methallylsulfone **257** and tributylamine in acetonitrile was attempted and gave compound **235** with an optimum yield of 68% (Table 18 entry 7).

The proposed mechanism for this photocatalyzed transformation is shown in (**Scheme 43**). Thus, visible-light-excitation of *fac*-Ir(ppy)₃ results in the radical cleavage of carbon–iodide bond on compound **234** through a single electron transfer (SET) process. The glucopyranoside radical **315** generated then directly adds onto the 2-pyridyl methallylsulfone **257** thereby generating compound **235** and 2-pyridyl sulfonyl radical **316**. Subsequently, the excited *fac*-Ir(ppy)₃ form of the catalyst is reduced to its ground state by a sacrificial electron donor such as tributylamine. The carbon radical **315** generated can as well undergo hydrogen atom abstraction probably from the methallylsulfone **257** to give the reduced product **306**.

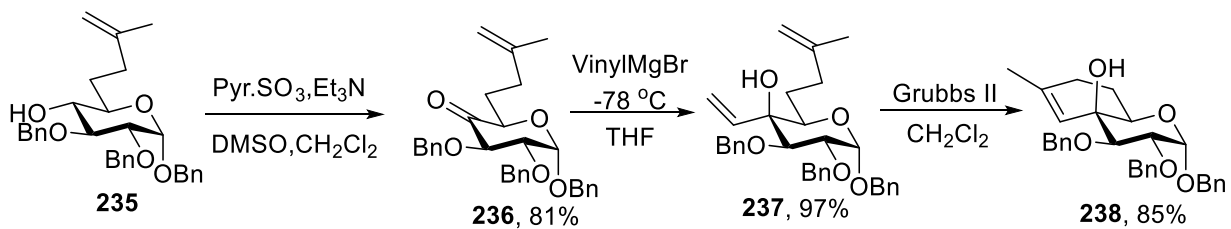


Scheme 43. Proposed mechanism for the visible-light mediated formation of compound **235**

using *fac*-Ir(ppy)₃ as a catalyst

2.1.3.3 Construction of the bicyclic scaffold

The oxidation of **235** under Parikh-Doering conditions¹¹² gave ketone **236**, which on treatment with vinyl magnesium bromide afforded allylic alcohol **236** as a single diastereoisomer. The generation of compound **236** as a single diastereoisomer was consistent with the earlier observation on the corresponding methyl glycoside (**Scheme 44**).¹¹³



Scheme 44. Synthesis of the bicyclic intermediate **238**

As previously, the configuration of compound **237** was confirmed by NOE studies that revealed the existence of NOE correlations between H4' and H3 and, H9 and H5 (**Figure 24**).

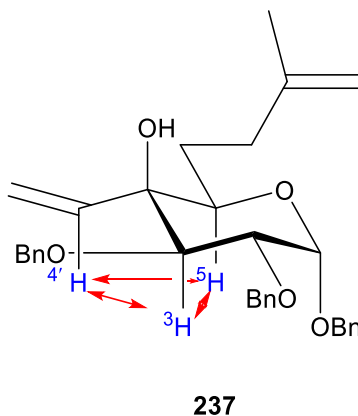
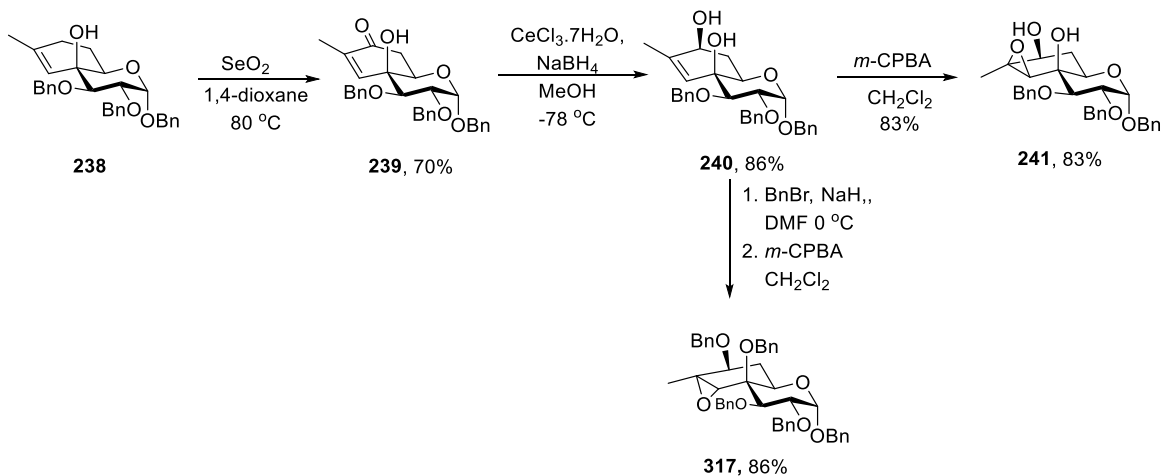


Figure 24. NOE correlations between H4' and H3 and H5 in compound **237**

The requisite bicyclic scaffold was then obtained by ring closing methathesis in excellent yield and it functioned as with the methyl glycoside (**Scheme 29**)

2.1.3.4. Stereoselective synthesis of oxiranes **241** and **317**

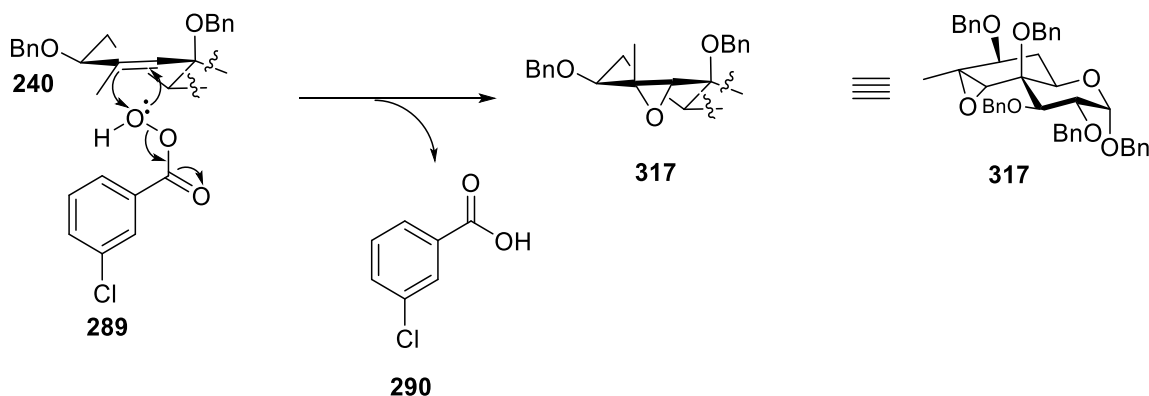


Scheme 45. Derivatization of **241** and **317** from intermediate **240**

As previously observed with the methyl glycoside, the regioselective allylic oxidation of **238** with SeO₂ in 1,4-dioxane at 80 °C gave enone **239** in 70% yield.¹¹⁶ Subsequently, the regio- and stereoselective reduction of the enone derivative **239** under Luche's conditions,¹¹⁷ resulted in

the isolation of the allylic alcohol **240** in 86% yield as a single diastereoisomer as previously observed with the methyl glycoside (**Scheme 32**).

Functionalization of the alkene group in compound **240** was then attempted next to access the epoxide derivative **312**. Thus, benzylation followed by epoxidation on compound **240** using *m*-CPBA¹¹⁸ at room temperature in 1,2 di-chloromethane furnished oxirane **315** in 86% yield (**Scheme 45**). Mechanistically, the observed stereochemical outcome of this reaction suggests that in the indicated half-chair conformation, the epoxidation preferentially occurs from the bottom face of the alkene which is less sterically hindered (**Scheme 46**).



Scheme 46. Proposed mechanism for epoxidation leading to compound **317**

The assigned structure of **317** is consistent with the NOE studies that revealed the existence of the NOE correlations between H9 and the axial C8-methyl group as well as the benzylic methylene resonances of the 4-*O*-benzyl ether. Similarly, an NOE correlation of the axial C8 methyl group to the benzylic methylene resonances of the 7-*O*-benzyl ether was observed (**Figure 25**).

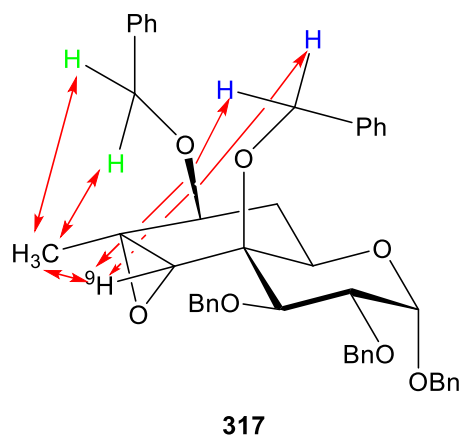


Figure 25. NOE correlations between H9, C8-methyl group and the benzylic methylene hydrogens in compound **317**

The regio- and stereoselective epoxide ring opening of **317** was then investigated under various conditions intended to involve S_N2 -attack of the external nucleophile at the secondary site. As summarized in (**Table 19**), subjection of the epoxide **317** under mild conditions or thermal/microwave conditions proved unsuccessful as they led to recovery of starting materials or decomposition of the epoxide.

Table 19. Attempted regioselective epoxide ring opening under various conditions

Entry	Oxirane	Reagent	Temp. (°C)	Heat source	Solvent	Yield (%)
1	317	TBAOAc	rt	-	CH ₂ Cl ₂	NR
2	317	TBAOAc	40	Δ	CH ₂ Cl ₂	NR
3	317	TBAOAc	75	Δ	CH ₃ CN	NR
4	317	TBAOAc	100	water bath	neat	NR
5	317	TBAOAc	80-170	μW	CH ₃ CN	decompose
6	317	TBANO ₂	0-120	Δ	DMF	decompose
7	317	TBANO ₂	100-140	μW	DMSO	decompose
8	317	5% KOH	0-rt	-	1,4 dioxane, H ₂ O	NR

Reverting to the H-bonded directed epoxidation achieved with the methyl glycoside (**Scheme 33**), epoxide **241** was obtained in 83% yield as a single diastereoisomer, via treatment of compound **240** with *m*-CPBA at room temperature in 1,2 di-chloromethane (**Scheme 45**).¹¹⁸ Similar to the observations made with the methyl glycoside, the relative configuration of epoxide **241** was confirmed by the observation of strong NOE correlations of H9 with the C8-methyl group, H3, H5 and H7 (**Figure 26**).

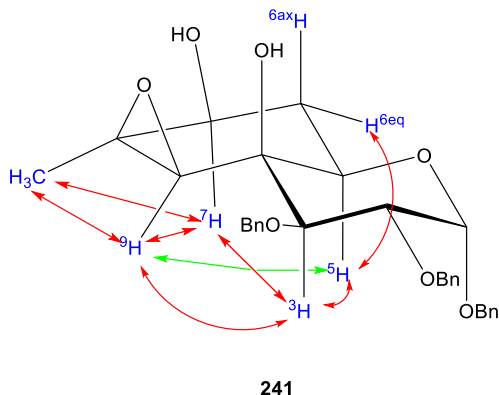


Figure 26. NOE correlations of H^9 , C8-methyl group, H^3 , H^5 and H^7 in compound **241**

Regioselective opening of **241** was attempted under a variety of acidic conditions (**Table 20**). Thus, in dry solvents (Table 20, entry 2) the enone **239** was isolated as the only product. Reactions conducted under aqueous acidic conditions without excessive heating proved unsuccessful due to the insolubility of epoxide **241** (Table 20, entries 6 and 7). Finally, consistent with the studies on the methyl glycoside (**Scheme 34**) regio- and stereoselective access to the desired tetraol **242** was realized by employing sulfuric acid as catalyst in a homogeneous solution mixture of 1,4-dioxane:water 1:3 at 65 °C (Table 3, entry 5). Thus, tetraol **242** was obtained in 50% yield alongside 45% of the enone **239**.

Table 20. Regioselective epoxide ring opening under various acidic conditions

Entry	Oxirane	Reagent	Temp (°C)	Solvent	Yield (%)	
					242	239
1	241	wet triflic acid	0-45	CH ₂ Cl ₂	NR	NR
2	241	H ₂ SO ₄	65	1,4 dioxane	0	78
3	241	H ₂ SO ₄	65	1,4 dioxane:H ₂ O (1:1)	20	68
4	241	H ₂ SO ₄	65	1,4 dioxane:H ₂ O (1:2)	37	35
5	241	H ₂ SO ₄	65	1,4 dioxane: H ₂ O (1:3)	50	45
6	241	H ₂ SO ₄	65	1,4 dioxane:H ₂ O (1:4)	13	0
7	241	H ₂ SO ₄	65	1,4 dioxane:H ₂ O (1:6)	10	0
8	241	Sc(SO ₃ CF ₃) ₃	rt-45	THF	NR	NR

Consistent with the previous observations made in the establishment of the relative configuration of the methyl tetraol **289**, NOE studies on tetraol **242** revealed the presence of strong NOE correlations of H9 with H3, H5 and H7. Moreover, NOE correlation of the axial C8 methyl group to H6_{axial} was also observed (**Figure 27**).

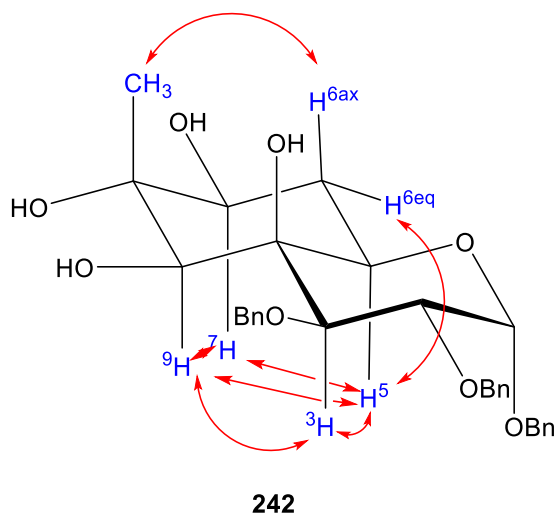
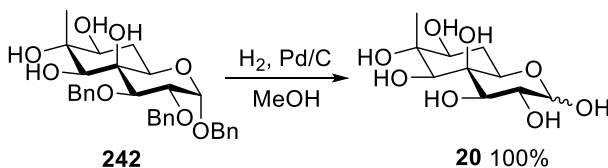


Figure 27. NOE correlations between H9, H3, H5 and H7 in compound **242**

2.1.3.5 Deprotection of **242** to give **20**

The synthesis of bradyrhizose **20** was completed by hydrogenolysis of the benzyl ethers over 10% Pd/C in methanol in quantitative yield (**Scheme 47**).⁴⁸

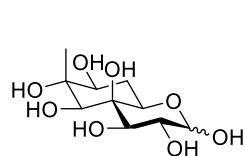


Scheme 47. Completion of synthesis

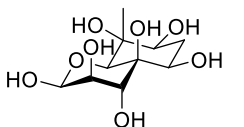
2.1.4 Comparison of ^1H and ^{13}C spectral data of bradyrhizose

Upon completion of the synthesis of compound **20**, a comparison of the NMR spectral data with the reported literature data was carried out as outlined in (**Table 21**).

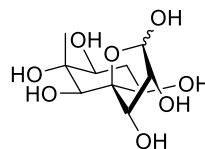
Table 21. Comparison of ^1H and ^{13}C spectral data of bradyrhizose synthesis with literature syntheses



β -D-bradyrhizose **a**
 α -D-bradyrhizose **b**



regioisomeric
 1,9-pyranose form **c**



β -furanose form **d**
 α -furanose form **e**

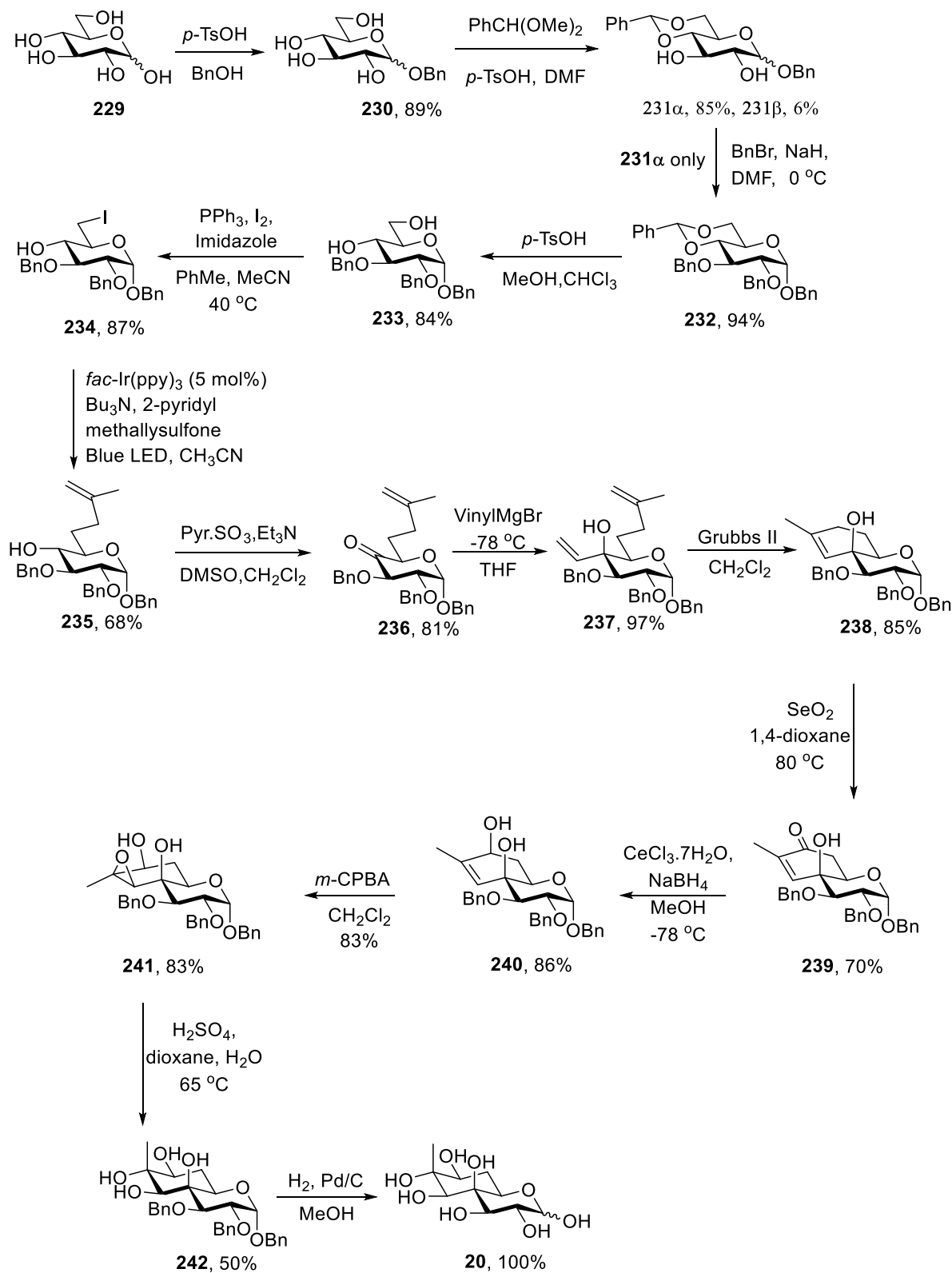
Data source	20a	20b	20c	20d	20e	Solvent	Chemical shift reference
Research data							
δ_{H}	4.61	5.21	5.04	5.05	5.25		
Multiplicity	d	d	s	s	d	D_2O	internal HOD at δ_{H} 4.79
$^3J_{\text{H1,H2}}$	(8.1 Hz)	(4.3 Hz)			(3.7 Hz)		
δ_{C}	96.5	92.2	100.0				
Yu data⁴⁸							
δ_{H}	4.50	5.10	4.93	4.93	5.14	D_2O	internal acetone at δ_{H} 2.225, δ_{C} 31.45
Multiplicity	d	d	d	d			
$^3J_{\text{H1,H2}}$	(8.07 Hz)	(3.9 Hz)	(5.0 Hz)	(1.9 Hz)			
δ_{C}	96.5	92.2	100.0	93.2	93.6		
Lowary data⁵⁰							
δ_{H}	4.62	5.23	5.07-5.05	5.07-5.05	5.27	D_2O	external acetone at δ_{H} 2.225, δ_{C} 31.07
Multiplicity	d	d	m	m	d		
$^3J_{\text{H1,H2}}$	(8.1 Hz)	(4.0 Hz)			(5.3 Hz)		
δ_{C}	97.6	93.3					
Molinaro data⁴⁷							
δ_{H}		4.97					internal acetone at δ_{H} 2.225, δ_{C} 31.45
Multiplicity		d				D_2O	
$^3J_{\text{H1,H2}}$		(3.9 Hz)					
δ_{C}		96.6					

The spectral data of the synthesized bradyrhizose were consistent with the literature data from Yu and Lowary syntheses^{48,50} as an inspection of the ^1H NMR spectra of **20** in D_2O with HOD as an internal standard revealed that the structure of bradyrhizose give rise in solution to an equilibrium mixture consisting of two different pyranose forms **a** and **b**, the regioisomer **c**, and the

furanose forms **d** and **e** (**Table 21**). The anomeric signals of H-1 at δ_{H} 4.61 and 5.21 ppm corresponds to the β - and α -anomers of pyranose forms **a** and **b** with $^3J_{\text{H1,H2}}$ coupling constants of 8.1 and 4.3 Hz, respectively. The H-1 anomeric signals observed at δ_{H} 5.05 and 5.25 ppm corresponds to the α - and β -anomers of furanose forms **d** and **e**, respectively, while the anomeric signal observed at 5.04 ppm is attributed to the regioisomeric form **c**. As was previously highlighted in Chapter 1, the deviations in both the ^1H and ^{13}C NMR spectra chemical shifts observed in (**Table 21**) results from the use of different internal standards.

2.2 Conclusions

In summary, an effective synthesis of bradyrhizose has been developed from D-glucose in 14 steps and 6% overall yield (**Scheme 48**). This synthesis differs from the known literature methods as it involves the fusion of the bicyclic ring onto an existing pyranose framework as opposed to the fusion of a pyranose ring onto a preformed inositol skeleton. It is worth noting that this synthesis also involves fewer steps with minimal usage of protecting groups in comparison to the literature syntheses described in Chapter 1.



Scheme 48. Synthesis of bradyrhizose **20** from D-glucose **229**

CHAPTER 3 STEREOSELECTIVE SYNTHESIS OF THE EQUATORIAL GLYCOSIDES OF 3-DEOXY-D-MANNO-OCT-2-ULOSONIC ACID

3.1 Background

As a virulence factor, the bacterial capsule is an important factor in the propagation of bacterial infections by Gram-negative in humans. KDO, a constituent of the bacterial capsule, has been found to commonly form (2→3) or (2→6) equatorial glycosidic linkages with other sugar residues.⁷¹⁻⁷⁶ Therefore, the development of stereocontrolled synthetic methods for accessing equatorial KDO glycosides in high yields and selectivity as well as use of such pure glycosides as candidates in the development of antibacterial vaccines is of importance. As discussed in chapter 1, very few selective glycosylation methods have been reported for synthesizing β -KDO glycosides, with only few cases demonstrating high selectivity, hence there is a need to develop an efficient method.

Crich and co-workers demonstrated that excellent equatorial selectivity was attainable in the pseudaminic acid series with donor 219, that was shown to take up the least reactive and most equatorially selective conformation about its C6-C7 bond (**Figure 28**).⁹⁸

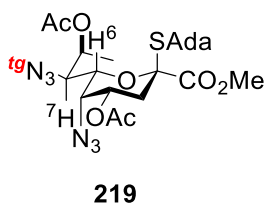


Figure 28. Pseudaminic donor 219 with a predominant *tg* conformation about its exocyclic C6-C7 bond

Recognition of the pseudo-enantiomeric relationship between pseudaminic acid **228** and 3-deoxy-D-manno-oct-2-ulosonic acid (KDO) **102** (**Figure 19**), leads to the prediction that KDO donors will populate the *tg* conformation about their exocyclic 6,7-bond and will display excellent

equatorial selectivity under the standard conditions used by Crich and co-workers.⁹⁸ Accordingly, the synthesis of KDO donors with strategic protecting groups and their use in the stereocontrolled synthesis of KDO glycosides are the focus of this chapter.

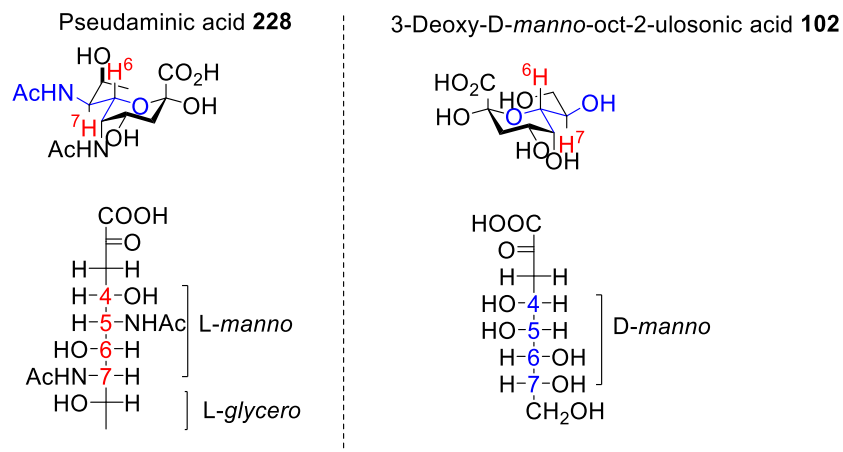


Figure 19. Pseudo-enantiomeric relationship of pseudaminic acid **228** and KDO **102**

3.2 Results and discussion

3.2.1 Synthesis of a key KDO acetonide intermediate

The synthesis of KDO in general is relatively trivial and many syntheses have been reported in the literature. The synthesis of KDO derivative **326** from D-mannose **323** as reported by Chai and co-workers was adopted for these studies as it provides the targeted KDO derivative in a minimum number of steps that use practical chemistry.¹³¹ Thus, isopropylidenation of **323** with 2,2-dimethoxypropane in the presence of a catalytic amount of *p*-TsOH monohydrate gave **324** in 95% yield (**Scheme 50**). The TBS protected phosphonate ester¹³¹ **322** was prepared according to (**Scheme 49**) and utilized in the HWE condensation with **324** in the presence of *t*-BuOLi in THF yielding **325** in 84% yield. TBAF mediated cleavage of the silyl ether followed by cyclization afforded compound **326** in 76% yield.¹³¹ Subsequently, acetylation on **326** in the presence of pyridine and acetic anhydride gave **327** in good yield (**Scheme 50**).

323

$\xrightarrow[p\text{-TsOH}]{\text{DMF}}$

324, 95%

$\xrightarrow[t\text{-BuOLi}]{\text{THF, 0 } ^\circ\text{C}}$

325, 84%

$\xrightarrow[\text{THF, 0 } ^\circ\text{C}]{\text{TBAF}}$

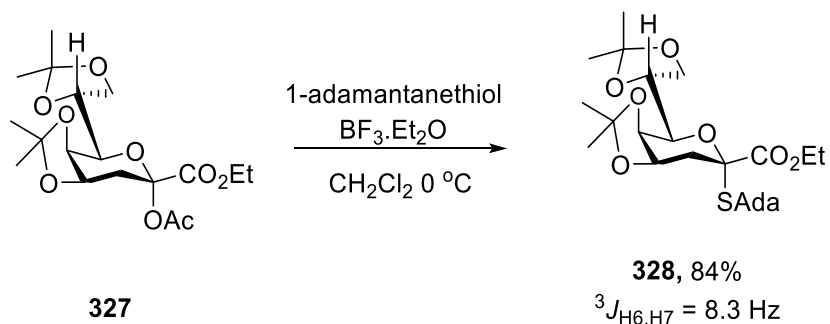
326, 76%

$\xrightarrow[\text{pyridine 0 } ^\circ\text{C}]{\text{DMAP, Ac}_2\text{O}}$

327, 91%

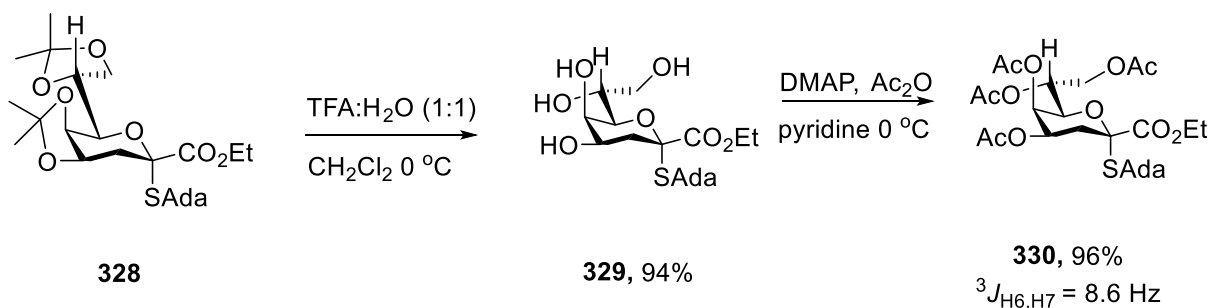
3.2.2 Synthesis of KDO thioglycosyl donors

Attention was then turned to the synthesis of KDO thioglycosyl donors using compound **327** as the precursor, and to establishing the conformation about their exocyclic bond by measurement of the $^3J_{6,7}$ coupling constant. Thus, thioglycoside **328** was obtained in 84% yield from compound **327** by treatment with 1-adamantanethiol in the presence of $\text{BF}_3 \cdot \text{Et}_2\text{O}$ (**Scheme 51**). Adamantanethiol was selected for this reaction because it presents less odor problems and most importantly, it poses good electron donating properties.¹³²



Scheme 51. Preparation of thioglycoside **328** and its H6,H7 coupling constant

Inspection of the ^1H NMR spectrum of compound **328** revealed a $^3J_{6,7}$ coupling constant of 8.3 Hz (Scheme 51). This value was comparable to those obtained previously by Unger and co-workers in ammoniated KDO salts⁹⁹ as well as in the pseudaminic acid series by Crich and co-workers.⁹⁸ This observation confirmed the existence of a predominant *tg* conformation about the exocyclic bond in the thioglycoside **328**. Thioglycosyl donor **330** was obtained by a two-step reaction sequence involving cleavage of the acetonide groups with aqueous trifluoroacetic to give tetraol **329** and acetylation of **329** with an overall 96% yield (**Scheme 52**).

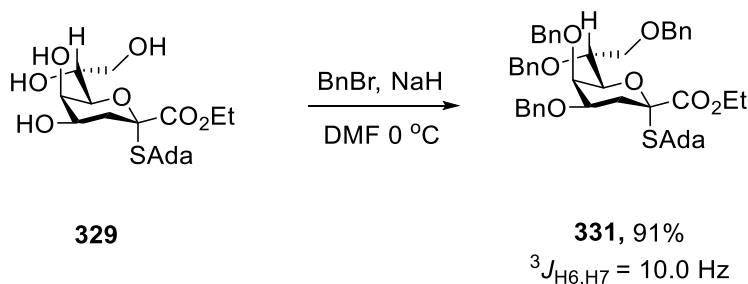


Scheme 52. Preparation of KDO thioglycosyl donor **330** from the acetonide derivative **328**

The ^1H NMR spectrum of compound **330** also revealed a $^3J_{6,7}$ coupling constant of 8.6 Hz, thus confirming the predominant *tg* conformation of its exocyclic bond.

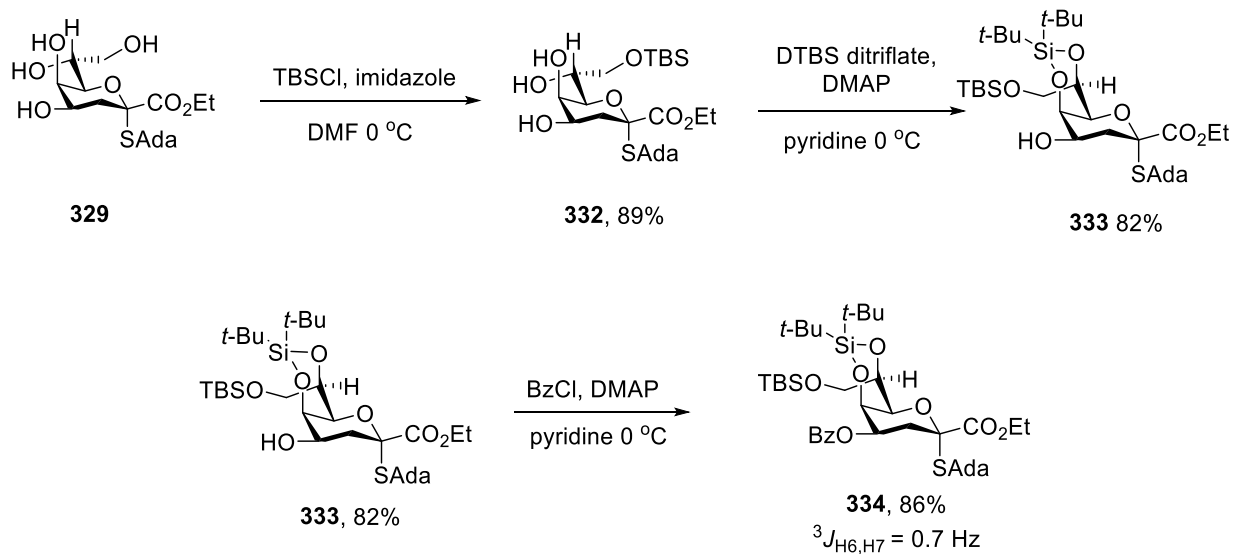
Next, thioglycoside **331** was obtained in excellent yield by treating tetraol **329** with benzyl bromide and sodium hydride in dimethylformamide (**Scheme 53**). A $^3J_{6,7}$ coupling constant of 10.0

Hz observed in the ^1H NMR spectrum of compound **331** demonstrated the predominant *tg* conformation about its exocyclic bond.



Scheme 53. Synthesis of benzylated thioglycoside **331** from tetraol **329**

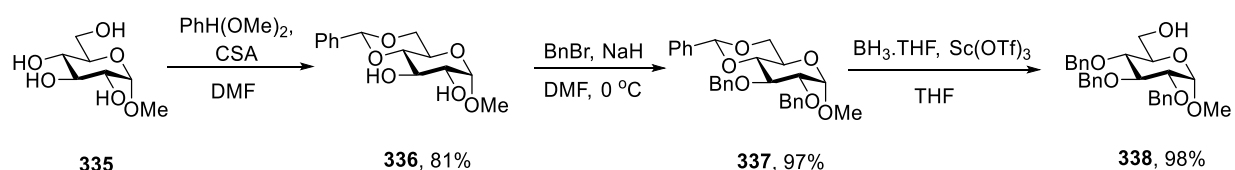
Subsequently, KDO thioglycosyl donor **334** was obtained from tetraol **329** via selective silylation of the primary alcohol to give **332**, followed by installation of the di-*tert*-butylsilylene acetal in compound **333**, and eventually benzylation, all in excellent yields (**Scheme 54**). As expected, the $^3J_{\text{H6,H7}}$ coupling constant of 0.7 Hz in the ^1H NMR spectrum of **334** confirmed that the 6,7-bond in the bicyclic donor **334** is locked in an approximate *gg* conformation.



Scheme 54. Synthesis of a silyl protected KDO donor **334**

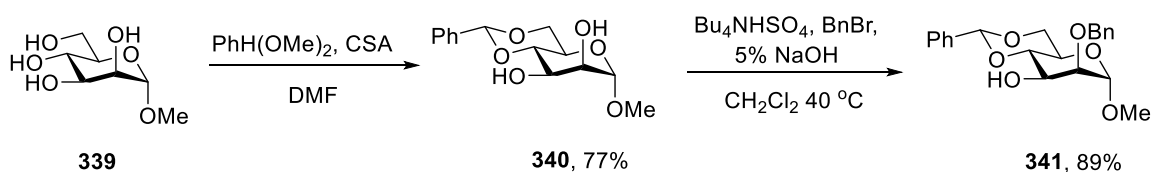
3.2.3 Preparation of acceptors

Turning to acceptor preparation, the selection of acceptors **338**, **341**, **346**, **351**, **360** and **368** as models having free hydroxyl group at either C-3 or C-6 positions was based on their presence in various bacterial KDO equatorial glycosides as discussed in chapter 1. Methyl glycosyl acceptor **338** was obtained from methyl α -D-glucopyranoside **335** via installation of a benzylidene acetal in **336** followed by benzylation and finally selective cleavage of the benzylidene acetal, with modest yields observed in all the steps (**Scheme 55**).¹³³



Scheme 55. Preparation of the methyl glucosyl acceptor **338**

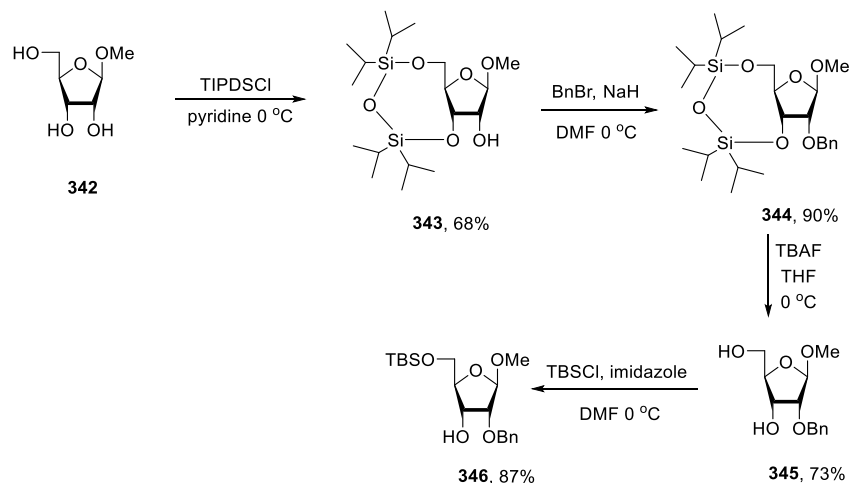
As previously reported in the literature, methyl α -D-mannoside **339** was converted to benzylidene acetal derivative **340**. Reaction of **340** with tetrabutylammonium hydrogen sulfate, benzyl bromide and aqueous sodium hydroxide in dichloromethane at reflux selectively afforded the 2-O-benzyl ether **341** in 89% yield (**Scheme 56**).¹³⁴



Scheme 56. Synthesis of mannosyl acceptor **341** from D-mannoside

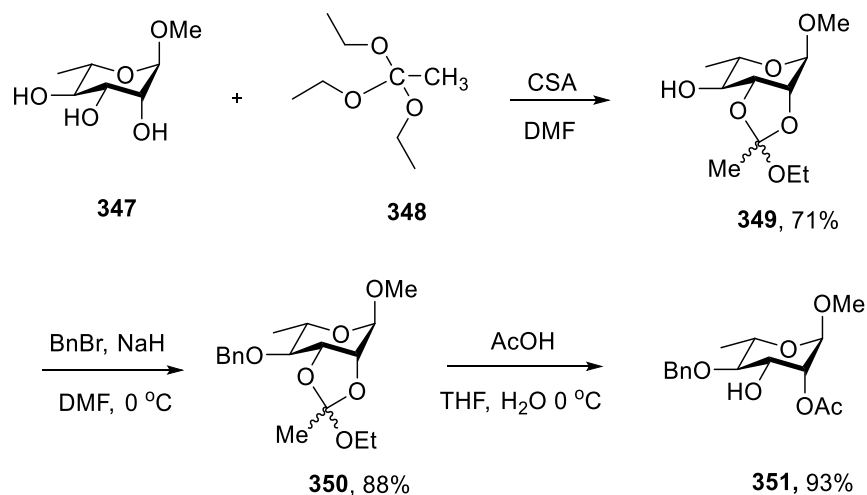
Ribofuranosyl acceptor **346** was obtained in four steps from methyl β -D-ribofuranoside **342**. Thus, treatment of methyl β -D-ribofuranoside **342** with 1,3-dichloro-1,1,3,3-tetraisopropylidisiloxane led to selective protection of C3-OH and C5-OH resulting in compound **343**. Subsequent benzylation of compound **343** followed by cleavage of the silyl protecting group

with TBAF gave diol **345**. Selective silylation of the primary C5-OH with TBSCl then gave acceptor **346** in 87% yield.¹³⁵



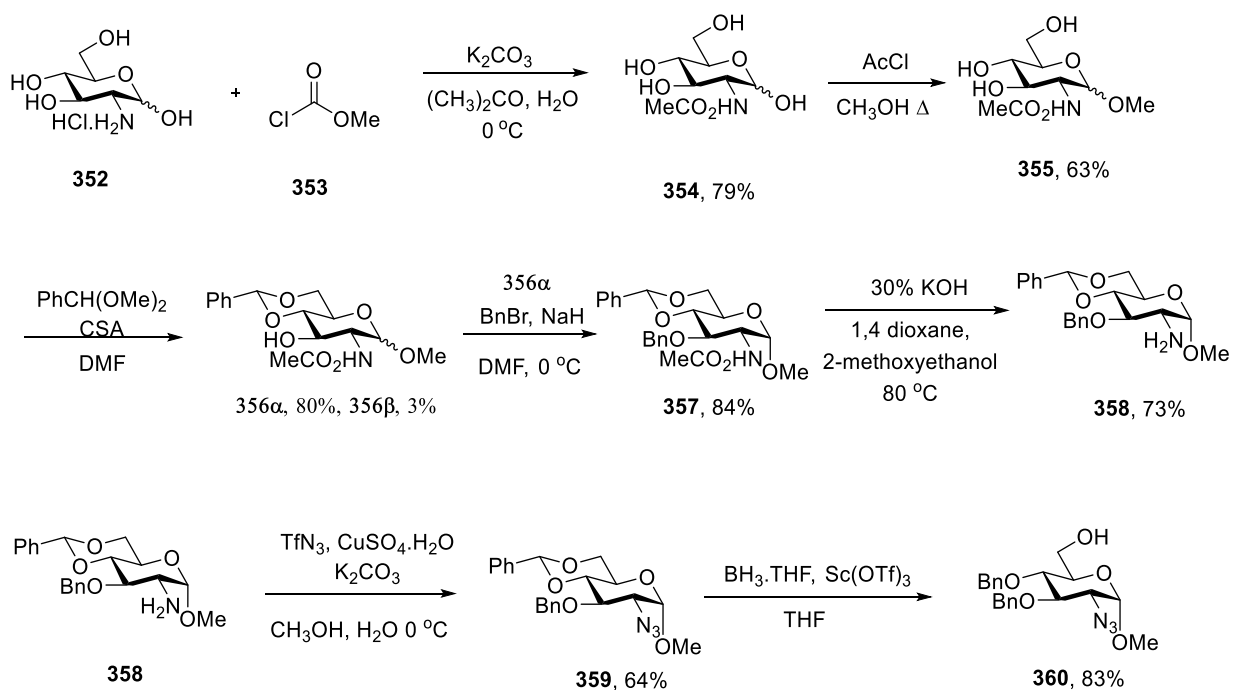
Scheme 57. Synthesis of the methyl ribofuranosyl acceptor **346**

Methyl α -L-rhamnosyl acceptor **351** was obtained by a reaction sequence involving treatment of methyl rhamnoside **347** with triethyl orthoacetate in the presence of 10-camphorsulfonic acid to yield to the 2,3-ortho ester **349** as a mixture of diastereoisomers. Benzylation at the C4-OH position and acid-catalyzed regioselective ring opening of the ortho ester then afforded the desired acceptor **351** in 93% yield (**Scheme 58**).¹³⁶



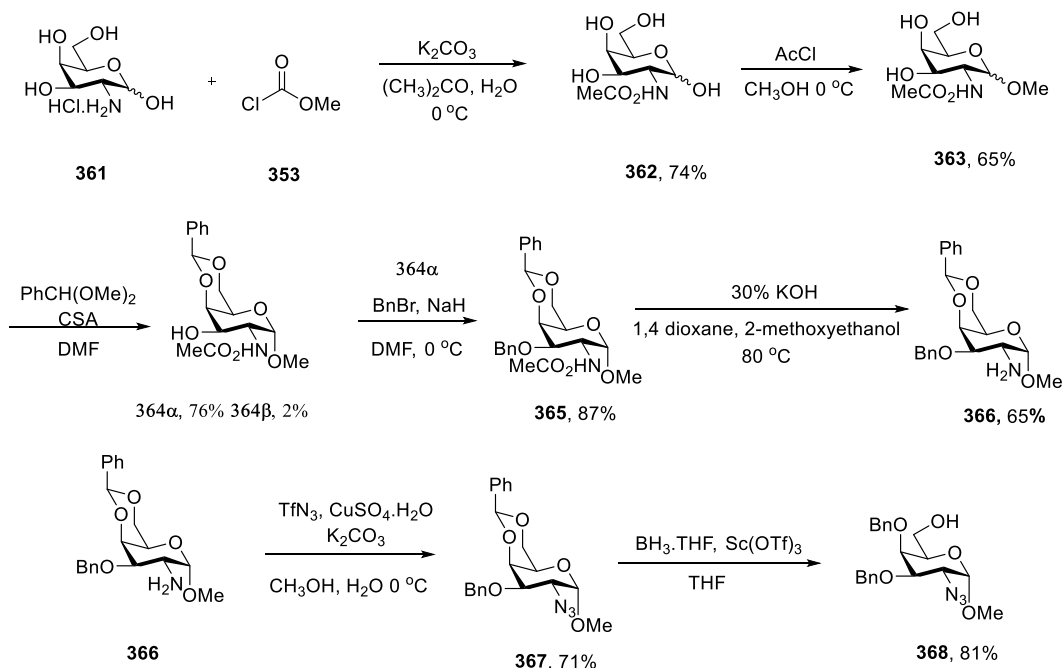
Scheme 58. Preparation of acceptor **351**

Starting from D-glucosamine hydrochloride **352**, methyl 2-deoxy-2-azido-4,6-*O*-benzylidene- α -D-glucopyranoside **360** was synthesized using a known literature protocol.¹³⁷ Thus, D-glucosamine hydrochloride was treated with methyl chloroformate **353** in the presence of potassium carbonate to give carbamate **354**, which was dissolved in methanolic hydrogen chloride solution and heated under reflux to give **355**. Installation of the benzylidene acetal followed by cleavage of the carbamate protecting group gave **358**. Azidation in the presence of triflyl azide with subsequent selective cleavage of the benzylidene acetal gave the desired acceptor **360** in 83% yield (**Scheme 59**).



Scheme 59. Synthesis of acceptor **360**

The galactosyl **368** was obtained in 81% yield from intermediate **367** by adopting the synthetic protocol used in the synthesis of acceptor **360** (**Scheme 60**).



Scheme 60. Preparation of galactosyl acceptor **368**

3.3 Glycosylation reactions of KDO thioglycosyl donors

Glycosylation reactions were conducted under the standard conditions employed by Crich and co-workers⁹⁷⁻⁹⁸ for ease of comparison. Thus, activation of the donors was done in a 2/1 dichloromethane/acetonitrile solvent system at -78 °C using *N*-iodosuccinimide and trifluoromethanesulfonic acid in the presence of acid-washed 4 Å molecular sieves. Acid-washed molecular sieves were used to improve on yield and selectivity. Reaction mixtures were quenched by the addition of triethylamine at -78 °C before warming to room temperature and workup. All the coupling reactions afforded equatorial KDO glycosides in excellent yields and selectivity as outlined in (**Figure 29**).

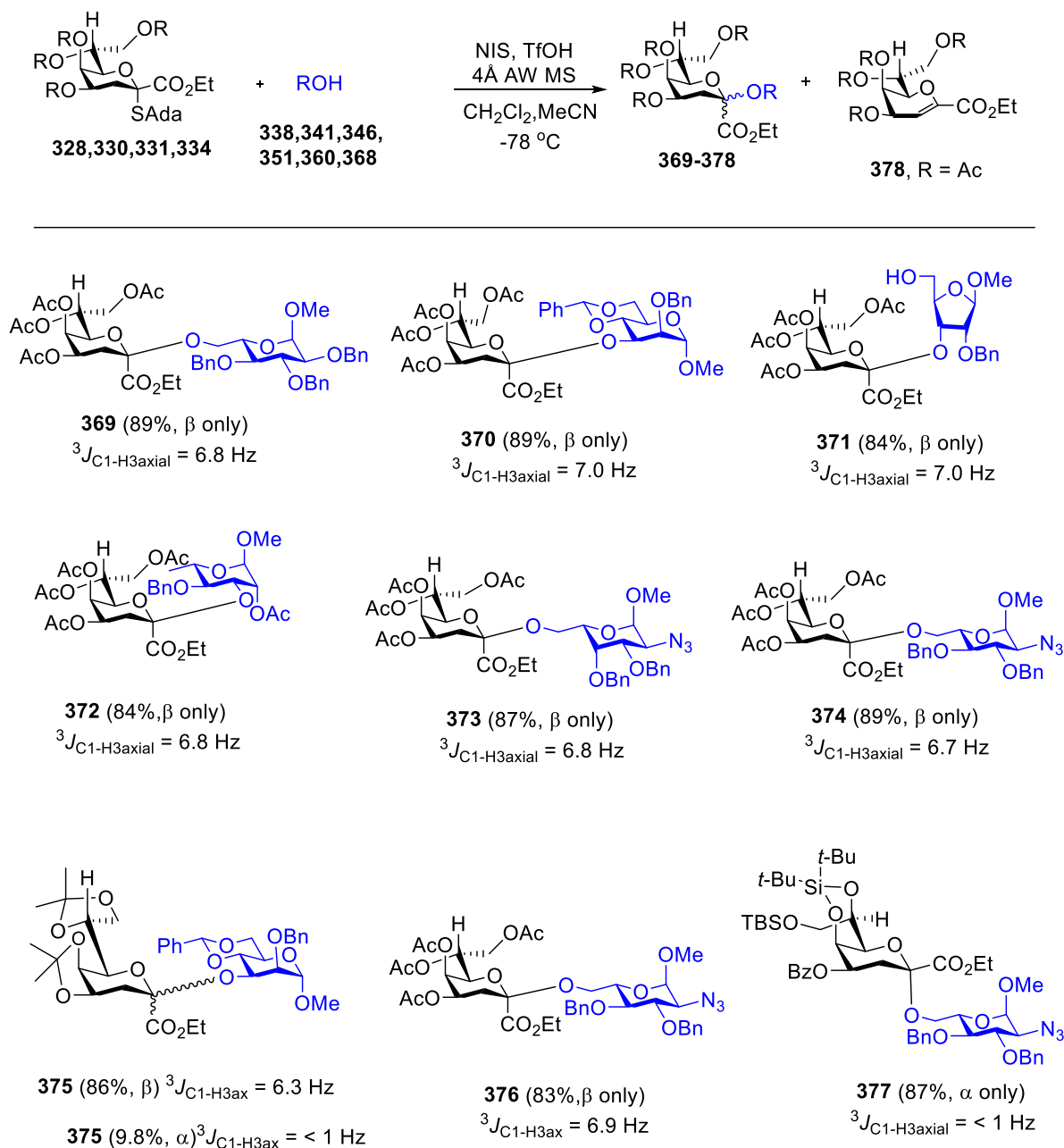


Figure 29. Synthesis of equatorially linked KDO glycosides

3.3.1 Assignment of configuration for coupled KDO glycosides

The assignment of anomeric configuration of KDO glycosides can be achieved by measurement of the $^3J_{C-1/H-3ax}$ heteronuclear coupling constant, as long as the KDO pyranose ring exists in the 5C_2 chair conformation.^{99,138} The configurational assignment using a $^3J_{C-1/H-3ax}$

heteronuclear coupling constant is based on the correlation of coupling constants with torsional angle.¹³⁹ As such, KDO glycosides with equatorial linkages have a $^3J_{C-1/H-3ax}$ value of 5.0–7.0 Hz, while the axially linked KDO glycosides have a value of ≤ 1.0 Hz. This difference observed for the $^3J_{C-1/H-3ax}$ coupling constants can be rationalized by a Karplus relationship¹⁴⁰ in which the dihedral angle of C1-C2-C3-H_{3ax} of the equatorial KDO anomer **378** is 180° while that of the axial KDO anomer **379** is 60° (**Figure 30**).

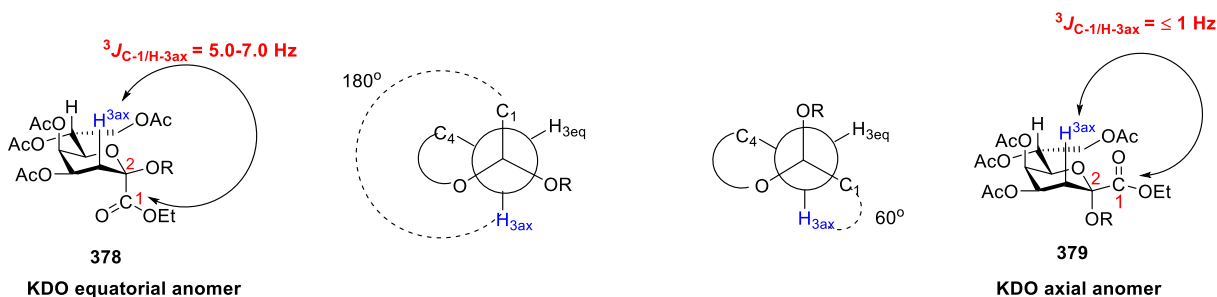
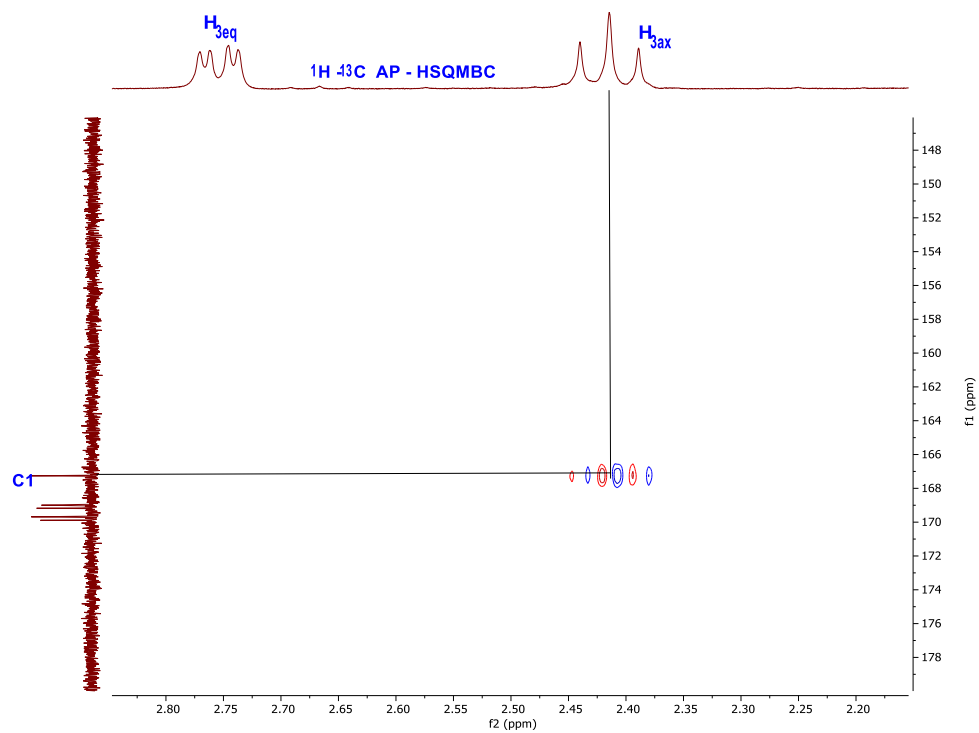
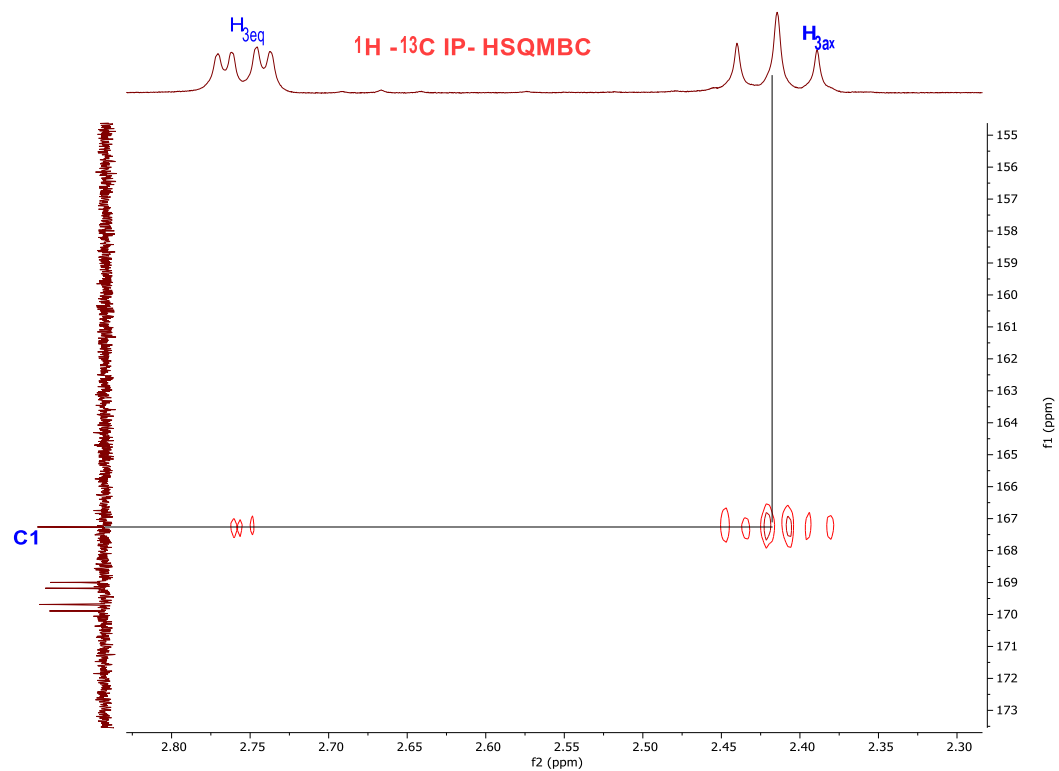


Figure 30. Karplus relationship showing the dihedral angle of equatorial and axial KDO glycosides and their corresponding coupling constants

The $^3J_{C-1/H-3ax}$ values of KDO glycosides were determined using HSQMBC experiments as illustrated in Figure 31. Thus, two complementary in-phase (IP) and anti-phase (AP) spectra were acquired from the HSQMBC experiments using data set points of 4096 x 512 with the inter-pulse delay optimized to 8 Hz, and then the difference spectrum was obtained to provide spin-state HSQMBC spectra from which the $^3J_{C-1/H-3ax}$ values were measured by comparing the relative displacement of a given cross-peak in both spectra (**Figure 31**).¹⁴¹



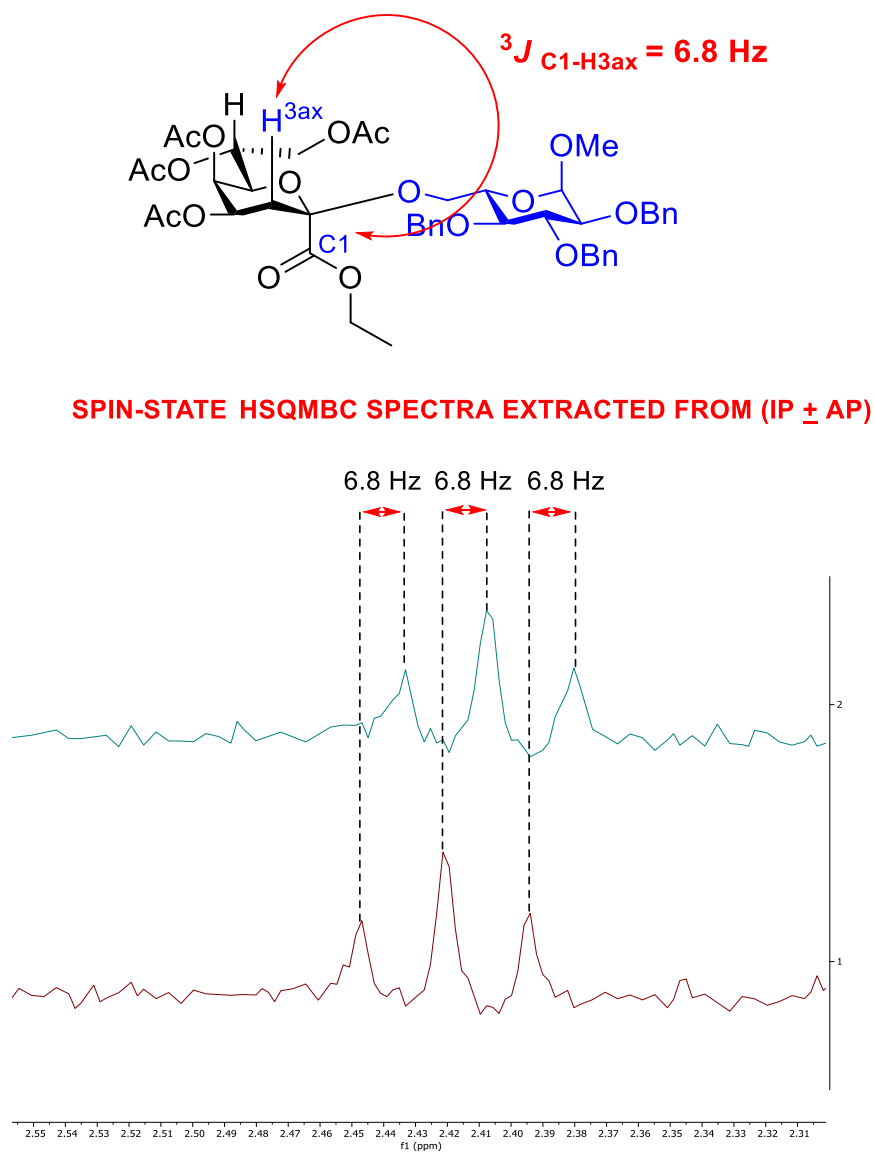


Figure 31. Determination of the configuration of KDO glycosides using the IPAP-HSQMBC experiment

Consistent with the literature findings, analysis of $^3J_{H,H}$ coupling constants around the pyranoside ring of the synthesized KDO thioglycosyl donors employed in this study revealed that donors **330**, **331**, and **334** adopted the 5C_2 chair conformation. However, minor distortion in the chair conformation of compound **328** and its glycosides caused by the *cis*-fused 4,5-*O*-acetonide

group was evident from a $^2J_{\text{H3eq,H3ax}}$ geminal coupling constant of 15.6 Hz, which contrasted with that of ~12.0 Hz seen in all other thioglycoside donors and their glycosides (**Table 22** and **23**).

Table 22. Chemical shifts of the synthesized KDO thioglycosyl donors

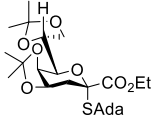
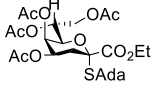
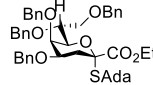
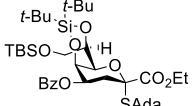
									
KDO donor	H _{3ax}	H _{3eq}	H-4	H-5	H-6	H-7	H _{8ax}	H _{8eq}	NMR solvent
328									
δ_{H}	2.07	2.66	4.52	4.32	3.59	4.37	4.08	3.85	CDCl ₃
multiplicity	t	dd	dt	dd	dd	ddd	dd	dd	
330									
δ_{H}	2.14	2.19	5.23	5.32 - 5.28	4.65	5.15	4.01	4.54	CD ₃ CN
multiplicity	t	dd	ddd	m	dd	ddd	dd	dd	
331									
δ_{H}	1.98	2.38	4.85 - 4.81	4.56 - 4.53	4.38	4.62	4.22-4.16	4.22-4.16	CDCl ₃
multiplicity	t	dd	m	m	dd	ddd	m	m	
334									
δ_{H}	2.85	2.67	5.70	4.92	4.86	4.53	3.86 - 3.81	3.86 - 3.81	CDCl ₃
multiplicity	t	dd	ddd	d	t	ddd	m	m	

Table 23. $^2J_{\text{H,H}}$ and $^3J_{\text{H,H}}$ coupling constants around the pyranoside ring of the synthesized KDO thioglycosyl donors

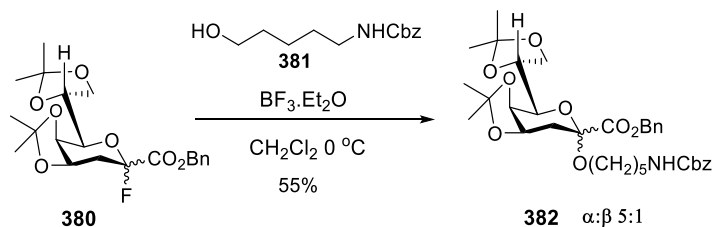
KDO donor	H _{3ax}	H _{3eq}	H-4	H-5	H-6	H-7	H _{6ax}	H _{8eq}	NMR solvent
328 ($J_{\text{H,H}}$)	15.6 Hz	15.6, 3.7 Hz	7.3, 3.5 Hz	3.4, 2.0 Hz	8.3, 2.0 Hz	8.3, 6.1, 3.7 Hz	9.1, 6.1 Hz	9.1, 3.7 Hz	CDCl ₃
330 ($J_{\text{H,H}}$)	12.1 Hz	12.1, 5.3 Hz	12.1, 5.3, 3.1 Hz	-	8.6, 1.5 Hz	8.6, 5.9, 2.7 Hz	12.2, 5.9 Hz	12.2, 2.8 Hz	CD ₃ CN
331 ($J_{\text{H,H}}$)	12.1	12.1, 4.0 Hz	-	-	10.2, 1.6 Hz	10.2, 5.0, 3.1 Hz	-	-	CDCl ₃
334 ($J_{\text{H,H}}$)	12.7 Hz	13.1, 4.6 Hz	12.2, 4.7, 2.7 Hz	2.8 Hz	0.7 Hz	6.5, 4.8, 0.7 Hz	-	-	CDCl ₃

Glycosylation of the peracetylated thioglycoside donor **330** with the methyl 2,3,4-tri-*O*-benzyl- α -D-glucopyranoside **338** afforded the desired equatorial glycoside **369** in 89% yield as a single anomer with a $^3J_{\text{C-1/H-3ax}}$ value of 6.8 Hz (**Figure 29**). In the same manner, coupling of donor **338** with mannopyranosyl acceptor **341**, ribofuranosyl acceptor **346**, rhamnopyranosyl acceptor **351**, glucopyranosyl acceptor **360**, and galactopyranosyl acceptor **368** afforded the expected equatorial glycosides **370-374** each as single equatorial anomers in excellent isolated yield. All products were found to display $^3J_{\text{C-1/H-3ax}}$ coupling constants ranging from 6.7 to 7.0 Hz. The glycal ester **378** was also isolated in minor amounts from these coupling reactions.

Of note is that the glycosylation reaction involving use of peracetylated thioglycoside donor **330** with the ribofuranosyl acceptor **346** was accompanied by cleavage of the primary silyl ether with no competing glycosylation at the primary position of the acceptor **346** observed. This observation suggested that the silyl cleavage occurred during workup and not in the course of the glycosylation.

Coupling of 4,5;7,8-di-*O*-isopropylidene-protected donor **328** to the mannosyl acceptor **341** resulted in the formation of the equatorial glycoside **375 β** in 86% isolated yield with a

$^3J_{C-1/H-3ax}$ coupling constant of 6.3 Hz. The α -anomer of **375** was also isolated in 10% yield with a $^3J_{C-1/H-3ax}$ coupling constant of <1.0 Hz. Since the *tg* conformation predominates in the side chain of donors **328**, **330** and **331** (Figure 29), it would be expected that all the three systems display high equatorial selectivity in the coupling reactions. The reduced selectivity observed with donor **328** is likely the result of the distortion of the pyranoside ring imposed by the presence of the *cis*-fused 4,5-*O*-acetonide group. This distortion is evident by a change in the $^2J_{H3ax, H3eq}$ coupling constant outlined in (Table 22). Indeed, the distortion of the 5C_2 chair conformation of related KDO glycosyl donors by cyclic isopropylidene at *O*-4/*O*-5 positions has been shown in the literature as an effective means of achieving α -selectivity in glycosylation reactions (Scheme 61).^{76, 142}



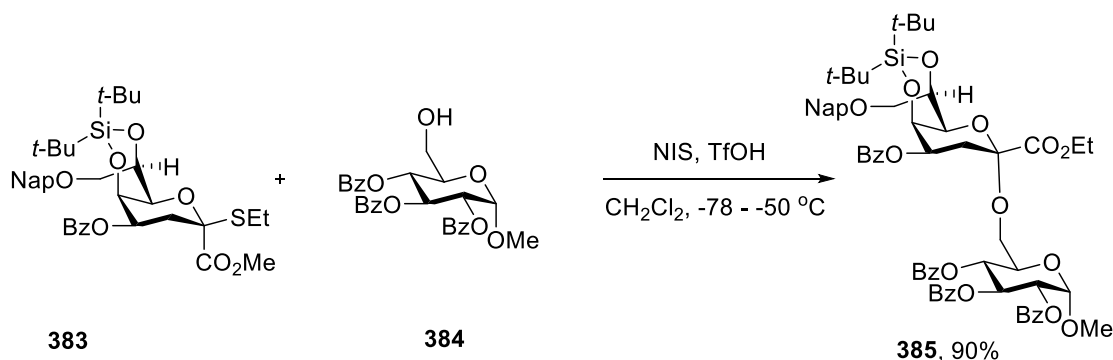
Scheme 61. Enhancement of α -selectivity by distortion of the 5C_2 chair conformation of donor

380

Gratifyingly, coupling of the perbenzylated donor **331** to the glucosyl acceptor **360** gave the desired equatorial glycoside **376** in 83% isolated yield. It was characterized by a $^3J_{C-1/H-3ax}$ value of 6.9 Hz. Both the peracetylated donor **328** and the perbenzylated donor **331** show excellent equatorial selectivity, suggesting that other donors containing different combinations of benzyl ether and acetate esters will also be good precursors for the selective synthesis of equatorial glycosides of KDO from bacterial capsular polysaccharides.

Yang and co-workers demonstrated that the closely related 5,7-*O*-silylene-protected KDO thioglycosides are excellent donors for the formation of axial glycosides (Scheme 62).¹⁴³ They

hypothesized that this selectivity arose from steric shielding of the β -face of the donor imposed by the bulky 5,7-di-*O*-*tert*-butylsilylene substituent.



Scheme 62. Synthesis of axial KDO glycosides using 5,7-di-*O*-*tert*-butylsilylene protected donor

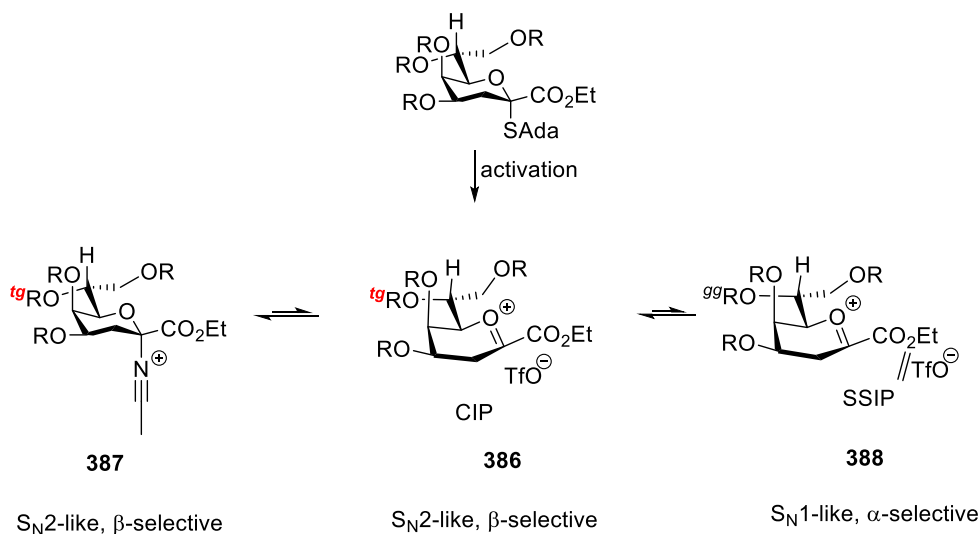
383

Consistent with the Yang findings, coupling of 5,7-di-*O*-*tert*-butylsilyl donor **334** with the acceptor **360** gave the axial glycoside **377**, which had a $^3J_{\text{C-1/H-3ax}}$ value of <1 Hz, in 87% isolated yield. In addition to the steric shielding of the β -face suggested by Yang and coworkers, the α -selectivity of donor **334** is likely a result of imposition of the *gg* conformation of the side chain by the 5,7-*O*-silylene acetal. Moreover, cleavage of the silyl group was consistent with the observation made during the formation of glycoside **371**.

The β -selectivity observed in the coupling reactions of KDO donors **328**, **330** and **331** results from the protecting groups ability to favor the *tg* conformation of the KDO side chain in which the electron withdrawing effect of the C6–O6 bond is maximized. This conformation stabilizes the covalent axial glycosyl triflate or its functional equivalent the contact ion pair **386**, or the glycosyl nitrilium ion **387**, and so the β -face attack of the covalent axial glycosyl triflate by the acceptor results in formation of the equatorial KDO glycosides.

On the other hand, when the protecting group imposes the *gg* conformation on the side chain, a looser solvent separated ion pair **388** is populated to a greater extent, which results in α -

selectivity, because the acceptor approaches the SSIP from the α -face to form the thermodynamically stable axial KDO glycosides (**Scheme 63**).



Scheme 63. Mechanistic hypothesis outlining the importance of side chain conformation on reactivity and selectivity of KDO glycosyl donors

3.4 Conclusions

In conclusion, the vital lessons learnt from recent work by Crich and co-workers on studies involving the role of configuration and conformation on the reactivity and selectivity of pseudaminic acid glycosyl donor led to the prediction that KDO donors would be highly equatorially selective in glycosylation reactions conducted under standard conditions as long as the KDO protecting group favors the predominant *tg* conformation of the KDO side chain. These predictions were borne out by the experimental findings that revealed excellent equatorial selectivity with the peracetyl and perbenzyl-protected KDO donors **330** and **331**, and to a lesser degree by the 4,5;7,8-di-*O*-isopropylidene-protected donor **328**. As would be expected, a change in the side conformation to the *gg* conformation in donor **334** led to a reversal in selectivity. This concept provides an effective and selective method for the synthesis of KDO equatorial glycosides similar to those found in numerous pathogenic bacteria.

CHAPTER 4 PROGRESS TOWARDS A STEREOCONTROLLED CONVERGENT SYNTHESIS OF A PENTASACCHARIDE CONTAINING THE TETRASACCHARIDE REPEATING UNIT OF *K. kingae* TYPE C CAPSULAR POLYSACCHARIDE

4.1 Background

Isolated in 1960, *Kingella kingae* is a Gram-negative bacterium belonging to the *Neisseriaceae* family. It is commonly known to cause pediatric bacteremia, osteomyelitis and septic arthritis in children aged 6 to 36 months. This pathogen is carried asymptotically in the oropharynx and spreads by close interpersonal contact. The colonization of the human mucosae by the bacterium occurs via its attachment to the respiratory epithelium using surface factors such as the type 4 pili, the trimeric autotransporter protein (Knh), and the polysaccharide capsule. The attachment enables the bacterium to penetrate into the host blood stream where its replication and spread to other sites in the human body occurs.^{144, 71, 72} Currently, the containment of *K. kingae* infections is through the administration of a wide array of antimicrobial drugs including β -lactam antibiotics that have been developed for treating infections caused by other bacterial pathogens.¹⁴⁵ As previously discussed in chapter 1, three structurally distinct *K. kingae* polysaccharide capsules have been identified in which 3-deoxy-D-manno-oct-2-ulosonic acid forms β -(2 \rightarrow 3)-linkages with 2-acetamido-2-deoxygalactose and D-ribose in capsules a and c respectively, while in capsule b, it forms β -(2 \rightarrow 6)-linkages with 2-acetamido-2-deoxyglucose.⁷¹⁻⁷²

There is a continuous need for the development of capsular polysaccharide-based vaccines against infections caused by bacterial pathogens; such efforts are often limited by the scarcity of pure bacterial isolates as well as the complexity of the bacterial glycan structures. As a result, selective chemical syntheses have been developed as an alternative solution for synthesis of such vaccine candidates.⁷⁵ In continuation of this quest, a stereocontrolled chemical synthesis of a

pentasaccharide containing the *K. kingae* type c capsular polysaccharide repeating unit capped by a suitable linker for conjugation was planned. The polymer of Rib- β -D-(1 \rightarrow 2)-Rib- β -D-(1 \rightarrow 2)-Rib- β -D-(1 \rightarrow 4)-KDO- β -D-(2 \rightarrow O)-linker containing a hydrophobic linker equipped with a terminal primary amine group **403** was targeted (**Figure 32**).

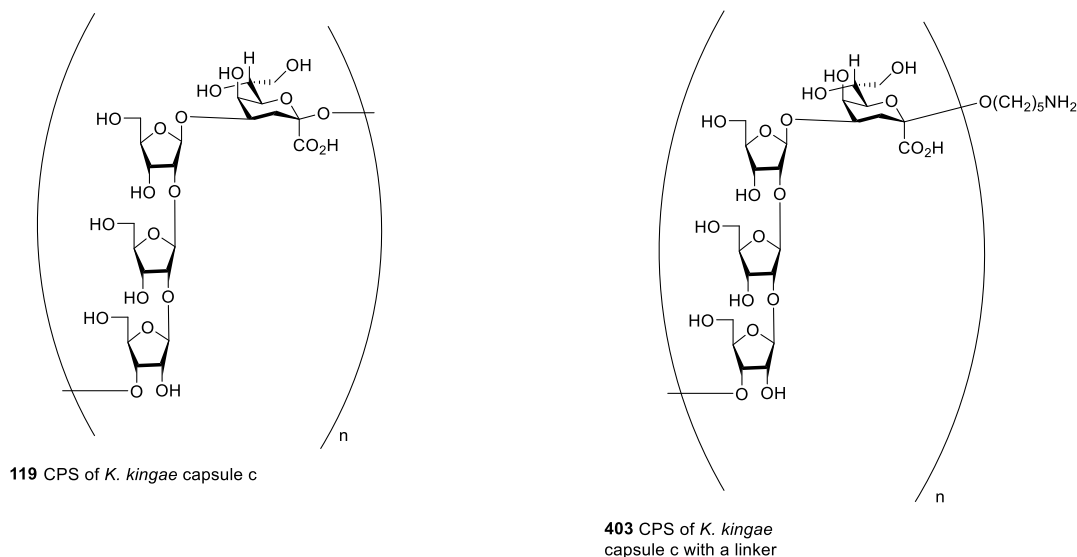


Figure 32. *K. kingae* capsule c repeating unit **119** and its derivative **403** containing a linker

Building on the results presented in chapter three, a similar trend in selectivity outcome was predicted to be observed for the construction of the (2 \rightarrow O-linker) equatorial glycosidic linkage present in **403** by employing the equatorially selective peracetylated KDO donor **330** (**Figure 33**).

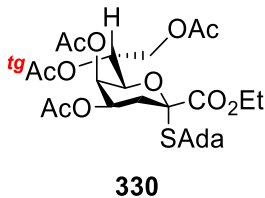
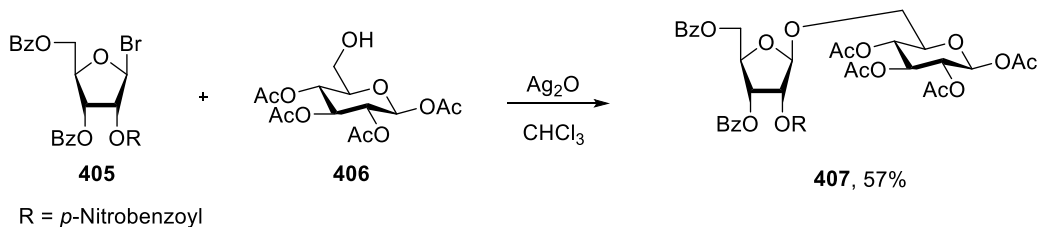


Figure 33. Equatorially selective peracetylated donor **330**

Similarly, the stereocontrolled construction of β -(1 \rightarrow 2) and β -(1 \rightarrow 4) glycosidic linkages in compound **403** (**Figure 32**) can be straightforwardly achieved using ribofuranosyl donors

possessing acyl-protecting group on O2. 1,2 *trans*- β -Glycosidic linkages in pyranose or furanose systems are known to be stereoselectively formed with the help of stereodirecting participation by C2 acyloxy groups in such systems.¹⁴⁶ For example, Gorin and co-workers demonstrated that coupling of β -D-ribofuranosyl bromide **405** and acceptor **406** under the mediation of silver oxide resulted in the formation of ribofuranoside **407** (Scheme 64).¹⁴⁷



Scheme 64. Synthesis of a β -ribofuranoside via neighboring participation of the *p*-nitrobenzoyl group

Therefore, it is anticipated that the neighboring group participation by an acyl group can be used to facilitate the formation of a predominant 1,2 *trans*- β -glycosidic linkage. Progress towards a stereocontrolled convergent synthesis of the pentasaccharide **404** is described in this chapter.

4.2 Results and discussion

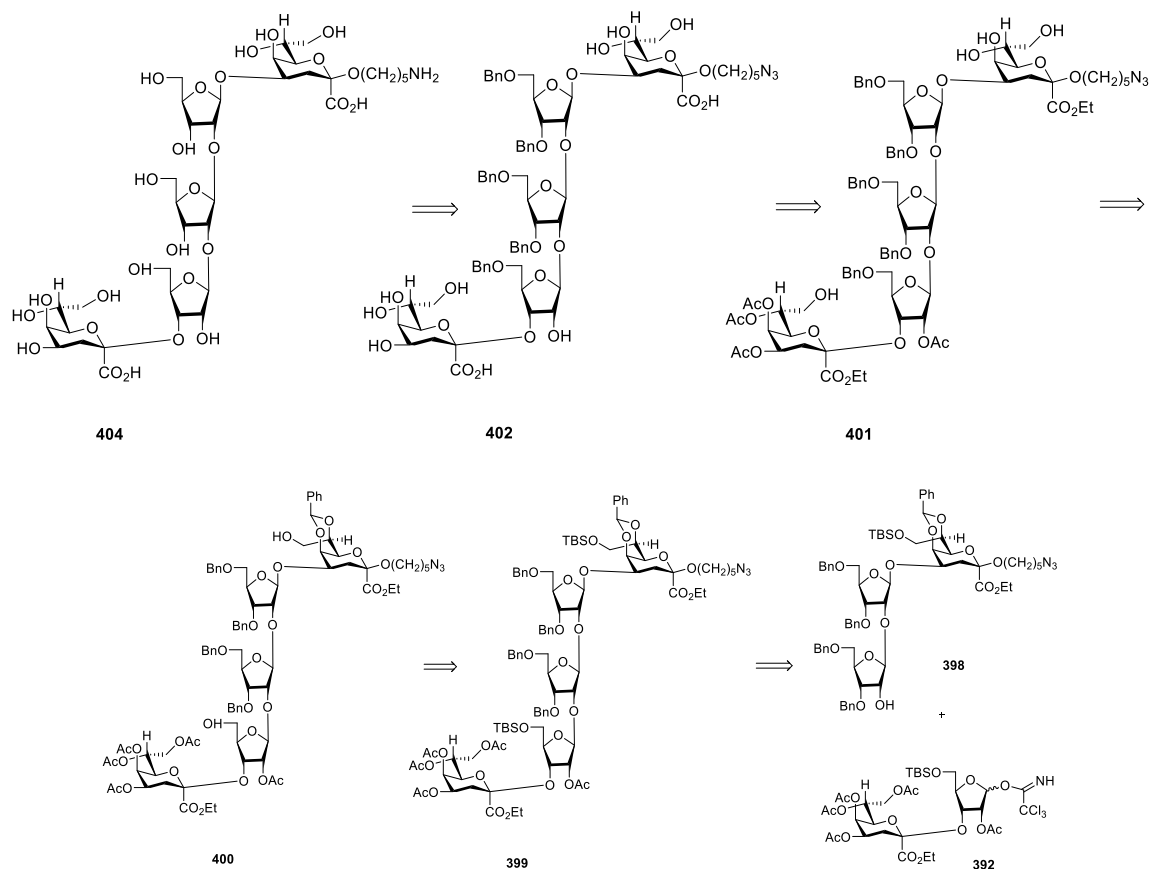
4.2.1 Retrosynthesis of compound 404

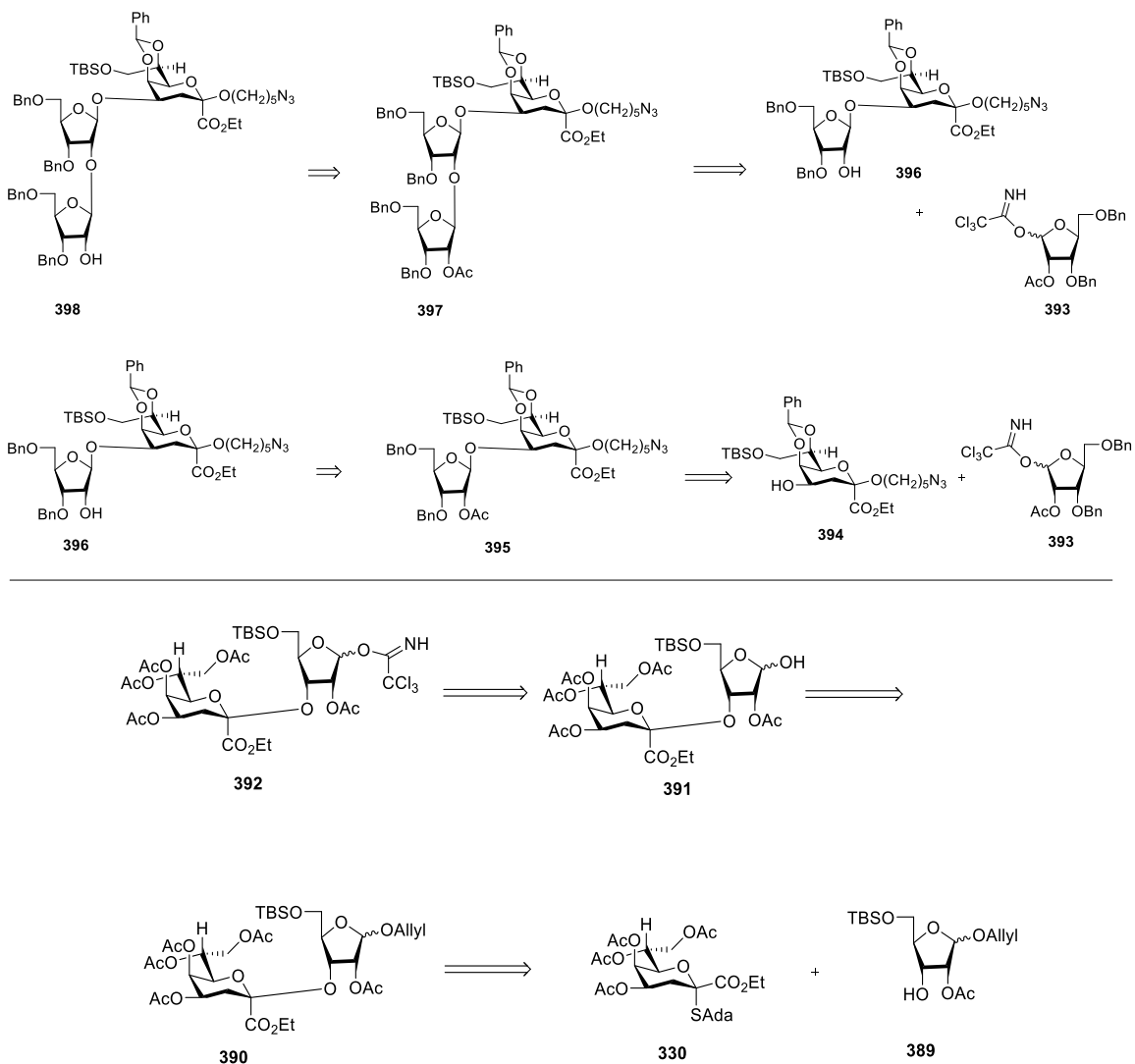
Rather than targeting the exact repeating unit, which is a tetrasaccharide, an extended pentasaccharide **404** was targeted (Scheme 65). This pentasaccharide was selected as the target for synthesis because it contained two KDO equatorial linkages, one from a primary alcohol (linker) and one from a secondary alcohol (ribose); it is therefore a better test of the synthetic methodology developed for synthesis of equatorial KDO linkages.

Pentasaccharide **404** can be obtained from the protected derivative **399** via a sequence of reactions involving desilylation, benzylidene acetal cleavage, deacetylation and debenzoylation

(Scheme 65). Compound **399** can be formed from a stereoselective convergent 3+2 glycosylation approach by employing trisaccharide acceptor **398** and the ribofuranosyl imidate donor **392**. Acceptor **398** can be obtained from **397** under Zemplén deacetylation conditions. As a key intermediate, masked acceptor **397** can be obtained by first performing the assembly of the β -(1 \rightarrow 4)-linkage using benzylidene protected KDO acceptor **394** and ribofuranosyl imidate donor **393**, followed by elongation at O2' of **396** using donor **393** (Scheme 66).

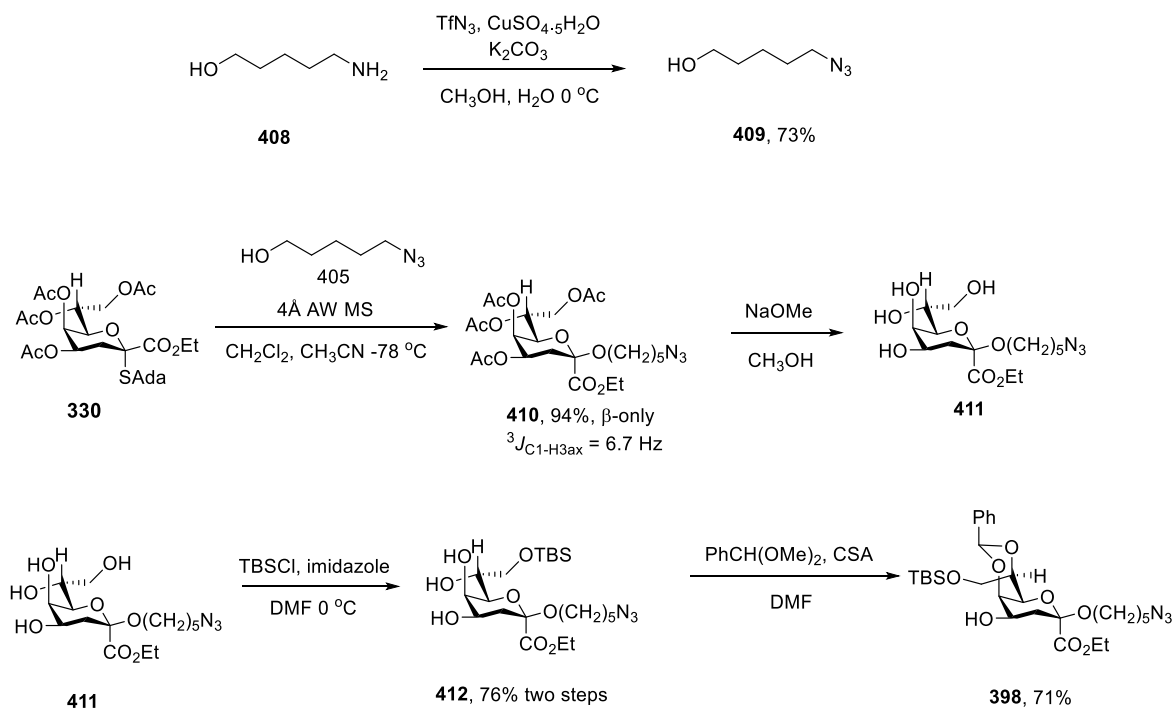
The formation of imidate donor **392** can be realized by first forming the β -(2 \rightarrow 3)-linkage using the equatorially selective peracetylated KDO donor **330** and ribofuranosyl acceptor **389** under well-established standard glycosylation conditions. Subsequent selective cleavage of the allyl ether followed by installation of the imidate group should result in the desired donor **392** (Scheme 66).



Scheme 65. Retrosynthetic analysis of the convergent 3 + 2 synthesis of pentasaccharide **404****Scheme 66.** Retrosynthetic analysis of the synthesis of trisaccharide acceptor **398** and ribofuranosyl donor **392**.**4.2.2 Preparation of KDO donor 330 and acceptor 398**

The synthesis of pentasaccharide **404** began with preparation of key KDO donor **330**, which was achieved as described in chapter three. The preparation of acceptor **398** from **330** required the use of 5-azido-1-pentanol **409** as an acceptor. This acceptor was readily made in 73% yield by treatment of the commercial amino alcohol **408** with triflyl azide and copper sulfate

(Scheme 67).¹⁴⁸ As would be expected, excellent equatorial selectivity and a $^3J_{C-1/H-3ax}$ value of 6.7 Hz observed for the glycoside in the glycosylation step were consistent with the observations described in chapter three. Deacetylation and subsequent selective protection of the C6 hydroxyl with *tert*-butyldimethylsilyl chloride afforded compound **412** in good yield. Regioselective installation of the benzylidene group on O4 and O6 under acidic conditions then furnished the targeted KDO acceptor **398** in 71% yield (Scheme 67).

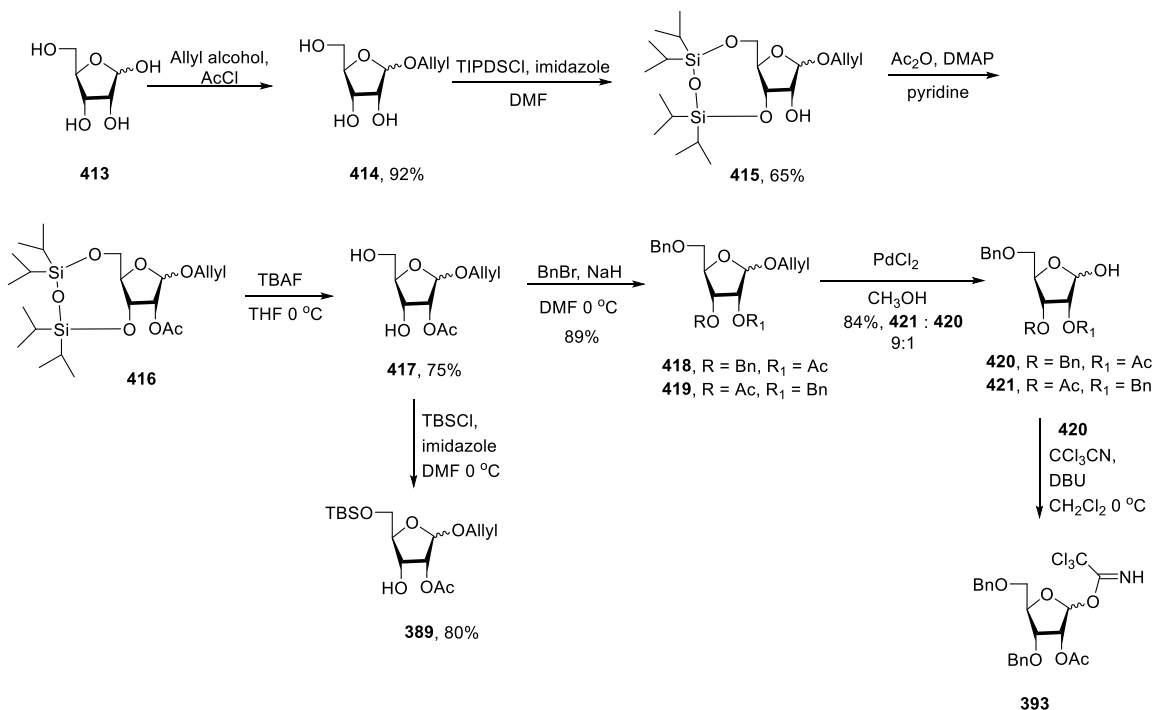


Scheme 67. Preparation of KDO acceptor **398** from donor **330**

4.2.3 Preparation of the ribofuranosyl imidate donor **393** and the ribosyl acceptor **389**

Attention was then focused on the synthesis of ribofuranosyl derivative **393** and acceptor **389**. Starting from D-ribose, compound **417** was obtained in four steps (Scheme 68). Thus, Fischer glycosylation of allyl alcohol with D-ribose **413** followed by selective silylation on C3-OH and C5-OH of **414** with a cyclic disiloxane group gave **415**. Subsequent acetylation at C2-OH followed by cleavage of the silyl protecting group with TBAF gave diol **417**. Treatment of diol **417** with

sodium hydride and benzyl bromide yielded to an inseparable mixture of **418** and **419** that were carried to the next step, which involved selective cleavage of the allyl ether using palladium chloride¹⁴⁹ yielding to **421** and **420** in a ratio of 9:1 as determined from the reaction mixture. The verification of the intramolecular acetyl group migration to C3 position of **417** at the benzylation step was confirmed by 1D and 2D spectral analysis of the inseparable mixture of **421** and **420**. Thus, a comparison of the proton and carbon chemical shifts observed in the mixture in relation to the 1D and 2D spectra of **417**, revealed acetyl migration leading to compound **421** (Table 23). Unfortunately, the separation of **420** and **421** could not be achieved in a timely manner due to the COVID-19 outbreak. Hypothetically, treatment of form of **420** with trichloroacetonitrile and DBU would furnish the desired imidate donor **393**. In parallel, ribofuranosyl acceptor **389** was obtained in 80% yield via treatment of diol **417** with *tert*-butyldimethylsilyl chloride and imidazole.



Scheme 68. Synthesis of acceptor **389** from diol **417** and the proposed preparation of imidate donor **393** from **420**

Table 24. Comparison of ^1H and ^{13}C chemical shifts of a mixture of compounds 420 and 421 in relation to compound 417

		H-2	H-3	
417	δ_{H}	5.07	3.90	
	δ_{C}	69.5	67.3	
420	δ_{H}	5.09	3.61	
	δ_{C}	70.3	62.8	
421	δ_{H}	3.22	5.87	
	δ_{C}	76.3	67.4	

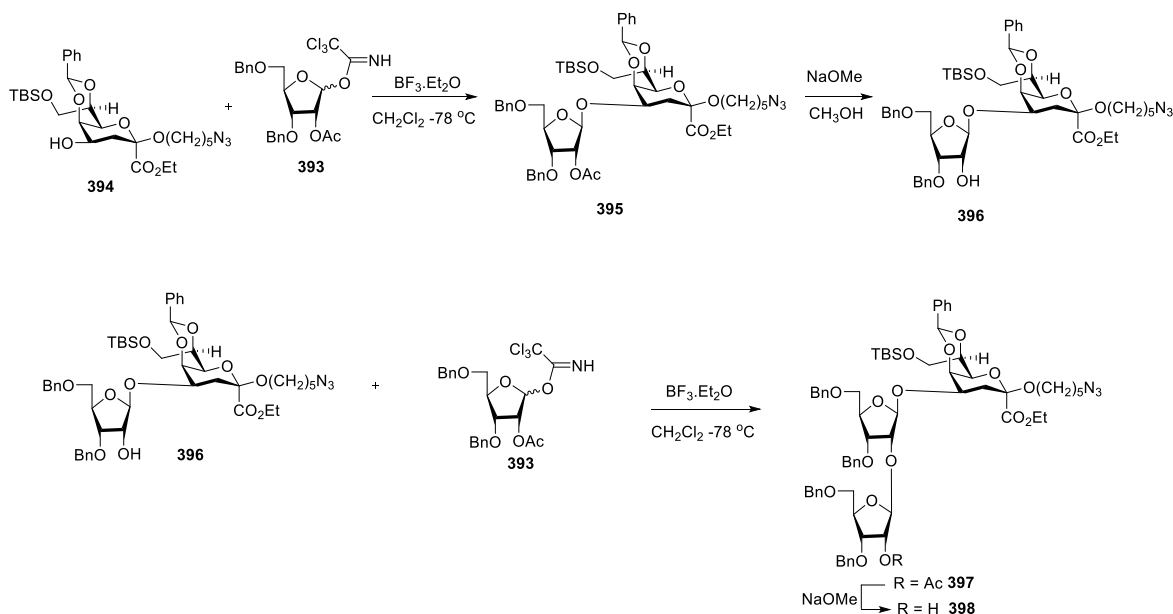
4.3 Intended completion of syntheses

Unfortunately, the intended syntheses had to be curtailed because of the shutdown following the COVID-19 outbreak. The intended route is described here in the hope that it may be of use to a later worker.

4.3.1 Preparation of key trisaccharide acceptor 398

Future directions will involve preparation of acceptor **398** from donor **393** and acceptor **394** (Scheme 69). It is predicted that $\text{BF}_3 \cdot \text{Et}_2\text{O}$ mediated coupling of donor **393** with acceptor **394** will lead to the stereoselective formation of the β -(1 \rightarrow 4)-linkage in compound **395**. It is reasoned that the stereoselective formation of the β -linkage will be facilitated by neighboring group participation of the C2 acetyl group in donor **393**. Deacetylation using sodium methoxide in methanol will furnish acceptor **396**, which then will be coupled to imidate donor **393** under the mediation of $\text{BF}_3 \cdot \text{Et}_2\text{O}$ resulting in disaccharide **397**. Again, stereodirecting participation by the C2 acetyl group in donor **393** is expected to aid in the stereoselective formation of the β -(1 \rightarrow 2)-

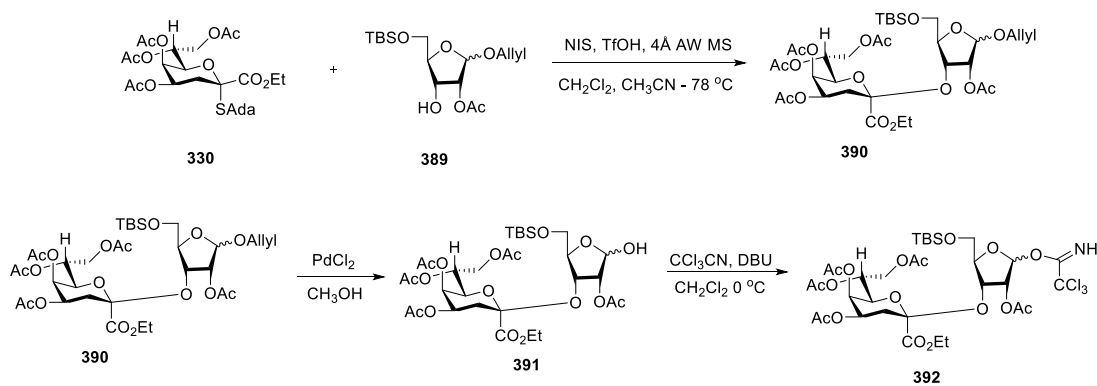
linkage in compound **397**. Subsequent cleavage of the acetyl group will furnish the desired trisaccharide acceptor **398**.



Scheme 69. Proposed preparation of trisaccharide acceptor **398**

4.3.2 Preparation of key imidate donor **392**

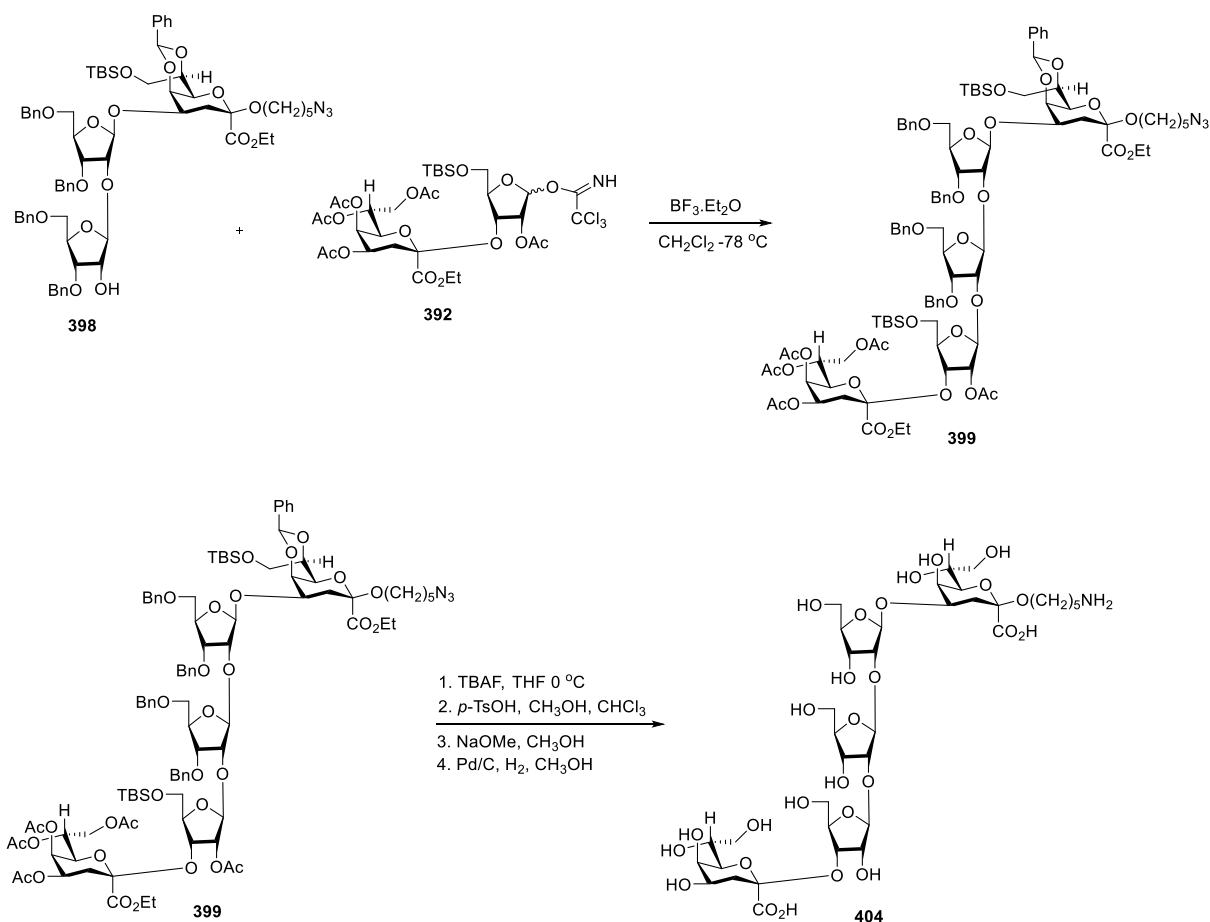
Based on the work described in chapter three, it is envisioned that the masked donor **390** containing a β -(2 \rightarrow 3)-linkage would be stereoselectively achieved through the glycosylation of an equatorially selective peracetylated KDO thioglycosyl donor **330** with ribofuranosyl acceptor **389** under the mediation of NIS/TfOH at -78 °C in a 2/1 CH₂Cl₂/CH₃CN solvent system (**Scheme 70**). Cleavage of the allyl ether in the presence of palladium chloride¹⁴⁹ followed by installation of the imidate group at the anomeric position using DBU and trichloroacetonitrile will furnish the desired donor **392**.



Scheme 70. Proposed stereoselective synthesis of **390** and preparation of imidate donor **392**

4.3.3 Stereocontrolled construction of the β -(1 \rightarrow 2)-linkage via a convergent 3+2 glycosylation approach

Stereoselective convergent 3+2 glycosylation of ribofuranosyl donor **392** and trisaccharide acceptor **398** under the activation of $\text{BF}_3 \cdot \text{Et}_2\text{O}$ in dichloromethane is expected to lead to the formation of pentasaccharide **399** containing the new β -D-Rib-(1 \rightarrow 2)- β -Rib linkage. Subsequent global deprotection (desilylation, benzylidene cleavage, removal of the acetyl-protecting groups under Zemplén conditions and debenzylation) would be expected to successfully yield to the compound **404** containing the tetrasaccharide repeating unit of *K. kingae* type c capsular polysaccharide (**Scheme 71**).



Scheme 71. Proposed preparation of the pentasaccharide via a stereocontrolled convergent 3+2 glycosylation approach

4.5 Conclusion

In summary, convergent synthesis of the pentasaccharide **404** containing the tetrasaccharide repeating unit of the capsular polysaccharide of *K. kingae* type c has been designed and partially accomplished. Thus, the use of peracetylated thioglycoside donor in glycosylation to furnish the desired β -KDO linkage, applying the concept of the side chain control of reactivity discussed in chapter three, yielded to an equatorially-linked KDO glycoside in good selectivity and yield. Additionally, key donors and acceptors were synthesized in good yields by employing practical chemistry. Such results clearly demonstrate that with the right trisaccharide acceptor and

donor at hand, a stereocontrolled convergent 3 + 2 glycosylation mediated by a Lewis acid at low temperature, followed by global deprotection would be anticipated to furnish the desired pentasaccharide.

CHAPTER 5. CONCLUSIONS

The unusual structure of bradyrhizose coupled with its immunologically silent nature stimulated an interest in its chemical synthesis. An effective and short synthesis was developed in which bradyrhizose was synthesized in 14 steps and 6% overall yield from D-glucose. The synthesis involved the elaboration of a *trans*-fused carbocyclic ring onto the pre-existing glucopyranose framework with key steps involving photocatalyzed radical extension of the glucopyranose side chain, construction of the bicyclic framework via ring closing metathesis, regioselective allylic oxidation, regio- and stereoselective Luche reduction, hydroxy-directed epoxidation and regio- and stereoselective acid-catalyzed epoxide opening at the more substituted position. The final step involved global deprotection through hydrogenolysis. This synthesis is significantly shorter than the two previous syntheses.

The widespread occurrence of equatorial glycosides of KDO in the capsular polysaccharides of numerous pathogenic bacteria, coupled with the challenges encountered in isolation of such glycosides in pure form, necessitates the need to synthesize them in a stereocontrolled fashion. However, there exists few methods for accessing β -KDO glycosides and only a few examples display high level of β -selectivity. Conformational analysis of the likely side chain conformation of KDO, and analogy with the pseudoenantiomeric pseudaminic acid, predicted the equatorially selective coupling of peracetyl KDO donor to typical acceptors at low temperature. This hypothesis was borne out by experiment and confirms the important role of side chain conformation in regulating glycosyl donor reactivity and selectivity.

The successful demonstration of synthesis of equatorial KDO glycosides as a function of side chain conformation provides an effective and alternative route for selective synthesis of KDO equatorial glycosides commonly found in numerous pathogenic bacteria.

CHAPTER 6. EXPERIMENTAL SECTION

General Experimental: All reactions were carried out under argon unless otherwise stated. Solvents used for column chromatography were analytical grade and were purchased from commercial suppliers. Thin-layer chromatography was carried out with 250 μm glass backed silica (XHL) plates. Detection of compounds was achieved by UV absorption (254 nm) and by staining with 10% sulfuric acid in ethanol. Purification of crude residues was performed over silica gel chromatography using 230–400 mesh grade 60 silica unless otherwise stated. Specific rotations were measured in chloroform on an automatic polarimeter with a path length of 10 cm. NMR spectra were recorded in acetonitrile- d_3 , CDCl_3 , D_2O or CD_3OD using a 400 or 600 MHz Varian spectrometers, a 900 MHz Bruker Avance spectrometer and EZZ500 JEOL instrument (500 MHz). High-resolution (HRMS) mass spectra were recorded in the electrospray mode using a time of flight mass analyzer (ESI-TOF). Heating of reaction mixtures were carried out on an aluminum heating block of appropriate size. volumetric glass. The chemical shifts (δ) were recorded in ppm and the multiplicity were abbreviated as follows: s (singlet), m (multiplet), br (broad), d (doublet), t (triplet) and q (quartet).

Methyl 2,3-di-*O*-benzyl-6-deoxy-6-iodo- α -D-glucopyranoside (247). This compound was prepared according to the literature method in (20 g, 83% yield) as a colorless syrup. $[\alpha]_{\text{D}}^{23} = +19.4$ ($c = 1.0$, CHCl_3), ^1H NMR (400 MHz, CDCl_3) δ 7.47 – 7.29 (m, 10H), 5.03 (d, $J = 11.5$ Hz, 1H), 4.77 (d, $J = 12.0$ Hz, 1H), 4.69 (s, 1H), 4.67-4.64 (m, 3H), 3.78 (t, $J = 9.1$ Hz, 1H), 3.57 – 3.50 (m, 2H), 3.48 – 3.37 (m, 4H), 3.34 – 3.19 (m, 2H). ^{13}C NMR (101 MHz, CDCl_3) δ 138.5, 137.9, 128.7, 128.6, 128.11, 128.07, 128.0, 98.1, 80.7, 79.9, 75.4, 73.7, 73.2, 69.8, 55.6, 7.1. ESI-HRMS: m/z calcd for $\text{C}_{21}\text{H}_{25}\text{O}_5\text{INa}$ [$\text{M} + \text{Na}$] 507.0645, found 507.0644.

2-pyridyl methallyl sulfone (257). To a solution of 2-mercaptopyridine (6.31 g, 56.8 mmol) and 3-chloro-2-methylpropene (25.7 g, 283.8 mmol) in CH₃CN (81 mL) was Et₃N (23 mL). The mixture was stirred at rt till completion. The solvent was then removed at reduced pressure and the residual crude dissolved in diethyl ether (100 mL) and washed with 5% sodium hydroxide (30 mL) and sodium chloride. The combined organic layer was dried in MgSO₄, filtered, and concentrated under reduced pressure. The residual crude (8.5 g, 51.4 mmol) was dissolved in CH₂Cl₂ (200 mL). The solution was treated with *m*-Chloroperoxybenzoic acid (17.8 g, 102.9 mmol) and stirred at 0 °C till completion. After completion, the reaction mixture was concentrated under reduced pressure, diluted with CH₂Cl₂ (20 mL) and neutralized with 0.2 M aqueous sodium bicarbonate (15 mL). The aqueous layer was extracted with CH₂Cl₂ twice and the combined organic layer was dried over anhydrous MgSO₄, filtered, and concentrated. The crude was purified by silica gel column chromatography (hexane:ethyl acetate 5:1) to give (7.7 g, 76%) as a colorless liquid. ¹H NMR (400 MHz, CDCl₃) δ 8.67 (dd, *J* = 7.8, 7.7, 1H), 7.96 (dd, *J* = 7.9, 7.9 Hz, 1H), 7.88 (dd, *J* = 7.7, 7.7 Hz, 1H), 7.49 (dd, *J* = 7.6, 7.7 Hz, 1H), 4.93 (s, 1H), 4.68 (s, 1H), 3.99 (s, 2H), 1.78 (s, 3H). ¹³C NMR (101 MHz, CDCl₃) δ 156.5, 150.1, 138.1, 132.8, 127.5, 122.8, 120.9, 59.8, 22.8. ESI-HRMS: *m/z* calcd for C₉H₁₁O₂NSNa [M + H] 198.0363, found 198.0358.

Methyl 2,3-di-*O*-benzyl-6,7,8,9-tetradecoxy-8-methyl- α -D-non-8-enoglucopyranoside (253). Compound **247** (3.0 g, 6.2 mmol) was dissolved in dry α,α,α -Trifluorotoluene (31 mL) and treated with 2-pyridyl methallylsulfone (1.2 g, 6.2 mmol). Lauroyl peroxide (5.0 g, 12.4 mmol) was added to the reaction mixture in two portions at 80 °C. The reaction mixture was stirred at 80 °C for 2 h with monitoring by TLC (hexane:ethyl acetate 6:1, *R_f* = 0.6). After completion, the reaction mixture was concentrated under reduced pressure and the residue was purified by silica gel column chromatography (hexane:ethyl acetate 15:1 to 10:1 to 6:1) to give **253** (1.2 g, 50%) as

a colorless syrup and **260** (0.9 g, 40%) also as a colorless syrup. $[\alpha]_D^{23} = +58$ ($c = 0.4$, CHCl_3), ^1H NMR (400 MHz, CDCl_3) δ 7.42 – 7.20 (m, 10H), 5.02 (d, $J = 11.5$ Hz, 1H), 4.82 – 4.51 (m, 6H), 3.73 (t, $J = 9.3$ Hz, 1H), 3.55 – 3.46 (m, 2H), 3.36 (s, 3H), 3.23 (t, $J = 9.2$ Hz, 1H), 2.26 – 2.17 (m, 1H), 2.02–1.94 (m, 1H), 1.61 – 1.45 (m, 2H). ^{13}C NMR (101 MHz, CDCl_3) δ 145.4, 138.7, 138.0, 128.6, 128.5, 128.1, 128.0, 127.96, 127.9, 110.0, 97.9, 81.5, 79.98, 75.4, 73.7, 72.99, 70.1, 55.1, 33.5, 29.8. ESI-HRMS: m/z calcd for $\text{C}_{25}\text{H}_{32}\text{O}_5\text{Na}$ [$\text{M} + \text{Na}$] 435.1764, found 435.1762.

4-toluy methyl sulfone (259). To a solution of 4-toluene sulfinate (10 g, 56.1 mmol) in DMF (40 mL) was added 3-Chloro-2-methylpropene (2.7 mL, 27.6 mmol). The mixture was stirred at reflux till completion. The solvent was then removed at reduced pressure and the residual crude dissolved in ethyl acetate (50 mL) and washed with saturated sodium bicarbonate (2×20 mL). The aqueous layer was extracted twice with ethyl acetate and the combined organic layer dried in MgSO_4 , filtered, and concentrated under reduced pressure. The residual crude was purified by silica gel column chromatography (hexane:ethyl acetate 5:1) to give **259** (10.9 g 92%) as white solid. ^1H NMR (400 MHz, CDCl_3) δ 7.74 (d, $J = 8.2$ Hz, 2H), 7.32 (d, $J = 8.4$ Hz, 2H), 5.02 (br, 1H), 4.68 (br, 1H), 3.74 (br, 2H), 2.43 (s, 3H), 1.85 (s, 3H). ^{13}C NMR (101 MHz, CDCl_3) δ 144.6, 135.5, 133.5, 129.6, 128.5, 120.6, 64.5, 22.7, 21.6. ESI-HRMS: m/z calcd for $\text{C}_{11}\text{H}_{14}\text{O}_2\text{SNa}$ [$\text{M} + \text{Na}$] 233.0308, found 233.0304.

Methyl 2,3-di-O-benzyl-6,7-dideoxy-8,8-dimethyl- α -D-glucopyranoside (261). Compound **247** (2.95 g, 6.09 mmol) was dissolved in dry α,α,α -trifluorotoluene (30 mL) and treated with 4-toluy methyl sulfone (2.6 g, 12.18 mmol). Lauroyl peroxide (2.4 g, 6.09 mmol) was added to the reaction mixture in two portions at 80 °C. The reaction was stirred at 80 °C for 4 h with monitoring by TLC (hexane:ethyl acetate 5:1, $R_f = 0.5$). After completion, the reaction

mixture was concentrated under reduced pressure and the residue was purified by silica gel column chromatography (hexane:ethyl acetate 20:1 to 10:1 to 5:1) to give **261** (1.4 g, 57%) as a colorless syrup. $[\alpha]_D^{23} = +47.4$ ($c = 0.5$, CHCl_3), ^1H NMR (400 MHz, CDCl_3) δ 7.56 – 6.99 (m, 10H), 4.95 – 4.79 (m, 2H, 2PhCH₂), 4.79 – 4.63 (m, 2H, 2PhCH₂), 4.54 (d, $J = 3.7$ Hz, 1H, H-1), 3.79 (dd, $J = 9.5, 9.5$ Hz, 1H, H-3), 3.53 – 3.18 (m, 6H, H-2, H-4, H-5, OCH₃), 1.87-1.76 (m, 2H, H-6, H-7), 1.63-1.62 (m, 2H, H-6', H-7'), 1.26 (s, 6H). ^{13}C NMR (101 MHz, CDCl_3) δ 139.4, 138.5, 129.6, 128.4, 128.2, 128.1, 128.0, 127.7, 127.4, 99.1, 79.8, 79.1, 75.9, 75.2, 73.7, 72.0, 67.4, 55.2, 35.8, 31.1, 25.8, 22.3. ESI-HRMS: m/z calcd for $\text{C}_{25}\text{H}_{32}\text{O}_5\text{Na}$ [$\text{M} + \text{Na}$] 435.1464, found 435.1462.

Methyl 2,3-di-O-benzyl-6,7,8,9-tetradexoxy-8-methyl-4-keto- α -D-non-8-enoglucopyranoside (271). Compound **253** (1.21 g, 2.9 mmol) was dried under vacuum overnight and dissolved in anhydrous solution of DMSO:dichloromethane 2:1 (7 mL) under argon. The mixture was cooled to 0 °C. A solution of sulfur trioxide pyridine complex (1.4 g, 8.8 mmol) in DMSO (3 mL) was stirred at rt for 20 minutes then added dropwise to the sugar solution at 0 °C. The reaction mixture was allowed to come to rt and stirred till completion with monitoring by TLC (hexane:ethyl acetate 5:1, $R_f = 0.5$). The reaction mixture was concentrated under reduced pressure and the residue diluted with dichloromethane (30 mL) and water (20 mL). The aqueous layer was extracted with dichloromethane twice and the combined organic layer was dried over anhydrous MgSO_4 , filtered, and concentrated. The residue was purified by silica gel column chromatography (hexane:ethyl acetate 5:1) to give **271** (0.93 g, 77%) as a colorless syrup. $[\alpha]_D^{23} = +130$ ($c = 0.8$, CHCl_3). ^1H NMR (CDCl_3 , 400 MHz): δ 8.09 – 6.75 (m, 10H), 4.96 (d, $J = 11.3$ Hz, 1H), 4.87 (d, $J = 12.1$ Hz, 1H), 4.75 – 4.69 (m, 3H), 4.67 (m, 1H), 4.43 (d, $J = 10.1$ Hz, 1H), 4.06 (dd, $J = 8.5, 3.6$ Hz, 1H), 3.75 (dd, $J = 10.0, 3.6$ Hz, 1H), 3.46 (s, 3H), 2.15 (m, 1H), 2.11 – 1.99 (m, 2H), 1.72 (s, 3H), 1.65 (m, 1H). ^{13}C NMR (CDCl_3) δ 203.24, 144.80, 128.47, 128.40, 128.13, 128.02, 127.97,

127.81, 110.55, 98.40, 82.83, 80.27, 74.35, 73.92, 72.03, 55.99, 33.08, 26.21, 22.33. HRMS (ESI) m/z calc. for $C_{25}H_{30}O_5Na$ $[M+Na]^+$, 433.2004; found, 433.1991.

Methyl 2,3-di-*O*-benzyl-6,7,8,9-tetradecoxy-8-methyl-4-*C*-vinyl- α -D-non-8-enogalactopyranoside (274). A solution of **271** (0.43 g, 1.0 mmol) in dry THF (10 mL) was cooled to -78 °C under argon and treated with vinylmagnesium bromide (2.09 mL, 2.1 mmol). The reaction mixture was stirred at -78 °C for 2 h with monitoring by TLC (hexane:ethyl acetate 5:1, R_f = 0.5). After completion, the reaction mixture was concentrated and the residue purified by silica gel column chromatography (hexane:ethyl acetate 5:1) to give **274** (0.35 g, 76%) as a colorless syrup. $[\alpha]_D^{23}$ = +85 (c = 1.0, $CHCl_3$), 1H NMR (400 MHz, $CDCl_3$) δ 7.44 – 7.10 (m, 10H), 5.75 (dd, J = 17.2, 10.7 Hz, 1H), 5.47 (dd, J = 17.2, 1.4 Hz, 1H), 5.33 (d, J = 10.6, 1H), 4.80 (d, 11.3 Hz, 2H), 4.71 – 4.61 (m, 4H), 3.80 (s, 2H), 3.40 (s, 3H), 2.28-2.20 (m, 1H), 2.04 – 1.90 (m, 1H), 1.74 – 1.64 (m, 4H), 1.30-1.21(m, 1H). ^{13}C NMR (101 MHz, $CDCl_3$) δ 145.5, 139.6, 138.3, 138.1, 128.4, 128.31, 128.27, 128.1, 127.9, 127.8, 116.5, 110.1, 98.2, 80.1, 77.7, 77.2, 76.0, 73.3, 70.7, 55.3, 34.5, 25.5, 22.4. HRMS (ESI) m/z calc. for $C_{27}H_{34}O_5Na$ $[M+Na]^+$, 461.2306; found, 461.2304.

Methyl 2,3-di-*O*-benzyl-6,7,8,9-tetradecoxy-8-methyl- α -D-non-8-enogalactopyranoside (278). A solution of **274** (2 g, 4.6 mmol) in dry dichloromethane (11 mL) was treated with 2nd gen. Grubbs catalyst (29 mg, 0.5 mmol). The reaction mixture was heated at 40 °C till completion with monitoring by TLC (hexane:ethyl acetate 4:1, R_f = 0.5). After completion, the reaction mixture was concentrated and the concentrate purified by silica gel column chromatography (hexane:ethyl acetate 4:1) to give **278** (1.57 g, 84%) as a light brown syrup. $[\alpha]_D^{23}$ = +60 (c = 0.6, $CHCl_3$), 1H NMR (400 MHz, $CDCl_3$) δ 7.48 – 7.18 (m, 10H), 5.50 (s, 1H), 5.04 (d, J = 11.2 Hz, 1H), 4.77 (d, J = 12.0 Hz, 1H), 4.72 – 4.60 (m, 3H), 4.00 (dd, J = 9.4,

3.9 Hz, 1H), 3.68 (dd, $J = 12.3, 3.7$ Hz, 1H), 3.61 (d, $J = 9.4$ Hz, 1H), 3.39 (s, 3H), 2.13 – 1.98 (m, 3H), 1.70-1.64 (m, 1H). ^{13}C NMR (101 MHz, CDCl_3) δ 139.2, 138.5, 138.3, 128.43, 128.40, 128.23, 128.21, 127.9, 127.8, 122.0, 98.8, 80.0, 75.97, 73.4, 70.7, 68.9, 55.3, 30.3, 23.2, 21.7. HRMS (ESI) m/z calc. for $\text{C}_{25}\text{H}_{30}\text{O}_5\text{Na}$ $[\text{M}+\text{Na}]^+$, 433.1997; found, 433.1991.

Methyl 2,3-di-*O*-benzyl-6,8,9-trideoxy-8-methyl-7-keto- α -D-non-8-enogalactopyranoside (279). A solution of **278** (94.4 mg, 0.2 mmol) in dry 1,4 dioxane (10 mL) was treated with selenium dioxide (10 mg, 0.1 mmol) added in four portions over the period of the reaction. The reaction mixture was heated at 80 °C till completion with monitoring by TLC (hexane:ethyl acetate 2:1, $R_f = 0.4$). After completion, the reaction mixture was concentrated and the residue purified by silica gel column chromatography (hexane:ethyl acetate 2:1) to give first, **279** (55 mg, 65%) as a white form then, **280** (6 mg, 7%) as a colorless syrup. **279**: $[\alpha]_{\text{D}}^{23} = +59$ ($c = 0.53$, CHCl_3), ^1H NMR (400 MHz, CDCl_3) δ 7.56 – 7.08 (m, 10H), 6.42 (s, 1H), 5.09 (d, $J = 11.4$ Hz, 1H), 4.85 – 4.51 (m, 4H), 4.14 – 3.91 (m, 2H), 3.72 (d, $J = 9.3$ Hz, 1H), 3.37 (s, 3H), 3.00 – 2.83 (m, 1H), 2.57 – 2.52 (m, 1H). ^{13}C NMR (101 MHz, CDCl_3) δ 197.5, 141.1, 137.9, 128.62, 128.55, 128.4, 128.2, 128.1, 98.9, 78.5, 78.2, 75.9, 73.4, 70.5, 66.6, 55.6, 38.0, 15.6. HRMS (ESI) m/z calc. for $\text{C}_{25}\text{H}_{28}\text{O}_6\text{Na}$ $[\text{M}+\text{Na}]^+$, 447.1196; found, 447.1193.

Methyl 2,3-di-*O*-benzyl-6,7,8,9-tetradecoxy- α -D-non-8-enogalactopyranoside (280). ^1H NMR (400 MHz, CDCl_3) δ 9.22 (s, 1H), 7.56 – 7.15 (m, 10H), 5.09 (d, $J = 11.5$ Hz, 1H), 4.88 – 4.55 (m, 4H), 4.14 – 3.91 (m, 1H), 3.68 – 3.59 (m, 1H), 2.62 – 2.38 (m, 2H), 2.22 – 2.05 (m, 1H), 2.05 – 1.88 (m, 1H), 1.85 – 1.65 (m, 1H). ^{13}C NMR (101 MHz, CDCl_3) δ 196.4, 141.0, 137.9, 128.6, 128.5, 128.4, 128.2, 128.1, 98.9, 78.6, 78.3, 75.9, 73.5, 70.4, 66.6, 55.7, 38.1, 15.5. HRMS (ESI) m/z calc. for $\text{C}_{25}\text{H}_{28}\text{O}_6\text{Na}$ $[\text{M}+\text{Na}]^+$, 447.1300; found, 447.1296.

Benzyl 2,3-di-*O*-benzyl-6,8,9-trideoxy -8-methyl- α -D-non-8-enogalactopyranoside

(287). A solution of **279** (58 g, 0.1 mmol) in dry methanol (1.4 mL) was treated with cerium (III) chloride heptahydrate (61 mg, 0.2 mmol) and stirred at rt for 1 h. The reaction mixture was cooled to -78 °C and sodium borohydride (8 mg, 0.2 mmol) was added, with monitoring by TLC (hexane:ethyl acetate 1:1, R_f = 0.2). After completion, the reaction mixture was concentrated and the crude diluted with ethyl acetate (10 mL) and washed with water (10 mL). The aqueous layer was extracted with ethyl acetate and the combined organic layer dried over anhydrous $MgSO_4$, filtered, and concentrated. The residue was purified by silica gel column chromatography (hexane:ethyl acetate 1:1) to give **287** (47 mg, 80%) as a colorless liquid. $[\alpha]_D^{23} = +50.1$ (c = 0.67, $CHCl_3$), 1H NMR (400 MHz, $CDCl_3$) δ 7.41 – 7.28 (m, 10H), 5.50 (s, 1H), 5.04 (d, J = 11.3 Hz, 1H), 4.76 (d, J = 11.9 Hz, 1H), 4.70 – 4.52 (m, 3H), 4.11 (t, J = 8.3 Hz, 1H), 3.97 (dd, J = 9.4, 3.8 Hz, 1H), 3.63 (dd, J = 12.9, 3.5 Hz, 1H), 3.58 (d, J = 9.4 Hz, 1H), 3.38 (s, 3H), 2.19-2.13 (m, 1H), 2.05-1.97 (m, 1H), 1.71 (s, 3H). ^{13}C NMR (101 MHz, $CDCl_3$) δ 141.4, 138.3, 128.5, 128.3, 128.2, 127.95, 127.9, 123.99, 98.9, 79.4, 78.5, 75.9, 73.4, 70.9, 70.1, 66.7, 55.5, 32.2, 19.1. HRMS (ESI) m/z calc. for $C_{25}H_{30}O_6Na$ $[M+Na]^+$, 449.1948; found, 449.1940.

Methyl 8,9-anhydro-2,3-di-*O*-benzyl-6-deoxy-8-methyl- α -D-nonagalactopyranoside

(288). A solution of **287** (32 mg, 0.1 mmol) in dry THF (0.75 mL) was treated with *m*-chloroperoxybenzoic acid (13 mg, 0.1 mmol) and stirred at rt, with monitoring by TLC (hexane:ethyl acetate:methanol 1:1:0.1, R_f = 0.2). After completion, the reaction mixture was concentrated under reduced pressure, diluted with ethyl acetate (15 mL) and neutralized with 0.2 M aqueous sodium bicarbonate (30 mL). The aqueous layer was extracted with ethyl acetate twice and the combined organic layer was dried over anhydrous $MgSO_4$, filtered, and concentrated. The crude product was purified by silica gel column chromatography (hexane:ethyl acetate:methanol

1:1:0.1) to give **288** (26 mg, 78%) as a syrup. $[\alpha]_{\text{D}}^{23} = +25.7$ ($c = 0.4$, CHCl_3), ^1H NMR (400 MHz, CDCl_3) δ 7.41 – 7.26 (m, 10H), 5.05 (d, $J = 11.7$ Hz, 1H), 4.79 (d, $J = 11.9$ Hz, 1H), 4.69 (d, $J = 11.8$ Hz, 1H), 4.64 (d, $J = 11.9$ Hz, 1H), 4.56 (d, $J = 3.8$ Hz, 1H), 4.06 (dd, $J = 9.5, 3.8$ Hz, 1H), 3.91 – 3.81 (m, 2H), 3.62 (d, $J = 9.5$ Hz, 1H), 3.33 (s, 3H), 3.18 (dd, $J = 12.7, 2.5$ Hz, 1H), 2.70 (s, 1H), 1.76 – 1.70 (m, $J = 12.4, 6.3, 2.7$ Hz, 1H), 1.60 – 1.48 (m, 1H), 1.22 (s, 3H). ^{13}C NMR (101 MHz, CDCl_3) δ 162.7, 138.1, 137.98, 128.9, 128.6, 128.51, 128.48, 128.5, 128.2, 128.0, 127.97, 98.9, 78.2, 77.3, 75.3, 73.54, 70.50, 67.2, 62.6, 55.6, 28.5, 19.1. HRMS (ESI) m/z calc. for $\text{C}_{25}\text{H}_{30}\text{O}_7\text{Na}$ $[\text{M}+\text{Na}]^+$, 465.1891; found, 465.1889.

Methyl 2,3-di-*O*-benzyl-8- α -D-bradyrhizopyranoside (291). A solution of **288** (0.17 g, 0.4 mmol) in 1,4 dioxane:water 2:1 (4 mL), was treated with concentrated sulphuric acid (4 μL , 0.1 mmol) added dropwise in three portions at 65 °C. The reaction was monitored by TLC (hexane:ethyl acetate:methanol 1:1:0.1, $R_f = 0.1$). After completion, the mixture was diluted with ethyl acetate (10 mL) and neutralized with saturated aqueous sodium bicarbonate (5 mL). The aqueous layer was extracted with ethyl acetate twice and the combined organic layer was dried over anhydrous MgSO_4 , filtered, and concentrated. The crude product was purified by silica gel column chromatography (hexane:ethyl acetate:methanol 1:1:0.1) to give first, **279** (58.6 mg, 35%) then, **291** (67.2 mg, 37%) as a white form. $[\alpha]_{\text{D}}^{23} = +64$ ($c = 0.5$, CHCl_3), ^1H NMR (400 MHz, CDCl_3) δ 7.43 – 7.20 (m, 11H), 5.09 (d, $J = 10.7$ Hz, 1H), 4.75 – 4.59 (m, 4H), 4.03 (dd, $J = 9.4, 3.7$ Hz, 1H), 3.91 (d, $J = 9.4$ Hz, 1H), 3.73 (br, 1H), 3.66 – 3.55 (m, 2H), 3.51 (br, 1H), 3.38 (s, 3H), 2.76 (s, 1H), 1.94 – 1.80 (m, 2H), 1.26 (s, 3H). ^{13}C NMR (101 MHz, CDCl_3) δ 137.7, 137.2, 128.9, 128.6, 128.52, 128.46, 128.3, 128.2, 98.2, 82.9, 78.8, 78.3, 77.5, 75.8, 73.7, 73.1, 72.2, 66.3, 55.6, 30.3, 15.5. HRMS (ESI) m/z calc. for $\text{C}_{25}\text{H}_{32}\text{O}_8\text{Na}$ $[\text{M}+\text{Na}]^+$, 483.1995; found, 483.1990.

Benzyl α,β -D-glucopyranoside (230). This compound was prepared according to the literature method in 89% yield as a white solid (26.7g) in the form of a 12.5:1 $\alpha:\beta$ mixture. ^1H NMR (400 MHz, CD_3OD) δ 7.47 – 7.16 (m, 10H), 4.94-4.90 (m, 2H), 4.76 (d, J = 11.9 Hz, 1H), 4.66 (d, J = 11.9 Hz, 1H), 4.55 (d, J = 12.0 Hz, 1H), 4.36 (d, J = 7.8 Hz, 1H), 3.93 – 3.88 (m, 1H), 3.82 – 3.77 (m, 1H), 3.75 – 3.58 (m, 5H), 3.42 (dd, J = 9.7, 3.8 Hz, 1H), 3.41 – 3.21 (m, 5H). ^{13}C NMR (101 MHz, CD_3OD) δ 140.4, 137.6, 128.4, 127.92, 127.88, 127.86, 127.8, 127.3, 125.6, 101.9, 97.8, 76.7, 76.6, 73.71, 73.68, 72.5, 72.1, 70.4, 70.34, 70.27, 68.8, 61.4, 61.2. HRMS (ESI): m/z calcd for $\text{C}_{13}\text{H}_{18}\text{O}_6\text{Na}$ [$\text{M} + \text{Na}$] 293.0957, found 293.0952.

Benzyl 4,6-*O*-benzylidene- α,β -D-glucopyranoside (231). To a solution of **230** (25 g, 92.5 mmol) in DMF (500 mL) was added benzaldehyde dimethyl acetal (17.3 mL, 111.0 mmol) and *p*-TsOH monohydrate (3.5 g, 18.0 mmol). The mixture was stirred at rt till completion. The solvent was then removed at reduced pressure and the residual crude dissolved in ethyl acetate (100 mL) and washed with saturated sodium bicarbonate (2×30 mL). The aqueous layer was extracted twice with ethyl acetate and the combined organic layer dried in MgSO_4 , filtered, and concentrated under reduced pressure. The residual crude was purified by silica gel column chromatography (hexane:ethyl acetate 3:1) to give first compound **231 β** as a white solid (2.1 g, 6%) and then **231 α** as a white solid (28 g, 85%). **231 α** . Mp 155 -162 °C $[\alpha]_{\text{D}}^{23} = +103$ (c = 0.98, CHCl_3) ^1H NMR (400 MHz, CDCl_3) δ 8.05 – 7.16 (m, 10H), 5.48 (s, 1H, benzylidene), 4.95 (d, J = 3.9 Hz, 1H, H-1), 4.73 (d, J = 11.8 Hz, 1H, PhCH_2), 4.53 (d, J = 11.8 Hz, 1H, PhCH_2), 4.19 (dd, J = 10.1, 4.8 Hz, 1H, H-6_{eq}), 3.94 (t, J = 9.3 Hz, 1H, H-3), 3.82 (td, J = 9.9, 4.8 Hz, 1H, H-5), 3.69 (q, J = 10.4 Hz, 1H, H-6_{ax}), 3.60 (dd, J = 9.2, 3.9 Hz, 1H, H-2), 3.46 (t, J = 9.4 Hz, 1H, H-4). ^{13}C NMR (101 MHz, CDCl_3) δ 162.7, 137.1, 136.8, 129.1, 128.5, 128.2, 128.12, 128.08, 126.3, 101.8, 98.3, 81.0, 72.9,

71.4, 70.0, 68.9, 62.7. HRMS (ESI): m/z calcd for $C_{20}H_{22}O_6Na$ [$M + Na$] 381.1314, found 381.1316.

231 β . Mp 120 -125 °C $[\alpha]_D^{23} = +98$ ($c = 1.0$, $CHCl_3$) 1H NMR (400 MHz, $CDCl_3$) δ 7.57 – 7.30 (m, 10H), 5.50 (s, 1H, benzyldiene), 4.91 (d, $J = 11.6$ Hz, 1H, , $PhCH_2$), 4.61 (d, $J = 11.6$ Hz, 1H, $PhCH_2$), 4.45 (d, $J = 7.7$ Hz, 1H, H-1), 4.34 (dd, $J = 10.5, 5.0$ Hz, 1H, H-6_{eq}), 3.84 – 3.70 (m, 2H, H-6_{ax}, H-3), 3.60 – 3.47 (m, 2H, H-2, H-4), 3.39 (td, $J = 9.7, 4.9$ Hz, 1H, H-5). ^{13}C NMR (101 MHz, $CDCl_3$) δ 137.0, 136.7, 129.3, 128.6, 128.4, 128.18, 128.16, 126.3, 102.1, 101.9, 80.5, 74.5, 73.1, 71.4, 68.7, 66.4. HRMS (ESI): m/z calcd for $C_{20}H_{22}O_6Na$ [$M + Na$] 381.1314, found 381.1319.

Benzyl 2,3-di-*O*-benzyl-4,6-*O*-benzyldiene- α -D-glucopyranoside (232). A solution of **231** (8 g, 22.2 mmol) in dry DMF (222 mL) was placed in an ice bath at 0 °C under argon. Sodium hydride (2.7 g, 66.7 mmol) and benzyl bromide were then added. The reaction mixture was stirred at 0 °C for 3 h then at ambient temperature for 4 h, with monitoring by TLC (hexane:ethyl acetate 6:1, $R_f = 0.6$). After completion, the reaction mixture was quenched with methanol (10 mL) followed by water (100 mL) and extracted with ethyl acetate (100 mL). The aqueous layer was extracted with ethyl acetate thrice and the combined organic layer dried over anhydrous $MgSO_4$, filtered, and concentrated. The residue was purified by silica gel column chromatography (hexane:ethyl acetate 6:1) to give **232** as a white amorphous solid (11.3 g, 94%). Mp 114 -117 °C. $[\alpha]_D^{23} = +21.9$ ($c = 0.54$, $CHCl_3$), 1H NMR (400 MHz, $CDCl_3$) δ 7.76 – 6.96 (m, 20H), 5.56 (s, 1H, benzyldiene), 4.94 (d, $J = 11.2$ Hz, 1H, $PhCH_2$), 4.86 (d, $J = 11.4$ Hz, 1H, $PhCH_2$), 4.84 (d, $J = 3.8$ Hz, 1H, H-1), 4.77 (d, $J = 12.0$ Hz, 1H, $PhCH_2$), 4.74 (d, $J = 12.3$ Hz, 1H, $PhCH_2$), 4.60 (d, $J = 12.2$ Hz, 2H, 2 $PhCH_2$), 4.21 (dd, $J = 10.2, 4.9$ Hz, 1H, H-6_{eq}), 4.12 (t, $J = 9.3$ Hz, 1H, H-3), 3.92 (dt, $J = 9.9, 4.8$ Hz, 1H, H-5), 3.70 (t, $J = 10.3$ Hz, 1H, H-6_{ax}), 3.63 (t, $J = 9.4$ Hz, 1H, H-

4), 3.57 (dd, $J = 9.3, 3.8$ Hz, 1H, H-2). ^{13}C NMR (101 MHz, CDCl_3) δ 138.8, 138.1, 137.4, 136.9, 128.9, 128.5, 128.41, 128.36, 128.3, 128.2, 127.97, 127.9, 127.8, 127.6, 126.0, 101.2, 96.5, 82.2, 79.2, 78.7, 75.4, 73.5, 69.3, 69.0, 62.6. HRMS (ESI): m/z calcd for $\text{C}_{34}\text{H}_{34}\text{O}_6\text{Na}$ [$\text{M} + \text{Na}$] 561.2253, found 561.2258.

Benzyl 2,3-di-*O*-benzyl- α -D-glucopyranoside (233). A solution of **232** (19.0 g, 35.2 mmol) in methanol:chloroform 2:1 (300 mL), was treated with *p*-TsOH monohydrate (2.7 g, 14.07 mmol) at rt. The reaction was monitored by TLC (hexane:ethyl acetate 2:1, $R_f = 0.3$). After completion, the reaction mixture was concentrated under reduced pressure, diluted with ethyl acetate (250 mL) and neutralized with saturated aqueous sodium bicarbonate (100 mL). The aqueous layer was extracted with ethyl acetate twice and the combined organic layer was dried over anhydrous MgSO_4 , filtered, and concentrated. The residual syrup was purified by silica gel column chromatography (hexane:ethyl acetate 2:1) to give **233** (13.3 g, 84%) as white amorphous solid. Mp 95-98 °C. $[\alpha]_D^{23} = +53.6$ ($c = 0.64$, CHCl_3), ^1H NMR (400 MHz, CDCl_3) δ 7.75 – 6.96 (m, 15H), 5.05 (d, $J = 11.4$ Hz, 1H, PhCH_2), 4.85 (d, $J = 3.6$ Hz, 1H, H-1), 4.75 (d, $J = 11.4$ Hz, 1H, PhCH_2), 4.72 (d, $J = 12.3$ Hz, 1H, PhCH_2), 4.64 (d, $J = 11.9$ Hz, 1H, PhCH_2), 4.57 (d, $J = 12.3$ Hz, 1H, PhCH_2), 4.54 (d, $J = 11.9$ Hz, 1H, PhCH_2), 3.89 (t, $J = 9.2$ Hz, 1H, H-3), 3.75-3.73 (m, 2H, H-6, H-6'), 3.72 – 3.66 (m, 1H, H-5), 3.57 (t, $J = 9.2$ Hz, 1H, H-4), 3.51 (dd, $J = 9.5, 3.6$ Hz, 1H, H-2). ^{13}C NMR (101 MHz, CDCl_3) δ 138.8, 138.0, 137.1, 128.6, 128.5, 128.43, 128.39, 127.8, 127.91, 127.85, 95.5, 81.4, 79.8, 75.4, 72.7, 71.1, 70.3, 69.2, 62.2. HRMS (ESI): m/z calcd for $\text{C}_{27}\text{H}_{30}\text{O}_6\text{Na}$ [$\text{M} + \text{Na}$] 473.1940, found 473.1947.

Benzyl 2,3-di-*O*-benzyl-6-deoxy-6-iodo- α -D-glucopyranoside (234). A solution of **233** (8.6 g, 19.0 mmol) in toluene:acetonitrile 1:1 (190 mL), was treated with triphenyl phosphine (5.5 g, 20.9 mmol), iodine (5.3 g, 20.9 mmol), and imidazole (3.9 g, 57.1 mmol). The mixture was

heated at 40 °C and monitored by TLC (hexane:ethyl acetate 6:1, R_f = 0.6). After completion, the reaction mixture was concentrated under reduced pressure. The residual syrup was purified by silica gel column chromatography (hexane:ethyl acetate 6:1) to give **234** (9.3 g, 87%) as a colorless syrup. $[\alpha]_D^{23} = +46.6$ ($c = 0.98$, CHCl_3), ^1H NMR (400 MHz, CDCl_3) δ 7.64 – 7.03 (m, 15H), 5.06 (d, $J = 11.5$ Hz, 1H, PhCH_2), 4.87 (d, $J = 3.6$ Hz, 1H, H-1), 4.81 (d, $J = 12.1$ Hz, 1H, PhCH_2), 4.69 (d, $J = 11.5$ Hz, 1H, PhCH_2), 4.63 (d, $J = 12.7$ Hz, 2H, 2PhCH_2), 4.55 (d, $J = 11.9$ Hz, 1H, PhCH_2), 3.87 (t, $J = 9.2$ Hz, 1H, H-3), 3.57 – 3.46 (m, 3H, H-2, H-4, H-6), 3.33 (td, $J = 9.2, 2.5$ Hz, 1H, H-5), 3.26 (dd, $J = 10.9, 7.5$ Hz, 1H, H-6'). ^{13}C NMR (101 MHz, CDCl_3) δ 138.6, 137.8, 136.8, 128.70, 128.65, 128.5, 128.04, 128.01, 128.0, 127.9, 94.97, 80.8, 79.8, 75.4, 73.7, 72.6, 70.1, 68.99, 7.3. HRMS (ESI): m/z calcd for $\text{C}_{27}\text{H}_{29}\text{IO}_5\text{Na}$ [$\text{M} + \text{Na}$] 583.0957, found 583.0953.

Benzyl 2,3-di-O-benzyl-6,7,8,9-tetradecoxy-8-methyl- α -D-non-8-enoglucopyranoside (235). Compound **234** (5.89 g, 10.5 mmol) was dissolved in dry α,α,α -Trifluorotoluene (117 mL) and treated with 2-pyridyl methallylsulfone (7.3 g, 36.8 mmol). Lauroyl peroxide (20.9 g, 52.6 mmol) was added to the reaction mixture in two portions at 80 °C. The reaction mixture was stirred at 80 °C for 2 h with monitoring by TLC (hexane:ethyl acetate 6:1, R_f = 0.6). After completion, the reaction mixture was concentrated under reduced pressure and the residue was purified by silica gel column chromatography (hexane:ethyl acetate 15:1 to 10:1 to 6:1) to give **235** (2.7 g, 54%) as a colorless syrup and **306** (1.6g, 36%) also as a colorless syrup. $[\alpha]_D^{23} = +60.1$ ($c = 0.57$, CHCl_3), ^1H NMR (400 MHz, CDCl_3) δ 7.46 – 7.22 (m, 15H), 5.06 (d, $J = 11.5$ Hz, 1H, PhCH_2), 4.81 (d, $J = 3.6$ Hz, 1H, H-1), 4.76 – 4.68 (m, 4H, 2PhCH_2 , 2H-vinyl), 4.62 (d, $J = 11.9$ Hz, 1H, PhCH_2), 4.53 – 4.48 (m, 2H, 2PhCH_2), 3.83 (t, $J = 9.3$ Hz, 1H, H-3), 3.65 (t, $J = 8.8$ Hz, 1H, H-5), 3.52 (dd, $J = 9.5, 3.6$ Hz, 1H, H-2), 3.27 (t, $J = 9.3$ Hz, 1H, H-4), 2.26 – 2.18 (m, 1H, H-7), 2.07 – 1.98 (m, 2H, H-7', H-6), 1.74 (s, 3H, methyl), 1.56 – 1.46 (m, 1H, H-6'). ^{13}C NMR (101 MHz, CDCl_3) δ

145.5, 138.8, 138.0, 137.1, 128.6, 128.42, 128.39, 127.93, 127.89, 127.8, 110.1, 94.8, 81.5, 79.9, 75.3, 73.8, 72.5, 70.4, 68.7, 33.5, 29.9, 22.5. HRMS (ESI): m/z calcd for $C_{31}H_{36}O_5Na$ [$M + Na$] 511.2460, found 511.2459.

Benzyl 2,3-di-*O*-benzyl-6-deoxy- α -D-glucopyranoside (306). $[\alpha]_D^{23} = +19.5$ ($c = 1.1$, $CHCl_3$) 1H NMR (500 MHz, $CDCl_3$) δ 7.37 – 7.25 (m, 15H), 5.05 (d, $J = 11.5$ Hz, 1H, $PhCH_2$), 4.80 (d, $J = 3.6$ Hz, 1H, H-1), 4.71 (dd, $J = 11.9, 5.5$ Hz, 2H, $PhCH_2$), 4.62 (d, $J = 11.9$ Hz, 1H, $1PhCH_2$), 4.55 (d, $J = 12.0$ Hz, 2H), 3.81 (t, $J = 9.2$ Hz, 1H, H-3), 3.76 – 3.68 (m, 1H, H-5), 3.52 (dd, $J = 9.5, 3.7$ Hz, 1H, H-2), 3.18 (t, $J = 9.2$ Hz, 1H, H-4), 1.21 (d, $J = 6.3$ Hz, 3H, CH_3). ^{13}C NMR (126 MHz, $CDCl_3$) δ 138.9, 138.2, 137.4, 128.7, 128.50, 128.45, 128.0, 95.4, 81.5, 80.2, 75.5, 75.4, 72.7, 69.1, 67.3, 17.8. HRMS (ESI): m/z calcd for $C_{27}H_{30}O_5Na$ [$M + Na$] 457.1963, found 457.1968.

Photocatalyzed allylation using *fac*-Ir(ppy)₃ catalyst

Benzyl 2,3-di-*O*-benzyl-6,7,8,9-tetradexy-8-methyl- α -D-non-8-enoglucopyranoside (235). To an oven-dried 100 mL Pyrex volumetric flask was added compound **234** (0.23 g, 0.4 mmol), 2-pyridyl methallylsulfone (0.16 g, 0.8 mmol) and tributylamine (0.2 mL, 0.8 mmol). Ir(ppy)₃ catalyst (5 mol%, 14 mg, 0.02 mmol), purified according to the literature protocol² and anhydrous acetonitrile (41 mL) were then added, and the mixture degassed with argon for 30 minutes. The flask was then placed in a 600 mL beaker lined with 12V blue LED strips and covered with aluminum foil. The reaction mixture was irradiated with a blue LED light till completion with monitoring by TLC (hexane:ethyl acetate 5:1, $R_f = 0.5$). The mixture was then diluted with acetonitrile, concentrated at reduced pressure and the residue purified via silica gel chromatography (5:1) to give **235** (0.14 g, 68%) as a colorless syrup and **306** (23 mg, 13%). The

spectral data were consistent with the data acquired from allylation procedure utilizing lauroyl peroxide as the initiator.

Procedure for preparation of 3-pyridyl methallylsulfone (301)

3-pyridyl sulfonyl chloride (1.21 g, 6.8 mmol,) and Na₂SO₃ (1.7 g, 13.6 mmol,) were dissolved in H₂O (10 mL) and heated to 80 °C. NaHCO₃ (1.2 g, 13.6 mmol) was then added portionwise over 1 hr. The reaction was stirred at 80 °C till completion and was then removed from the heating bath and allowed to reach ambient temperature. The reaction was concentrated under reduced pressure and the residual water was co-evaporated with toluene to give a white solid that was directly dissolved in DMF (20 mL) at room temperature and 3-chloro-2-methylpropene (0.9 mL) was added. The reaction was heated to 70 °C till completion. The reaction was diluted with EtOAc and H₂O was added. The layers were separated and the aqueous layer was extracted with EtOAc. The organic layer was dried with Na₂SO₄, filtered and concentrated at reduced pressure. The residue was purified via silica gel chromatography (3:1) to give **301** (0.85 g, 62%) as a colorless liquid.

Procedure for allylation reaction using 3-pyridyl methallylsulfone (301)

Benzyl 2,3-di-O-benzyl-6,7,8,9-tetradecoxy-8-methyl- α -D-non-8-enoglucopyranoside (235). Compound **234** (100 mg, 0.2 mmol) was dissolved in dry α,α,α -Trifluorotoluene (10 mL) and treated with 3-pyridyl methallylsulfone (0.1 g, 0.5 mmol). Lauroyl peroxide (0.36 g, 0.9 mmol) was added to the reaction mixture in two portions at 80 °C. The reaction mixture was stirred at 80 °C for 2 h with monitoring by TLC (hexane:ethyl acetate 6:1, R_f = 0.6). After completion, the reaction mixture was concentrated under reduced pressure and the residue was purified by silica gel column chromatography (hexane:ethyl acetate 15:1 to 10:1 to 6:1) to give **235** (43 mg, 50%) as a colorless syrup and **306** (29.3 mg, 38%) also as a colorless syrup. The spectral data were

consistent with the data acquired from allylation procedure utilizing 2-pyridyl methallylsulfone as the allyl source.

Procedure for preparation of methallyl ethylsulfone (**304**)

A solution of ethanethiol (5 ml, 67.6 mmol) in DMF (5 mL) was cooled to 0 °C, then sodium hydride (2.7 g, 67.6 mmol) was added portionwise over 15 minutes. 3-chloro-2-methylpropene (6.6 g, 67.6 mmol) was added and the mixture was stirred at 0 °C for 1 h then at ambient temperature for 2 h. After completion, the reaction mixture was quenched with methanol (5 mL) followed by water (15 mL) and extracted with ethyl acetate (30 mL). The aqueous layer was extracted with ethyl acetate thrice and the combined organic layer dried over anhydrous MgSO₄, filtered, and concentrated. The residual crude (7.86 g, 67.6 mmol) was dissolved in CH₂Cl₂ (150 mL). The solution was treated with *m*-Chloroperoxybenzoic acid (23 g, 135.2 mmol) and stirred at 0 °C till completion. After completion, the reaction mixture was concentrated under reduced pressure, diluted with CH₂Cl₂ (20 mL) and neutralized with 0.2 M aqueous sodium bicarbonate (100 mL). The aqueous layer was extracted with CH₂Cl₂ twice and the combined organic layer was dried over anhydrous MgSO₄, filtered, and concentrated. The crude was purified by silica gel column chromatography (hexane:ethyl acetate 4:1) to give **304** (8.1 g, 81%) as a colorless liquid. ¹H NMR (400 MHz, CDCl₃) δ 5.08 (s, 1H), 4.97 (s, 1H), 3.55 (s, 2H), 2.94-2.88 (m, 2H), 1.84 (s, 3H), 1.26-1.22 (m, 3H). ¹³C NMR (101 MHz, CDCl₃) δ 134.0, 120.2, 60.1, 45.6, 22.6, 6.4. HRMS (ESI): *m/z* calcd for C₆H₁₂O₂SNa [M + Na] 171.0278, found 171.0270.

Procedure for allylation reaction using methallyl ethylsulfone (**304**)

Benzyl 2,3-di-*O*-benzyl-6,7,8,9-tetradecoxy-8-methyl- α -D-non-8-enoglucopyranoside (235**)**. Compound **234** (50 mg, 0.1 mmol) was dissolved in a solvent mixture of heptane:PhCl 1:1 (2 mL) and treated with ethyl methallylsulfone (26 mg, 0.2 mmol). AIBN (3 mg, 0.02 mmol) was

then added. The reaction mixture was stirred at 80 °C for 2 h with monitoring by TLC (hexane:ethyl acetate 3:1, R_f =0.6). After completion, the reaction mixture was concentrated under reduced pressure and the residue was purified by silica gel column chromatography (hexane:ethyl acetate 3:1) to give **7** (4 mg, 10%) as a colorless syrup and **306** (2.6 mg, 6%). The spectral data were consistent with the data acquired from allylation procedure utilizing lauroyl peroxide as the initiator.

Procedure for allylation reaction using triethylborane as the initiator

Benzyl 2,3-di-O-benzyl-6,7,8,9-tetradecoxy-8-methyl- α -D-non-8-enoglucopyranoside (235). Compound **234** (0.16 g, 0.3 mmol) and 2-pyridyl methallylsulfone (57 mg, 0.7 mmol) were dissolved in dry α,α,α -Trifluorotoluene (3.2 mL) and the mixture cooled to 0 °C. Triethylborane (1.45 mL, 1.5 mmol) was then added to the reaction mixture in a dropwise fashion via a syringe pump. The reaction mixture was stirred at 0 °C for 2 h in an open air and gradually brought to rt with monitoring by TLC (hexane:ethyl acetate 6:1, R_f =0.6). After completion, the reaction mixture was concentrated under reduced pressure and the residue was purified by silica gel column chromatography (hexane:ethyl acetate 6:1) to give **7** (57 mg, 40%) as a colorless syrup and **306** (64 mg, 51%) as a colorless syrup. The spectral data were consistent with the data acquired from allylation procedure utilizing lauroyl peroxide as the initiator.

Benzyl 2,3-di-O-benzyl-6,7,8,9-tetradecoxy-8-methyl-4-keto- α -D-non-8-enoglucopyranoside (236). Compound **235** (1.85 g, 3.8 mmol) was dried under vacuum overnight and dissolved in anhydrous solution of DMSO:dichloromethane 2:1 (10.8 mL) under argon. The mixture was cooled to 0 °C. A solution of sulfur trioxide pyridine complex (1.81 g, 11.4 mmol) in DMSO (2 mL) was stirred at rt for 20 minutes then added dropwise to the sugar solution at 0 °C. The reaction mixture was allowed to come to rt and stirred till completion with monitoring by TLC

(hexane:ethyl acetate 4:1, R_f = 0.5). The reaction mixture was concentrated under reduced pressure and the residue diluted with dichloromethane (50 mL) and water (50 mL). The aqueous layer was extracted with dichloromethane twice and the combined organic layer was dried over anhydrous $MgSO_4$, filtered, and concentrated. The residue was purified by silica gel column chromatography (hexane:ethyl acetate 4:1) to give **236** (1.50 g, 81%) as a colorless syrup. $[\alpha]_D^{23} = +135.1$ ($c = 1.2$, $CHCl_3$), 1H NMR (400 MHz, $CDCl_3$) δ 7.54 – 7.20 (m, 15H), 5.03 – 4.94 (m, 2H, $PhCH_2$, H-1), 4.84 – 4.57 (m, 7H, $5PhCH_2$, $2H_{gem}$), 4.52 (d, $J = 10.1$ Hz, 1H, H-3), 4.16 (dd, $J = 8.4, 3.4$ Hz, 1H, H-5), 3.78 (dd, $J = 10.1, 3.6$ Hz, 1H, H-2), 2.21 – 2.01 (m, 3H, H-7, H-7', H-6), 1.80 – 1.63 (m, 4H, H-6', CH_3). ^{13}C NMR (101 MHz, $CDCl_3$) δ 203.4, 144.9, 138.0, 137.9, 136.8, 128.5, 128.40, 128.38, 128.3, 128.2, 128.1, 128.0, 127.9, 127.83, 127.79, 110.6, 95.7, 82.98, 80.6, 74.4, 73.6, 72.5, 69.8, 33.2, 26.3, 22.4. HRMS (ESI): m/z calcd for $C_{31}H_{34}O_5Na$ [$M + Na$] 509.2304, found 509.2310.

Benzyl 2,3-di-*O*-benzyl-6,7,8,9-tetradecoxy-8-methyl-4-*C*-vinyl- α -D-non-8-enogalactopyranoside (237). A solution of **236** (0.86 g, 1.8 mmol) in dry THF (18 mL) was cooled to -78 °C under argon and treated with vinylmagnesium bromide (5.32 mL, 5.3 mmol). The reaction mixture was stirred at -78 °C for 2 h with monitoring by TLC (hexane:ethyl acetate 6:1, $R_f = 0.6$). After completion, the reaction mixture was concentrated and the residue purified by silica gel column chromatography (hexane:ethyl acetate 6:1) to give **237** (0.86 g, 97%) as a colorless syrup. $[\alpha]_D^{23} = +89.3$ ($c = 1.35$, $CHCl_3$), 1H NMR (400 MHz, $CDCl_3$) δ 7.54 – 7.22 (m, 15H), 5.82 (dd, $J = 17.2, 10.6$ Hz, 1H, H-vinyl), 5.52 (dd, $J = 17.2, 1.1$ Hz, 1H, H-vinyl), 5.38 (dd, $J = 10.7, 1.0$ Hz, 1H, H-vinyl), 4.94 (d, $J = 3.6$ Hz, 1H, H-1), 4.88 (d, $J = 10.4$ Hz, 1H, $PhCH_2$), 4.80 (d, $J = 12.3$ Hz, 1H, $PhCH_2$), 4.77 – 4.73 (m, 2H), 4.69 (d, $J = 11.9$ Hz, 1H, $PhCH_2$), 4.66 (d, $J = 10.4$ Hz, 1H, $PhCH_2$), 4.59 (d, $J = 12.3$ Hz, 1H, $PhCH_2$), 4.56 (d, $J = 11.9$ Hz, 1H, $PhCH_2$),

3.92 (d, $J = 9.6$ Hz, 1H, H-3), 3.85 (dd, $J = 9.6, 3.7$ Hz, 1H, H-2), 3.78 (dt, $J = 9.8, 3.51$ Hz, 1H, H-5), 2.63 (s, 1H, OH), 2.35 – 2.28 (m, 1H), 2.07 – 2.00 (m, 1H), 1.83 – 1.65 (m, 5H). ^{13}C NMR (101 MHz, CDCl_3) δ 145.5, 139.7, 138.3, 138.2, 137.2, 128.5, 128.4, 128.3, 128.24, 128.17, 127.93, 127.87, 127.8, 127.7, 116.6, 110.3, 95.1, 80.1, 72.9, 71.0, 68.7, 34.6, 25.6, 22.5. HRMS (ESI): m/z calcd for $\text{C}_{33}\text{H}_{38}\text{O}_5\text{Na}$ [$\text{M} + \text{Na}$] 537.2617, found 537.2622.

Benzyl **2,3-di-*O*-benzyl-6,7,8,9-tetradecoxy-8-methyl- α -D-non-8-enogalactopyranoside (238).** A solution of **237** (0.76 g, 1.5 mmol) in dry dichloromethane (4 mL) was treated with 2nd gen. Grubbs catalyst (0.1 g, 0.2 mmol). The reaction mixture was heated at 40 °C till completion with monitoring by TLC (hexane:ethyl acetate 3:1, $R_f = 0.5$). After completion, the reaction mixture was concentrated and the concentrate purified by silica gel column chromatography (hexane:ethyl acetate 3:1) to give **238** (0.62 g, 85%) as a light brown syrup. $[\alpha]_D^{23} = +65.6$ ($c = 0.8$, CHCl_3), ^1H NMR (400 MHz, CDCl_3) δ 7.66 – 7.04 (m, 15H), 5.55 (s, 1H), 5.08 (d, $J = 11.2$ Hz, 1H), 4.93 (d, $J = 3.9$ Hz, 1H, H-1), 4.71 (d, $J = 12.2$ Hz, 2H, PhCH_2), 4.69 – 4.60 (m, 2H, PhCH_2), 4.55 (d, $J = 11.8$ Hz, 1H, PhCH_2), 4.01 (dd, $J = 9.4, 4.0$ Hz, 1H, H-2), 3.74 (dd, $J = 11.9, 3.7$ Hz, 1H, H-5), 3.68 (d, $J = 9.4$ Hz, 1H, H-3), 2.15 – 1.94 (m, 3H, H-7, H-7', H-6), 1.74 – 1.53 (m, 4H, CH_3 , H-6'). ^{13}C NMR (101 MHz, CDCl_3) δ 139.2, 138.6, 138.3, 137.5, 128.5, 128.39, 128.35, 128.1, 128.0, 127.80, 127.75, 127.7, 122.1, 96.2, 80.2, 78.6, 75.96, 72.9, 70.7, 69.3, 69.3, 30.3, 23.3, 21.7. HRMS (ESI): m/z calcd for $\text{C}_{31}\text{H}_{34}\text{O}_5\text{Na}$ [$\text{M} + \text{Na}$] 509.2304, found 509.2316.

Benzyl **2,3-di-*O*-benzyl-6,8,9-trideoxy-8-methyl-7-keto- α -D-non-8-enogalactopyranoside (239).** A solution of **238** (0.48 g, 1.0 mmol) in dry 1,4 dioxane (10 mL) was treated with selenium dioxide (0.11 g, 1.0 mmol) added in four portions over the period of the reaction. The reaction mixture was heated at 80 °C till completion with monitoring by TLC

(hexane:ethyl acetate 4:1, $R_f = 0.3$). After completion, the reaction mixture was concentrated and the residue purified by silica gel column chromatography (hexane:ethyl acetate 4:1 to 2:1) to give **239** (0.34 g, 70%) as an off white crystalline solid. Mp 117-120 °C. $[\alpha]_D^{23} = +64.6$ ($c = 0.35$, CHCl_3), ^1H NMR (400 MHz, CDCl_3) δ 7.50 – 7.20 (m, 15H), 6.47 (s, 1H), 5.12 (d, $J = 11.3$ Hz, 1H, PhCH_2), 4.94 (d, $J = 3.8$ Hz, 1H, H-1), 4.74 (d, $J = 11.4$ Hz, 1H, PhCH_2), 4.68 (d, $J = 12.2$ Hz, 1H, PhCH_2), 4.63 (d, $J = 11.7$ Hz, 1H, PhCH_2), 4.57 (d, $J = 12.2$ Hz, 1H, PhCH_2), 4.54 (d, $J = 11.7$ Hz, 1H, PhCH_2), 4.10 (dd, $J = 12.8, 4.9$ Hz, 1H, H-5), 4.03 (dd, $J = 9.3, 3.9$ Hz, 1H, H-2), 3.78 (d, $J = 9.3$ Hz, 1H, H-3), 2.91 (dd, $J = 16.5, 12.8$ Hz, 1H, H-6_{ax}), 2.48 (dd, $J = 16.5, 4.9$ Hz, 1H, H-6_{eq}), 1.70 (s, 3H, CH_3). ^{13}C NMR (101 MHz, CDCl_3) δ 197.5, 141.2, 137.9, 137.8, 136.9, 128.6, 128.5, 128.4, 128.3, 128.2, 128.1, 128.0, 127.9, 127.8, 96.2, 78.4, 78.3, 75.9, 72.9, 70.5, 69.6, 67.0, 37.99, 15.6. HRMS (ESI): m/z calcd for $\text{C}_{31}\text{H}_{32}\text{O}_6\text{Na}$ [$\text{M} + \text{Na}$] 523.2097, found 523.2096.

Benzyl 2,3-di-*O*-benzyl-6,8,9-trideoxy -8-methyl- α -D-non-8-enogalactopyranoside (240). A solution of **239** (0.39 g, 0.8 mmol) in dry methanol (7 mL) was treated with cerium (III) chloride heptahydrate (0.44 g, 1.2 mmol) and stirred at rt for 1 h. The reaction mixture was cooled to -78 °C and sodium borohydride (50 mg, 1.3 mmol) was added, with monitoring by TLC (hexane:ethyl acetate 1:1, $R_f = 0.3$). After completion, the reaction mixture was concentrated and the crude diluted with ethyl acetate (50 mL) and washed with water (20 mL). The aqueous layer was extracted with ethyl acetate and the combined organic layer dried over anhydrous MgSO_4 , filtered, and concentrated. The residue was purified by silica gel column chromatography (hexane:ethyl acetate 1:1) to give **240** (0.34 g, 86%) as a colorless liquid. $[\alpha]_D^{23} = +55.5$ ($c = 0.95$, CHCl_3), ^1H NMR (400 MHz, CD_3OD) δ 7.51 – 7.13 (m, 15H), 5.50 (s, 1H, H-9), 5.01 – 4.92 (m, 2H, PhCH_2 , H-1), 4.69 – 4.63 (m, 2H, 2PhCH_2), 4.63 – 4.52 (m, 3H, 3PhCH_2), 4.05 – 3.94 (m, 2H,

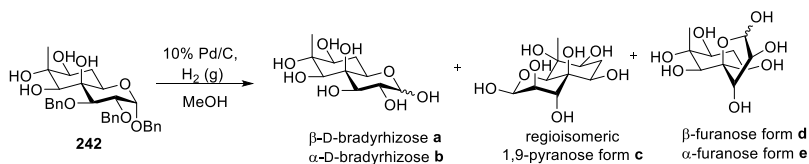
H-2, H-7), 3.62 (dd, $J = 12.2, 4.1$ Hz, 1H, H-5), 3.54 (d, $J = 9.6$ Hz, 1H, H-3), 2.02 – 1.86 (m, 2H, H-6, H-6'), 1.66 (s, 3H, CH₃). ¹³C NMR (101 MHz, CD₃OD) δ 141.4, 138.6, 138.3, 137.6, 128.2, 128.1, 128.0, 127.96, 127.9, 127.8, 127.5, 127.4, 127.3, 122.9, 96.5, 79.7, 78.4, 75.3, 72.4, 70.5, 69.1, 69.0, 67.7, 31.4, 17.96. HRMS (ESI): m/z calcd for C₃₁H₃₄O₆Na [M + Na] 525.2253, found 525.2252.

Benzyl-2,3,4,7-tetra-*O*-benzyl-8,9-epoxy- α -D-bradyrhizopyranoside (317). A solution of **240** (42 mg, 0.08 mmol) in dry DMF (0.8 mL) was placed in an ice bath at 0 °C under argon. Sodium hydride (3 mg, 0.08 mmol) and benzyl bromide (10 μ L, 0.08 mmol) were added. The reaction mixture was stirred at 0 °C for 1 h then at ambient temperature for 2 h, with monitoring by TLC (hexane:ethyl acetate 20:1, $R_f = 0.5$). After completion, the reaction mixture was quenched with methanol (2 mL) followed by water (5 mL) at 0 °C and extracted with ethyl acetate (10 mL). The aqueous layer was extracted with ethyl acetate thrice and the combined organic layer dried over anhydrous MgSO₄, filtered, and concentrated. The unreacted benzyl bromide was removed via flash column chromatography yielding 52 mg of desired intermediate by weight. A solution of intermediate (52 mg, 0.08 mmol) in dry THF (0.6 mL) was treated with *m*-Chloroperoxybenzoic acid (0.03 mg, 0.15 mmol) and stirred at RT, with monitoring by TLC (hexane:ethyl acetate 10:1, $R_f = 0.6$). After completion, the reaction mixture was concentrated under reduced pressure, diluted with ethyl acetate (5 mL) and neutralized with 0.2 M aqueous sodium bicarbonate (3 mL). The aqueous layer was extracted with ethyl acetate twice and the combined organic layer was dried over anhydrous MgSO₄, filtered, and concentrated. The crude was purified by silica gel column chromatography (hexane:ethyl acetate 10:1) to give **317** (51 mg, 86%) as a syrup. $[\alpha]_D^{23} = +30.9$ ($c = 0.25$, CHCl₃) ¹H NMR (900 MHz, Acetonitrile-*d*₃) δ 7.42 – 7.31 (m, 25H), 5.08 – 5.01 (m, 3H), 4.85 (d, $J = 10.7$ Hz, 1H), 4.76 (d, $J = 11.3$ Hz, 1H), 4.69 – 4.65 (m, 4H, H-1, 3PhCH₂), 4.54

(d, $J = 11.7$ Hz, 1H), 4.52 (d, $J = 12$ Hz, 1H), 4.06 (dd, $J = 9.9, 3.8$ Hz, 1H, H-2), 3.93 (d, $J = 9.9$ Hz, 1H, H-3), 3.84 – 3.78 (m, 2H, H-5, H-7), 3.63 (s, 1H, H-9), 1.94-1.93 (m, 1H, H-6), 1.84 – 1.81 (m, 1H, H-6'), 1.36 (s, 3H). ^{13}C NMR (226 MHz, CD_3CN) δ 139.7, 139.0, 138.7, 138.2, 128.4, 128.3, 128.3, 128.3, 128.2, 127.99, 127.9, 127.8, 127.7, 127.7, 127.6, 127.6, 127.5, 127.4, 96., 80.3, 77.7, 75.8, 75.1, 74.1, 72.1, 71.5, 69.3, 67.8, 65.1, 61.5, 60.7, 28.8, 18.7. ESI-HRMS: m/z calcd for $\text{C}_{45}\text{H}_{46}\text{O}_7\text{Na}$ [$\text{M} + \text{Na}$] 721.3141, found 721.3143.

Benzyl 8,9-anhydro-2,3-di-*O*-benzyl-6-deoxy-8-methyl- α -D-nonagalactopyranoside (241). A solution of **240** (0.34 g, 0.7 mmol) in dry THF (6.7 mL) was treated with *m*-chloroperoxybenzoic acid (72 mg, 0.4 mmol) and stirred at rt, with monitoring by TLC (hexane:ethyl acetate:methanol 1:1:0.1, $R_f = 0.3$). After completion, the reaction mixture was concentrated under reduced pressure, diluted with ethyl acetate (50 mL) and neutralized with 0.2 M aqueous sodium bicarbonate (100 mL). The aqueous layer was extracted with ethyl acetate twice and the combined organic layer was dried over anhydrous MgSO_4 , filtered, and concentrated. The crude product was purified by silica gel column chromatography (hexane:ethyl acetate:methanol 1:1:0.1) to give **241** (0.29 g, 83%) as a syrup. $[\alpha]_D^{23} = +28.9$ ($c = 0.7$, CHCl_3), ^1H NMR (600 MHz, CDCl_3) δ 7.51 – 7.16 (m, 15H), 5.09 (d, $J = 11.7$ Hz, 1H, PhCH_2), 4.85 (d, $J = 3.9$ Hz, 1H, H-1), 4.72 (d, $J = 11.7$ Hz, 1H, PhCH_2), 4.69 (d, $J = 11.8$ Hz, 1H, PhCH_2), 4.62 – 4.59 (m, 2H, 2PhCH_2), 4.56 (d, $J = 11.8$ Hz, 1H, PhCH_2), 4.07 (dd, $J = 9.4, 3.9$ Hz, 1H, H-2), 3.73 (dd, $J = 10.4, 6.3$ Hz, 1H, H-7), 3.69 (d, $J = 9.4$ Hz, 1H, H-3), 3.19 (dd, $J = 12.7, 2.7$ Hz, 1H, H-5), 2.78 (s, 1H, H-9), 1.63 (ddd, $J = 12.3, 6.3, 2.8$ Hz, 1H, H-6_{eq}), 1.48 (td, $J = 12.6, 10.4$ Hz, 1H, H-6_{ax}), 1.24 (s, 3H, methyl). ^{13}C NMR (151 MHz, CDCl_3) δ 138.0, 137.3, 128.7, 128.5, 128.41, 128.39, 127.99, 127.97, 127.8, 96.7, 78.3, 75.3, 73.1, 70.8, 69.9, 69.6, 67.4, 63.4, 62.95, 28.5, 19.1. HRMS (ESI): m/z calcd for $\text{C}_{31}\text{H}_{34}\text{O}_7\text{Na}$ [$\text{M} + \text{Na}$] 541.2202, found 541.2210.

Benzyl 2,3-di-*O*-benzyl-8- α -D-bradyrhizopyranoside (242). A solution of **241** (135 mg, 0.3 mmol) in 1,4 dioxane:water 05:1.5 (5 mL), was treated with concentrated sulphuric acid (30 μ L, 0.6 mmol) added dropwise in three portions at 65 °C. The reaction was monitored by TLC (hexane:ethyl acetate:methanol 1:1:0.2, R_f = 0.2). After completion, the mixture was diluted with ethyl acetate (20 mL) and neutralized with saturated aqueous sodium bicarbonate (50 mL). The aqueous layer was extracted with ethyl acetate twice and the combined organic layer was dried over anhydrous $MgSO_4$, filtered, and concentrated. The crude product was purified by silica gel column chromatography (hexane:ethyl acetate:methanol 1:1:0.2) to give **15** (70 mg, 50%) as a white amorphous solid. Mp, 148-152 °C. $[\alpha]_D^{23} = +66.3$ ($c = 0.75$, $CHCl_3$), 1H NMR (600 MHz, CD_3OD) δ 7.49 – 7.11 (m, 15H), 4.95 – 4.92 (m, 2H, $PhCH_2$, H-1), 4.78 (d, $J = 10.4$ Hz, 1H, $PhCH_2$), 4.66 (d, $J = 12.2$ Hz, 1H, $PhCH_2$), 4.57 (d, $J = 12.2$ Hz, 1H, $PhCH_2$), 4.55 (d, $J = 11.5$ Hz, 1H, $PhCH_2$), 4.52 (d, $J = 11.5$ Hz, 1H, $PhCH_2$), 3.93 (dd, $J = 9.5, 3.7$ Hz, 1H, H-2), 3.89 (d, $J = 9.6$ Hz, 1H, H-3), 3.70 (dd, $J = 12.4, 4.0$ Hz, 1H, H-5), 3.48 (s, 1H, H-9), 3.43 (dd, $J = 12.2, 4.3$ Hz, 1H, H-7), 1.82 (q, $J = 12.2$ Hz, 1H, H-6_{ax}), 1.64 (dt, $J = 11.9, 4.2$ Hz, 1H, H-6_{eq}), 1.22 (s, 3H, methyl). ^{13}C NMR (151 MHz, CD_3OD) δ 138.14, 138.08, 137.5, 128.14, 128.09, 128.0, 127.99, 127.96, 127.9, 127.8, 127.54, 127.47, 127.4, 95.97, 82.7, 78.8, 78.0, 77.2, 74.95, 73.8, 72.5, 72.3, 69.2, 66.6, 31.1, 14.0. HRMS (ESI): m/z calcd for $C_{31}H_{36}O_8Na$ [$M + Na$] 559.2308, found 559.2311.



α,β -D-Bradyrhizose (20). Compound **242** (45 mg, 0.08 mmol) was dissolved in dry methanol (5 ml) then 10% Pd/C (79 mg, 0.1 mmol) was added and the mixture degassed with argon. The reaction mixture was then purged with H_2 gas then put under H_2 gas at rt till completion.

The palladium on carbon was filtered and the filtrate concentrated at reduced pressure. The residual crude was purified by reversed phase column chromatography (on a C-18 silica gel) using H₂O as the eluent yielding compound **20** (21 mg, 100% , as an equilibrium mixture of α -D-bradyrhizose, β -D-bradyrhizose, α,β -furanoses and a regioisomeric 1,9-pyranose) as a white foam with spectral data consistent with the literature.³ ¹H NMR (900 MHz, D₂O) δ 5.25 (d, J = 3.7 Hz, 0.08H, H-1e), 5.23 (d, J = 4.1 Hz, 0.08H), 5.21 (d, J = 4.3 Hz, 0.42H, H-1b), 5.05 (s, 0.03H, H-1d), 5.04 (s, 0.17H, H-1c), 4.61 (d, J = 8.1 Hz, 1H, H-1a), 4.37 – 4.25 (m, 0.28H), 4.18 – 4.08 (m, 0.24H), 4.06 – 3.96 (m, 0.53H), 3.94 - 3.91 (m, 0.57H), 3.85 – 3.77 (m, 3.14H), 3.78 – 3.67 (m, 4.83H), 3.50 – 3.42 (m, 0.98H), 2.02 – 1.92 (m, 0.17H), 1.92 – 1.82 (m, 0.40H), 1.34 – 1.30 (m, 0.55H), 1.25 - 1.21 (m, 3.09H), 1.19 – 1.15 (m, 0.80H). ¹³C NMR (151 MHz, D₂O) δ 96.5, 92.2, 78.4, 78.2, 77.6, 77.3, 74.3, 73.3, 72.8, 72.5, 72.0, 70.4, 70.3, 69.0, 65.4, 30.9, 30.8, 14.0, 14.0. HRMS (ESI): m/z calcd for C₁₀H₁₈O₈Na [M + Na] 289.0899, found 289.0900. The chemical shifts for both ¹H for (**20**) were referenced to HOD (δ_H 4.79).

Methyl 2,3,4-tri-*O*-benzyl- α -D-glucopyranoside (338). This acceptor was prepared according to the literature method in (1.4 g, 98%) yield as a colorless syrup. ¹H NMR (400 MHz, CDCl₃) δ 7.41 – 7.25 (m, 15H), 5.00 (d, J = 10.9 Hz, 1H), 4.93 – 4.77 (m, 3H), 4.66 (dd, J = 11.6, 8.2 Hz, 2H), 4.58 (d, J = 3.6 Hz, 1H), 4.02 (t, J = 9.2 Hz, 1H), 3.78 (dd, J = 11.6, 2.5 Hz, 1H), 3.74 – 3.62 (m, 2H), 3.57 – 3.46 (m, 2H), 3.37 (s, 3H). ¹³C NMR (101 MHz, CDCl₃) δ 138.7, 138.14, 138.11, 128.5, 128.4, 128.1, 128.0, 127.94, 127.92, 127.9, 127.6, 98.2, 81.95, 79.99, 77.4, 75.7, 75.0, 73.4, 70.7, 61.9, 55.2. HRMS (ESI): m/z calcd for C₂₈H₃₂O₆Na [M + Na] 487.2271, found 487.2265.

Methyl 2-*O*-benzyl-4,6-*O*-benzylidene- α -D-mannopyranoside (341). This acceptor was prepared according to the literature method in (1.2 g, 89%) yield as a colorless syrup. ¹H NMR

(499 MHz, CDCl₃) δ 7.53 – 7.49 (m, 2H), 7.43 – 7.30 (m, 8H), 5.57 (s, 1H), 4.77 – 4.75 (m, 1H), 4.74 – 4.66 (m, 2H), 4.27 (dd, J = 9.7, 4.3 Hz, 1H), 4.12 – 4.06 (m, 1H), 3.92 (t, J = 9.5 Hz, 1H), 3.87 – 3.73 (m, 3H), 3.37 (s, 3H). ¹³C NMR (126 MHz, CDCl₃) δ 137.7, 137.4, 129.1, 128.6, 128.3, 128.1, 127.96, 126.3, 102.1, 99.5, 79.5, 78.5, 73.8, 68.8, 68.7, 63.4, 54.99. HRMS (ESI): m/z calcd for C₂₁H₂₄O₆Na [M + Na] 395.1252, found 395.1248.

Methyl 2-*O*-benzyl-5-*O*-*tert*-butyldimethylsilyl- β -D-ribofuranoside (346). This acceptor was prepared according to the literature method in (97 mg, 87%) yield as a colorless syrup. ¹H NMR (600 MHz, CDCl₃) δ 7.39 – 7.18 (m, 5H), 4.81 (s, 1H, H-1), 4.72 (d, J = 11.9 Hz, 1H, PhCH₂), 4.60 (d, J = 11.9 Hz, 1H, PhCH₂), 4.34 (dd, J = 7.2, 4.6 Hz, 1H, H-3), 4.09 (dt, J = 7.4, 3.1 Hz, 1H, H-4), 3.79 (dt, J = 12.1, 2.6 Hz, 1H, H-5_{eq}), 3.70 (d, J = 4.5 Hz, 1H, H-2), 3.54 (ddd, J = 11.9, 8.0, 3.5 Hz, 1H, H-5_{ax}), 3.34 (s, 3H), 2.92 (s, 3H), 2.84 (s, 3H), 0.87 (s, 9H). ¹³C NMR (151 MHz, CDCl₃) δ 162.5, 137.97, 128.98, 128.3, 128.2, 127.8, 127.7, 106.7, 83.4, 82.3, 72.6, 71.1, 61.7, 55.5, 36.4, 31.4, 25.7, 18.1. HRMS (ESI): m/z calcd for C₁₉H₃₂O₅Na [M + Na] 391.1960, found 391.1957.

Methyl 2-*O*-acetyl-4-*O*-benzyl- α -L-rhamnopyranoside (351). This acceptor was prepared according to the literature method in (120 mg, 93%) yield as a colorless syrup. ¹H NMR (500 MHz, CDCl₃) δ 7.37 – 7.30 (m, 5H), 5.07 (dd, J = 3.6, 1.6 Hz, 1H), 4.82 (d, J = 11.1 Hz, 1H), 4.68 (d, J = 11.1 Hz, 1H), 4.60 – 4.59 (m, 1H), 4.06 (dd, J = 9.4, 3.6 Hz, 1H), 3.70 (dq, J = 9.5, 6.2 Hz, 1H), 3.34 – 3.29 (m, 4H), 2.13 (s, 3H), 1.33 (d, J = 6.3 Hz, 3H). ¹³C NMR (126 MHz, CDCl₃) δ 171.0, 138.4, 128.6, 127.95, 98.5, 81.7, 75.2, 72.9, 70.2, 67.3, 54.96, 21.1, 18.1. HRMS (ESI): m/z calcd for C₁₆H₂₂O₆Na [M + Na] 333.1361, found 333.1356.

Methyl 2-azido-3,4-di-*O*-benzyl-2-deoxy- α -D-galactopyranoside (368). This compound was prepared according to the literature method⁵ in (0.25 g, 81%) yield as a colorless syrup. ¹H

NMR (500 MHz, CDCl₃) δ 7.39 – 7.31 (m, 10H), 4.95 – 4.89 (m, 1H), 4.82-4.80 (m, 1H), 4.80 – 4.67 (m, 3H), 4.57 (d, J = 11.6 Hz, 1H), 3.97 – 3.91 (m, 3H), 3.76-3.72 (m, 1H), 3.57 – 3.50 (m, 1H), 3.39 (s, 3H). ¹³C NMR (126 MHz, CDCl₃) δ 137.98, 137.6, 128.7, 128.7, 128.6, 128.22, 128.16, 128.0, 127.1, 99.2, 77.9, 74.6, 73.4, 72.8, 70.8, 62.3, 60.2, 55.5. HRMS (ESI): m/z calcd for C₂₁H₂₅N₃O₅Na [M + Na] 422.1889, found 422.1878.

Methyl 2-azido-3,4-di-*O*-benzyl-2-deoxy- α -D-glucopyranoside (360). This compound was prepared according to the literature method⁵ in (0.34 g, 83%) yield as a colorless syrup. ¹H NMR (500 MHz, CDCl₃) δ 7.41-7.30 (m, 10H), 4.93-4.88 (m, 2H), 4.78 (d, J = 3.5 Hz, 1H), 4.72 – 4.65 (m, 2H), 4.02 (dd, J = 10.2, 8.6 Hz, 1H), 3.84-3.81 (m, 1H), 3.77 – 3.69 (m, 2H), 3.65 (t, J = 9.3 Hz, 1H), 3.41 (s, 3H). ¹³C NMR (126 MHz, CDCl₃) δ 138.1, 138.0, 128.7, 128.6, 128.24, 128.20, 128.12, 128.08, 128.0, 127.99, 127.1, 98.9, 80.5, 78.1, 75.6, 75.2, 71.5, 63.8, 61.5, 55.3. HRMS (ESI): m/z calcd for C₂₁H₂₅N₃O₅Na [M + Na] 422.1910, found 422.1901.

Ethyl (2-*O*-acetyl-4,5,7,8-di-*O*-isopropylidene-3-deoxy- α -D-manno-oct-2-ulopyranosyl) onate (327). This compound was prepared according to the literature method in (2.6g, 91 %) yield as a white foam. ¹H NMR (600 MHz, CDCl₃) δ 4.52 (dt, J = 7.3, 3.5 Hz, 1H, H-4), 4.37 (ddd, J = 8.4, 6.1, 3.7 Hz, 1H, H-7), 4.32 (dd, J = 7.8, 2.0 Hz, 1H, H-5), 4.24 – 4.19 (m, 2H), 4.08 (dd, J = 9.1, 6.1 Hz, 1H, H-8_{ax}), 3.85 (dd, J = 9.1, 3.7 Hz, 1H, H-8_{eq}), 3.59 (dd, J = 8.3, 2.0 Hz, 1H, H-6), 2.66 (dd, J = 15.6, 3.7 Hz, 1H, H-3_{eq}), 2.07 – 2.03 (m, 4H, H-3_{ax}, CH₃), 1.47 (s, 3H), 1.40 (s, 3H), 1.34 (s, 3H), 1.30 (s, 3H), 1.26 (t, J = 7.1 Hz, 3H). ¹³C NMR (151 MHz, CDCl₃) δ 168.9, 168.0, 109.8, 109.5, 96.9, 73.3, 72.9, 71.2, 69.5, 67.1, 62.0, 32.1, 27.0, 25.5, 25.1, 24.8, 21.0, 13.8. HRMS (ESI): m/z calcd for C₁₈H₂₈O₉Na [M + Na] 411.1751, found 411.1743.

Ethyl (1-adamantanyl 4,5,7,8-di-*O*-isopropylidene-3-deoxy-2-thio- α -D-manno-oct-2-ulopyranosid) onate (328). To a stirred mixture of the Kdo donor **327** (0.23 g, 0.6 mmol), and 1-

adamantanethiol (0.15 g, 0.9 mmol) in anhydrous CH_2Cl_2 (2 mL) at 0 °C, was added dropwise boron trifluoride etherate (0.2 mL) under argon. The reaction mixture was stirred at 0 °C for 30 min with monitoring by TLC (hexane:ethyl acetate 2:1, $R_f = 0.3$). After completion, the reaction mixture was diluted with CH_2Cl_2 , and neutralized with saturated aqueous sodium bicarbonate (10 mL). The aqueous layer was extracted with CH_2Cl_2 twice and the combined organic layer was dried over anhydrous Na_2SO_4 , filtered, and concentrated at reduced pressure. The residual crude was purified by silica gel column chromatography (hexane/EtOAc: 2/1) to provide **328** (0.26 g, 84%) as a colorless syrup. $[\alpha]_D^{23} = +20$ ($c = 0.6$, CHCl_3) ^1H NMR (600 MHz, CDCl_3) δ 4.45-4.43 (m, 1H), 4.35 – 4.25 (m, 3H), 4.16 – 4.06 (m, 3H), 3.71 (dd, $J = 7.9, 1.9$ Hz, 1H), 2.87 (dd, $J = 15.2, 3.9$ Hz, 1H), 2.01 – 1.94 (m, 6H), 1.88-1.85 (m, 3H), 1.79 (dd, $J = 15.2, 2.6$ Hz, 1H), 1.63-1.62 (m, 6H), 1.42 (s, 3H), 1.39 (s, 3H), 1.36 (s, 3H), 1.32 (t, $J = 7.1$ Hz, 3H), 1.28 (s, 3H). ^{13}C NMR (151 MHz, CDCl_3) δ 171.2, 109.6, 109.1, 84.5, 73.8, 72.1, 71.5, 70.3, 67.7, 61.7, 49.99, 43.6, 36.1, 34.3, 29.8, 26.9, 25.5, 25.3, 24.9, 14.0. HRMS (ESI): m/z calcd for $\text{C}_{26}\text{H}_{40}\text{O}_7\text{SNa}$ [$M + \text{Na}$] 519.2647, found 519.2640.

Ethyl (1-adamantanyl-3-deoxy-2-thio- α -D-manno-oct-2-ulopyranosid) onate (329). A solution of **328** (0.89 g, 1.8 mmol) in CH_2Cl_2 (5 mL), was treated with a solution mixture of trifluoroacetic acid:water 1:1 (1 mL) at 0 °C. The reaction mixture was stirred at 0 °C till completion with monitoring by TLC (hexane:ethyl acetate:methanol 1:1:0.5, $R_f = 0.1$). After completion, the mixture was diluted with CH_2Cl_2 (10 mL) and neutralized with saturated aqueous sodium bicarbonate (20 mL). The aqueous layer was extracted with ethyl acetate three times and the combined organic layer was dried over anhydrous Na_2SO_4 , filtered, and concentrated. The residual crude was purified by silica gel column chromatography (hexane:ethyl acetate:methanol 1:1:0.5) to give **329** (0.35 g, 94%) as a light yellow syrup $[\alpha]_D^{23} = +98$ ($c = 0.4$, CD_3OD) ^1H NMR

(500 MHz, CD₃OD) δ 4.34-4.29 (m, 1H), 4.23-4.16 (m, 2H), 4.04 – 3.96 (m, 3H), 3.78 (dd, J = 11.3, 5.5 Hz, 1H), 3.63 (dd, J = 11.1, 6.6 Hz, 1H), 2.05 – 1.93 (m, 8H), 1.91 – 1.86 (m, 3H), 1.70-1.63 (m, 6H), 1.32 (t, J = 7.1 Hz, 3H). ¹³C NMR (126 MHz, CD₃OD) δ 172.5, 86.4, 78.2, 72.4, 71.6, 67.17, 7.91, 63.1, 62.0, 49.3, 43.5, 36.5, 35.9, 29.9, 13.1. HRMS (ESI): m/z calcd for C₂₀H₃₂O₇SNa [M + Na] 439.1757, found 439.1710.

Ethyl (1-adamantanyl 4,5,7,8-tetra-*O*-acetyl-3-deoxy-2-thio- α -D-manno-oct-2-ulopyranosid) onate (330). A solution of **329** (0.18 g, 0.4 mmol) in pyridine (5 mL), was cooled to 0 °C. 4-dimethylaminopyridine (26 mg, 0.2 mmol) was added followed by the addition of acetic anhydride (0.2 mL, 2.2 mmol). The reaction mixture was stirred at 0 °C till completion with monitoring by TLC (hexane:ethyl acetate 3:1, R_f = 0.3). After completion, the reaction mixture was concentrated under reduced pressure and the residue purified by silica gel column chromatography (hexane:ethyl acetate 3:1) to give **330** (0.24 g, 96%) as an off white form. $[\alpha]_D^{23}$ = +136 (c = 0.3, CHCl₃) ¹H NMR (600 MHz, CD₃CN) δ 5.32 – 5.28 (m, 1H, H-5), 5.23 (ddd, J = 12.1, 5.3, 3.1 Hz, 1H, H-4), 5.15 (ddd, J = 8.6, 5.9, 2.7 Hz, 1H, H-7), 4.65 (dd, J = 8.6, 1.5 Hz, 1H, H-6), 4.54 (dd, J = 12.2, 2.8 Hz, 1H, H-8_{eq}), 4.31 (dq, J = 10.8, 7.1 Hz, 1H, OCH₂CH₃), 4.21 (dq, J = 10.8, 7.1 Hz, 1H, OCH₂CH₃), 4.01 (dd, J = 12.2, 5.9 Hz, 1H, H-8_{ax}), 2.22 – 2.17 (m, 1H), 2.16 – 2.13 (m, 1H), 2.06 – 1.94 (m, 15H), 1.93 – 1.89 (m, 5H), 1.71-1.65 (m, 6H), 1.32 (t, J = 7.1 Hz, 3H). ¹³C NMR (151 MHz, CD₃CN) δ 170.4, 170.1, 169.6, 169.4, 86.2, 69.3, 68.3, 66.6, 64.8, 62.2, 61.9, 49.9, 43.1, 35.7, 34.1, 29.8, 19.98, 19.96, 19.92, 19.85, 13.3. HRMS (ESI): m/z calcd for C₂₈H₄₀O₁₁SNa [M + Na] 607.2206, found 607.2189.

Ethyl (1-adamantanyl 8-*O*-tert-butyldimethylsilyl-3-deoxy-2-thio- α -D-manno-oct-2-ulopyranosid) onate (332). To a solution mixture of thioglycoside **329** (0.15 g, 0.4 mmol) in DMF (3.7 mL) was added imidazole (50 mg, 0.7 mmol) and TBSCl (55 mg, 0.4 mmol) at 0 °C. The

reaction mixture was gradually warmed to rt and stirred for 1 h while monitoring by TLC (hexane:ethyl acetate 1:1, $R_f = 0.2$). The reaction was then quenched by addition of saturated aqueous NH_4Cl , and then diluted with ethyl acetate. The organic layer was washed with water and brine, dried over anhydrous Na_2SO_4 , filtered and concentrated at reduced pressure. The residual syrup was purified by silica gel column chromatography (hexane:ethyl acetate 1:1) to give **332** (0.17 g, 89%) as an off white foam. $[\alpha]_D^{23} = +105$ ($c = 1.4$, CH_3OH) ^1H NMR (500 MHz, CD_3CN) δ 4.27 – 4.17 (m, 1H), 4.17 – 4.08 (m, 2H), 3.94-3.92 (m, 1H), 3.89-3.85 (m, 2H), 3.81 (dd, $J = 10.3, 5.5$ Hz, 1H), 3.62 – 3.58 (m, 1H), 1.99 – 1.89 (m, 8H), 1.88 – 1.81 (m, 3H), 1.66 – 1.62 (m, 5H), 1.27 (t, $J = 7.1$ Hz, 3H), 0.91-0.82 (m, 9H), 0.06 (s, 6H). ^{13}C NMR (126 MHz, CD_3CN) δ 170.9, 86.5, 72.0, 71.6, 66.9, 66.0, 64.9, 61.6, 49.3, 43.4, 37.1, 35.9, 29.9, 25.5, 18.1, 13.5, 0.9, 0.7, 0.6, 0.4, 0.2, 0.07. HRMS (ESI): m/z calcd for $\text{C}_{26}\text{H}_{46}\text{O}_7\text{SSiNa}$ $[\text{M} + \text{Na}]$ 553.2632, found 553.2626.

Ethyl (1-adamantanyl 5,7-di-*O*-*tert*-butylsilyl-8-*O*-*tert*-butyldimethylsilyl-3-deoxy-2-thio- α -D-manno-oct-2-ulopyranosid) onate (333). A solution of **332** (60 mg, 0.1 mmol) in pyridine (1.1 mL) was cooled to 0 °C. 4-dimethylaminopyridine (7 mg, 0.06 mmol) was added followed by the addition of di-*tert*-butylsilyl bis(trifluoromethanesulfonate) (37 μL). The reaction mixture was stirred at 0 °C till completion with monitoring by TLC (hexane:ethyl acetate 4:1, $R_f = 0.5$). The reaction was then quenched by addition of saturated aqueous NH_4Cl , and then diluted with ethyl acetate. The organic layer was washed with water and brine, dried over anhydrous Na_2SO_4 , filtered and concentrated under reduced pressure. The residual crude was purified by silica gel column chromatography (hexane:ethyl acetate 4:1) to give **333** (62 mg, 82%) as a colorless syrup. $[\alpha]_D^{23} = +82$ ($c = 0.3$, CHCl_3) ^1H NMR (500 MHz, C_6D_6) δ 4.68 (br, 1H, H-6), 4.45 (t, $J = 5.7$ Hz, 1H, H-7), 4.34 (, $J = 3.0$ Hz, 1H, H-5), 4.26 – 4.12 (m, 1H, H-4), 4.02-3.99 (

2H, 2CH₂), 3.79 – 3.71 (m, 2H, H-8_{ax}, H-8_{eq}), 2.59 (dd, $J = 13.5, 4.8$ Hz, 1H, H-3_{ax}), 2.26 – 2.10 (m, 2H), 2.00 (d, $J = 12.0$ Hz, 3H), 1.83 (br, 4H), 1.59-1.56 (m, 5H), 1.46 (d, $J = 12.4$ Hz, 4H), 1.14 (s, 9H), 1.03 (s, 6H), 1.00 (s, 9H), 0.88 (s, 9H). ¹³C NMR (126 MHz, C₆D₆) δ 170.1, 86.6, 77.4, 77.0, 70.6, 69.1, 66.6, 66.0, 61.0, 49.6, 43.4, 38.2, 36.1, 30.0, 27.9, 27.8, 27.4, 27.3, 25.9, 21.96, 21.5, 20.5, 18.4, 13.8. HRMS (ESI): m/z calcd for C₃₄H₆₂O₇SSi₂Na [M + Na] 694.3673, found 694.3665.

Ethyl (1-adamantanyl 4-*O*-benzoyl-5,7-di-*O*-*tert*-butylsilyl-8-*O*-*tert*-butyldimethylsilyl-3-deoxy-2-thio- α -D-manno-oct-2-ulopyranosid) onate (334). To a solution of **333** (70.7 mg, 0.1 mmol) in pyridine (1.1 mL) was added 4-dimethylaminopyridine (6 mg, 0.05 mmol) and benzoyl chloride (12 μ L, 0.3 mmol) at 0 °C. The reaction mixture was stirred at 0 °C till completion with monitoring by TLC (hexane:ethyl acetate 6:1, $R_f = 0.5$). The reaction was then quenched by addition of methanol. The resulting mixture was concentrated under reduced pressure. The obtained residue was purified by silica gel column chromatography (hexane:ethyl acetate 6:1) to afford **334** (75 mg, 86%) as a colorless syrup. $[\alpha]_D^{23} = +63$ ($c = 0.1$, CHCl₃) ¹H NMR (900 MHz, C₆D₆) δ 8.13 – 8.08 (m, 2H), 7.02 – 6.98 (m, 1H), 6.96 – 6.92 (m, 2H), 5.70 (ddd, $J = 12.2, 4.7, 2.7$ Hz, 1H, H-4), 4.92 (d, $J = 2.8$ Hz, 1H, H-5), 4.86 (t, $J = 0.7$ Hz 1H, H-6), 4.53 (ddd, $J = 6.5, 4.8, 0.7$ Hz, 1H, H-7), 4.07 – 3.99 (m, 2H, 2OCH₂CH₃), 3.86 – 3.81 (m, 2H, H-8_{ax}, H-8_{eq}), 2.85 (t, $J = 12.7$ Hz, 1H, H-3_{ax}), 2.67 (dd, $J = 13.1, 4.6$ Hz, 1H, H-3_{eq}), 2.23 (d, $J = 11.8$ Hz, 3H), 2.07 (d, $J = 11.9$ Hz, 3H), 1.85 (s, 3H), 1.60 (d, $J = 11.8$ Hz, 3H), 1.48 (d, $J = 12.1$ Hz, 3H), 1.22 (s, 11H), 1.03 (s, 11H), 0.97 (d, $J = 7.1$ Hz, 3H), 0.94 (s, 11H). ¹³C NMR (226 MHz, C₆D₆) δ 169.9, 165.4, 132.6, 130.6, 129.6, 128.2, 127.98, 127.96, 127.9, 127.8, 127.74, 127.69, 127.63, 127.59, 127.4, 86.6, 77.2, 70.7, 66.6, 66.1, 61.1, 49.8, 43.4, 36.1, 34.0, 29.99, 29.9, 27.95,

27.2, 25.98, 21.96, 21.4, 18.5, 13.8. HRMS (ESI): m/z calcd for $C_{41}H_{66}O_8SSi_2Na$ [$M + Na$] 797.3909, found 797.3889.

Ethyl (1-adamantanyl 4,5,7,8-tetra-*O*-benzyl-3-deoxy-2-thio- α -D-manno-oct-2-ulopyranosid) onate (331). To a solution of **329** (0.12 g, 0.3 mmol) in dry DMF (2.9 mL) were added sodium hydride (46.1 mg, 1.2 mmol) and BnBr (138 μ L, 1.2 mmol) at 0 °C. The reaction mixture was gradually warmed to room temperature and stirred till completion with monitoring by TLC (hexane:ethyl acetate 10:1, R_f = 0.6). The reaction was quenched by the addition methanol, then was diluted with ethyl acetate. The organic layer was washed with water and brine, dried over anhydrous Na_2SO_4 , filtered and concentrated in at reduced pressure. The residual syrup was purified by silica gel column chromatography (hexane:ethyl acetate 10:1) to afford **331** (0.2 g, 91%) as a colorless syrup. . $[\alpha]_D^{23} = +138$ (c = 0.8, $CHCl_3$). 1H NMR (500 MHz, C_6D_6) δ 7.33-7.31 (m, 4H), 7.29 – 7.26 (m, 3H), 7.14-7.08 (7H), 7.04 – 7.01 (m, 6H), 5.09 (dd, J = 11.4, 3.7 Hz, 1H), 4.99 (d, J = 12.5 Hz, 1H), 4.92 (d, J = 12.4 Hz, 1H), 4.85 – 4.81 (m, 1H), 4.62 (ddd, J = 10.0, 8.2, 1.4 Hz, 1H, H-7), 4.56 – 4.53 (m, 1H), 4.41 – 4.37 (m, 2H), 4.34-.30 (m, 2H), 4.22-4.16 (m, 3H), 4.10 – 4.07 (m, 1H), 3.96 – 3.91 (m, 2H), 2.74 – 2.68 (m, 2H), 2.14 – 2.00 (m, 6H), 1.82 – 1.75 (m, 3H), 1.48 – 1.42 (m, 6H), 0.87 (t, J = 7.1 Hz, 3H). ^{13}C NMR (126 MHz, C_6D_6) δ 169.97, 169.9, 139.54, 139.48, 139.1, 138.8, 138.7, 129.0, 128.37, 128.35, 128.23, 128.20, 128.0, 127.95, 127.9, 127.8, 127.7, 127.6, 127.5, 127.4, 127.31, 127.25, 127.23, 127.16, 87.2, 87.1, 77.5, 77.4, 76.3, 74.7, 74.6, 73.4, 73.0, 72.97, 72.7, 72.6, 72.23, 72.17, 70.43, 70.40, 70.2, 70.0, 66.9, 61.1, 49.6, 49.5, 43.5, 36.2, 36.1, 35.7, 30.09, 30.06, 13.7. HRMS (ESI): m/z calcd for $C_{48}H_{56}O_7SNa$ [$M + Na$] 800.3672, found 800.3671.

Ethyl (4,5,7,8-tetra-*O*-acetyl-3-deoxy- β -D-manno-oct-2-ulopyranosyl) onate-(2 \rightarrow 6)-methyl 2,3,4-tri-*O*-benzyl- α -D-glucopyranoside (369). A mixture of donor **330** (59 mg, 0.1

mmol) acceptor **338** (70.3 mg, 0.2 mmol) and activated 4Å acid-washed powdered molecular sieves (59 mg) in CH₂Cl₂:CH₃CN 2:1 (0.5 mL, 0.2M) was stirred for 30 min at rt under argon, then cooled to -78 °C. The reaction mixture was then treated with *N*-iodosuccinimide (25 mg, 0.1 mmol) and TfOH (9 µL, 0.1 mmol) and stirred at -78 °C till completion, then quenched with triethylamine (10 µL) at -78 °C and gradually stirred to rt. The reaction mixture was diluted with CH₂Cl₂ (5 mL) filtered through celite and washed with 20% aqueous Na₂S₂O₃ (5 mL). The aqueous layer was extracted with CH₂Cl₂ (3 mL) twice and the combined organic layer was dried over Na₂SO₄ and concentrated at reduced pressure. The residual crude was purified via silica gel column chromatography eluting with (hexane/ethyl acetate 4:1) yielding **369** (79 mg, 89%) as a colorless syrup. $[\alpha]_D^{23} = +33$ ($c = 0.8$, CHCl₃) ¹H NMR (500 MHz, C₆D₆) δ 7.45 (m, 1H), 7.29 (m, 2H), 7.21 (d, $J = 7.6$ Hz, 2H), 7.10 – 7.02 (m, 10H), 5.54 – 5.52 (m, 1H), 5.49 (ddd, $J = 9.4, 5.4, 2.0$ Hz, 1H), 5.13 – 5.09 (m, 1H), 5.07 (d, $J = 11.1$ Hz, 1H), 4.90 (d, $J = 11.4$ Hz, 1H), 4.72 (d, $J = 11.1$ Hz, 1H), 4.63 (d, $J = 11.8$, 1H), 4.61 (d, $J = 12.0$, 1H), 4.55 – 4.49 (m, 2H), 4.36 (dd, $J = 12.3, 5.6$ Hz, 1H), 4.19 (dd, $J = 9.8, 5.4$ Hz, 1H), 4.16 (d, $J = 7.6$ Hz, 1H), 4.11 – 4.07 (m, 1H), 4.03-3.98 (m, 2H), 3.89-3.84 (m, 1H), 3.80 – 3.75 (m, 2H), 3.45 (t, $J = 5.9$ Hz, 1H), 3.34-3.31 (m, 4H), 2.73 (dd, $J = 12.3, 4.1$ Hz, 1H), 2.39 (t, $J = 12.7$ Hz, 1H), 1.74 (s, 3H), 1.73 (s, 3H), 1.69 (s, 3H), 1.56 (s, 3H), 0.86 (t, $J = 7.1$ Hz, 3H). ¹³C NMR (126 MHz, C₆D₆) δ 169.99, 169.8, 169.3, 169.1, 167.4, 139.6, 139.2, 139.1, 128.3, 128.13, 128.06, 128.0, 127.9, 127.84, 127.75, 127.7, 127.6, 127.5, 127.44, 127.41, 127.2, 105.1, 99.8, 82.2, 79.8, 75.1, 74.92, 74.86, 73.5, 72.9, 71.4, 68.1, 67.3, 64.3, 64.1, 62.7, 61.9, 56.2, 32.8, 20.2, 20.1, 19.98, 13.7. HRMS (ESI): m/z calcd for C₄₆H₅₆O₁₇Na [M + Na] 903.3417, found 903.3407.

Ethyl (4,5,7,8-tetra-*O*-acetyl-3-deoxy- β -D-manno-oct-2-ulopyranosyl) onate-(2→3)-methyl 2-*O*-benzyl-4,6-*O*-benzylidene- α -D-mannopyranoside (370). A mixture of donor **330**

(110 mg, 0.2 mmol) acceptor **341** (110 mg, 0.3 mmol) and activated 4Å acid-washed powdered molecular sieves (110 mg) in CH₂Cl₂:CH₃CN 2:1 (0.95 mL, 0.2M) was stirred for 30 min at rt under argon, then cooled to -78 °C. The reaction mixture was then treated with *N*-iodosuccinimide (47 mg, 0.2 mmol) and TfOH (17 µL, 0.2 mmol) and stirred at -78 °C till completion, then quenched with triethylamine (20 µL) at -78 °C and gradually stirred to rt. The reaction mixture was diluted with CH₂Cl₂ (5 mL) filtered through celite and washed with 20% aqueous Na₂S₂O₃ (5 mL). The aqueous layer was extracted with CH₂Cl₂ (5 mL) twice and the combined organic layer was dried over Na₂SO₄ and concentrated at reduced pressure. The residual crude was purified via silica gel column chromatography eluting with (hexane/ethyl acetate 3:1) yielding **370** in (0.13 g, 89%) as a colorless syrup and **378** in (4.7 mg, 6%) as an off-white foam. $[\alpha]_D^{23} = +56$ ($c = 0.9$, CHCl₃) ¹H NMR (600 MHz, CD₃CN) δ 7.48 – 7.46 (m, 2H), 7.45 – 7.35 (m, 8H), 5.63 (m, 1H), 5.23 (m, 1H), 5.02 (m, 2H), 4.87 (d, $J = 11.6$ Hz, 1H), 4.73 (d, $J = 1.6$ Hz, 1H), 4.70 (d, $J = 11.6$ Hz, 1H), 4.53 (dd, $J = 10.3, 3.3$ Hz, 1H), 4.34 (dd, $J = 12.2, 2.3$ Hz, 1H), 4.26 – 4.15 (m, 4H), 4.05-4.02 (m, 1H), 4.00 – 3.96 (m, 1H), 3.81 – 3.75 (m, 3H), 3.36 (s, 3H), 2.37 (dd, $J = 13.0, 5.1$ Hz, 1H), 2.24 (t, $J = 12.8$ Hz, 1H), 2.03 (s, 3H), 2.00 (s, 3H), 1.96 (s, 3H), 1.92 (s, 3H), 1.25 (t, $J = 7.1$ Hz, 3H). ¹³C NMR (151 MHz, CD₃CN) δ 170.3, 170.1, 169.6, 167.7, 138.8, 138.1, 128.7, 128.3, 128.1, 127.9, 127.6, 125.96, 100.98, 100.7, 99.7, 78.8, 76.5, 73.9, 71.6, 70.9, 68.3, 67.9, 67.4, 64.4, 63.97, 62.4, 62.2, 54.2, 30.5, 19.95, 13.3. HRMS (ESI): m/z calcd for C₃₉H₄₈O₁₇Na [M + Na] 811.2775, found 811.2784.

Ethyl (4,5,7,8-tetra-*O*-acetyl-3-deoxy- β -D-manno-oct-2-ulo pyranosyl) onate-(2 \rightarrow 3)-methyl 2-*O*-benzyl- β -D-ribofuranoside (371**). A mixture of donor **330** (30 mg, 0.1 mmol) acceptor **346** (28 mg, 0.1 mmol) and activated 4Å acid-washed powdered molecular sieves (30 mg) in CH₂Cl₂:CH₃CN 2:1 (0.3 mL, 0.2M) was stirred for 30 min at rt under argon, then cooled**

to -78 °C. The reaction mixture was then treated with *N*-iodosuccinimide (14 mg, 0.1 mmol) and TfOH (45 μ L, 0.1 mmol) and stirred at -78 °C till completion, then quenched with triethylamine (5 μ L) at -78 °C and gradually stirred to rt. The reaction mixture was diluted with CH₂Cl₂ (5 mL) filtered through celite and washed with 20% aqueous Na₂S₂O₃ (5 mL). The aqueous layer was extracted with CH₂Cl₂ (4 mL) twice and the combined organic layer was dried over Na₂SO₄ and concentrated at reduced pressure. The residual crude was purified via silica gel column chromatography eluting with (hexane/ethyl acetate 1:1) yielding **371** in (29 mg, 84%) as a colorless syrup and **378** in (1.1 mg, 5%) as an off-white foam. $[\alpha]_D^{23} = +41$ ($c = 0.9$, CHCl₃). ¹H NMR (600 MHz, C₆D₆) δ 7.13-7.03 (m, 5H), 5.56 – 5.48 (m, 2H), 5.10 (ddd, $J = 13.2, 4.6, 2.9$ Hz, 1H), 4.84 (br, 1H), 4.56 (dd, $J = 12.3, 2.2$ Hz, 1H), 4.45 (dd, $J = 12.3, 5.5$ Hz, 1H), 4.39 – 4.34 (m, 1H), 4.32 – 4.16 (m, 5H), 3.91 – 3.80 (m, 2H), 3.76 (d, $J = 4.8$ Hz, 1H), 3.69 (dd, $J = 10.1, 4.9$ Hz, 1H), 3.19 (s, 3H), 2.66 (dd, $J = 12.4, 4.4$ Hz, 1H), 2.40 (t, $J = 12.8$ Hz, 1H), 1.78 – 1.53 (m, 12H), 0.90 (t, $J = 7.1$ Hz, 3H). ¹³C NMR (151 MHz, C₆D₆) δ 169.9, 169.2, 169.0, 167.6, 137.7, 127.8, 127.6, 127.5, 105.6, 99.7, 82.96, 82.2, 72.3, 71.4, 68.1, 67.2, 65.7, 64.1, 62.7, 61.6, 54.4, 32.6, 20.1, 13.6. HRMS (ESI): m/z calcd for C₃₁H₄₂O₁₆Na [M + Na] 693.2376, found 693.2369.

Ethyl (4,5,7,8-tetra-*O*-acetyl-3-deoxy- β -D-manno-oct-2-ulopyranosyl) onate-(2 \rightarrow 3)-methyl 2-*O*-acetyl-4-*O*-benzyl- α -L-rhamnopyranoside (372). A mixture of donor **330** (69 mg, 0.1 mmol) acceptor **351** (55 mg, 0.2 mmol) and activated 4Å acid-washed powdered molecular sieves (69 mg) in CH₂Cl₂:CH₃CN 2:1 (0.6 mL, 0.2M) was stirred for 30 min at rt under argon, then cooled to -78 °C. The reaction mixture was then treated with *N*-iodosuccinimide (29 mg, 0.1 mmol) and TfOH (10 μ L, 0.1 mmol) and stirred at -78 °C till completion, then quenched with triethylamine (5 μ L) at -78 °C and gradually stirred to rt. The reaction mixture was diluted with CH₂Cl₂ (5 mL) filtered through celite and washed with 20% aqueous Na₂S₂O₃ (5 mL). The aqueous

layer was extracted with CH₂Cl₂ (3 mL) twice and the combined organic layer was dried over Na₂SO₄ and concentrated at reduced pressure. The residual crude was purified via silica gel column chromatography eluting with (hexane/ethyl acetate 3:1) yielding **372** in (73 mg, 84%) as a colorless syrup and **378** in (3.5 mg, 7%) as an off-white foam. $[\alpha]_D^{23} = +65$ ($c = 0.8$, CHCl₃) ¹H NMR (499 MHz, C₆D₆) δ 7.56 (d, $J = 7.1$ Hz, 2H), 7.22 (t, $J = 7.8$ Hz, 2H), 7.01 (t, $J = 7.5$ Hz, 1H), 5.65-5.60 (m, 1H), 5.50-5.46 (m, 1H), 5.36 – 5.33 (m, 1H), 5.27-5.25 (m, 1H), 4.82 – 4.77 (m, 2H), 4.76 – 4.70 (m, 2H), 4.69 (br, 1H), 4.51 (d, $J = 10.7$ Hz, 1H), 4.23 – 4.18 (m, 1H), 4.18 – 4.12 (m, 1H), 4.01 (dq, $J = 10.8, 7.1$ Hz, 1H), 3.91 (dq, $J = 9.2, 6.2$ Hz, 1H), 3.66 (t, $J = 9.7$ Hz, 1H), 3.00 (s, 3H), 2.60 (dd, $J = 12.7, 4.5$ Hz, 1H), 2.32 (t, $J = 12.8$ Hz, 1H), 1.80 (s, 3H), 1.71 (s, 3H), 1.67 (s, 3H), 1.64 (s, 3H), 1.63 (s, 3H), 1.30 (d, $J = 6.3$ Hz, 3H), 0.99 (t, $J = 7.1$ Hz, 3H). ¹³C NMR (126 MHz, C₆D₆) δ 169.9, 169.7, 169.5, 169.2, 169.0, 167.4, 137.5, 128.5, 127.90, 127.85, 127.7, 127.5, 98.2, 96.9, 80.1, 75.8, 70.6, 70.4, 69.0, 68.4, 67.57, 66.63, 64.3, 62.9, 62.2, 54.3, 32.6, 20.3, 20.0, 18.0, 13.3. HRMS (ESI): m/z calcd for C₃₄H₄₆O₁₇Na [M + Na] 749.2628, found 749.2627.

Ethyl (4,5,7,8-tetra-*O*-acetyl-3-deoxy- β -D-manno-oct-2-ulopyranosyl) onate-(2 \rightarrow 6)-methyl 2-azido-3,4-di-*O*-benzyl-2-deoxy- α -D-galactopyranoside (373). A mixture of donor **330** (50 mg, 0.1 mmol) acceptor **368** (51 mg, 0.1 mmol) and activated 4Å acid-washed powdered molecular sieves (50 mg) in CH₂Cl₂:CH₃CN 2:1 (0.43 mL, 0.2M) was stirred for 30 min at rt under argon, then cooled to -78 °C. The reaction mixture was then treated with *N*-iodosuccinimide (21.3 mg, 0.1 mmol) and TfOH (8 μ L, 0.1 mmol) and stirred at -78 °C till completion, then quenched with triethylamine (5 μ L) at -78 °C and gradually stirred to rt. The reaction mixture was diluted with CH₂Cl₂ (5 mL) filtered through celite and washed with 20% aqueous Na₂S₂O₃ (5 mL). The aqueous layer was extracted with CH₂Cl₂ (3 mL) twice and the combined organic layer was dried over Na₂SO₄ and concentrated at reduced pressure. The residual crude was purified via silica gel

column chromatography eluting with (hexane/ethyl acetate 1:1) yielding **373** in (61 mg, 87%) as a colorless syrup and **378** in (1.1 mg, 3%) as an off-white foam. $[\alpha]_D^{23} = +37$ ($c = 0.5$, CHCl_3) ^1H NMR (500 MHz, C_6D_6) δ 7.38 (d, $J = 7.7$ Hz, 2H), 7.34 (d, $J = 7.8$ Hz, 2H), 7.19 (t, $J = 7.5$ Hz, 3H), 7.14-7.10 (m, 3H), 5.56 – 5.49 (m, 2H), 5.10 (dt, $J = 13.2, 3.6$ Hz, 1H), 4.92 (d, $J = 10.9$ Hz, 1H), 4.63 (d, $J = 11.0$ Hz, 1H), 4.53 (br, 1H), 4.47 (d, $J = 3.7$ Hz, 1H), 4.44 (br, 2H), 4.17 – 4.11 (m, 2H), 3.94 – 3.87 (m, 5H), 3.81 – 3.73 (m, 2H), 3.36 (d, $J = 8.4$ Hz, 1H), 3.08 (s, 3H), 2.71 (dd, $J = 12.3, 4.7$ Hz, 1H), 2.39 (t, $J = 12.7$ Hz, 1H), 1.77 (s, 3H), 1.73 (s, 3H), 1.69 (s, 3H), 1.57 (s, 3H), 0.83 (t, $J = 7.1$ Hz, 3H). ^{13}C NMR (126 MHz, C_6D_6) δ 169.9, 169.8, 169.3, 167.3, 138.8, 138.1, 99.7, 99.4, 77.3, 75.0, 74.3, 71.9, 71.4, 70.1, 68.2, 67.3, 64.6, 64.2, 62.6, 61.8, 60.1, 54.8, 32.97, 20.2, 20.1, 20.1, 19.98, 13.7. HRMS (ESI): m/z calcd for $\text{C}_{39}\text{H}_{49}\text{N}_3\text{O}_{16}\text{Na}$ [$\text{M} + \text{Na}$] 838.3005, found 838.3000.

Ethyl (4,5,7,8-tetra-*O*-acetyl-3-deoxy- β -D-manno-oct-2-ulopyranosyl) onate-(2 \rightarrow 6)-methyl 2-azido-3,4-di-*O*-benzyl-2-deoxy- α -D-glucopyranoside (374**). A mixture of donor **330** (50 mg, 0.1 mmol) acceptor **360** (51 mg, 0.1 mmol) and activated 4Å acid-washed powdered molecular sieves (50 mg) in $\text{CH}_2\text{Cl}_2:\text{CH}_3\text{CN}$ 2:1 (0.43 mL, 0.2M) was stirred for 30 min at rt under argon, then cooled to -78°C . The reaction mixture was then treated with *N*-iodosuccinimide (21.3 mg, 0.1 mmol) and TfOH (8 μL , 0.1 mmol) and stirred at -78°C till completion, then quenched with triethylamine (5 μL) at -78°C and gradually stirred to rt. The reaction mixture was diluted with CH_2Cl_2 (5 mL) filtered through celite and washed with 20% aqueous $\text{Na}_2\text{S}_2\text{O}_3$ (5 mL). The aqueous layer was extracted with CH_2Cl_2 (3 mL) twice and the combined organic layer was dried over Na_2SO_4 and concentrated at reduced pressure. The residual crude was purified via silica gel column chromatography eluting with (hexane/ethyl acetate 1:1) yielding **374** in (62.4 mg, 89%) as a colorless syrup and **378** in (1.0 mg, 2.7%) as an off-white foam. $[\alpha]_D^{23} = +44$ ($c = 0.38$, CHCl_3)**

^1H NMR (500 MHz, C_6D_6) δ 7.27 (d, $J = 7.2$ Hz, 4H), 7.16 (d, $J = 7.5$ Hz, 3H), 7.09 (m, 3H), 5.52 – 5.50 (br, 1H), 5.49-5.45 (m, 1H), 5.08 (dt, $J = 13.0, 3.8$ Hz, 1H), 4.82 (d, $J = 11.3$ Hz, 1H), 4.75 – 4.70 (m, 2H), 4.68-4.64 (m, 2H), 4.50 (dd, $J = 12.2, 4.9$ Hz, 1H), 4.45 – 4.41 (m, 1H), 4.37 (d, $J = 3.5$ Hz, 1H), 4.25-4.23 (m, 1H), 4.14 (d, $J = 11.7$ Hz, 1H), 4.02 – 3.98 (m, 1H), 3.86-3.80 (m, 2H), 3.72 (dd, $J = 10.4, 5.0$ Hz, 1H), 3.66 (dd, $J = 10.7, 7.1$ Hz, 1H), 3.51 (t, $J = 9.4$ Hz, 1H), 3.03 (s, 3H), 2.94 (dd, $J = 10.3, 3.5$ Hz, 1H), 2.68 (dd, $J = 12.3, 4.6$ Hz, 1H), 2.42 (t, $J = 12.7$ Hz, 1H), 1.77 (s, 3H), 1.71 (s, 3H), 1.68 (s, 3H), 1.56 (s, 3H), 0.81 (t, $J = 7.1$ Hz, 3H). ^{13}C NMR (126 MHz, C_6D_6) δ 170.0, 169.7, 169.2, 169.1, 167.3, 138.8, 138.5, 127.9, 127.8, 127.6, 99.9, 98.8, 80.2, 78.3, 74.9, 74.4, 71.3, 70.1, 68.1, 67.3, 64.1, 63.6, 62.5, 61.8, 54.6, 32.8, 20.2, 20.1, 20.04, 19.97, 13.7. HRMS (ESI): m/z calcd for $\text{C}_{39}\text{H}_{49}\text{N}_3\text{O}_{16}\text{Na}$ [$\text{M} + \text{Na}$] 838.3005, found 838.2988.

Ethyl (4,5,7,8-di-*O*-isopropylidene-3-deoxy- α,β -D-manno-oct-2-ulopyranosyl) onate-(2 \rightarrow 3)-methyl 2-*O*-benzyl-4,6-*O*-benzylidene- α -D-mannopyranoside (375). A mixture of donor **328** (79.3 mg, 0.1 mmol) acceptor **341** (89.3 mg, 0.2 mmol) and activated 4Å acid-washed powdered molecular sieves (79 mg) in CH_2Cl_2 : CH_3CN 2:1 (0.8 mL, 0.2M) was stirred for 30 min at rt under argon, then cooled to -78°C . The reaction mixture was then treated with *N*-iodosuccinimide (40 mg, 0.2 mmol) and TfOH (14.2 μL , 0.2 mmol) and stirred at -78°C till completion, then quenched with triethylamine (5 μL) at -78°C and gradually stirred to rt. The reaction mixture was diluted with CH_2Cl_2 (5 mL) filtered through celite and washed with 20% aqueous $\text{Na}_2\text{S}_2\text{O}_3$ (5 mL). The aqueous layer was extracted with CH_2Cl_2 (5 mL) twice and the combined organic layer was dried over Na_2SO_4 and concentrated at reduced pressure. The residual crude was purified via silica gel column chromatography eluting with (hexane/ethyl acetate 5:1) to give first compound **375a** (11 mg, 9.8%) as a colorless syrup and then **375b** (96 mg, 86%) as a colorless syrup.

Ethyl (4,5,7,8-di-*O*-isopropylidene-3-deoxy- α -D-manno-oct-2-ulopyranosyl) onate-(2 \rightarrow 3)-methyl 2-*O*-benzyl-4,6-*O*-benzylidene - α -D-mannopyranoside (375 α). $[\alpha]_{\text{D}}^{23} = +25$ ($c = 0.7$, CHCl_3). ^1H NMR (500 MHz, CD_3CN) δ 7.45-7.43 (m, 2H), 7.42 – 7.11 (m, 8H), 5.55 (s, 1H), 4.85 (d, $J = 11.5$ Hz, 1H), 4.71 (dd, $J = 10.1$, 3.4 Hz, 1H), 4.66 – 4.62 (m, 2H), 4.45 – 4.41 (m, 1H), 4.19 – 4.06 (m, 7H), 3.96 (dd, $J = 8.2$, 6.0 Hz, 1H), 3.86 (t, $J = 9.6$ Hz, 1H), 3.77 – 3.60 (m, 3H), 3.36 (dd, $J = 7.5$, 2.1 Hz, 1H), 3.26 (s, 3H), 2.41 (dd, $J = 15.9$, 5.5 Hz, 1H), 2.27 (dd, $J = 15.9$, 4.5 Hz, 1H), 1.45 (s, 3H), 1.32 (s, 3H), 1.27 (s, 3H), 1.26 (s, 3H), 1.18 (t, $J = 7.1$ Hz, 3H). ^{13}C NMR (126 MHz, CD_3CN) δ 169.3, 139.1, 138.3, 128.9, 128.4, 128.2, 128.0, 127.6, 126.2, 108.9, 108.5, 101.3, 100.99, 100.2, 79.1, 77.1, 74.0, 73.99, 73.6, 71.5, 70.6, 70.0, 68.5, 66.2, 64.2, 61.9, 53.9, 31.5, 26.3, 26.1, 24.6, 24.2, 13.4 HRMS (ESI): m/z calcd for $\text{C}_{37}\text{H}_{48}\text{O}_{13}\text{Na}$ [$\text{M} + \text{Na}$] 723.2987, found 723.2982.

Ethyl (4,5,7,8-di-*O*-isopropylidene-3-deoxy- β -D-manno-oct-2-ulopyranosyl) onate-(2 \rightarrow 3)-methyl 2-*O*-benzyl-4,6-*O*-benzylidene- α -D-mannopyranoside (375 β). $[\alpha]_{\text{D}}^{23} = +31$ ($c = 1.0$, CHCl_3) ^1H NMR (499 MHz, CD_3CN) δ 7.49 – 7.44 (m, 4H), 7.43 – 7.37 (m, 5H), 7.35 (d, $J = 7.1$, 1H), 5.53 (s, 1H), 4.80 (d, $J = 11.6$ Hz, 1H), 4.74 (d, $J = 1.6$ Hz, 1H), 4.69 (d, $J = 11.6$ Hz, 1H), 4.48 (dt, $J = 8.1$, 2.9 Hz, 1H), 4.38 (dd, $J = 10.3$, 3.4 Hz, 1H), 4.28 – 4.23 (m, 1H), 4.18 – 4.15 (m, 2H), 4.07 – 4.03 (m, 2H), 3.97 (dd, $J = 8.6$, 6.5 Hz, 1H), 3.94 – 3.89 (m, 1H), 3.74 (dd, $J = 7.2$, 3.6 Hz, 1H), 3.70 (td, $J = 6.0$, 3.3 Hz, 3H), 3.36 (s, 3H), 3.31 (td, $J = 7.0$, 3.8 Hz, 1H), 3.00 (dd, $J = 15.4$, 3.4 Hz, 1H), 1.80 (dd, $J = 15.4$, 2.2 Hz, 1H), 1.44 (s, 3H), 1.34 (s, 3H), 1.24 (s, 3H), 1.22 (s, 3H), 0.85 (t, $J = 7.2$ Hz, 3H). ^{13}C NMR (126 MHz, CD_3CN) δ 167.2, 138.9, 138.1, 128.98, 128.3, 128.14, 128.06, 127.7, 126.7, 117.3, 108.8, 107.9, 102.1, 100.2, 97.7, 79.4, 77.4, 74.7, 73.8, 72.6, 70.8, 69.9, 69.5, 68.5, 64.98, 64.2, 60.7, 54.2, 31.7, 25.7, 24.5, 24.4, 23.9, 13.2. HRMS (ESI): m/z calcd for $\text{C}_{37}\text{H}_{48}\text{O}_{13}\text{Na}$ [$\text{M} + \text{Na}$] 723.2987, found 723.2961.

Ethyl (4,5,7,8-tetra-*O*-benzyl-3- β -D-manno-oct-2-ulopyranosyl) onate (2 \rightarrow 6)-methyl 2-azido-3,4-di-*O*-benzyl-2-deoxy- α -D-glucopyranoside (376). A mixture of donor **331** (68.3 mg, 0.1 mmol) acceptor **360** (52.6 mg, 0.1 mmol) and activated 4Å acid-washed powdered molecular sieves (68 mg) in CH₂Cl₂:CH₃CN 2:1 (0.44 mL, 0.2M) was stirred for 30 min at rt under argon, then cooled to -78 °C. The reaction mixture was then treated with *N*-iodosuccinimide (21.8 mg, 0.1 mmol) and TfOH (7.8 μ L, 0.1 mmol) and stirred at -78 °C till completion, then quenched with triethylamine (5 μ L) at -78 °C and gradually stirred to rt. The reaction mixture was diluted with CH₂Cl₂ (5 mL) filtered through celite and washed with 20% aqueous Na₂S₂O₃ (5 mL). The aqueous layer was extracted with CH₂Cl₂ (5 mL) twice and the combined organic layer was dried over Na₂SO₄ and concentrated at reduced pressure. The residual crude was purified via silica gel column chromatography eluting with (hexane/ethyl acetate 7:1) yielding **376** in (73 mg, 83%) as a colorless syrup. $[\alpha]_D^{23} = +86$ ($c = 0.98$, CHCl₃). ¹H NMR (500 MHz, C₆D₆) δ 7.33 – 7.23 (m, 12H), 7.09 – 7.02 (m, 18H), 5.13 (d, $J = 11.2$ Hz, 1H), 4.85 (d, $J = 11.5$ Hz, 1H), 4.80 (br, 1H), 4.77 – 4.72 (m, 2H), 4.67 (d, $J = 11.1$ Hz, 1H), 4.55 (d, $J = 11.4$ Hz, 1H), 4.38 – 4.35 (m, 3H), 4.25 (br, 2H), 4.19 – 4.14 (m, 3H), 4.00 (ddd, $J = 10.2, 5.0, 3.1$ Hz, 2H), 3.86 – 3.81 (m, 4H), 3.77 – 3.70 (m, 1H), 3.62 – 3.57 (m, 1H), 3.51 (ddd, $J = 12.2, 4.3, 2.3$ Hz, 1H), 2.99 (s, 3H), 2.95 (dd, $J = 10.3, 3.5$ Hz, 1H), 2.77 (dd, $J = 12.1, 4.0$ Hz, 1H), 2.70 (t, $J = 12.2$ Hz, 1H), 0.76 (t, $J = 7.1$ Hz, 3H). ¹³C NMR (126 MHz, C₆D₆) δ 168.4, 139.6, 139.3, 139.1, 138.9, 138.7, 138.6, 128.2, 127.9, 127.8, 127.6, 100.2, 98.8, 80.3, 78.5, 76.8, 74.6, 74.5, 74.3, 73.4, 72.3, 72.1, 70.8, 70.4, 70.2, 63.6, 62.8, 61.2, 54.6, 32.3, 13.8. HRMS (ESI): m/z calcd for C₅₉H₆₅N₃O₁₂Na [M + Na] 1030.4460, found 1030.4451.

Ethyl (4-*O*-benzoyl-5,7-di-*O*-*tert*-butylsilyl-3-deoxy- α -D-manno-oct-2-ulopyranosyl) onate (2 \rightarrow 6)-methyl 2-azido-3,4-di-*O*-benzyl-2-deoxy- α -D-glucopyranoside (377). A mixture

of donor **334** (11 mg, 0.01 mmol) acceptor **360** (8.5 mg, 0.02 mmol) and activated 4Å acid-washed powdered molecular sieves (5 mg) in CH₂Cl₂:CH₃CN 2:1 (0.1 mL, 0.2M) was stirred for 30 min at rt under argon, then cooled to -78 °C. The reaction mixture was then treated with *N*-iodosuccinimide (3.5 mg, 0.02 mmol) and TfOH (2.1 µL, 0.01 mmol) and stirred at -78 °C till completion, then quenched with triethylamine (2 µL) at -78 °C and gradually stirred to rt. The reaction mixture was diluted with CH₂Cl₂ (5 mL) filtered through celite and washed with 20% aqueous Na₂S₂O₃ (3 mL). The aqueous layer was extracted with CH₂Cl₂ (3 mL) twice and the combined organic layer was dried over Na₂SO₄ and concentrated at reduced pressure. The residual crude was purified via silica gel column chromatography eluting with (hexane/ethyl acetate 3:1) yielding **377** in (11 mg, 87%) as a colorless syrup. $[\alpha]_D^{23} = +68$ ($c = 0.3$, CHCl₃). ¹H NMR (600 MHz, C₆D₆) δ 8.14 (br, 1H), 7.28 – 7.25 (m, 4H), 7.05 – 6.93 (m, 10H), 5.65-5.61 (m, 1H), 4.75 (t, $J = 11.3$ Hz, 3H), 4.67 (d, $J = 2.7$ Hz, 1H), 4.63 (d, $J = 11.1$ Hz, 1H), 4.50 (d, $J = 3.6$ Hz, 1H), 4.44 – 4.37 (m, 2H), 4.22 (br, 1H), 4.10 (dd, $J = 10.6, 1.8$ Hz, 1H), 4.03 – 3.96 (m, 3H), 3.96 – 3.90 (m, 2H), 3.90 – 3.82 (m, 2H), 3.48 (dt, $J = 10.6, 5.2$ Hz, 1H), 3.42 – 3.36 (m, 1H), 3.26 (s, 3H), 3.15 (dd, $J = 10.3, 8.6$ Hz, 1H), 3.01 (dd, $J = 10.3, 3.5$ Hz, 1H), 2.75 (t, $J = 12.1$ Hz, 1H), 2.42 (dd, $J = 12.3, 4.8$ Hz, 1H), 1.28 (s, 11H), 1.03 (s, 7H), 0.93 (t, $J = 7.1$ Hz, 3H). ¹³C NMR (151 MHz, C₆D₆) δ 167.0, 165.7, 141.2, 138.38, 138.36, 132.8, 130.5, 129.6, 127.9, 127.7, 127.5, 98.7, 98.6, 80.2, 79.3, 77.1, 74.95, 74.7, 70.8, 70.5, 69.9, 66.8, 64.9, 63.5, 63.3, 61.1, 54.8, 27.7, 26.96, 21.8, 21.7, 13.7. HRMS (ESI): m/z calcd for C₄₆H₆₁O₁₃SiN₃Na [M + Na] 915.2286, found 915.2282.

Ethyl (4,5,7,8-tetra-*O*-acetyl-2,3-dideoxy-D-manno-oct-2-ulopyranosyl) onate (378).

$[\alpha]_D^{23} = +56$ ($c = 0.7$, CHCl₃). ¹H NMR (500 MHz, CDCl₃) δ 5.86 (d, $J = 6.5$ Hz, 1H), 5.69 (br, 1H), 5.46 (br, 1H), 5.27-5.23 (m, 1H), 4.62-4.58 (m, 1H), 4.41 – 4.17 (m, 5H), 2.06 (br, 6H), 2.01

(br, 6H), 1.30 (t, $J = 6.7$ Hz, 3H). ^{13}C NMR (126 MHz, CDCl_3) δ 170.6, 170.4, 170.1, 169.6, 161.1, 144.96, 107.3, 73.4, 67.4, 64.9, 61.97, 61.8, 60.9, 20.8, 20.7, 20.6, 14.2. HRMS (ESI): m/z calcd for $\text{C}_{18}\text{H}_{24}\text{O}_{11}\text{Na}$ [$\text{M} + \text{Na}$] 439.1008, found 439.1000.

5-azido-1-pentanol (409). A solution of triflic anhydride (3 mL, 17.9 mmol) in dry MeCN (10 mL) was cooled to 0 °C, then, sodium azide (2.3g, 35.7 mmol) was added and the reaction mixture stirred at 0 °C for 2 h. A solution of 5-aminopentanol (0.2 g, 1.9 mmol) in methanol (5mL) was added to reaction mixture followed by the dropwise addition of a solution mixture of $\text{CuSO}_4 \cdot \text{H}_2\text{O}$ (20 mg, 0.1 mmol) and K_2CO_3 (0.2 g, 1.6 mmol) in MeOH:H₂O 1:5 (10 mL). The resulting mixture was gradually brought to rt and stirred till completion with monitoring by TLC (dichloromethane:ethyl acetate 1:1, $R_f = 0.4$). The solvent was carefully concentrated under reduced pressure and the residue taken up in ethyl acetate and washed with water and brine. The aqueous layer was extracted with ethyl acetate and the combined organic layer was dried over anhydrous Na_2SO_4 , filtered, and concentrated at reduced pressure. The residual crude was purified by silica gel column chromatography (dichloromethane:ethyl acetate 1:1) to give **2** in (0.18 g, 73%) yield as a colorless oil and the spectral data were consistent with the literature. ^1H NMR (500 MHz, CD_3OD) δ 3.53 (t, $J = 6.4$ Hz, 2H), 3.32 (t, $J = 7.2$ Hz, 2H), 1.63 – 1.43 (m, 4H), 1.41 – 1.19 (m, 2H). ^{13}C NMR (126 MHz, CD_3OD) δ 61.3, 42.2, 31.8, 27.5, 22.9. HRMS (ESI): m/z calcd for $\text{C}_5\text{H}_{11}\text{ON}_3\text{Na}$ [$\text{M} + \text{Na}$] 152.0804, found 152.0800.

Ethyl (4,5,7,8-tetra-*O*-acetyl-2,3-dideoxy-D-manno-oct-2-ulopyranosyl) onate-(2→*O*)-5-azido-pentane (410). A mixture of donor **330** (117 mg, 0.2 mmol), acceptor **409** (39 mg, 0.3 mmol) and activated 4Å acid-washed powdered molecular sieves (117 mg) in $\text{CH}_2\text{Cl}_2:\text{CH}_3\text{CN}$ 2:1 (1 mL, 0.2M) was stirred for 30 min at rt under argon, then cooled to -78 °C. The reaction mixture was then treated with *N*-iodosuccinimide (49.7 mg, 0.2 mmol) and TfOH

(17.8 μ L, 0.2 mmol) and stirred at -78 °C till completion, then quenched with triethylamine (7 μ L) at -78 °C and gradually stirred to rt. The reaction mixture was diluted with CH₂Cl₂ (10 mL), filtered through celite and washed with 20% aqueous Na₂S₂O₃ (5 mL). The aqueous layer was extracted with CH₂Cl₂ (5 mL) twice and the combined organic layer was dried over Na₂SO₄ and concentrated at reduced pressure. The residual crude was purified via silica gel column chromatography eluting with (hexane/ethyl acetate 2:1) yielding **410** in (102 mg, 94%) as a colorless syrup. $[\alpha]_D^{23} = +30$ ($c = 1.3$, CHCl₃), ¹H NMR (500 MHz, C₆D₆) δ 5.57 – 5.50 (m, 2H), 5.08 (dt, $J = 13.2, 4.2$ Hz, 1H), 4.58 – 4.50 (m, 2H), 4.24 (d, $J = 9.7$ Hz, 1H), 3.89-3.81 (m, 3H), 3.30 (dt, $J = 9.2, 6.3$ Hz, 1H), 2.67 (dd, $J = 12.3, 4.3$ Hz, 1H), 2.57 (t, $J = 6.0$ Hz, 2H), 2.40 (t, $J = 12.7$ Hz, 1H), 1.80 (s, 3H), 1.70 (s, 3H), 1.55 (s, 3H), 1.30-1.27 (m, 3H), 1.12 – 1.08 (m, 3H), 0.89 (d, $J = 6.9$ Hz, 3H). ¹³C NMR (126 MHz, C₆D₆) δ 170.1, 169.8, 169.3, 169.2, 167.8, 99.6, 71.3, 68.3, 67.3, 64.3, 64.2, 62.8, 61.6, 50.9, 32.99, 29.0, 28.3, 23.1, 20.2, 20.13, 20.07, 19.99, 13.8. HRMS (ESI): m/z calcd for C₂₃H₃₅O₁₂Na [M + Na] 568.2113, found 568.2109.

Ethyl (8-*O*-*tert*-butyldimethylsilyl-3-deoxy- β -D-manno-oct-2-ulopyranosyl) onate-(2 \rightarrow *O*)-5-azido-pentane (412). A solution of **410** (0.1 g, 0.2 mmol) in dry methanol (10 mL) was treated with sodium methoxide (40 mg, 0.7 mmol) added in four portions over the period of the reaction. The reaction mixture was stirred at rt till completion. After completion, the reaction mixture was neutralized with IR 120 resin and concentrated at reduced pressure. The residue was dissolved in DMF (3 mL) and the solution mixture treated with imidazole (18 mg, 0.3 mmol) and TBSCl (30 mg, 0.2 mmol) at 0 °C. The reaction mixture was gradually warmed to rt and stirred till completion with monitoring by TLC (hexane:ethyl acetate 1:1, $R_f = 0.2$). The reaction was then quenched by addition of saturated aqueous NH₄Cl, and then diluted with ethyl acetate. The organic layer was washed with water and brine, dried over anhydrous Na₂SO₄, filtered and concentrated at

reduced pressure. The residual syrup was purified by silica gel column chromatography (hexane:ethyl acetate 1:1) to give **412** (86.5 mg, 88%) as a colorless syrup. $[\alpha]_{\text{D}}^{23} = +57$ ($c = 0.2$, CH₃OH), ¹H NMR (500 MHz, CD₆CO) δ 4.30-4.26 (m, 2H), 4.02 (dd, $J = 10.5, 3.3$ Hz, 1H), 3.93 – 3.82 (m, 2H), 3.82 – 3.73 (m, 1H), 3.69 (dd, $J = 10.5, 7.0$ Hz, 1H), 3.65-3.61 (m, 1H), 3.53 (d, $J = 8.0$ Hz, 1H), 3.45-3.40 (m, 1H), 3.37 (t, $J = 6.9$ Hz, 2H), 3.21 (d, $J = 5.4$ Hz, 1H), 3.17 – 3.07 (m, 2H), 2.29 (dd, $J = 12.3, 4.6$ Hz, 1H), 2.23 (s, 6H), 1.88 (t, $J = 12.3$ Hz, 1H), 1.69-1.58 (m, 4H), 1.51 – 1.43 (m, 2H), 1.36 (t, $J = 7.0$ Hz, 3H), 1.01 (s, 9H). ¹³C NMR (126 MHz, CD₆CO) δ 168.9, 99.4, 74.6, 70.7, 67.1, 66.2, 65.4, 63.6, 61.5, 51.3, 34.97, 29.2, 28.4, 25.5, 23.2, 18.2, 13.7. HRMS (ESI): m/z calcd for C₂₁H₄₁O₈N₃SiNa [M + Na] 514.1461, found 514.1457.

Ethyl (5,7-*O*-benzylidene-8-*O*-*tert*-butyldimethylsilyl-3-deoxy- β -D-manno-oct-2-ulopyranosyl) onate-(2 \rightarrow *O*)-5-azido-pentane (398). To a solution of **412** (31 mg, 0.1 mmol) in DMF (0.3 mL) was added benzaldehyde dimethyl acetal (11.7 μ L, 0.1 mmol) and CSA (3 mg, 0.01 mmol). The mixture was stirred at rt till completion. The solvent was then removed at reduced pressure and the residual crude dissolved in ethyl acetate (10 mL) and washed with saturated sodium bicarbonate (2 \times 10 mL). The aqueous layer was extracted twice with ethyl acetate and the combined organic layer dried in MgSO₄, filtered, and concentrated under reduced pressure. The residual crude was purified by silica gel column chromatography (hexane:ethyl acetate 2:1) to give **398** (41 mg, 71%) as a colorless syrup. $[\alpha]_{\text{D}}^{23} = +61$ ($c = 0.6$, CHCl₃), ¹H NMR (500 MHz, CD₃CN) δ 7.58-7.56 (m, 2H), 7.38 – 7.36 (m, 3H), 5.74 (s, 1H), 4.50 (dt, $J = 8.0, 4.1$ Hz, 1H), 4.33 (dd, $J = 7.8, 2.0$ Hz, 1H), 4.20-4.13 (m, 2H), 4.05 (dd, $J = 10.8, 2.6$ Hz, 1H), 3.77 – 3.67 (m, 3H), 3.60 (dd, $J = 10.7, 7.4$ Hz, 1H), 3.51 (dd, $J = 8.7, 2.0$ Hz, 1H), 3.26 (dt, $J = 9.3, 6.7$ Hz, 1H), 3.20-3.17 (m, 3H), 3.04 (d, $J = 5.2$ Hz, 1H), 1.50 – 1.44 (m, 4H), 1.27 – 1.24 (m, 5H), 0.88 (s, 14H). ¹³C NMR (126 MHz, CD₃CN) δ 169.9, 137.9, 129.5, 128.2, 127.4, 103.2, 98.6, 72.3, 72.1, 71.5, 70.9,

65.6, 63.99, 61.3, 51.1, 32.6, 29.1, 28.3, 25.4, 23.1, 18.1, 13.6. HRMS (ESI): m/z calcd for $C_{28}H_{45}O_8N_3SiNa$ [$M + Na$] 602.1575, found 602.1570.

Allyl 3,5-di-*O*-tetraisopropylidisiloxy- α,β -D-ribofuranoside (415). A solution of **414** (0.94 g, 4.9 mmol) in pyridine (3.7 mL) was treated with TIPDSCl₂ (1.6 mL, 4.9 mmol) at 0 °C. The reaction mixture was gradually warmed to rt and stirred for 1 h while monitoring by TLC (hexane:ethyl acetate 2:1, R_f = 0.7). The reaction was then quenched by addition of saturated aqueous NH₄Cl, and then diluted with ethyl acetate. The organic layer was washed with water and brine, dried over anhydrous Na₂SO₄, filtered and concentrated at reduced pressure. The residual syrup was purified by silica gel column chromatography (hexane:ethyl acetate 2:1) to give **415** (1.38 g, 65%) as a colorless syrup. ¹H NMR (500 MHz, CDCl₃) δ 5.97 – 5.86 (m, 2H), 5.33 – 5.07 (m, 5H), 4.79 (d, J = 3.7 Hz, 1H), 4.68 (dd, J = 7.8, 4.1 Hz, 1H), 4.29 – 4.19 (m, 3H), 4.18 – 4.10 (m, 2H), 4.06 – 3.90 (m, 5H), 3.89 – 3.82 (m, 2H), 3.70 (dd, J = 11.8, 4.8 Hz, 1H), 3.63-3.60 (m, 1H), 3.36-3.34 (m, 1H), 3.18 (d, J = 9.8 Hz, 1H), 1.07 – 0.91 (m, 57H). ¹³C NMR (126 MHz, CDCl₃) δ 134.5, 133.9, 133.5, 117.9, 117.4, 99.6, 98.1, 73.5, 73.3, 73.0, 71.9, 71.8, 71.1, 705, 69.9, 69.6, 69.3, 68.5, 67.96, 67.8, 64.7, 63.8, 17.7, 17.6, 17.5, 17.44, 17.38, 17.34, 17.29, 17.22, 17.15, 13.9, 13.63, 13.57, 13.5, 13.44, 13.38, 13.3, 13.2, 13.1, 12.99, 12.9. HRMS (ESI): m/z calcd for $C_{20}H_{40}O_6Si_2Na$ [$M + Na$] 455.0120, found 455.0115.

Allyl 2-*O*-acetyl- α,β -D-ribofuranoside (417). A solution of **415** (0.84 g, 1.9 mmol) in pyridine (2 mL), was cooled to 0 °C. 4-dimethylaminopyridine (0.12 g, 1.0 mmol) was added followed by the addition of acetic anhydride (0.18 mL, 1.9 mmol). The reaction mixture was stirred at 0 °C till completion with monitoring by TLC (hexane:ethyl acetate 3:1, R_f = 0.5). After completion, the reaction mixture was concentrated under reduced pressure and the residue (0.88 g, 1.9 mmol) was dissolved in THF (5 mL). The solution mixture was then treated with TBAF (1.9

ml) at 0 °C. The reaction mixture was gradually warmed to rt and stirred for 3 h while monitoring by TLC (hexane:ethyl acetate 1:1, R_f = 0.1). The reaction was then quenched by addition of saturated aqueous NH_4Cl , and then diluted with ethyl acetate. The organic layer was washed with water and brine, dried over anhydrous Na_2SO_4 , filtered and concentrated at reduced pressure. The residual syrup was purified by silica gel column chromatography (hexane:ethyl acetate 1:1) to give **417** (0.33 g, 75%) as a colorless syrup ^1H NMR (500 MHz, CD_3OD) δ 6.00 – 5.82 (m, 2H), 5.39 – 5.21 (m, 2H), 5.15-5.10 (m, 3H), 4.99 – 4.81 (m, 2H), 4.79 – 4.68 (m, 2H), 4.61 (d, J = 3.0 Hz, 1H), 4.29 – 4.21 (m, 2H), 4.19-4.15 (m, 1H), 4.10 – 3.97 (m, 3H), 3.97 – 3.84 (m, 1H), 3.84 – 3.75 (m, 3H), 3.75 – 3.64 (m, 2H), 3.64 – 3.53 (m, 1H), 3.53 – 3.38 (m, 1H), 2.10-2.08 (m, 4H), 2.07-2.05 (m, 2H). ^{13}C NMR (126 MHz, CD_3OD) δ 168.9, 99.4, 74.6, 70.7, 67.1, 66.2, 65.4, 63.6, 61.5, 51.3, 34.97, 29.2, 28.4, 25.5, 23.2, 18.2, 13.7. HRMS (ESI): m/z calcd for $\text{C}_{10}\text{H}_{16}\text{O}_6\text{Na}$ [$\text{M} + \text{Na}$] 255.1125, found 255.1119.

Allyl 2-*O*-acetyl-5-*O*-*tert*-butyldimethylsilyl- α,β -D-ribofuranoside (389). To a solution mixture of **417** (0.1 g, 0.4 mmol) in DMF (4.3 mL) was added imidazole (38 mg, 0.6 mmol) and TBSCl (65 mg, 0.4 mmol) at 0 °C. The reaction mixture was gradually warmed to rt and stirred for 2 h while monitoring by TLC (hexane:ethyl acetate 2:1, R_f = 0.3). The reaction was then quenched by addition of saturated aqueous NH_4Cl , and then diluted with ethyl acetate. The organic layer was washed with water and brine, dried over anhydrous Na_2SO_4 , filtered and concentrated at reduced pressure. The residual syrup was purified by silica gel column chromatography (hexane:ethyl acetate 2:1) to give **389** (0.11 g, 80%) as a colorless syrup. ^1H NMR (500 MHz, CDCl_3) δ 5.94 – 5.81 (m, 2H), 5.29-5.26 (m, 1H), 5.25-5.20 (m, 1H), 5.18-5.16 (m, 2H), 4.98 (t, J = 3.1 Hz, 1H), 4.90 (d, J = 2.3 Hz, 1H), 4.86 – 4.76 (m, 2H), 4.27 – 4.13 (m, 3H), 4.13 – 4.06 (m, 2H), 4.01-3.98 (m, 1H), 3.96 – 3.84 (m, 2H), 3.80-3.77 (m, 1H), 3.72 (dd, J = 11.6, 4.3 Hz, 1H),

3.62-3.59 (m, 2H), 0.93 – 0.88 (m, 18H). ^{13}C NMR (126 MHz, CDCl_3) δ 170.4, 133.9, 133.8, 117.7, 117.3, 100.6, 97.2, 77.4, 77.1, 76.8, 71.4, 69.95, 69.8, 69.5, 68.5, 68.4, 68.1, 64.0, 63.6, 25.8, 25.7, 21.3, 21.1, 18.1. HRMS (ESI): m/z calcd for $\text{C}_{16}\text{H}_{30}\text{O}_6\text{SiNa}$ [$\text{M} + \text{Na}$] 369.2300, found 369.2296.

Allyl 2-*O*-acetyl-3,5-di-*O*-benzyl- α,β -D-ribofuranoside (420) and Allyl 3-*O*-acetyl-2,5-di-*O*-benzyl- α,β -D-ribofuranoside (421). To a solution of **417** (0.2 g, 0.9 mmol) in dry DMF (8.6 mL) were added sodium hydride (0.14 g, 3.4 mmol) and BnBr (0.4 ml, 3.4 mmol) at 0 °C. The reaction mixture was gradually warmed to room temperature and stirred till completion with monitoring by TLC (hexane:ethyl acetate 20:1, R_f = 0.5). The reaction was quenched by the addition methanol, then was diluted with ethyl acetate. The organic layer was washed with water and brine, dried over anhydrous Na_2SO_4 , filtered and concentrated at reduced pressure. The unreacted benzyl bromide was removed via flash column chromatography yielding to (0.33 g, 89%) of desired intermediate **418** and the regioisomeric form **419**. A solution mixture of **418** and **419** (0.33 g, 0.8 mmol) in methanol was treated with PdCl_2 (28 mg, 0.2 mmol) and stirred at rt till completion. The solid residue was filtered, and the filtrate concentrated at reduced pressure. The residual syrup was purified by silica gel column chromatography (hexane:ethyl acetate 2:1) to afford a mixture of **420** and **421** (0.25 g, 84%) as a colorless syrup. ^1H NMR (500 MHz, CDCl_3) δ 7.42 – 7.20 (m, 18H), 5.87 (d, J = 3.5 Hz, 1H), 4.97 – 4.92 (m, 1H), 4.73 (d, J = 11.6, 1H), 4.67 – 4.55 (m, 4H), 4.45 (t, J = 12.1 Hz, 1H), 4.14 – 4.07 (m, 1H), 3.90 – 3.77 (m, 2H), 3.74 – 3.67 (m, 1H), 3.60-3.55 (m, 2H), 3.24-3.22 (m, 1H). ^{13}C NMR (126 MHz, CDCl_3) δ 170.6, 137.8, 137.7, 137.5, 128.7, 128.62, 128.58, 128.5, 128.1, 127.98, 127.9, 106.96, 94.6, 91.4, 82.4, 80.3, 72.8, 72.6, 72.5, 72.4, 71.96, 71.7, 71.3, 70.9, 68.1, 67.1, 63.1, 62.8, 56.7, 55.7. HRMS (ESI): m/z calcd for $\text{C}_{21}\text{H}_{24}\text{O}_6\text{Na}$ [$\text{M} + \text{Na}$] 395.1907, found 395.190.

REFERENCES

1. McNaught, A. D. *Carbohydr. Res.* **1997**, 297, 1–92.
2. Sharon, N.; Lis H, *Science*. **1989**, 246, 227–234, b) Ghazarian, H.; Idoni, B.; Oppenheimer, S. B. *Acta. Histochem.* **2011**, 113, 236–247.
3. Seeberger, P. H. *Acc. Chem. Res.* **2015**, 48, 1450–1463.
4. a) Hsu, C.-H.; Hung, S.-C.; Wu, C.-Y.; Wong, C.-H. *Angew. Chem. Int. Ed.* **2011**, 50, 11872–11923
 b) Saliba, R. C.; Wooke, Z. J.; Nieves, G. A.; Chu, A.-H. A.; Bennett, C. S.; Pohl, N. L. B. *Org. Lett.* **2018**, 20, 800–803. c) C.-Y. Huang, D. A. Thayer, A.-Y. Chang, M. D. Best, J. Hoffmann, S. Head, C.-H. Wong, *Proc. Natl. Acad. Sci. USA.* **2006**, 103, 15 – 20.
5. a) Love, K. R.; Seeberger, P. H. *Angew. Chem. Int. Ed.* **2004**, 43, 612 – 615; *Angew. Chem. Int. Ed.* **2004**, 43, 602 – 605. b) Pistorio, S. G.; Geringer, S. A.; Stine, K. J.; Demchenko, A. V. *J. Org. Chem.* **2019**, 84, 6576–6588. c) Panza, M.; Stine, K. J.; Demchenko, A. V. *Chem. Comm.* **2020**, 56, 1333–1336.
6. Schuerch, C.; Fréchet, J. M. *J. Am. Chem. Soc.* **1971**, 93, 492–496.
7. a) Bartetzko, M.; Pfrengle, F. *Chem. Bio. Chem.* **2019**, 20, 877–885. b) Jeyakumar, K.; Hurevitch, M.; Seeberger, P. H. *Chem. Comm.* **2013**, 49, 4453–4455.
8. a) Cheng, C.-W., Wu, C.-Y., Hsu, W.-L., & Wong, C.-H. *Biochemistry*. **2019**, doi:10.1021/acs.biochem.9b00613. b) Schmidt, D.; Schuhmacher, F.; Geissner, A.; Seeberger, P. H.; Pfrengle, F. *Chem. Eur. J.* **2015**, 21, 5709–5713.
9. a) Andrade, R. B.; Plante, O. J.; Melean, L. G.; Seeberger, P. H. *Org. Lett.* **1999**, 1, 1811–1814. b) Plante, O. J.; Palmacci, E. R.; Seeberger, P. H. *Science* **2001**, 291, 1523–1527. c) Love, K. R.; Seeberger, P. H. *Angew. Chem., Int. Ed.* **2004**, 43, 602–605.
10. a) Werz, D. B.; Castagner, B.; Seeberger, P. H. *J. Am. Chem. Soc.* **2007**, 129, 2770–2771. b) Baek, J. Y.; Choi, T. J.; Jeon, H. B.; Kim, K. S. *Angew. Chem. Int. Ed.* **2006**, 45, 7436–7440. c) Walvoort, M. T. C.; Van den Elst, H.; Plante, O. J.; Kröck, L.; Seeberger, P. H.; Overkleeft, H. S.; Van der Marel, G. A.; Codee, J. D. C. *Angew. Chem. Int. Ed.* **2012**, 51, 4393–4396.

11. a) Linhardt, R. J.; Toida, T. *Acc. Chem. Res.* **2004**, 37, 431–438. b) Gama, C. I.; Hsieh-Wilson, L. C. *Curr. Opin. Chem. Biol.* **2005**, 9, 609–619. c) Noti, C.; Seeberger, P. H. *Chem. Biol.* **2005**, 12, 731–756. d) Kandasamy, J.; Hahm, H. S.; Schuhmacher, F.; Klein, J. C.; Seeberger, P. H. *Chem. Comm.* **2014**, 50, 1875–1877.
12. a) Winter, C.; Schwegmann-Webels, C.; Cavanagh, D.; Neumann, U.; Herrler, G. *J. Gen. Virol.* **2006**, 87, 1209–1216. b) Crocker, P. R.; Paulson, J. C.; Varki, A. *Nat. Rev. Immunol.* **2007**, 7, 255–266. c) Chen, X.; Varki, A. *ACS Chem. Biol.* **2010**, 5, 163–176. d) Ernst, B.; Oehrlein, R. *Glyconj. J.* **1999**, 16, 161–170.
13. a) Brandley, B. K.; Schnaar, R. L. **1986**, 40, 97–111. b) Albersheim, P.; Anderson-Prouty, A. *Ann. Rev. Plant Physiol.* **1975**, 26, 31–52. c) Cummings, R. D. *Glyconj. J.* **2019**, 36, 241–257.
14. a) Hook, M.; Kjehlen, L.; Johansson, S.; Robinson, J. *Annu. Rev. Biochem.* **1984**, 53, 847–850. b) Kobata, A. New York: John Wiley and Sons, **1984**, p. 87–161.
15. a) Monsigny, M. *Biol. Cell.* **1984**, 51, 113–116. b) Frazier, W.; Glaser, L. *Annu. Rev. Biochem.* **1979**, 48, 491–497.
16. Van den Bosch, J. F.; Verboom-Sohmer, U.; Postma, P.; de Graaff, J.; MacLaren, D. M. *Infect. Immun.* **1980**, 29, 226–229.
17. Paulson, J. C. Vol. II (Conn, P.M., Ed.) New York: Academic Press, **1985**, p. 131.
18. a) Pierce, M.; Ballou, C. E. *J. Biol. Chem.* **1983**, 258, 3576–3578. b) Burke, D.; Mendonca-Previato, L.; Ballou, C. E. *Proc. Natl. Acad. Sci. U.S.A.* **1980**, 77, 318–329.
19. a) Loomis, W. F. *Develop. Biol.* **1979**, 70, 1–10. b) Muller, K.; Gerisch, O.; Fromme, I.; Mayer, H.; Tsugita, A. A. *Eur. J. Biochem.* **1979**, 99, 419–430. c) Ray, J.; Shinnick, T.; Lerner, R. *Nature.* **1979**, 279, 215–223.
20. a) Muller, W. E. G. *Mol. Cell. Biochem.* **1980**, 29, 131–136. b) Hirsch, A. M. *Curr. Opi. Plant Biol.* **1999**, 2, 320–326.
21. Vacquier, V. D.; Moy, G. W. *Proc. Natl. Acad. Sci. U.S.A.* **1977**, 74, 2456–2460. b) Schmidt, E. L. *Ann. Rev. Microbiol.* **1979**, 33, 355–376.

22. a) Shur, B. D.; Hall, N. G. *J. Cell Biol.* **1982**, 95, 567-571. b) Shur, B. D.; Hall, N. G. *J. Cell Biol.* **1982**, 95, 574-578.
23. Kato, G.; Maruyama, Y.; Nakamura, M. *Agric. Biol. Chem.* **1979**, 43, 1085-1092.
24. Lagarda-Diaz, I.; Guzman-Partida, M. A.; Vazquez-Moreno, L. *Int. J. Mol. Sci.* **2017**, 18, 1242-1246.
25. Rini, J. M. *Annu. Rev. Biophys. Biomol. Struct.* **1995**, 24, 551-77.
26. Bohlool, B. B.; Schmidt, E. *Science*. **1974**, 185, 269-272.
27. a) Medford, A. J.; Hatzell, M. C. *ACS Catal.* **2017**, 7, 2624–2643). b) Gemperline, E.; Jayaraman, D.; Maeda, J.; Ané, J-M.; Li, L. *J. Am. Soc. Mass Spectrom.* **2015**, 26, 149-158. c) Li, X-H.; Chen, W-L.; Tan, H-Q.; Li, F-R.; Li, J-P.; Li, Y-G.; Wang, E-B. *ACS Appl. Mater. Interfaces.* **2019**, 11, 37927–37938. d) Shi, R.; Zhao, Y.; Waterhouse, G. I. N.; Zhang, S.; Zhang, T. *ACS Catal.* **2019**, 9, 9739–9750.
28. Sulieman, S.; Tran, P. S.-L., *Int. J. Mol. Sci.* **2014**, 15, 19389-19393.
29. Mus, F.; Crook, M. B.; Garcia, K.; Costas, A. G.; Geddes, B. A.; Kouri, E. D.; Paramasivan, P.; Ryu, M.-H.; Oldroyd, G. E. D.; Poole, P. S.; Udvardi, M. K.; Voigt, C. A.; Ane, J.-M.; Peters, J. W., *Appl. Environ. Microbiol.* **2016**, 82, 3698-3710.
30. Mylona, P.; Pawloski, K.; Bisseling, T. *Plant Cell.* **1995**, 7, 869-885.
31. Hoffman, B.M.; Lukoyanov, D.; Yang, Z-Y.; Dean, D. R.; Seefeldt, L.C. *Chem. Rev.* **2014**, 114, 4041–4062.
32. Biswas, B.; Gresshof, P. M., *Int. J. Mol. Sci.* **2014**, 15, 7380-7397.
33. Price, N. P. J.; Carlson, R. W. *Glycobiology*, **1995**, 5, 233–242.
34. Schultze, M.; Kondorosi, Á. *Curr. Opin. Genet. Dev.* **1996**, 6, 631–638.
35. Price, N. P. J. *Carbohydr. Res.* **1999**, 317, 1–9.
36. a) Geremia, R. A.; Mergaert, P.; Geelen, D.; Van Montagu, M.; Holsters, M. *Proc. Natl. Acad. Sci. USA*, **1994**, 91, 2669–2673. b) Spaink, H. P.; Wijffjes, A. H. M.; Van der drift, K. M. G. M.; Haverkamp, J.; Thomas-Oates, J. E.; Lugtenberg, B. J. J. *Mol. Microbiol.* **1994**, 13, 821–831.

37. John, M.; Röhrig, H.; Schmidt, J.; Wieneke, U.; Schell, J. *Proc. Natl. Acad. Sci. USA*, **1993**, 90, 625–629.
38. a) Atkinson, E. M.; Palcic, M. M.; Hindsgaul, O.; Long, S. R. *Proc. Natl. Acad. Sci. USA*, **1994**, 91, 8418–8422. b) Rohrig, H.; Schmidt, J.; Wieneke, U.; Kondorosi, A.; Barlier, I.; Schell Jr., J.; John, M. *Proc. Natl. Acad. Sci. USA*, **1994**, 91, 3122–3126.
39. Lerouge, I.; Vanderleyden, J. *FEMS. Micro. Rev.* **2001**, 26, 17-47.
40. Silipo, A.; Erbs, G.; Shinya, T.; Dow, J. M.; Parrilli, M.; Lanzetta, R.; Shibuya, N.; Newman, M. A.; Molinaro, A. *Glycobiology*. **2010**, 20, 406.
41. Garozzo, D.; D’Errico, G.; Giraud, E.; Molinaro, A. *Nat. Commun.* **2014**, 5, 5106.
42. Okazaki, S.; Tittabutr, P.; Teulet, A.; Thouin, J.; Fardoux, J.; Chaintreuil, C.; Gully, D.; Arrighi, J.-F.; Furuta, N.; Miwa, H.; Yasuda, M.; Nouwen, N.; Teaumroong, N.; Giraud, E. *ISME. J.* **2016**, 10, 64-74.
43. Nouwen, N.; Fardoux, J.; Giraud, E. *PLoS One*. 11.
44. Frayssé, N.; Couderc, F.; Poinot, V. *Eur. J. Biochem.* **2003**, 270, 1365-1380.
45. Lerouge, I.; Vanderleyden, J. *FEMS. Micro. Rev.* **2001**, 26, 17-47.
46. Giraud, E.; Moulin, L.; Vallenet, D.; Barbe, V.; Cytryn, E.; Avarre, J.-C.; Jaubert, M.; Simon, D.; Cartieaux, F.; Prin, Y.; Bena, G.; Hannibal, L.; Fardoux, J.; Sadowsky, M. *Science*. **2007**, 316, 1307-1312.
47. Silipo, A.; Leone, M. R.; Erbs, G.; Parrilli, M.; Lanzetta, R.; Chang, W.-S.; Newman, M. A.; Molinaro, A. *Angew. Chem. Int. Ed.* **2011**, 50, 12610-12612.
48. Li, W.; Silipo, A.; Molinaro, A.; Yu, B. *Chem. Commun.* **2015**, 51, 6964-6967
49. Li, W.; Silipo, A.; Gersby, L. B. A.; Newman, M. A.; Molinaro, A.; Yu, B. *Angew. Chem. Int. Ed.* **2017**, 56, 2092-2096.
50. Aboussafy, C. L.; Gersby, L. B. A.; Molinaro, A.; Newman, M-A.; Lowary, T. L. A. *J. Org. Chem.* **2019**, 84, 14-41.
51. Menzel, M.; Ziegler, T. *Eur. J. Org. Chem.* **2014**, 7658–7663.

52. Borowski, D.; Zweiböhmer, T.; Ziegler, T. *Eur. J. Org. Chem.* **2016**, 31, 5248–5256.
53. Amarasekara, H.; Dharuman, S.; Kato, T.; Crich, D. *J. Org. Chem.* **2018**, 83, 881–897.
54. Lazzara, N. C.; Rosano, R. J.; Vagadia, P. P.; Giovine, M. T.; Bezpalko, M. W.; Piro, N. A.; Giuliano, R. M. *J. Org. Chem.* **2019**, 84, 2, 666–678.
55. a) Cosgrove, D. J. *Annu. Rev. Cell Dev. Biol.* **1997**, 13, 171–201. b) Inoue, S.; Kitajima, K. *Glycoconj. J.* **2006**, 23, 277–290. c) Schauer, R. *Adv. Carbohydr. Chem. Biochem.* **1982**, 40, 131–234. d) Chen, C-C.; Ress, D.; Linhardt, R. J. *ACS Symposium Series.* **2005**, 896, 53–80.
56. Imoto, M.; Kusumoto, S.; Shiba, T. *Tetrahedron Lett.* **1987**, 28, 6235–6238. b). Kohlbrenner, W. E.; Fesik, S. W. *J. Biol. Chem.* **1985**, 260, 14695–1470.
57. Trattnig, N.; Farcet, J-B.; Gritsch, P.; Christler, A.; Pantophlet, R.; Kosma, P. *J. Org. Chem.* **2017**, 82, 12346–12358.
58. Knirel, Y. A.; Shevelev, S. D.; Perepelov, A. V. *Mendeleev Commun.* **2011**, 21, 173–182.
59. a) Levine, D. H.; Racker, E. *J. Biol. Chem.* **1959**, 234, 2532–2539. b) Unger, F. M. *Advances Carbohydr. Chem. Biochem.* **1981**, 323–388.
60. Lodowska, J.; Wolny, D.; Glarz, L. W. *Can. J. Microbiol.* **2013**, 59, 645–655.
61. Klein, G.; Lindner, B.; Brade, H.; Raina, S. J. *Biol. Chem.* **2011**, 286, 42787–42807.
62. Moll, H.; Knirel, Y. A.; Helbig, J. H.; Zahring, U. *Carbohydr. Res.* **1997**, 304, 91–95.
63. Silipo, A.; Molinaro, A.; Comegna, D.; Sturiale, L.; Cescutti, P.; Garozzo, D.; Lanzetta, R.; Parrilli, M. *Eur. J. Org. Chem.* **2006**, 21, 4784–4883.
64. Kocharova, N. A.; Ovchinnikova, O. G.; Torzewska, A.; Shashkov, A. S.; Knirel, Y. A.; Rozalski, A. *Carbohydr. Res.* **2007**, 342, 665–670.
65. a) Cox, A. D.; St. Michael, F.; Neelamegan, D.; Lacelle, S.; Cairns, C. M.; Giuliani, M. M.; Biolchi, A.; Hoe, C. J.; E. Moxon, R. E.; Richards, J. C. *Glycoconj. J.* **2010**, 27, 643–648. b) Gidney, M. A. J.; Plested, J. S.; Lacelle, S.; Coull, P. A.; Wright, J. C.; Makepeace, K.; Brisson, J-R.; Cox, A. D.; Moxon, R. E.; Richards, J. C. *Infect. Immun.* **2003**, 72, 559–569. c) Parker, M. J.; Gomery, K.; Richard, G.; MacKenzie, C. R.; Cox, A. D.; Richards, J. C.; Evans, S. V. *Glycobiology*, **2014**, 24,

- 442–449. d) Zdorovenko, E. L.; Vinogradov, E.; Zdorovenko, G. M.; Lindner, B.; Bystrova, O. V.; Shashkov, A. S.; Rudolph, K.; Zähringer, U.; Knirel, Y. A. *Eur. J. Biochem.* **2004**, 271, 4968–4977.
66. Vinogradov, E. V.; Petersen, B. O.; Thomas-Oates, J. E.; Duus, J. Ø.; Brade, H.; Holst, O. J. *Biol. Chem.* **1998**, 273, 28122.
67. Willis, L. M.; Whitfield, C. *Carbohydr. Res.* **2013**, 378, 35–44.
68. MacLean, L. L.; Vinogradov, E.; Pagotto, F.; Perry, M. B. *Can. J. Microbiol.* **2012**, 58, 540–546.
69. Willis, L. M.; Whitfield, C. *Proc Natl Acad Sci U S A.* **2013**, 110, 20753–20758.
70. a) Muñoz, V. L.; Porsch, E. A.; St. Geme, J. W. *Current Opinion in Microbiology* **2020**, 54, 37–42. b) Starr, K. F.; Porsch, E. A.; Seed, P. C.; St. Geme, J. W. *Infect Immun.* **2016**, 73:1491–1505.
71. Vanhaverbeke, C.; Heyraud, A.; Achouak, W.; Heulin, T. *Carbohydr. Res.* **2001**, 334, 127–133.
72. Muldoon, J.; Perepelov, A. V.; Shashkov, A. S.; Nazarenko, E. L.; Zubkov, V. A.; Gorshkova, R. P.; Ivanova, E. P.; Gorshkova, N. M.; Knirel, Y. A.; Savage, A. V. *Carbohydr. Res.* **2003**, 338, 459–462.
73. Reistad, R.; Zähringer, U.; Bryn, K.; Alstad, J.; Bøvre, K.; Jantzen, E. *Carbohydr. Res.* **1993**, 245, 129–136.
74. a) Zhuang, L.; Chen, Y.; Lou, Q.; Yang, Y. *Org. Biomol. Chem.* **2019**, 17, 1694–1697. b) Paulsen, H.; Krogmann, C. *Carbohydr. Res.* **1990**, 205, 31–44. c) Bernlind, C.; Oscarson, S. *J. Org. Chem.* **1998**, 63, 7780–7788. d) Hanuszkiewicz, A.; Hübner, G.; Vinogradov, E.; Lindner, B.; Brade, L.; Brade, H.; Debarry, J.; Hein, H.; Holst, O. *Chem. Eur. J.* **2008**, 14, 10251 – 10258. e) Yang, Y.; Martin, C. E.; Seeberger, P. H. *Chem. Sci.* **2012**, 3, 896–899. f) Shinefield, H. R. *Vaccine* **2010**, 28, 4335–4339. g) Gu, X. X.; Tsai, C. M.; Ueyama, T.; Barenkamp, S. J.; Robbins, J. B.; Lim, D. J. *Infect. Immun.* **1996**, 64, 4047–4053. h) Paulsen, H.; Stiem, M.; Unger, F. M. *Tetrahedron Lett.* **1986**, 27, 1135–1138. i) Bernlind, C.; Oscarson, S. *Carbohydr. Res.* **1997**, 297, 251–260. j) Seeberger, P. H. *Chem. Soc. Rev.* **2008**, 37, 19–28. 29. k) Hsu, C.-H.; Hung, S.-C.; Wu, C.-Y.; Wong, C.-H. *Angew. Chem. Int. Ed.* **2011**, 50, 11872–11923. l) Boltje, T. J.; Zhong, W.;

- Park, J.; Wolfert, M. A.; Chen, W.; Boons, G.-J. *J. Am. Chem. Soc.* **2012**, 134, 14255–14262. m)
- Yang, Y.; Oishi, S.; Martin, C. E.; Seeberger, P. H. *J. Am. Chem. Soc.* **2013**, 135, 6262–6271. n)
- Kosma, P.; Hofinger, A.; Muller-Loennies, S.; Brade, H. *Carbohydr. Res.* **2010**, 345, 704–708. o)
- Kosma, P.; Zamyatina, A. DOI 10.1007/978-3-7091-0733-1_5. p) Zhuang, L.; Chen, Y.; Lou, Q.; Yang, Y. *Org. Biomol. Chem.* **2019**, 17, 1694–1697.
75. Kong, L.; Vijayakrishnan, B.; Kowarik, M.; Park, J.; Zakharova, A. N.; Neiwert, L.; Faridmoayer, A.; Davis, B. G. *Nat. Chem.* **2016**, 8, 242–249.
76. a) Trattinig, N.; Blaukopf, M.; Bruxelle, J.-F.; Pantophlet, R.; Kosma, P. *J. Am. Chem. Soc.* **2019**, 141, 7946–7954. b) Kosma, P. *Carbohydr. Chem.* **2017**, 42, 116–164.
77. a) Huang, J.-S.; Huang, W.; Meng, X.; Wang, X.; Gao, P.-C.; Yang, J. S. *Angew. Chem. Int. Ed.* **2015**, 54, 10894–10898. b) Imoto, M.; Kusunose, N.; Matsuura, Y.; Kusumoto, S.; Shiba, T. *Tetrahedron Lett.* **1987**, 28, 6277–6280. c) Imoto, M.; Kusunose, N.; Kusumoto, S.; Shiba, T. *Tetrahedron Lett.* **1988**, 29, 2227–2230. d) Yoshizaki, H.; Fukuda, N.; Sato, K.; Oikawa, M.; Fukase, K.; Suda, Y.; Kusumoto, S. *Angew. Chem. Int. Ed.* **2001**, 40, 1475–1480. e) Zhang, Y.-H.; Gaekwad, J.; Wolfert, M. A.; Boons, G.-J. *Chem. - Eur. J.* **2008**, 14, 558–569. f) Li, Y.-T.; Wang, L.-X.; Pavlova, N. V.; Li, S.-C.; Lee, Y. C. *J. Biol. Chem.* **1997**, 272, 26419–26424. g) Baasov, T.; Kohen, A. *J. Am. Chem. Soc.* **1995**, 117, 6165–6174.
78. a) Pokorny, B.; Kosma, P. *Org. Lett.* **2015**, 17, 110–113. b) Pokorny, B.; Kosma, P. *Chem. Eur. J.* **2015**, 21, 305–313. c) Pokorny, B.; Kosma, P. *Chemistry Open* **2015**, 4, 722–728. d) Blaukopf, M.; Müller, B.; Hofinger, A.; Kosma, P. *Eur. J. Org. Chem.* **2012**, 2012, 119–131.
79. a) Yang, Y.; Martin, C. E.; Seeberger, P. H. *Chem. Sci.* **2012**, 3, 896–899. b) Tanaka, H.; Takahashi, D.; Takahashi, T. *Angew. Chem. Int. Ed.* **2006**, 45, 770–773.
80. Yang, Y.; Oishi, S.; Martin, C. E.; Seeberger, P. H. *J. Am. Chem. Soc.* **2013**, 135, 6262–6271.
81. a) Boons, G. J. P. H.; van Delft, F. L.; van der Klein, P. A. M.; van der Marel, G. A.; van Boom, J. H. *Tetrahedron* **1992**, 48, 885–904. b) Van der Klein, P. A. M.; Filemon, W.; Boons, G. J. P. H.; Veeneman, G. H.; van der Marel, G. A.; van Boom, J. H. *Tetrahedron*. **1992**, 48, 4649–4658.

82. Qian, Y.; Feng, J.; Parvez, M.; Ling, C.-C. *J. Org. Chem.* **2012**, 77, 96-107.
83. Pradhan, T. K.; Lin, C. C.; Mong, K. K. *Org. Lett.* **2014**, 16, 1474-1477.
84. Mannerstedt, K.; Ekelöf, K.; Oscarson, S. *Carbohydr. Res.* **2007**, 342, 631-637
85. Mazur, M.; Barycza, B.; Andriamboavonjy, H.; Lavoie, S.; Kenfack, M. T.; Laroussarie, A.; Blériot, Y.; Gauthier, C. *J. Org. Chem.* **2016**, 81, 10585-10599.
86. Huang, W.; Zhou, Y.-Y.; Pan, X.-L.; Zhou, X.-Y.; Lei, J.-C.; Liu, D.; Chu, Y.; Yang, J.-S. *J. Am. Chem. Soc.* **2018**, 140, 3574-3582.
87. Mi, X.-M.; Lou, Q.-X.; Fan, W.-J.; Zhuang, L.-Q.; Yang, Y. *Carbohydr. Res.* **2017**, 448, 161-165.
88. Adero, P. O.; Amarasekara, H.; Wen, P.; Bohé, L.; Crich, D. *Chem. Rev.* **2018**, 118, 8242-8284.
89. Bock, K.; Duus, J. O. J. *Carbohydr. Chem.* **1994**, 13, 513-543.
90. a) Crich, D.; Sun, S. *J. Org. Chem.* **1996**, 61, 4506-4507. b) Crich, D.; Sun, S. *J. Org. Chem.* **1997**, 62, 1198-1199.
91. Andrews, C. W.; Rodebaugh, R.; Fraser-Reid, B. *J. Org. Chem.* **1996**, 61, 5280-5289.
92. Jensen, H. H.; Nordstrom, M.; Bols, M. *J. Am. Chem. Soc.* **2004**, 126, 9205-9213.
93. Moume-Pymbock, M.; Furukawa, T.; Mondal, S.; Crich, D. *J. Am. Chem. Soc.* **2013**, 135, 14249-14255.
94. Dharuman, S.; Crich, D. *Chem. Eur. J.* **2016**, 22, 4535-4542.
95. Kancharla, P. K.; Crich, D. *J. Am. Chem. Soc.* **2013**, 135, 18999-19007.
96. Dhakal, B.; Buda, S.; Crich, D. *J. Org. Chem.* **2016**, 81, 10617-10630.
97. Dhakal, B.; Crich, D. *J. Am. Chem. Soc.* **2018**, 140, 15008-15015.
98. Unger, F. M.; Stix, D.; Schulz, G. *Carbohydr. Res.* **1980**, 80, 191-195.
99. McMahon, C. M.; Isabella, C. R.; Windsor, I. W.; Kosma, P.; Raines, R. T.; Kiessling, L. L. *J. Am. Chem. Soc.* **2020**, 142, 5, 2386-2395.
100. Dong, L.; Roosenberg, M. J.; Miller, J. M. *J. Am. Chem. Soc.* **2002**, 124, 15001-15005.
101. Degenstein, J. C.; Murria, P.; Easton, M. *J. Org. Chem.* **2015**, 80, 1909-1914.
102. Elchert, B.; Li, J.; Wang, J.; Hui, Y.; Rai, R. *J. Org. Chem.* **2004**, 69, 1513-1523.

103. Li, J.; Todaro, L. J.; Mootoo, D. R. *Org. Lett.* **2008**, 10, 1337-1340.
104. Sadaaki, Nu.; Yuhsuke, K.; Yuya, Y. *Bull. Chem. Soc. Jpn.* **1981**, 54, 2831-2054.
105. Kawakami, Y.; Yamashita, Y. *J. Org. Chem.* **1983**, 48, 1912-1914.
106. Tamao, K.; Sumitani, K.; Kiso, Y. *Bull. Chem. Soc. Jpn.* **1976**, 49, 1958-1969.
107. Ohmiya, H.; Tsuji, T.; Yorimitsu, H.; Oshima, K. *Chem. Eur. J.* **2004**, 10, 5640 – 5648.
108. Masahiro, S.; Hideki, Y.; Koichiro, O. *Bull. Chem. Soc. Jpn.* **2009**, 82, 1194-1196.
109. Someya, H.; Ohmiya, H.; Yorimitsu, H.; Oshima, K. *Org. Lett.* **2008**, 10, 969-971.
110. Perez, V. M.; Fregoso-Lopez, D.; Miranda, L. D. *Tetrahedron Lett.* **2017**, 58, 1326-
111. Mobley, J. K.; Yao, S. G.; Crocker, M.; Meier, M. *RSC. Adv.* **2015**, 105136-105148.
112. Cardona, F.; D'Orazio, G.; Silva, A. M. S. *Eur. J. Org. Chem.* **2014**, 2549-2556.
113. Cram, D. J.; Kopecky, K. R. *J. Am. Chem. Soc.* **1959**, 81, 2748–2755.
114. a) Grubbs, R. H.; Chang, S. *Tetrahedron*. **1998**, 54, 4413-4450. b) Chatterjee, A. K.; Sanders, D. P.; Grubbs, R. H. *Org. Lett.* **2002**, 4, 1939-1942. c) Fu, G. C.; Grubbs, R. H. *J. Am. Chem. Soc.* **1993**, 115, 3800-3801. d) Miller, J. F.; Termin, A.; Koch, K.; Piscopio, A. D. *J. Org. Chem.* **1998**, 63, 3158-3159. e) Peeck, L. H.; Plenio, H. *Organometallics* **2010**, 29, 2761–2766.
115. a) Trachtenberg, E. N.; Carver, J. R. *J. Org. Chem.* **1970**, 35, 1646-1653. b) Guillemonat, A. *Ann. Chim.* **1939**, 11, 143-211.
116. a) Luche, J-L.; Rodriguez-Hahn, L.; Crabbé, P. *Chem. Commun.* **1978**, 601-602. b) Ching, T. K. M.; Cheng, H. M.; Wong, W. F.; Kwong, C. S. K.; Li, J.; Lau, C. B. S.; Leung, P. S.; Cheng, C. H. K. *Org. Lett.* **2008**, 10, 3145-3148.
117. Davies, S. G.; Fletcher, A. M.; Thomson, J. E. *Org. Biomol. Chem.* **2014**, 12, 4544-4549.
118. a) Graham, A. R.; Millidge, A. F.; Young, D. P. *J. Chem. Soc.* **1954**, 2180-2200. b) Winstein, S.; Ingraham, L. L. *J. Am. Chem. Soc.* **1952**, 74, 1160-1164. c) Parker, R. E.; Isaacs, N. S. *Chem. Rev.* **1959**, 59, 737-799.
119. a) Fürst, A.; Plattner, P. A. *Helv. Chim. Acta.* **1949**, 32, 275–283. b) Alt, G. H.; Barton, D. H. R. *J. Chem. Soc.* **1954**, 4284-4294.

120. Chiu, M. K. T.; Sigillo, K.; Gross, H. P.; Franz, H. A. *Synth. Commun.* **2007**, 37, 2355-2381.
121. Panchaud, P.; Renaud, P. *Adv. Synth. Catal.* **2004**, 346, 925-928.
122. a) Brown, H. C.; Midland, M. M. *Angew. Chem., Int. Ed. Engl.* **1972**, 11, 692–700. b) Kabalka, G. W.; Brown, H. C.; Suzuki, A.; Honma, S.; Arase, A.; Itoh, M. *J. Am. Chem. Soc.* **1970**, 92, 710–712. c) Brown, H. C.; Midland, M. M. *J. Am. Chem. Soc.* **1971**, 93, 1506–1508.
123. a) Nozaki, K.; Oshima, K.; Utimoto, K. *Tetrahedron Lett.* **1988**, 29, 1041-1044. b) Nozaki, K.; Oshima, K.; Uchimoto, K. *J. Am. Chem. Soc.* **1987**, 109, 2547–2549.
124. Matsushita, T.; Sati, G. C.; Kondasinghe, N.; Pirrone, M. G.; Kato, T.; Waduge, P.; Kumar, H. S.; Sanchon, A. C.; Dobosz-Bartoszek, M.; Shcherbakov, D.; Juhas, M.; Hobbie, S. N.; Schrepfer, T.; Chow, C. S.; Polikanov, Y. S.; Schacht, J.; Vasella, A.; Böttger, E. C.; Crich, D. *J. Am. Chem. Soc.* **2019**, 141, 5051-5061.
125. Ogawa, A.; Curran, D. P. *J. Org. Chem.* **1997**, 62, 450-451.
126. Curran, D. P.; McFadden, T. R. *J. Am. Chem. Soc.* **2016**, 138, 7741–7752.
127. Keck, G. E.; Enhdln, E. J.; Yates, J. B.; Wiley, M. R. *Tetrahedron.* **1985**, 41, 4079-4094.
128. a) Guyader, L. E.; Quiclet-Sire, B.; Seguin, S.; Zard, S. Z. *J. Am. Chem. Soc.* **1997**, 119, 7410-7411. b) Quiclet-Sire, B.; Zard, S. Z. *J. Am. Chem. Soc.* **1996**, 118, 1209-1210. c) Kim, S.; Kim, S. *Bull. Chem. Soc. Jpn.* **2007**, 80, 809–822.
129. Nguyen, J. D.; D'Amato, E. M.; Narayanam, J. M. R.; Stephenson, C. R. J. *Nat. Chem.* **2012**, 4, 854-859.
130. Feng, Y.; Dong, J.; Xu, F.; Liu, A.; Wang, L.; Zhang, Q.; Chai, Y. *Org. Lett.* **2015**, 17, 2388–2391.
131. Crich, D.; Li, W. *J. Org. Chem.* **2007**, 72, 7794–7797.
132. Wang, C.-C.; Luo, S.-Y.; Shie, C.-R.; Hung, S.-C. *Org. Lett.* **2002**, 4, 847–849.
133. Crich, D.; Li, W.; Li, H. *J. Am. Chem. Soc.* 2004, 126, 15081–15086. b) Garegg, P. J.; Iversen, T.; Oscarson, S. *Carbohydr. Res.* **1976**, 50, C12- C14.

134. Barandun, L. J.; Ehrmann, F. R.; Zimmerli, D.; Immekus, F.; Giroud, M.; Grünenfelder, C.; Schweizer, W. B.; Bernet, B.; Betz, M.; Heine, A.; Klebe, G.; Diederich, F. *J. Chem. Eur.* **2015**, 21, 126 – 135.
135. Jung, M. E.; Koch, P. *Org. Lett.* **2011**, 13, 3710–3713.
136. a) Crich, D.; Vinod, A. U. *Org. Lett.* **2003**, 5, 1297–1300. b) Bauer, T.; Tarasiuk, J.; Paśniczek, K. *Tetrahedron. Asymmetry*. **2002**, 13, 77-82.
137. Neszmélyi, A.; Jann, K.; Messner, P.; Unger, F. *J. Chem. Soc. Chem. Commun.* **1982**, 1017–1019.
138. a) Marshall, J. L.; Müller, D. E.; Conn, S. A.; Seiwel, R.; Ihrig, A. M. *Acc. Chem. Res.* **1974**, 7, 333-339; b) Krivdin, L. B.; Della, E. W. *Prog. Nucl. Magn. Reson. Spectrosc.* **1991**, 23, 301 – 610.
139. a) Karplus, M. *J. Am. Chem. Soc.* **1963**, 85, 2870-2871. b) Hori, H.; Nakajima, T.; Nishida, Y.; Ohru, H.; Meguro, H. *Tetrahedron Lett.* **1988**, 29, 6317-6320.
140. a) Williamson, R. T.; Márquez, B. L.; Gerwick, W. H.; Kövér, K. E. *Magn. Reson. Chem.* **2000**, 38, 265–273. b) Kover, K. E.; Batta, G.; Feher, K. *J. Magn. Reson.* **2006**, 181, 89–97. c) Krishnamurthy, V. *J. Magn. Reson.* **1996**, 121, 33–41. d) Gil, S.; Espinosa, J. F.; Parella, T. *J. Magn. Reson.* **2010**, 207, 312–321.
141. Zhang, Y.; Gaekwad, J.; Wolfert, M. A.; Boons, G.-J. *Chem. Eur. J.* **2008**, 14, 558-569.
142. Huang, J.-S.; Huang, W.; Meng, X.; Wang, X.; Gao, P.-C.; Yang, J. S. *Angew. Chem. Int. Ed.* **2015**, 54, 10894-10898.
143. Yagupsky, P. *Clin. Microbiol. Rev.* **2015**, 28, 54-79.
144. a) Bidet, P.; Collin, E.; Basmaci, R.; Courroux, C.; Prisse, V.; Dufour, V.; Bingen, E.; Grimpel, E.; Bonacorsi, S. *Pediatr. Infect. Dis. J.* **2013**, 32, 558–560. b) Kiang, K. M.; Ogunmodede, F.; Juni, B. A.; Boxrud, D. J.; Glennen, A.; Bartkus, J. M.; Cebelinski, E. A.; Harriman, K.; Koop, S.; Faville, R.; Danila, R.; Lynfield, R. *Pediatrics*. **2005**, 116, 206–213. c) Banerjee, A.; Kaplan, J. B.; Soherwardy, A.; Nudell, Y.; MacKenzie, G. A.; Johnson, S.; Balashova, N. V. *Antimicrob. Agents Chemother.* **2013**, 57, 4300-4306. d) Saphyakhajon, P.; Joshi, A.Y.; Huskins, W. C.; Henry, N. K.; Boyce, T. G. *Pediatr. Infect. Dis. J.* **2008**, 27, 765–767.

145. a) Goodman, L. *Adv. Carbohydr. Chem.* **1967**, 22, 109-175. b) Paulsen, H. *Adv. Carbohydr. Chem. Biochem.* **1971**, 26, 127-195. c) Lerner, L. M. *Carbohydr. Res.* **1990**, 199, 116-120. d) Gregersen, N.; Pedersen, C. *Acta Chem. Scand.* **1968**, 22, 1307-1316. e) Pedersen, C. *Acta Chem. Scand.* **1968**, 22, 1888-1897. f) Capon, B. *Chem. Rev.* **1969**, 69, 4, 407-498.
146. a) P. A. J. Gorin. *Can. J. Chem.* **1962**, 40, 275-282. b) Igarashi, K. *Adv. Carbohydr. Chem. Biochem.* **1977**, 34, 243-283.
147. Meng, G.; Guo, T.; Ma, T.; Zhang, J.; Shen, Y.; Sharpless, K. B.; Dong, J. *Nature*, **2019**, 574, 86-89.
148. Mereyala, H. B.; Guntha, S. *Tetrahedron Lett.* **1993**, 34, 6929-6930.

ABSTRACT**SYNTHESIS OF BRADYRHIZOSE AND THE EQUATORIAL GLYCOSIDES OF 3-DEOXY-D-MANNO-OCT-2-ULOSONIC ACID**

by

PHILEMON NGOJE**August 2020****Advisor:** Dr. David Crich**Major:** Chemistry (Organic)**Degree:** Doctor of Philosophy

Chapter one provides a general view on the background to the research in two parts. The first part begins with an introduction on the significance of the lectin-carbohydrate interactions in leguminous plants. Then the structure and role of *O*-antigen lipopolysaccharides in the symbiotic nitrogen cycle, and the mechanism and significance of the cycle in leguminous plants growth are introduced. The role, isolation and characterization of bradyrhizose are also introduced; and the previous syntheses of bradyrhizose and of related bicyclic compounds presented.

The second part of chapter one starts with an introduction on the biosynthesis, role and occurrence of KDO in bacterial LPS and CPS. The second part also introduces the implications of KDO in glycoconjugate vaccine development, and highlights literature syntheses of equatorial KDO glycosides. The role of side chain conformation in stereocontrolled glycosylation reactions, in particular the influence of side chain conformation in stereoselective synthesis of neuraminic and pseudaminic glycosides, are then broadly discussed.

Chapter two describes the synthesis of bradyrhizose in 14 steps and 6% overall yield from commercially available and cheap D-glucose. Unlike the literature synthetic approaches to this unusual bicyclic sugar, the synthesis involves the elaboration of a *trans*-fused carbocyclic ring onto

the pre-existing glucopyranose framework followed by adjustment of the oxidation levels by simple practical methods. The key steps in this synthesis are radical extension of the glucopyranose side chain under photocatalytic conditions using *fac*-Ir(ppy)₃ as the catalyst, construction of the bicyclic motif using ring closing metathesis, regioselective allylic oxidation, Luche reduction, hydroxy-directed epoxidation, regio- and stereoselective acid-catalyzed epoxide opening, and deprotection.

Chapter three begins with an introduction to the pseudosymmetric relationship of the bacterial pseudaminic acid and 3-deoxy-D-manno-oct-2-ulosonic acid. Then, a brief discussion on the excellent equatorial selectivity obtained with the pseudaminic acid donor having the equatorially selective *tg* conformation about its C6-C7 bond is presented. This is followed by a prediction that suitably protected KDO donors will adopt the *trans,gauche* conformation of their side chain and consequently be highly equatorially selective in their coupling reactions conducted under standard conditions. The synthesis and conformational analysis of peracetylated, perbenzylated KDO donors, acetonide protected donor, and the silylene-protected KDO donor is then described. Consistent with the predictions, good to excellent equatorial selectivity is observed on coupling of acetonide-protected, per-*O*-acetyl or benzyl-protected KDO donors at low temperatures, while axial selectivity is seen on coupling of the axially selective silylene-protected KDO donor at low temperature.

Chapter four presents progress on the proposed convergent synthesis of the pentasaccharide containing the tetrasaccharide repeating unit of *K. kingae* type c capsular polysaccharide. The chapter begins with the background on *K. kingae* and its mode of infection. The synthesis of key donors and acceptors as building blocks is then described. Finally, a plan for completion of the synthesis is described.

Chapter 6 provides the full experimental details and characterization data for all compounds prepared.

AUTOBIOGRAPHICAL STATEMENT**PHILEMON NGOJE****Education**

2015 – Present Ph.D. in Organic Chemistry, Department of Chemistry, Wayne State University, Detroit, Michigan, USA. Advisor: Prof. David Crich.

2014 – 2015 M.S. in Organic Chemistry, Department of Chemistry, Youngstown State University, Youngstown, Ohio, USA. Advisor: Prof. Peter Norris

2006 – 2010 B.S. Chemistry University of Eastern Africa Baraton, Eldoret, Kenya

Publications

“Synthesis of bradyrhizose from D-glucose” Philemon Ngoje and David Crich, *Org. Lett.* **2020**, 22, 523-527

“Stereocontrolled Synthesis of the Equatorial Glycosides of 3-Deoxy-D-manno-oct-2-ulosonic Acid: Role of Side Chain Conformation” Philemon Ngoje and David Crich, *J. Am. Chem. Soc.* **2020**, 142, 7760-7764.

Presentations

“Concise Synthesis of bradyrhizose from D-glucose” Oral presentation at the 257th American Chemical Society National Meeting and Exposition. Orlando, Florida. 30th March- April 4th 2019.

“Concise Synthesis of bradyrhizose from D-glucose” Oral presentation at the 14th Midwest Carbohydrate and Glycobiology Symposium. Lansing MI. September 21-22, 2018.